AGH University of Science and Technology

FIELD OF NATURAL SCIENCES

SCIENTIFIC DISCIPLINE MATHEMATICS

DOCTORAL THESIS

Statistical inference for harmonizable processes with spectral mass concentrated on lines

Bartosz Majewski

Supervised by dr hab. Anna Dudek

Completed at AGH University of Krakow, Faculty of Applied Mathematics

Kraków, 2025

I sincerely thank Professor Anna Dudek for her support and guidance, which have greatly influenced my scientific development. I am especially grateful for her trust, belief in me, and the many opportunities she provided during my PhD.

I also deeply appreciate the collaboration and support of Professor Łukasz Lenart, Professor Antonio Napolitano, and Professor Hernando Ombao.

Finally, I want to thank my family and friends, especially Ola and Patka, for always being there for me and supporting me throughout this journey.

CONTENTS

Abstract vii

Streszczenie ix

Introduction xi

List of Symbols xv

1 Harmonizable processes 1

1.1 Harmonizability and stationary processes 1

1.2 Harmonizable almost periodically correlated processes 3

1.3 Harmonizable processes with spectral mass concentrated on lines 6

1.4 Examples in acoustics and communications 7

2 Spectral density estimation problem 13

2.1 Periodogram frequency-smoothed along the line 13

2.2 Mean-square consistency of the spectral density estimator 16

2.2.1 Known support line case 16

2.2.2 Unknown support line case 18

2.2.3 Example of support lines estimation in specific model 20

2.3 Asymptotic distribution of the rescaled spectral estimators 22

2.3.1 Asymptotic distribution of the rescaled spectral density estimator 22

2.3.2 Asymptotic distribution of the rescaled spectral coherence estimator 24

2.4 Proofs of results presented in Chapter 2 25

3 Subsampling procedure in spectral analysis 31

3.1 Brief overview of the subsampling for time series 31

3.2 Subsampling for continuous-time processes 33

3.3 Subsampling estimators and their properties 34

3.4 Consistency of subsampling procedure 37

3.5 Subsampling-based confidence intervals 41

3.6 Proofs of results presented in Chapter 3 41

4 Simulation study **63**
4.1 Models used in the simulation study . . . 63
4.2 Validation of mean-square consistency . . . 64
4.2.1 Known support line case . . . 64
4.2.2 Unknown support line case . . . 69
4.3 Validation of confidence intervals . . . 72

5 Analysis of signals exhibiting irregular cyclicities **77**
5.1 Inference for signals exhibiting irregular statistical cyclicity with applications to electrocardiograms . . . 77
5.1.1 Amplitude-modulated time-warped periodically correlated processes . . . 78
5.1.2 Bootstrap inference . . . 80
5.1.3 Application of the bootstrap inference . . . 85
5.1.4 Real data example . . . 87
5.1.5 Proofs of results presented in Section 5.1 . . . 91
5.2 Statistical properties of oscillatory processes with stochastic modulation in amplitude and time . . . 93
5.2.1 Model construction . . . 93
5.2.2 Statistical properties of the model . . . 94
5.2.3 Mean-square consistent estimators of mean and autocovariance functions . . . 95
5.2.4 Investigate the rate of convergence of the autocovariance estimator . . . 96
5.2.5 Proofs of results presented in Section 5.2 . . . 97

6 Conclusions and further research **107**

A Complex-valued random variables and vectors **109**
A.1 Second-order characterization of complex-valued random variables and vectors . . . 109
A.2 Cumulant of complex-valued random vectors . . . 111
A.3 Complex normal vectors . . . 112

B Lemmas **115**

Bibliography **121**

ABSTRACT

Harmonizable processes are widely used to model nonstationary signals in fields such as economics, engineering, and medicine. They can be seen as a superposition of sine and cosine waves with random amplitudes. This representation allows us to analyze the dependency between their frequencies. In this context, spectral density and spectral coherence serve as frequency domain analogs of covariance and correlation, respectively.

In this thesis, we focus on harmonizable processes whose spectral measure is concentrated on a union of lines (so-called support lines), potentially with non-unit slopes. This class of processes is a generalization of almost periodically correlated processes. It has practical applications in communication, particularly in the location of moving sources such as aircrafts, rockets, or hostile jamming emitters that transmit signals.

First, we address the spectral density estimation problem. We propose a periodogram frequency-smoothed along the support line as its estimator. We establish its mean-square consistency, considering scenarios in which the parameters of the support line are known or unknown. In addition, we derive the asymptotic distribution of the rescaled estimator when the support line is known. Consequently, we obtain the asymptotic distribution of the rescaled spectral coherence estimator. In addition, we introduce a subsampling technique designed specifically for the class of processes considered. We establish its consistency and construct subsampling-based confidence intervals for the spectral characteristics of harmonizable processes. To illustrate the theoretical results, we present a simulation study for models commonly used in acoustics and communication.

Finally, we present our results obtained for other classes of nonstationary processes. These findings are related to modeling and statistical inference for signals exhibiting irregular cyclicities, which are observed, for example, in medicine.

Keywords

confidence interval, periodogram, harmonizability, nonstationarity, resampling methods, spectral analysis, spectral coherence

STRESZCZENIE

Procesy harmonizowalne są szeroko stosowane do modelowania sygnałów niestacjonarnych w dziedzinach takich jak ekonomia, inżynieria i medycyna. Procesy te można postrzegać jako superpozycję fal sinusoidalnych i cosinusoidalnych o losowych amplitudach. Representacja ta ułatwia nam analizować zależność między częstotliwościami tych procesów, przy czym rolę kowariancji w dziedzinie częstotliwości odgrywa gęstość spektralna, a koherencja spektralna odpowiada korelacji w dziedzinie częstotliwości.

W niniejszej rozprawie skupiamy się na procesach harmonizowalnych, których miara spektralna jest skupiona na sumie prostych (tzw. prostych nośnych) o współczynnikach kierunkowych, które niekoniecznie są równe jeden. Klasa ta stanowi uogólnienie procesów prawie okresowo skorelowanych. Ma ona praktyczne zastosowanie w telekomunikacji, m.in. w lokalizacji ruchomych źródeł, takich jak samoloty, rakiety czy wrogie nadajniki zakłócające sygnał.

W pierwszej części pracy zajmujemy się problemem estymacji gęstości spektralnej. Estymujemy ją używając periodogramu wygładzonego wzdłuż prostej nośnej. Wykazujemy zgodność w sensie średniokwadratowym rozważając przypadki, gdy parametry prostej nośnej są znane lub nieznane. Ponadto wyprowadzamy rozkład asymptotyczny przeskalowanego estymatora w sytuacji, gdy znamy postać prostej nośnej. W konsekwencji uzyskujemy również asymptotyczny rozkład przeskalowanego estymatora koherencji spektralnej. Dodatkowo wprowadzamy metodę subsamplingu dla rozważanej klasy procesów. Pokazujemy jej zgodność i konstruujemy przedziały ufności oparte na subsamplingu dla charakterystyk spektralnych procesów harmonizowalnych. Aby zilustrować wyniki teoretyczne, przedstawiamy symulacje dla modeli powszechnie stosowanych w akustyce i komunikacji.

W drugiej części pracy dodatkowo prezentujemy wyniki uzyskane dla innych klas procesów niestacjonarnych. Dotyczą one modelowania i wnioskowania statystycznego dla sygnałów charakteryzujących się nieregularną cyklicznością, które to są obserwowane na przykład w medycynie.

Słowa kluczowe

analiza spektralna, harmonizowalność, koherencja spektralna, metody resamplingowe, niestacjonarność, przedział ufności, periodogram

INTRODUCTION

The covariance function is a common tool for analyzing stochastic processes, which measures the relationship between processes at different time points. However, it is not always sufficient, since the nature of the dependency in the observed phenomenon may be more complex and not fully captured by covariance, which measures only a linear dependency. For example, many stochastic processes can be represented as superpositions of sine and cosine waveforms with random amplitudes [67]. For this reason, Michel Loève introduced the concept of harmonizable processes in [53, Section 27]. A harmonizable process $\{X(t),\, t \in \mathbb{R}\}$ is expressed as

$$X(t) = \int_{\mathbb{R}} e^{i2\pi\omega t}\, \mathrm{d}\xi_X(\omega),$$

where $\xi_X(\omega)$ can be interpreted as a random amplitude associated with a frequency $\omega \in \mathbb{R}$ (for a formal definition, see Definition 1.2). The spectral analysis of such processes involves examining how different signal frequencies are correlated. To achieve this, a spectral measure is used. In addition, there are two commonly used tools for describing such a spectral dependency. That is, the spectral density function, which corresponds to covariance in the frequency domain, and the coherence function, which corresponds to correlation in the frequency domain.

A fundamental subclass of harmonizable processes are stationary processes, which have uncorrelated frequency components (see [11, Chapter 4] and [53, Section 27]). That is, the spectral measure has a support contained in the main diagonal of the bifrequency plane $\mathbb{R}^2$. In contrast, nonstationary processes exhibit correlated frequencies. In recent decades, significant developments have been made in the spectral analysis of nonstationary processes. In particular, many results were obtained for almost periodically correlated harmonizable processes, that is, harmonizable processes with almost periodic mean and autocovariance functions with respect to time (see Section 1.2). Research on these processes was pioneered by Gladyshev in 1961 [36, 37]. Harmonizable almost periodically correlated processes are a suitable model for data generated by interacting randomness with periodic phenomena exhibiting incommensurate frequencies. They have applications in fields such as acoustics, biology, climatology, econometrics, mechanics, and telecommunications. For references, see, for example, [1, 33, 42, 62, 78].

Dehay [17] showed that the spectral measure of harmonizable almost periodically correlated processes has support contained in a countable union of lines parallel to the main diagonal of the bifrequency plane. In this thesis, we study the class that generalizes a class of harmonizable almost periodically correlated processes. Namely, we consider harmonizable processes with spectral measure concentrated on lines with possibly non-unit slopes. These processes may result from linear

time-varying transformations of almost periodically correlated processes, such as the multi-path Doppler channel [61, Section 4]. This model effectively represents the received complex envelope in the context of locating a moving source that emits a communication signal, using measurements from two sensors [63].

Statistical inference for almost periodically correlated processes is well established (see, for example, [42, 62]), including their spectral analysis [25, 50, 51, 82]. In contrast, results for harmonizable processes with spectral measure concentrated on lines with possibly non-unit slopes remain limited. Most studies on the spectral analysis of such processes focus on the periodogram and its various modifications as estimators of spectral densities. To estimate spectral density functions across the entire bifrequency plane, a time-smoothed bifrequency periodogram was proposed by Napolitano in [60]. However, Napolitano showed that this estimator lacks mean-square consistency. Another approach considered in the literature involves evaluating the periodogram along the (estimated) support line [81, 83]. Unfortunately, the non-smoothed periodogram is not a mean-square consistent estimator even for stationary processes [11, Theorem 10.3.2]. The periodogram frequency-smoothed along a support line serves as a mean-square consistent estimator of the spectral density function corresponding to that support line [52, 61]. Moreover, this estimator has been shown to be asymptotically normal [61].

First, we focus on the estimation of the spectral density in the case when the support line is not known. This case is crucial because, in many real-world data applications, the location of the support line is unknown (see, for example, [63]). In contrast to [81] and [83], we present a mean-square consistent estimator, that is, a periodogram frequency smoothed along an estimated support line. Another aspect of our research involves statistical inference that goes beyond point estimation of spectral density functions, specifically by constructing confidence intervals. To do this, one needs to derive the asymptotic distributions of the rescaled estimator. It is difficult because the asymptotic covariance has a very complicated structure. To address this, we introduce a resampling method that approximates the asymptotic distribution of statistics. Our approach is based on the subsampling method, where the estimator is computed on subsamples of the data and these values are used to approximate the sampling distribution. A key advantage of subsampling is its consistency under relatively mild assumptions. Specifically, it only requires the existence of a non-degenerate limiting distribution for the statistic of interest, without a prior knowledge of its exact form (including its asymptotic variance or covariance), see e.g., [72]. We propose a continuous counterpart to the subsampling method introduced by Politis and Romano in [74]. Although the subsampling technique has been explored in the continuous-time setting in [4], these results are not applicable to our problem because the required assumptions are not satisfied.

In Chapter 1, we introduce in detail the concept of harmonizable processes. We begin by comparing stationary processes with harmonizable nonstationary processes. Then, we discuss a class of harmonizable periodically correlated processes. Next, we introduce harmonizable processes whose spectral measure is concentrated on the union of lines. Finally, we provide examples of these processes and their applications in acoustics and communications. In Chapter 2, we address the problem

of point estimating of the spectral density for harmonizable processes with spectral mass concentrated on lines. As an estimator, we propose a periodogram frequency-smoothed along a known line. First, we establish the mean-square consistency of the proposed estimator under assumptions weaker than those presented in [61, Chapter 4]. Based on that, we prove mean-square consistency in the case where the support line is unknown but its estimator is available. We provide an example of an estimation of the support line in a specific model. Finally, we present a result on the asymptotic normality of the rescaled estimator. As a consequence of this result, we also derive the asymptotic distribution of the rescaled spectral coherence estimator. In Chapter 3, we introduce the subsampling procedure for harmonizable processes with spectral mass concentrated on lines. This chapter begins by reviewing the notation for subsampling in time series as presented in [72]. Next, we tailor this approach for our continuous-time processes. We establish the asymptotic properties of the subsampling counterpart of the frequency-smoothed periodogram. In particular, we establish the consistency of our subsampling procedure. Finally, we construct two types of subsampling-based confidence intervals for spectral density and spectral coherence functions. In Chapter 4, we describe the simulation study that illustrates the theoretical findings of Chapter 2 and Chapter 3. Specifically, we conduct Monte Carlo simulations to validate the mean-square consistency of the frequency-smoothed periodogram in both scenarios: with a known support line and an estimated support line. Furthermore, using Monte Carlo simulation, we compare asymptotic confidence intervals and two subsampling-based confidence intervals for spectral density and spectral coherence.

In Chapter 5, we present two results on analysis of nonstationary processes that go beyond spectral analysis. In particular, we focus on the analysis of processes that exhibit irregular cyclicity. This subject has gained increasing attention in recent years, as many biomedical signals contain such irregularities. An example is the electrocardiogram (ECG) signal. Modeling ECG signals as processes with cyclic regularities has significant limitations, as it requires the assumption of a constant heart rate over time. This assumption is quite restrictive and is valid only for very short time intervals [63]. To capture this phenomenon, many new models with modulation of time and amplitude have been developed recently [15, 34, 48, 49, 63, 65]. In [31], we provide a statistical approach for analyzing electrocardiogram signals using amplitude-modulated time-warped periodically correlated processes, originally proposed by Napolitano in [63]. We develop two bootstrap procedures, based on the well-known Circular Block Bootstrap method. In [26], we propose a model that is constructed as a superposition of cosines with a nonstationary phase-shift process and a stationary amplitude process. The properties of the first- and second-order moments of the process are analyzed. In addition, estimators for the asymptotic mean and autocovariance functions are introduced along their asymptotic properties.

Finally, in Chapter 6, we summarize the results presented in this dissertation and outline possible further research directions. Moreover, the thesis includes two appendices. Appendix A summarizes some properties of complex-valued random variables. Appendix B contains the auxiliary lemmas used in this thesis. In the bibliography, the PhD candidate's papers [26, 29, 30, 31] have been highlighted by bolding his name.

LIST OF SYMBOLS

$\mathbb{N} = \{1, 2, \ldots\}$	set of natural numbers
$\mathbb{Z} = \{\ldots, -2, -1, 0, 1, \ldots\}$	set of integers
$\mathbb{R} = (-\infty, \infty)$	set of real numbers
$\mathbb{C} = \{a + ib : a, b \in \mathbb{R}\}$	set of complex numbers
$i = \sqrt{-1}$	imaginary unit
$\overline{z}$	complex conjugate of $z \in \mathbb{C}$
$z^{[*]}$	optional complex conjugate of $z \in \mathbb{C}$, i.e., $z^{[*]} \in \{z, \overline{z}\}$
$\mathrm{Re}(z)$	real part of $z \in \mathbb{C}$
$\mathrm{Im}(z)$	imaginary part of $z \in \mathbb{C}$
$\lfloor x \rfloor = \max\{m \in \mathbb{Z} : m \leq x\}$	floor of a number $x \in \mathbb{R}$
$\lceil x \rceil = \min\{m \in \mathbb{Z} : m \geq x\}$	ceil of a number $x \in \mathbb{R}$
A^{T}	transposition of a matrix A
$\langle x, y \rangle = \sum_{j=1}^{d} x_i \overline{y_i}$	scalar product of $x = [x_1, \ldots, x_d] \in \mathbb{C}^d$ and $y = [y_1, \ldots, y_d] \in \mathbb{C}^d$
$(\Omega, \mathcal{F}, \mathbb{P})$	probability space
$\mathcal{L}(X)$	law of a random variable X
$\mathbb{E}(X)$	expected value of a random variable X
$\mathrm{Var}(X)$	variance of a random variable X
$\mathrm{Cov}(X, Y)$	covariance of two random variables X and Y
$\mathrm{cum}(X_1, \ldots, X_n)$	joint cumulant of random variables $X_1, \ldots, X_n$
$\mathcal{N}(\mu, \sigma^2)$	normal distribution with a mean μ and a variance σ^2
$\mathcal{N}_d(\mu, \Sigma)$	d-dimensional normal distribution with a mean vector $\mu \in \mathbb{R}^d$ and a covariance matrix $\Sigma \in \mathbb{R}^{d \times d}$
$\xrightarrow{d}$	convergence in distribution
$\xrightarrow{\mathbb{P}}$	convergence in probability

a.s	almost surely, i.e. except on a set of probability zero
a.e	almost everywhere, i.e. except on a set of measure zero
$L^p(X)$	set of all measurable functions $f : X \to \mathbb{C}$ whose absolute value raised to the p-th power has a finite integral (see [9, Chapter 4])
$L^\infty(X)$	set of all measurable bounded almost everywhere functions $f : X \to \mathbb{C}$ (see [9, Chapter 4])
$\|f\|_p = \left(\int_X \|f(x)\|^p \,\mathrm{d}x\right)^{1/p}$	p-th norm of a function $f : X \to \mathbb{C}$ with $p \geq 1$
$\|f\|_\infty = \inf\{C > 0 \,:\, \|f(x)\| \leq C \text{ a.e. on } X\}$	essential supremum of a function $f : X \to \mathbb{C}$
$(f * g)(x) = \int_{\mathbb{R}} f(t)g(x-t)\,\mathrm{d}t$	convolution of two functions $f, g : \mathbb{R} \to \mathbb{C}$
$\mathbb{1}_A(x) = \begin{cases} 1, & x \in A \\ 0, & x \notin A \end{cases}$	indicator function of a set A
$\delta_x = \begin{cases} 1, & x = 0 \\ 0, & x \neq 0 \end{cases}$	Kronecker delta function
$\operatorname{sinc}(x) = \begin{cases} \frac{\sin(\pi x)}{\pi x}, & x \neq 0 \\ 1, & x = 0 \end{cases}$	sinc function
$\delta(x)$	Dirac delta function (see [20, Chapter III])

For two functions $f, g : \mathbb{R} \mapsto \mathbb{R}$, we use the following asymptotic notation:

- $f(x) = \mathcal{O}(g(x))$ as $x \to \infty$ if and only if there exists $M > 0$ and $x_0 \in \mathbb{R}$ such that $|f(x)| \leq M|g(x)|$ for $x_0 \geq x$;
- $f(x) = o(g(x))$ as $x \to \infty$ if and only if for every $M > 0$ there exists $x_0 \in \mathbb{R}$ such that $|f(x)| \leq M|g(x)|$ for $x_0 \geq x$.

Throughout the thesis, we use the following abbreviations:

- PC – periodically correlated;
- APC – almost periodically correlated;
- JAPC – jointly almost periodically correlated;
- AM-TW APC – amplitude-modulated time-warping periodically correlated.

CHAPTER 1

HARMONIZABLE PROCESSES

This chapter reviews the concepts of spectral analysis to provide a deeper understanding of the processes studied in this thesis. Section 1.1 recalls the definition of harmonizable processes and demonstrates how they generalize stationary processes. Section 1.2 presents almost periodically correlated processes as examples of nonstationary harmonizable processes with a specific spectral dependence structure. Section 1.3 discusses a class of harmonizable processes characterized by spectral mass concentrated along lines. Finally, Section 1.4 illustrates the practical applications of these processes in acoustics and communication.

1.1 Harmonizability and stationary processes

First, we establish the basic notation for stochastic processes. A *stochastic process* $\{X(t),\, t \in \mathbb{R}\}$ is a family of complex-valued random variables defined on a common probability space $(\Omega, \mathcal{F}, \mathbb{P})$ and indexed by the set $\mathbb{R}$. A *second-order stochastic process* is a stochastic process $\{X(t),\, t \in \mathbb{R}\}$ such that $\mathbb{E}|X(t)|^2 < \infty$ for all $t \in \mathbb{R}$. A *mean function* of a second-order stochastic process $\{X(t),\, t \in \mathbb{R}\}$ is $\mu_X(t) = \mathbb{E}X(t)$. An *autocovariance function* of a second-order stochastic process $\{X(t), t \in \mathbb{R}\}$ is

$$R_{XX}(t,s) = \operatorname{Cov}\big(X(t), X(s)\big) = \mathbb{E}\big((X(t) - \mathbb{E}X(t))\overline{(X(s) - \mathbb{E}X(s))}\big), \quad t, s \in \mathbb{R}.$$

A *cross-covariance function* of two zero-mean second-order stochastic processes $\{X(t),\, t \in \mathbb{R}\}$ and $\{Y(t),\, t \in \mathbb{R}\}$ is

$$R_{XY}(t,s) = \operatorname{Cov}\big(X(t), Y(s)\big) = \mathbb{E}\big((X(t) - \mathbb{E}X(t))\overline{(Y(s) - \mathbb{E}Y(s))}\big), \quad t, s \in \mathbb{R}.$$

Furthermore, *conjugate autocovariance function* and *conjugate cross-covariance function* are given by $R_{X\overline{X}}(t,s) = \operatorname{Cov}\big(X(t), \overline{X(s)}\big)$ and $R_{X\overline{Y}}(t,s) = \operatorname{Cov}\big(X(t), \overline{Y(s)}\big)$, for $t, s \in \mathbb{R}$, respectively.

To fully characterize complex-valued processes at the second-order level, both the covariance and conjugate covariance functions must be considered (see, e.g. [69, 70, 79, 80]). However, for the sake of simplicity, we will focus only on the autocovariance and cross-covariance functions. To

obtain results for their conjugate versions, it suffices to replace the process $Y(t)$ with its complex conjugation $\overline{Y(t)}$. For details on complex-valued random variables, see Appendix A.

Throughout this dissertation up to Chapter 4, we assume that all the processes considered are *zero-mean second-order stochastic processes*, that is, $\mu_X(t) = 0$ for all $t \in \mathbb{R}$. Such processes are encountered in communication and acoustics, which are our main areas of interest. However, in general, stochastic processes may have a non-zero mean function. In particular, it is common for almost periodically correlated processes discussed in Section 1.2.

In the following, we present the definition of the harmonizability of the covariance and the process introduced by Michel Loève [53, Section 37].

Definition 1.1 (Harmonizable covariance [53, p. 140])**.** A covariance $R_{XY}(t,s)$ is said to be *harmonizable* if there exists a covariance function $F^{XY}(\omega,\nu)$ of bounded variation on $\mathbb{R}\times\mathbb{R}$ such that

$$R_{XY}(t,s) = \iint_{\mathbb{R}^2} e^{i2\pi(t\omega - s\nu)}\,\mathrm{d}F^{XY}(\omega,\nu). \tag{1.1}$$

Definition 1.2 (Harmonizable process [53, p. 140])**.** A second-order zero-mean stochastic process $\{X(t),\, t\in\mathbb{R}\}$ is said to be *harmonizable* if there exists a second-order stochastic process $\xi_X(\omega)$ with a covariance $F^{XX}(\omega,\nu)$ of bounded variation on $\mathbb{R}\times\mathbb{R}$ such that

$$X(t) = \int_{\mathbb{R}} e^{i2\pi\omega t}\,\mathrm{d}\xi_X(\omega) \quad \text{a.s.} \tag{1.2}$$

If a stochastic process is harmonizable, then its autocovariance function is also harmonizable. Conversely, if the covariance function of a stochastic process is harmonizable, then the process is harmonizable [53, Section 37].

Remark 1.1. In the literature, F^{XY} is sometimes considered as a measure (see, for example, [42, Chapter 5]), however, we follow the definition proposed by Loève.

Remark 1.2. In the literature, spectral representations sometimes use Fourier waveforms $e^{i\omega t}$ instead of $e^{i2\pi\omega t}$. This variation can lead to ambiguities in applications, implementations, and formulas. The presence or absence of the factor 2π may require an appropriate scaling of the Fourier transform. Note that in this thesis, the factor 2π is present in the exponent.

Observe that equation (1.2) can be seen as the decomposition of $X(t)$ into sine waves $e^{i2\pi\omega t}\,\mathrm{d}\xi_X(\omega)$ with frequencies ω and random amplitude $\mathrm{d}\xi_X(\omega)$. This provides a spectral representation of the process. The function F^{XX} associated with $R_{XX}(t,s)$, describes the covariance between the spectral components $\mathrm{d}\xi_X(\omega)$ of $X(t)$ and is called the *spectral measure*. For two harmonizable processes $X(t)$ and $Y(t)$, their dependency can be analyzed in terms of the covariance between their spectral components between frequencies using F^{XY}. This function is known as *cross-spectral measure*. A comprehensive explanation of the spectral dependence can be found in [67]. For a complete analysis of the complex-valued process, it is essential to consider not only the spectral measures F^{XX}, F^{YY} and F^{XY}, but also the *conjugate spectral measures* $F^{X\overline{X}}$ and $F^{Y\overline{Y}}$, and *conjugate cross-spectral measure* $F^{X\overline{Y}}$.

The following illustrates that the concept of a harmonizable process generalizes the spectral representation of a stationary process.

Definition 1.3 (Wide-sense stationary process [11, p. 11])**.** A zero-mean second-order stochastic process $\{X(t),\, t \in \mathbb{R}\}$ is called *(wide-sense) stationary* if for all $t, s \in \mathbb{R}$ we have $\mu_X(t) = \mu_X(s)$ and $R_{XX}(t,s) = R_{XX}(t-s,0)$.

For simplicity, we omit the term "wide-sense" throughout this dissertation. The autocovariance function of stationary processes depends only on $t-s$. Therefore, for a stationary process $X(t)$, we can consider autocovariance as a function of one variable, i.e., $R_{XX}(t-s)$ instead of $R_{XX}(t-s,0)$.

For a stationary process, we have the following spectral representation. Let $\{X(t),\, t \in \mathbb{R}\}$ be a zero-mean second-order stationary process. Then

$$X(t) = \int_{\mathbb{R}} e^{i2\pi\omega t}\, \mathrm{d}\xi_X(\omega), \quad t \in \mathbb{R},$$

and

$$R_{XX}(\tau) = \int_{\mathbb{R}} e^{i2\pi\omega\tau}\, \mathrm{d}F^{XX}(\omega), \quad \tau \in \mathbb{R},$$

where $F^{XX}(\omega)$ is a right-continuous, non-decreasing function with a bounded variation on $\mathbb{R}$, and $\xi_X(\omega)$ is a second-order complex-value process of orthogonal increments, i.e.,

$$\mathrm{Cov}(\xi_X(\omega_1) - \xi_X(\omega_2), \xi_X(\omega_3) - \xi_X(\omega_4)) = 0, \qquad (\omega_1, \omega_2] \cap (\omega_3, \omega_4] = \varnothing.$$

Moreover, $F^{XX}(\omega) = \mathbb{E}|\xi_X(\omega)|^2$. If the spectral measure of a stationary process $X(t)$ is absolutely continuous, then there exists a unique function $f(\omega)$ such that $\mathrm{d}F(\omega) = f(\omega)\,\mathrm{d}\omega$. The function $f(\omega)$ is called a *spectral density function* of the process $X(t)$. More discussion of the spectral representation of a stationary process can be found in [11, Chapter 4],[39, Chapter II] and [53, Chapter 37].

Observe that stationary processes are harmonizable processes with uncorrelated spectral components $\mathrm{d}\xi_X(\omega)$ at different frequencies. Thus, we can write $\mathrm{d}F^{XX}(\omega,\nu) = \mathrm{d}F^{XX}(\omega)\delta(\nu-\omega)$, where $\delta(\cdot)$ is a Dirac delta function. Nonstationary harmonizable processes, on the other hand, are characterized by the fact that there is a correlation between spectral components of different frequencies. This enables more complex dependency to be captured. In the next section, we discuss the spectral properties of almost periodically correlated processes that are examples of nonstationary harmonizable processes.

1.2 Harmonizable almost periodically correlated processes

In this section, we present harmonizable almost periodically correlated processes, an important class of harmonizable nonstationary processes with a specific structure of spectral dependence. We start our discussion with the definition of an almost periodic function introduced by Harald Bohr in [8].

Definition 1.4 (Almost periodic function [8])**.** A function $g : \mathbb{R} \to \mathbb{R}$ is called *almost periodic (in the sense of Bohr)* if, for every $\varepsilon > 0$, there exists $l_\varepsilon > 0$ such that for any interval I_ε of length l_ε, there exists $\tau_\varepsilon \in I_\varepsilon$ such that $\sup_{t\in\mathbb{R}} |g(t+\tau_\varepsilon) - g(t)| < \varepsilon$.

Almost periodic functions generalize periodic functions. For example, consider the function $\cos\left(\frac{2\pi t}{T_0}\right) + \cos\left(\frac{2\pi t}{T_0\sqrt{2}}\right)$. This function is a sum of two periodic components with periods $T_1 = T_0$ and $T_2 = T_0\sqrt{2}$, respectively. Since these periods are incommensurate (the ratio of periods $\frac{T_2}{T_1} = \sqrt{2}$ is irrational), the function is not periodic but is instead almost periodic. The crucial property of continuous almost periodic functions is that they can be represented as the limit of a uniformly convergent sequence of trigonometric polynomials, as shown in [5].

Definition 1.5 (Almost periodically correlated process [37])**.** A second-order stochastic process $\{X(t),\, t \in \mathbb{R}\}$ is said to be *almost periodically correlated (APC)* when its mean function $\mu_X(t)$ and autocovariance function $R_{XX}(t, t+\tau)$ are almost periodic with respect to t for all $\tau \in \mathbb{R}$.

Definition 1.6 (Jointly almost periodically correlated process [85])**.** Two second-order stochastic process $\{X(t),\, t \in \mathbb{R}\}$ and $\{Y(t),\, t \in \mathbb{R}\}$ are said to be *jointly almost periodically correlated (JAPC)* if for all $\tau \in \mathbb{R}$ cross-covariance function $R_{XY}(t, t+\tau)$ is an almost periodic function with respect to t.

The analysis of APC processes is often conducted by representing the covariance and conjugate covariance functions in terms of its Fourier series. Let us assume that $\{X(t),\, t \in \mathbb{R}\}$ and $\{Y(t),\, t \in \mathbb{R}\}$ are JAPC processes. Then for any $t, \tau \in \mathbb{R}$ we have

$$R_{XY}(t, t+\tau) = \sum_{\lambda \in \Lambda_{XY}^{\tau}} a_{XY}(\lambda, \tau) e^{i2\pi\lambda t}, \tag{1.3}$$

where $\Lambda_{XY}^{\tau} = \{\lambda \in \mathbb{R} : a_{XY}(\lambda, \tau) \neq 0\}$. Functions $a_{XY}(\lambda, \tau)$ are Fourier coefficients given by

$$a_{XY}(\lambda, \tau) = \lim_{T\to\infty} \frac{1}{T} \int_{-\frac{T}{2}}^{\frac{T}{2}} R_{XY}(t, t+\tau) e^{-i2\pi\lambda t}\, \mathrm{d}t$$

and are called *cyclic autocovariance functions*. The set $\Lambda_{XY} = \bigcup_{\tau\in\mathbb{R}} \Lambda_{XY}^{\tau}$ is countable, and its elements are known as *cycle frequencies*.

Every stationary process is harmonizable, but nonstationary processes are not necessarily harmonizable, in particular, not every APC process is harmonizable. However, if $\{X(t),\, t \in \mathbb{R}\}$ and $\{Y(t),\, t \in \mathbb{R}\}$ are both harmonizable processes, then their spectral measure F^{XY} is concentrated in the union of the straight lines $\{(\omega, \nu) \in \mathbb{R}^2 : \nu = \omega - \lambda\}$, with $\lambda \in \Lambda_{XY}$, parallel to the main diagonal $\{(\omega, \nu) \in \mathbb{R}^2 : \nu = \omega\}$, see [17]. That is, we can write

$$\mathrm{d}F^{XY}(\omega, \nu) = \sum_{\lambda \in \Lambda_{XY}} \mathrm{d}F_{\lambda}^{XY}(\omega)\delta(\nu - (\omega - \lambda)).$$

Note that a function F_{λ}^{XY} can be viewed as the restriction of the spectral measure F^{XY} to the line $\{(\omega, \nu) \in \mathbb{R}^2 : \nu = \omega - \lambda\}$. If F_{λ}^{XY} is absolutely continuous, there exists the *spectral density function* f_{λ}^{XY} corresponding to cyclic frequencies $\lambda \in \Lambda_{XY}$, such that $\mathrm{d}F_{\lambda}^{XY}(\omega) = f_{\lambda}^{XY}(\omega)\,\mathrm{d}\omega$. In addition,

$$f_{\lambda}^{XY}(\omega) = \int_{\mathbb{R}} a_{XY}(\lambda, \tau)\, e^{-i2\pi\omega\tau}\, \mathrm{d}\tau, \qquad a_{XY}(\lambda, \tau) = \int_{\mathbb{R}} f_{\lambda}^{XY}(\omega)\, e^{i2\pi\omega\tau}\, \mathrm{d}\omega. \tag{1.4}$$

This is a generalization of the known relationship between the covariance function and the spectral density in the stationary case. Spectral density functions are the Fourier transforms of the corresponding cyclic autocovariance functions. For more details on the spectral theory for APC processes, we refer to [17, 41, 42, 62].

An important subclass of APC processes is the class of *periodically correlated (PC)* processes [42, Definition 1.4]. For (jointly) periodically correlated processes, the autocovariance function and cross-covariance function are periodic with some period T_0. Consequently, the set of cycle frequencies is a subset of $\left\{\frac{k}{T_0} : k \in \mathbb{Z}\right\}$, which means that the cyclic frequencies are integer multiples of the reciprocal of the period T_0. Note that the spectral measure for PC processes is concentrated in a union of equidistant straight lines parallel to the main diagonal of $\mathbb{R}^2$.

In the following, we present an example of an APC process.

Example 1.1. Define

$$X(t) = \sum_{k=1}^{K} \cos(2\pi\lambda_k t) Z_k(t), \quad t \in \mathbb{R}, \tag{1.5}$$

where $Z_k(t)$ are mutually independent stationary processes, $0 \leq \lambda_1 < \ldots < \lambda_K < \infty$ and $K \in \mathbb{N}$ is fixed. By $\gamma_k(\tau)$ we denote the autocovariance function of $Z_k(t)$, and $\phi_k(\omega)$ represents its spectral density function. Then a process $X(t)$ is harmonizable APC with $\Lambda_{XX} = \{0, \pm 2\lambda_1, \ldots, \pm 2\lambda_K\}$,

$$a_{XX}(\lambda, \tau) = \begin{cases} \frac{1}{2} \sum_{k=1}^{K} \gamma_k(\tau) \cos(2\pi\lambda_k\tau), & \lambda = 0, \\ \frac{1}{4}\gamma_k(\tau) e^{i2\pi\lambda_k\tau}, & \lambda = \pm 2\lambda_k, \\ 0, & \text{otherwise}, \end{cases}$$

and

$$f_\lambda^{XX}(\omega) = \begin{cases} \frac{1}{4} \sum_{k=1}^{K} \left(\phi_k(\omega - \lambda_k) + \phi_k(\omega + \lambda_k)\right), & \lambda = 0, \\ \frac{1}{4}\phi_k(\omega \mp \lambda_k), & \lambda = \pm 2\lambda_k, \\ 0, & \text{otherwise}. \end{cases}$$

Observe that, there are $2K + 1$ cyclic frequencies. In Figure 1.1, we illustrate the support of the spectral measure in three cases:

- Stationary case: $K = 1$ and $\lambda_1 = 0$;
- PC case: $K = 2$, $\lambda_1 = \frac{1}{4}$, and $\lambda_2 = \frac{1}{2}$;
- APC case: $K = 4$, $\lambda_1 = \frac{1}{2}$, $\lambda_2 = \frac{\sqrt{2}}{4}$, $\lambda_3 = \frac{1}{4}$, and $\lambda_4 = \frac{\sqrt{2}}{8}$.

For the stationary case, the spectral measure is supported by the main diagonal of the bifrequency plane. For the PC case, the support consists of a union of equidistant straight lines parallel to the main diagonal. Finally, in the APC case, the support is constituted by a union of straight lines parallel to the main diagonal but with varying distances between the lines.

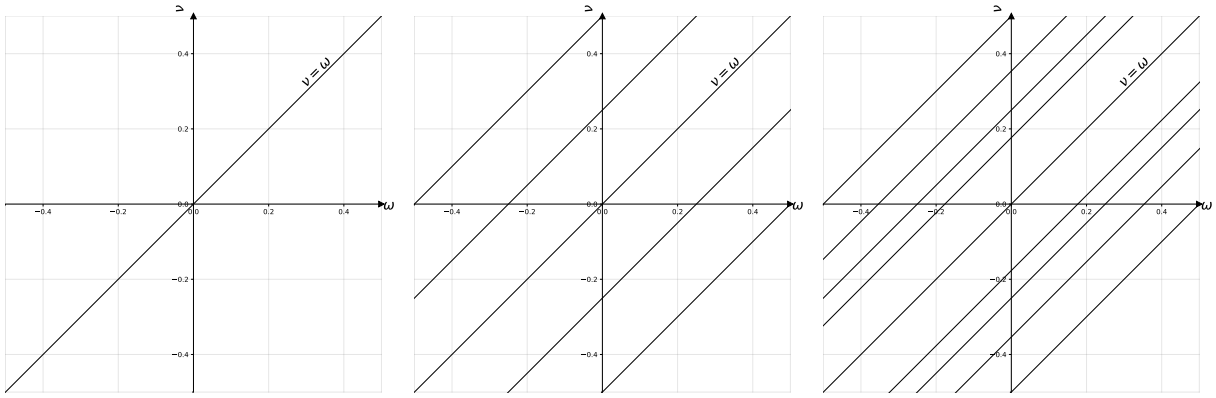

Figure 1.1: Spectral measure supports of the process given by (1.5) in three cases. Left panel: $K = 1$ and $\lambda_1 = 0$ (stationary case). Center panel: $K = 2$, $\lambda_1 = \frac{1}{4}$ and $\lambda_2 = \frac{1}{2}$ (PC case). Right panel: $K = 4$, $\lambda_1 = \frac{1}{2}$, $\lambda_2 = \frac{\sqrt{2}}{4}$, $\lambda_3 = \frac{1}{4}$ and $\lambda_4 = \frac{\sqrt{2}}{8}$ (APC case).

1.3 Harmonizable processes with spectral mass concentrated on lines

In this section, we introduce a class of processes that extend harmonizable APC processes by incorporating a more general spectral dependency structure.

Let $\{X(t),\, t \in \mathbb{R}\}$ and $\{Y(t),\, t \in \mathbb{R}\}$ be two zero-mean complex-valued harmonizable stochastic processes. We consider the case when the support of the spectral measure $F^{XY}(\omega, \nu)$ is contained in

$$\bigcup_{(\alpha,\beta)\in\mathcal{K}^{XY}} \left\{(\omega,\nu) \in \mathbb{R}^2 : \nu = \alpha\omega + \beta\right\},$$

where $\mathcal{K}^{XY} \subset \mathbb{R}^2$ is a countable set. This means that the spectral measure is constituted in the countable union of the lines with possibly non-unit slopes. Lines $\nu = \alpha\omega + \beta$, for $(\alpha, \beta) \in \mathcal{K}^{XY}$, are called a *support lines*. Note that we have

$$\mathrm{d}F^{XY}(\omega,\nu) = \sum_{(\alpha,\beta)\in\mathcal{K}^{XY}} \mathrm{d}F^{XY}_{\alpha,\beta}(\omega)\delta(\nu - (\alpha\omega + \beta)). \tag{1.6}$$

Such processes are the main interest of this thesis. They generalize harmonizable APC processes, as the support lines may have non-unit slopes compared to harmonizable APC processes. In that case, the support lines may even intersect. This makes their analysis more challenging. These processes can be encountered in communication as linear time-variant transformations of APC processes, which are widely recognized as suitable models for almost all modulated signals in this domain. A specific example of such linear time-variant transformations is the multipath Doppler channel, which introduces a different scaling amplitude, time delay, frequency shift, and time scale factor for each path [61, Chapter 4] and [62, Chapter 13].

In the following, we provide the formula for the cross-covariance function of $X(t)$ and $Y(t)$.

Proposition 1.1 ([61])**.** *Assume that*

$$\sum_{(\alpha,\beta)\in\mathcal{K}^{XY}} \int_{\mathbb{R}} |f_{\alpha,\beta}^{XY}(\omega)|\,\mathrm{d}\omega < \infty.$$

Then for $t, \tau \in \mathbb{R}$

$$R_{XY}(t,s) = \sum_{(\alpha,\beta)\in\mathcal{K}^{XY}} \left(\int_{\mathbb{R}} f_{\alpha,\beta}^{XY}(\omega) e^{i2\pi\omega(t-\alpha s)}\,\mathrm{d}\omega \right) e^{-i2\pi\beta s}.$$

Proof. The above property follows directly from (1.1) and (1.6). See [61, Theorem 4.2.9]. □

The formula shown in Proposition 1.1 recalls the Fourier representation (1.3) and relations (1.4) for APC processes (all slopes equal one). However, in the case considered, the "Fourier coefficients" depend on time t and s, not only on the lag parameter $\tau = t - s$. As a result, analyzing the characteristics of these processes in the time domain becomes difficult because of their complex structure. Therefore, spectral analysis provides a more efficient approach for their examination.

Remark 1.3. The processes introduced in this section are special cases of spectrally correlated processes, also known in the literature as simple processes [81, 83]. Spectrally correlated processes processes are characterized by a spectral measure that is supported by a countable union of curves. For further details, see [61, Chapter 4] and [81, 83].

1.4 Examples in acoustics and communications

In this section, we discuss possible applications in acoustics and communications of harmonizable processes with spectral mass concentrated on lines.

Example 1.2. Consider a process given by

$$X(t) = Z(t) + \sum_{k=1}^{K} c_k Z(s_k(t-\tau_k)) \cos(2\pi\lambda_k t), \quad t \in \mathbb{R}, \tag{1.7}$$

where the process $Z(t)$ is stationary, $c_1, \ldots, c_K \in \mathbb{C}$ are complex amplitudes, $0 < \lambda_1 < \ldots < \lambda_K < \infty$ are frequencies, $s_1, \ldots, s_K > 0$ are time-scale factors, $\tau_1, \ldots, \tau_K \in \mathbb{R}$ are time delays, and $K \in \mathbb{N}$. The model (1.7) can be used for acoustic and communication signals of a multi-path character. It contains time delays τ_k and Doppler stretches s_k, which arise due to different propagation speeds along different paths for a single receiver [52].

Let us now study the spectral properties of this model. While these proprieties are studied in [52] only for $K = 1$, we extend them to any $K \in \mathbb{N}$. For simplicity, we take $\tau_k = 0$ for all $k = 1, \ldots, K$. Since $Z(t)$ is stationary, its spectral measure can be expressed as $\mathrm{d}F_{ZZ}(\omega,\nu) = \phi(\omega)\delta(\nu-\omega)\,\mathrm{d}\omega$, where $\phi(\omega)$ is spectral density function of $Z(t)$. Then by (1.1)

$$\mathrm{Cov}(X(t), X(u)) = \sum_{k=0}^{K}\sum_{j=0}^{K} c_k\overline{c_j}\,\cos(2\pi\lambda_k t)\cos(2\pi\lambda_j u) \iint_{\mathbb{R}^2} e^{i2\pi(\xi s_k t - \zeta s_j u)}\,\mathrm{d}F_{ZZ}(\xi,\zeta),$$

wit $c_0 = s_0 = 1$ and $\lambda_0 = 0$. Using Euler formulas we get

$$\cos(2\pi\lambda_k t)\cos(2\pi\lambda_j u) = \frac{1}{4}\left(e^{i2\pi(\lambda_k t+\lambda_j u)} + e^{i2\pi(\lambda_k t-\lambda_j u)} + e^{-i2\pi(\lambda_k t-\lambda_j u)} + e^{-i2\pi(\lambda_k t+\lambda_j u)}\right).$$

By changing variables $\omega = \xi s_k \pm \lambda_k$ and $\nu = \zeta s_j \mp \lambda_j$, we have

$$e^{\pm i2\pi(\lambda_k t+\lambda_j u)} \iint\limits_{\mathbb{R}^2} e^{i2\pi(\xi s_k t-\zeta s_j u)}\,\mathrm{d}F_{ZZ}(\xi,\zeta) = \iint\limits_{\mathbb{R}^2} e^{i2\pi(\omega t-\nu u)}\,\mathrm{d}F_{ZZ}\left(\tfrac{\omega\mp\lambda_k}{s_k}, \tfrac{\nu\pm\lambda_j}{s_j}\right),$$

and by changing variables $\omega = \xi s_k \mp \lambda_k$ and $\nu = \zeta s_j \pm \lambda_j$, we have

$$e^{\pm i2\pi(\lambda_k t-\lambda_j u)} \iint\limits_{\mathbb{R}^2} e^{i2\pi(\xi s_k t-\zeta s_j u)}\,\mathrm{d}F_{ZZ}(\xi,\zeta) = \iint\limits_{\mathbb{R}^2} e^{i2\pi(\omega t-\nu u)}\,\mathrm{d}F_{ZZ}\left(\tfrac{\omega\mp\lambda_k}{s_k}, \tfrac{\nu\mp\lambda_j}{s_j}\right).$$

Consequently,

$$\mathrm{Cov}(X(t), X(u)) = \iint\limits_{\mathbb{R}^2} e^{i2\pi(\omega t-\nu u)}\,\mathrm{d}F_{XX}(\omega,\nu),$$

where

$$\begin{aligned}
\mathrm{d}F_{XX}(\omega,\nu) &= \frac{1}{4}\sum_{k=0}^{K}\sum_{j=0}^{K} c_k\overline{c_j}\Bigg(\mathrm{d}F_{ZZ}\left(\tfrac{\omega-\lambda_k}{s_k}, \tfrac{\nu+\lambda_j}{s_j}\right) + \mathrm{d}F_{ZZ}\left(\tfrac{\omega-\lambda_k}{s_k}, \tfrac{\nu-\lambda_j}{s_j}\right) \\
&\qquad + \mathrm{d}F_{ZZ}\left(\tfrac{\omega+\lambda_k}{s_k}, \tfrac{\nu+\lambda_j}{s_j}\right) + \mathrm{d}F_{ZZ}\left(\tfrac{\omega+\lambda_k}{s_k}, \tfrac{\nu-\lambda_j}{s_j}\right)\Bigg) \\
&= \frac{1}{4}\sum_{k=0}^{K}\sum_{j=0}^{K} \frac{c_k\overline{c_j}}{s_k}\Bigg(\phi\left(\tfrac{\omega-\lambda_k}{s_k}\right)\delta\left(\nu - \left(\tfrac{s_j}{s_k}(\omega-\lambda_k) - \lambda_j\right)\right)\mathrm{d}\omega \\
&\qquad + \phi\left(\tfrac{\omega-\lambda_k}{s_k}\right)\delta\left(\nu - \left(\tfrac{s_j}{s_k}(\omega-\lambda_k) + \lambda_j\right)\right)\mathrm{d}\omega \\
&\qquad + \phi\left(\tfrac{\omega+\lambda_k}{s_k}\right)\delta\left(\nu - \left(\tfrac{s_j}{s_k}(\omega+\lambda_k) - \lambda_j\right)\right)\mathrm{d}\omega \\
&\qquad + \phi\left(\tfrac{\omega+\lambda_k}{s_k}\right)\delta\left(\nu - \left(\tfrac{s_j}{s_k}(\omega+\lambda_k) + \lambda_j\right)\right)\mathrm{d}\omega.
\end{aligned}$$

From the above, we can identify six types of support lines and their corresponding spectral density functions.

- For the main diagonal $\{(\omega,\nu)\in\mathbb{R}^2 : \nu = \omega\}$, the spectral density is given by

$$f_{1,0}(\omega) = \phi(\omega) + \frac{1}{4}\sum_{k=1}^{K}\frac{|c_k|^2}{s_k}\left(\phi\left(\tfrac{\omega-\lambda_k}{s_k}\right) + \phi\left(\tfrac{\omega+\lambda_k}{s_k}\right)\right)$$

- For support lines $\{(\omega,\nu)\in\mathbb{R}^2 : \nu = \omega \pm 2\lambda_k\}$, where $k = 1,\ldots,K$, the spectral density is given by

$$f_{1,\beta}(\omega) = \frac{1}{2}\sum_{k=1}^{K}\frac{|c_k|^2}{s_k}\phi\left(\tfrac{\omega\pm\lambda_k}{s_k}\right),$$

- For support lines $\{(\omega,\nu)\in\mathbb{R}^2 : s_k\omega \pm \lambda_k\}$, where $k = 1,\ldots,K$, the spectral density is given by

$$f_{\alpha,\beta}(\omega) = \frac{1}{2}\sum_{k=1}^{K}\overline{c_k}\phi(\omega),$$

- For support lines $\{(\omega,\nu)\in\mathbb{R}^2 : \nu = \frac{1}{s_k}(\omega \pm \lambda_k)\}$, where $k = 1,\dots,K$, the spectral density is given by
$$f_{\alpha,\beta}(\omega) = \frac{1}{2}\sum_{k=1}^{K}\frac{c_k}{s_k}\phi\left(\tfrac{\omega\pm\lambda_k}{s_k}\right),$$

- For support lines $\{(\omega,\nu)\in\mathbb{R}^2 : \nu = \frac{s_j}{s_k}(\omega\pm\lambda_k)\pm\lambda_j\}$, where $k,j = 1,\dots K$, $k\neq j$, the spectral density is given by
$$f_{\alpha,\beta}(\omega) = \frac{c_k\overline{c_j}}{4s_k}\phi\left(\tfrac{\omega\pm\lambda_k}{s_k}\right)$$

- For support lines $\{(\omega,\nu)\in\mathbb{R}^2 : \nu = \frac{s_j}{s_k}(\omega\pm\lambda_k)\mp\lambda_j\}$, where $k,j = 1,\dots K$, $k\neq j$, the spectral density is given by
$$f_{\alpha,\beta}(\omega) = \frac{c_k\overline{c_j}}{4s_k}\phi\left(\tfrac{\omega\pm\lambda_k}{s_k}\right)$$

To simplify the indexing of spectral densities, the subscripts α and β in $f_{\alpha,\beta}(\omega)$ denote slope and intercept of the support lines, respectively.

Note that the number of support lines is $1+3\cdot 2K+2\cdot 2K(K-1) = 4K^2+2K+1$. For the case of $\tau_k\neq 0$, the formulas for the support lines are the same and spectral density formulas include an additional complex exponential depending on $s_k,\lambda_k,\tau_k,\omega$.

Figure 1.2 shows an example of the spectral measure support of $X(t)$ with $K=1$, $\lambda_1 = \frac{0.25}{\pi}$ and $s_1 = \frac{1}{2}$. Observe that there are 7 support lines in the bifrequency plane $(\omega,\nu)\in\mathbb{R}^2$, specifically
$$\nu = \omega,\quad \nu = s\omega\pm\eta,\quad \nu = \frac{\omega\pm\eta}{s},\quad \nu = \omega\pm 2\eta,$$
These support lines intersect at 12 points.

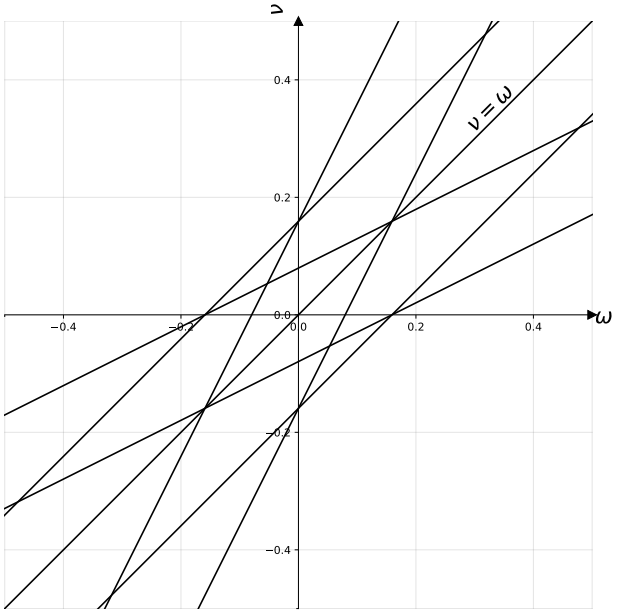

Figure 1.2: Spectral measure support of the process given by (1.7) with $K=1$, $\lambda_1 = \frac{0.25}{\pi}$ and $s_1 = \frac{1}{2}$.

Example 1.3. Consider two processes given by

$$X_j(t) = c_j Z(s_j(t-\tau_j))e^{i2\pi\eta_j t}, \quad j = 1, 2, \tag{1.8}$$

where $Z(t)$ is an APC process, $s_1, s_2 > 0$ are time-scale factors, $\eta_1, \eta_2 \in \mathbb{R}$ are frequency shifts, $\tau_1, \tau_2 \in \mathbb{R}$ are time delays, and $c_1, c_2 \in \mathbb{C}$ are complex amplitudes. A system of processes (1.8) is applicable in the problem of locating a moving source emitting a communication signal, based on measurements from two sensors [63]. Let $Z(t)$ be a signal transmitted by a moving source (e.g., aircraft, rockets, or other hostile jamming emitters) and received by the two sensors (as in Figure 1.3). If the relative radial speeds between the moving source and each receiver remain constant within the observation interval, the received complex envelope signals can be modeled as follows

$$Y_j(t) = X_j(t) + \varepsilon_j(t), \quad j = 1, 2,$$

where $\varepsilon_1(t)$ and $\varepsilon_2(t)$ are additive random noises generated by the same intentional jammer.

In [63], the following statistical properties of such a model have been shown. Assume that $Z(t)$ is harmonizable APC with

$$R_{ZZ}(t, t+\tau) = \sum_{\lambda \in \Lambda_{ZZ}} a_{ZZ}(\lambda, \tau)e^{i2\pi\lambda t},$$

where Λ_{ZZ} is a countable set. Let F^{ZZ} denote the spectral measure of $Z(t)$, and f_λ^{ZZ}, $\lambda \in \Lambda_{ZZ}$, represent the spectral density functions of $Z(t)$. Then the cross-covariance functions of $X_j(t)$ and $X_k(t)$ is given by

$$R_{X_jX_k}(t, t+\tau) = c_j\overline{c_k}e^{-i2\pi\eta_k\tau}e^{i2\pi(\eta_j-\eta_k)t}e^{-i2\pi\lambda s_j\tau_j}\sum_{\lambda \in \Lambda_{ZZ}} a_{ZZ}(\lambda, t(s_k-s_j)+s_j\tau_j+s_k(\tau-\tau_k))e^{i2\pi s_j\lambda t}.$$

Clearly, if $j = k$, we get that processes $X_j(t)$ are APC with cyclic frequencies $\Lambda_{X_jX_j} = \{s_j\lambda : \lambda \in \Lambda_{ZZ}\}$. If $j \neq k$, the function $R_{X_jX_k}(t, t+\tau)$ is almost periodic with respect to t if and only if $s_1 = s_2$. Consequently, $X_1(t)$ and $X_2(t)$ are not JAPC.

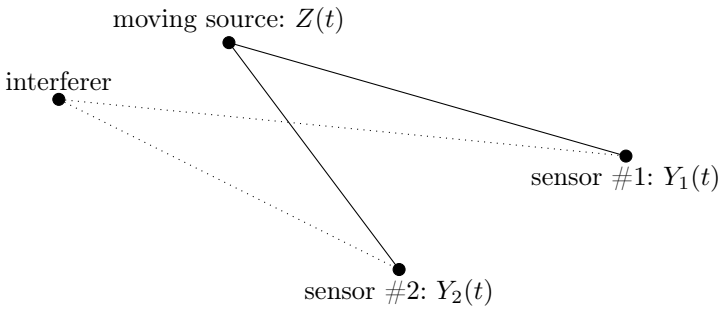

Figure 1.3: A moving source transmits a signal $Z(t)$, which is received by two sensors. The first sensor receives the signal $Y_1(t)$ and the second receives $Y_2(t)$. The interferer can come from intentional jamming.

Let us examine the spectral properties of these processes. Note that by (1.1)

$$\begin{aligned} R_{X_jX_k}(t,u) &= c_j\overline{c_k}\,\mathrm{Cov}(Z(s_j(t-\tau_j),Z(s_k(u-\tau_k))e^{i2\pi\eta_j t}e^{-i2\pi\eta_k u} \\ &= c_j\overline{c_k}\iint\limits_{\mathbb{R}^2} e^{i2\pi(\xi s_j(t-\tau_j)-\zeta s_k(u-\tau_k))}\,\mathrm{d}F_{ZZ}(\xi,\zeta)\,e^{i2\pi\eta_j t}e^{-i2\pi\eta_k u} \\ &= c_j\overline{c_k}\iint\limits_{\mathbb{R}^2} e^{i2\pi(\xi s_j+\eta_j)t}e^{-i2\pi(\zeta s_k+\eta_k)u}e^{-i2\pi s_j\xi\tau_j}e^{i2\pi s_k\zeta\tau_k}\,\mathrm{d}F^{ZZ}(\xi,\zeta). \end{aligned}$$

By changing variables $\omega = \xi s_j + \eta_j$ and $\nu = \zeta s_k + \eta_k$, we obtain

$$\begin{aligned} R_{X_jX_k}(t,u) &= c_j\overline{c_k}\iint\limits_{\mathbb{R}^2} e^{i2\pi\omega t}e^{-i2\pi\nu u}e^{-i2\pi(\omega-\eta_j)\tau_j}e^{i2\pi(\nu-\eta_k)\tau_k}\,\mathrm{d}F^{ZZ}\left(\tfrac{\omega-\eta_j}{s_j},\tfrac{\nu-\eta_k}{s_k}\right) \\ &= \iint\limits_{\mathbb{R}^2} e^{i2\pi(\omega t-\nu u)}\,\mathrm{d}F^{X_jX_k}(\omega,\nu), \end{aligned}$$

where

$$\begin{aligned} \mathrm{d}F^{X_jX_k}(\omega,\nu) &= c_j\overline{c_k}e^{-i2\pi(\omega-\eta_j)\tau_j}e^{i2\pi(\nu-\eta_k)\tau_k}\,\mathrm{d}F^{ZZ}\left(\tfrac{\omega-\eta_j}{s_j},\tfrac{\nu-\eta_k}{s_k}\right) \\ &= \tfrac{c_j\overline{c_k}}{s_j}\sum_{\lambda\in\Lambda_{ZZ}} e^{-i2\pi(\omega-\eta_j)\tau_j}e^{i2\pi(\nu-\eta_k)\tau_k}f_\lambda^{ZZ}\left(\tfrac{\omega-\eta_j}{s_j}\right)\delta\left(\tfrac{\nu-\eta_k}{s_k}-\left(\tfrac{\omega-\eta_j}{s_j}-\lambda\right)\right)\mathrm{d}\omega. \end{aligned}$$

Moreover,

$$\frac{\nu-\eta_k}{s_k}-\left(\frac{\omega-\eta_j}{s_j}-\lambda\right)=0$$

is equivalent to

$$\nu-\left(\tfrac{s_k}{s_j}(\omega-\eta_j)+\eta_k-s_k\lambda\right)=0.$$

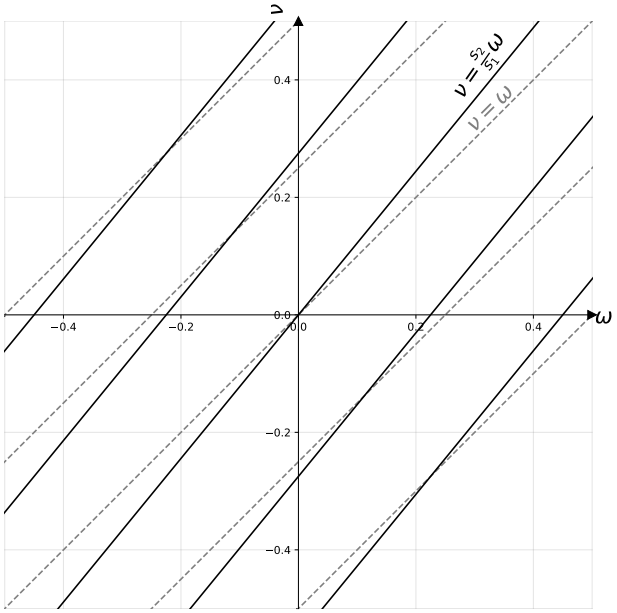

Figure 1.4: A comparison of the support of the cross-spectral measure $F^{X_1X_2}$ with parameters $\eta_1 = \eta_2 = 0$, $s_1 = 1.1$ and $s_2 = 0.9$ (black lines) with the support of spectral measure F^{ZZ} (dashed gray lines).

Therefore, the cross-spectral measure $F^{X_1X_2}$ is concentrated on the union of lines

$$\bigcup_{\lambda\in\Lambda_{ZZ}} \left\{(\omega,\nu)\in\mathbb{R}^2 : \nu = \tfrac{s_k}{s_j}(\omega-\eta_j)+\eta_k - s_k\lambda\right\}.$$

Note that all lines have the same slope $\frac{s_k}{s_j}$. The spectral density functions corresponding to these lines are expressed as

$$\begin{aligned} f^{X_jX_k}_{\alpha,\beta}(\omega) &= \tfrac{c_j\overline{c_k}}{s_j} f^{ZZ}_{\lambda}\left(\tfrac{\omega-\eta_j}{s_j}\right) e^{-i2\pi(\omega-\eta_j)\tau_j} e^{i2\pi\left(\left(\frac{s_k}{s_j}(\omega-\eta_j)+\eta_k-s_k\lambda\right)-\eta_k\right)\tau_k} \\ &= \frac{c_j\overline{c_k}}{s_j} f^{ZZ}_{\lambda}\left(\tfrac{\omega-\eta_j}{s_j}\right) e^{-i2\pi s_k\lambda\tau_k}\, e^{-i2\pi(\omega-\eta_j)\left(\tau_j-\frac{s_k}{s_j}\tau_k\right)}, \end{aligned}$$

with $(\alpha,\beta) = \left(\frac{s_k}{s_j}, -\frac{s_k}{s_j}\eta_j+\eta_k-s_k\lambda\right)$, $\lambda\in\Lambda_{ZZ}$.

In Figure 1.4, examples comparing the supports of the spectral measures F^{ZZ} and $F^{X_1X_2}$ are presented with $\eta_1=\eta_2=0$ and $s_1=1.1$ and $s_2=0.9$. Non-zero ν_j only influences the intercept of all the lines and is therefore omitted.

More motivating examples can be found in [44, p. 904], where a wideband communication scenario is discussed, and in [59, p. 204], who cover ocean acoustic tomography. A related case for seismic applications is presented in [12].

CHAPTER 2

SPECTRAL DENSITY ESTIMATION PROBLEM

In this chapter, we focus on the problem of spectral density estimation for harmonizable processes whose spectral measures are concentrated on a union of lines. In Section 2.1, we propose the frequency-smoothed periodogram along the support lines as an estimator of the spectral density function. In Section 2.2, we demonstrate the mean-square consistency of the normalized frequency-smoothed periodogram in two scenarios: when the support line is known and when it is unknown. Moreover, in Section 2.2.3, we present the estimation procedure of the support line in a specific model, with applications to locate a moving source. In Section 2.3, we provide the asymptotic distribution of the rescaled estimator in the case where the support lines are known. Finally, Section 2.4 includes proofs of the results.

All theorems, propositions, and corollaries in this chapter are original contributions. These results can be found in [29, 30].

2.1 Periodogram frequency-smoothed along the line

Let $X(t)$ and $Y(t)$ be two zero-mean complex-valued harmonizable stochastic processes with cross-spectral measure supported on a countable union of lines (see Section 1.3). Fix $T > 0$, and assume that we observe $X(t)$ and $Y(t)$ in the interval $\left[-\frac{T}{2}, \frac{T}{2}\right]$. The *bifrequency periodogram* of observed processes $X(t)$ and $Y(t)$ is defined as

$$I_T^{XY}(\omega, \nu) = \frac{1}{T}\, D_T^X(\omega)\, \overline{D_T^Y(\nu)}\,, \quad (\omega, \nu) \in \mathbb{R}^2,$$

where

$$D_T^X(\omega) = \int_{-\frac{T}{2}}^{\frac{T}{2}} X(t)\, w\left(\tfrac{t}{T}\right)\, e^{-i2\pi\omega t}\, \mathrm{d}t, \qquad D_T^Y(\omega) = \int_{-\frac{T}{2}}^{\frac{T}{2}} Y(t)\, w\left(\tfrac{t}{T}\right)\, e^{-i2\pi\omega t}\, \mathrm{d}t,$$

are the *short-time Fourier transform* of $X(t)$ and $Y(t)$, respectively. We assume that the function w is even with compact support $\left[-\frac{1}{2}, \frac{1}{2}\right]$. The function $w_T(t) = w\left(\frac{t}{T}\right)$ is referred to as the *data-tapering window*. Data tapering is applied in spectral density estimation to reduce spectral leakage

(the spectral power at a single frequency leaks into all frequencies around), particularly when the spectral density function exhibits high peaks (see, for example, [7]). Some authors consider the complex-valued window w since an appropriate choice of such a window can reduce the bias of the estimator by orders of magnitude [71]. Our consideration can be easily generalized to this case.

For stationary processes, the spectral density estimator is obtained by setting $\nu = \omega$, which corresponds to computing the periodogram along the main diagonal of the bifrequency plane [10, 11]. In the case of harmonizable APC processes, the periodogram is calculated along the line $\nu = \omega - \lambda$ to estimate the spectral density function associated with the cyclic frequency λ [42, 50, 62]. Therefore, in our case, it is natural to compute the periodogram along the support line of interest. This approach is considered in [81, 83]. However, it has been established that the periodogram is not mean-square consistent, even for stationary processes [11, Theorem 10.3.2]. To obtain a mean-square consistent spectral density estimator, smoothing techniques can be applied. We focus on the periodogram frequency-smoothed along the support line. This estimator is studied in [29, 30, 52, 61].

Let $q : \mathbb{R} \to \mathbb{R}$ be an even and continuous function on the interval $\left(-\frac{1}{2}, \frac{1}{2}\right)$ with compact support $\left[-\frac{1}{2}, \frac{1}{2}\right]$. The function $q_{h_T}(\omega) = \frac{1}{h_T} q\left(\frac{\omega}{h_T}\right)$ is referred to as the *frequency-smoothing window* with a *bandwidth* $h_T = \mathcal{O}\left(T^{-\kappa}\right)$, $\kappa \in (0, 1)$. Then the spectral density function corresponding to the line $\left\{(\omega, \nu) \in \mathbb{R}^2 : \nu = \alpha\omega + \beta\right\}$ can be estimated by the *normalized periodogram frequency-smoothed along the line*

$$\widehat{f}^{XY}_{\alpha,\beta}(\omega) = \frac{\widetilde{f}^{XY}_{\alpha,\beta}(\omega)}{\mathcal{E}(\alpha)}, \tag{2.1}$$

where $\widetilde{f}^{XY}_{\alpha,\beta}(\omega)$ is the *periodogram frequency-smoothed along the line*, defined as

$$\widetilde{f}^{XY}_{\alpha,\beta}(\omega) = \int_{\mathbb{R}} I^{XY}_T(\mu, \alpha\mu + \beta)\ \tfrac{1}{h_T} q\left(\tfrac{\omega - \mu}{h_T}\right) \mathrm{d}\mu,$$

and $\mathcal{E}(\alpha)$ is the *normalizing factor*, given by

$$\mathcal{E}(\alpha) = \int_{\mathbb{R}} W(\nu)\, W(-\alpha\nu)\, \mathrm{d}\nu.$$

By W we denote a Fourier transform of w, that is, $W(\nu) = \int_{\mathbb{R}} w(t) e^{-i2\pi\nu t}\, \mathrm{d}t$. Note that W is well defined if $w \in L^1(\mathbb{R})$, particularly when w is a continuous function on the interval $\left(-\frac{1}{2}, \frac{1}{2}\right)$ with compact support $\left[-\frac{1}{2}, \frac{1}{2}\right]$. For more details on Fourier transforms, see [77].

The normalizing factor $\mathcal{E}(\alpha)$ is required to obtain an asymptotically unbiased estimator of the spectral density function along the line with slope α [29, 30, 52, 61]. It depends only on the choice of data-tapering window w and considered slope α. Using the properties of the Fourier transform, we derive the formula for the normalizing factor in terms of w. Furthermore, we demonstrate that the normalizing factor has positive values. In particular, it is non-zero, and hence division by it is possible.

Window	$w(t)$	$W(\nu)$	$\mathcal{E}(\alpha)$
Rectangular	$\begin{cases} 1, & \lvert t\rvert \le \frac{1}{2} \\ 0, & \lvert t\rvert > \frac{1}{2} \end{cases}$	$\operatorname{sinc}(\nu)$	$\begin{cases} 1, & \lvert\alpha\rvert \le 1 \\ \frac{1}{\lvert\alpha\rvert}, & \lvert\alpha\rvert > 1 \end{cases}$
Triangular	$\begin{cases} 1-2\lvert t\rvert, & \lvert t\rvert \le \frac{1}{2} \\ 0, & \lvert t\rvert > \frac{1}{2} \end{cases}$	$\operatorname{sinc}^2(\nu)$	$\begin{cases} \frac{1}{2} - \frac{\lvert\alpha\rvert}{6}, & \lvert\alpha\rvert \le 1 \\ \frac{1}{2\lvert\alpha\rvert} - \frac{1}{6\lvert\alpha\rvert^2}, & \lvert\alpha\rvert > 1 \end{cases}$
Hann	$\begin{cases} \cos^2(\pi t), & \lvert t\rvert \le \frac{1}{2} \\ 0, & \lvert t\rvert > \frac{1}{2} \end{cases}$	$\frac{1}{2}\frac{\operatorname{sinc}(\nu)}{1-\nu^2}$	$1 + \operatorname{sinc}(\alpha) + \frac{1}{2}(\operatorname{sinc}(1-\alpha) + \operatorname{sinc}(1+\alpha))$

Table 2.1: Three examples of window functions $w(t)$, along with their Fourier transforms $W(\nu)$ and normalizing factors $\mathcal{E}(\alpha)$ as a function of α.

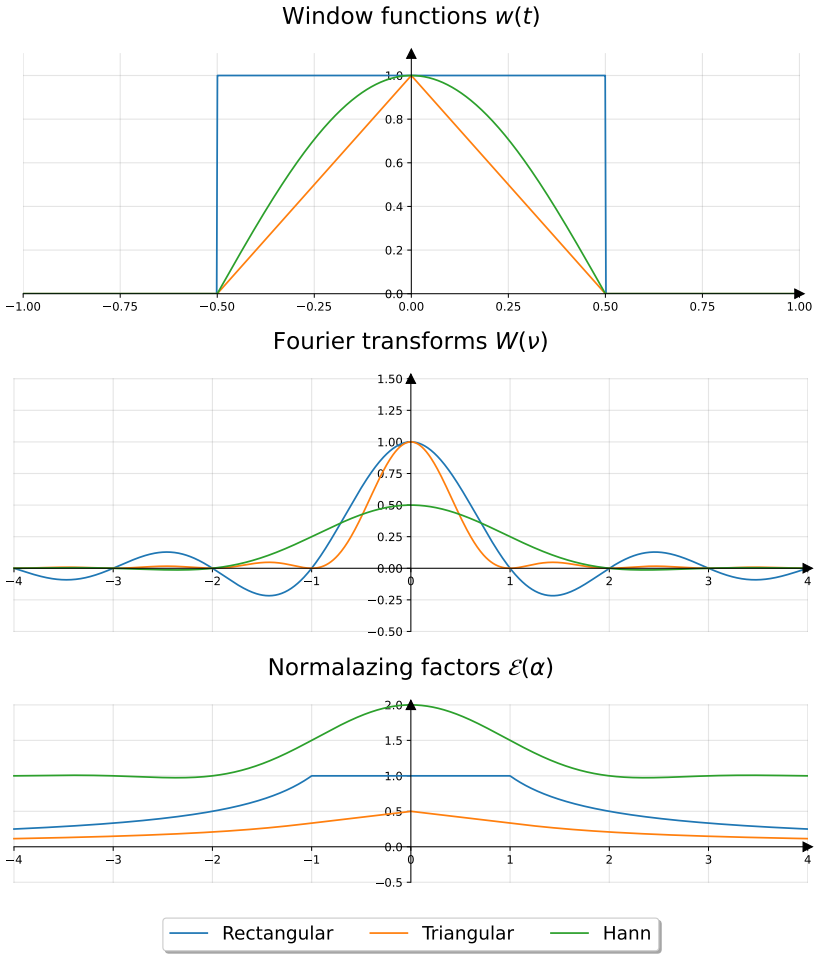

Figure 2.1: Top panel: windows $w(t)$. Middle panel: Fourier transforms $W(\nu)$. Bottom panel: the normalizing factor $\mathcal{E}(\alpha)$ as a function of α. Blue line: rectangular window function. Orange line: triangular window function. Green line: Hann window function.

Proposition 2.1. *Assume that w is a non-negative continuous function on the interval $\left(-\frac{1}{2}, \frac{1}{2}\right)$ with compact support $\left[-\frac{1}{2}, \frac{1}{2}\right]$. Then for all $\alpha \neq 0$*

$$\mathcal{E}(\alpha) = \int_{-\frac{1}{2}\min\left(1, \frac{1}{|a|}\right)}^{\frac{1}{2}\min\left(1, \frac{1}{|a|}\right)} w(t)\, w(\alpha t)\, \mathrm{d}t.$$

Moreover, for all $\alpha \neq 0$

$$0 < |\mathcal{E}(\alpha)| \leq \|w\|_\infty^2 \min\left(1, \tfrac{1}{|a|}\right). \tag{2.2}$$

Proof. This result is a special case of Proposition 3.1 given in Chapter 3. □

The normalizing factors $\mathcal{E}(\alpha)$ corresponding to some commonly used windows w are presented in Table 2.1. Here, $\mathrm{sinc}(\cdot)$ is a *sinc function* i.e. $\mathrm{sinc}(\nu) = \frac{\sin(\pi\nu)}{\pi\nu}$ for $\nu \neq 0$ and $\mathrm{sinc}(0) = 1$. Observe that the normalizing factor reaches the upper bound (2.2) for the rectangular window. Figure 2.1 illustrates window functions given in Table 2.1 with their Fourier transforms and normalizing factors.

In the following sections, we investigate the asymptotic properties of the normalized frequency-smoothed periodogram along the line.

2.2 Mean-square consistency of the spectral density estimator

In this section, we establish the mean-square consistency of the normalized frequency-smoothed periodogram along the line in two cases: when the support line is known and when it is unknown. The results discussed here are based on those presented in [30].

2.2.1 Known support line case

First, we focus on the scenario where the slope and intercept of the support line are known.

Assumption 2.1. Consider the following assumptions.

(i) For any $V_1, V_2 \in \{X, Y, \overline{X}, \overline{Y}\}$, processes $\{V_1(t),\, t \in \mathbb{R}\}$ and $\{V_2(t),\, t \in \mathbb{R}\}$ are zero-mean harmonizable and

$$\mathrm{Cov}\left(V_1(t), V_2(s)\right) = \sum_{(\alpha,\beta)\in\mathcal{K}^{V_1V_2}} \int_{\mathbb{R}} f_{\alpha,\beta}^{V_1V_2}(\omega)\, e^{i2\pi(\omega t - (\alpha\omega+\beta)s)}\, \mathrm{d}\omega,$$

where $\mathcal{K}^{V_1V_2}$ is a finite set in $\mathbb{R}^2$ and $\alpha > 0$, for $(\alpha, \beta) \in \mathcal{K}^{V_1V_2}$. The spectral density functions $f_{\alpha,\beta}^{V_1V_2}(\omega)$ are almost everywhere continuous and belong to $L^1(\mathbb{R}) \cap L^\infty(\mathbb{R})$.

(ii) The function w is even, non-negative, continuous on the interval $\left(-\frac{1}{2}, \frac{1}{2}\right)$, with compact support $\left[-\frac{1}{2}, \frac{1}{2}\right]$. Moreover, its Fourier transform W is continuous, and $W \in L^{\frac{4}{3}}(\mathbb{R}) \cap L^2(\mathbb{R}) \cap L^\infty(\mathbb{R})$.

(iii) The function q is even, non-negative, continuous on the interval $\left(-\frac{1}{2}, \frac{1}{2}\right)$, with compact support $\left[-\frac{1}{2}, \frac{1}{2}\right]$. Moreover, $\int_{\mathbb{R}} q(\omega)\, \mathrm{d}\omega = 1$.

(iv) For any $\boldsymbol{V} = (V_1, V_2, V_3, V_4)$, with $V_j \in \{X, Y, \overline{X}, \overline{Y}\}$, we have

$$\begin{aligned}&\operatorname{cum}\left(V_1(t_1), V_2(t_2), V_3(t_3), V_4(t_4)\right)\\ &\quad= \sum_{k=(\alpha_1,\alpha_2,\alpha_3,\beta)\in\mathcal{K}^{\boldsymbol{V}}} \iiint\limits_{\mathbb{R}^3} f_k^{\boldsymbol{V}}(\eta_1,\eta_2,\eta_3)\, e^{i2\pi\left(\eta_1 t_1+\eta_2 t_2+\eta_3 t_3+\Phi_k^{\boldsymbol{V}}(\eta_1,\eta_2,\eta_3) t_4\right)}\,\mathrm{d}\eta_1\,\mathrm{d}\eta_2\,\mathrm{d}\eta_3,\end{aligned}$$

where a set $\mathcal{K}^{\boldsymbol{V}}$ is a finite in $\mathbb{R}^3$, and $\Phi_k^{\boldsymbol{V}}(\eta_1,\eta_3,\eta_3) = \alpha_1\eta_1 + \alpha_2\eta_2 + \alpha_3\eta_3 + \beta$, with $\alpha_j > 0$, $j = 1,2,3$. The functions $f_k^{\boldsymbol{V}}(\eta_1,\eta_2,\eta_3)$ are almost everywhere continuous and belong to $L^1(\mathbb{R}^3)\cap L^\infty(\mathbb{R}^3)$.

By the condition (i) we impose mild regularity conditions on the spectral density functions. We assume a finite number of lines to ensure the validity of interchanging sums with integrals and limits in the proofs. The assumption (ii) on the data-tapering window is less restrictive than Assumption 4.6.2 in [61], where it is required that $W \in L^1(\mathbb{R})$. Moreover, the commonly used rectangular window function does not meet the assumption considered in [61]. The assumption (iii) is a typical condition for smoothing windows in spectral density estimation problems. This condition is met, for example, by the windows listed in Table 2.1, normalized to have a unit area. By the condition (iv) we establish the regularity of higher-order spectral densities. This assumption is satisfied by various signals, such as those encountered in telecommunications, which are often modifications of harmonizable APC processes with almost periodic fourth-order moments [61, 62]. For the definition of the joint cumulant of complex-valued random variables, see Appendix A.

In the following, we present results on the asymptotic expected value and covariance of the normalized frequency-smoothed periodogram along the line.

Theorem 2.1. *Let conditions (i),(ii) and (iii) in Assumption 2.1 hold. Let $(\alpha,\beta)\in\mathcal{K}^{XY}$ be fixed. Then for every $\omega\in\mathbb{R}$ such that $\alpha\omega+\beta \neq \alpha'\omega+\beta'$, for all $(\alpha',\beta')\in\mathcal{K}^{XY}\setminus\{(\alpha,\beta)\}$, we have*

$$\lim_{T\to\infty}\mathbb{E}\left[\widehat{f}_{\alpha,\beta}^{XY}(\omega)\right] = f_{\alpha,\beta}^{XY}(\omega).$$

Proof. See Section 2.4. □

Remark 2.1. In order to prove Theorem 2.1, the condition $W\in L^{\frac{4}{3}}(\mathbb{R})$ is not required.

Theorem 2.2. *Let Assumption 2.1 holds. Let $(\alpha_1,\beta_1),(\alpha_2,\beta_2)\in\mathcal{K}^{XY}$ be fixed. Then for $\omega_1,\omega_2\in\mathbb{R}$ excluding points of intersection of support lines, we have*

$$\begin{aligned}&\lim_{T\to\infty} Th_T \operatorname{Cov}\left(\widehat{f}_{\alpha_1,\beta_1}^{XY}(\omega_1), \widehat{f}_{\alpha_2,\beta_2}^{XY}(\omega_2)\right)\\ &\quad= \sum_{(\gamma_1,\delta_1)\in\mathcal{K}^{YY}}\sum_{(\gamma_2,\delta_2)\in\mathcal{K}^{\overline{XX}}} f_{\gamma_1,\delta_1}^{YY}(\omega_1)\; f_{\gamma_2,\delta_2}^{\overline{XX}}(-\alpha_1\omega_1-\beta_1)\; \mathcal{Q}(\gamma_1)\,\frac{\mathcal{W}_0(\alpha_2\gamma_1,\gamma_2,\alpha_2)}{\mathcal{E}(\alpha_1)\,\mathcal{E}(\alpha_2)}\\ &\qquad\qquad\times \delta_{\alpha_2\gamma_1-\gamma_2\alpha_1}\,\delta_{\alpha_2\delta_1-\gamma_2\beta_1+\delta_2+\beta_2}\,\delta_{\gamma_1\omega_1+\delta_2-\omega)2},\\ &\quad+ \sum_{(\gamma_1,\delta_1)\in\mathcal{K}^{Y\overline{X}}}\sum_{(\gamma_2,\delta_2)\in\mathcal{K}^{\overline{X}Y}} f_{\gamma_1,\delta_1}^{Y\overline{X}}(\omega_1)\, f_{\gamma_2,\delta_2}^{\overline{X}Y}(-\alpha_1\omega_1-\beta_1)\,\mathcal{Q}(\gamma_1\alpha_1)\,\frac{\mathcal{W}_0(\alpha_2\gamma_2,\alpha_2,\gamma_1)}{\mathcal{E}(\alpha_1)\,\mathcal{E}(\alpha_2)}\\ &\qquad\qquad\times \delta_{\gamma_1-\alpha_2\gamma_2\alpha_1}\,\delta_{\alpha_2\delta_2+\beta_2+\delta_1-\alpha_2\gamma_2\beta_1}\,\delta_{\omega_2+\gamma_2(\alpha_1\omega_1+\beta_1)-\delta_2},\end{aligned}$$

where

$$\mathcal{Q}(a) = \int_{\mathbb{R}} q(\lambda) q(a\lambda)\,\mathrm{d}\lambda,$$

$$\mathcal{W}_0(a_1, a_2, a_3) = \int_{\mathbb{R}}\int_{\mathbb{R}}\int_{\mathbb{R}} W(\eta_1) W(\eta_2) W(\eta_2)\, W(a_1\eta_1 + a_2\eta_2 + a_3\eta_3)\,\mathrm{d}\eta_1\,\mathrm{d}\eta_2\,\mathrm{d}\eta_3.$$

Proof. This result is a special case of Theorem 3.3 given in Chapter 3. □

Based on the above results, we establish the mean-square consistency of the normalized estimator for the spectral density function at points that are not the intersection of the support lines.

Corollary 2.1. *Let Assumption 2.1 holds. Let* $(\alpha, \beta) \in \mathcal{K}^{XY}$ *be fixed. Then for every* $\omega \in \mathbb{R}$ *such that* $\alpha\omega + \beta \neq \alpha'\omega + \beta'$*, for all* $(\alpha', \beta') \in \mathcal{K}^{XY} \setminus \{(\alpha, \beta)\}$*, we have*

$$\lim_{T\to\infty} \mathbb{E}\left|\widehat{f}^{XY}_{\alpha,\beta}(\omega) - f^{XY}_{\alpha,\beta}(\omega)\right|^2 = 0.$$

Proof. The proof follows immediately from Theorems 2.1 and 2.2. □

Mean-square consistency can also be achieved under alternative assumptions.

Remark 2.2. The theses of Theorem 2.2 and Corollary 2.1 hold if condition (iv) in Assumption 2.1 is substituted with any of the following:

(iv)′ For any $k \in \mathbb{N}$ and $l \in \mathbb{N}$, and for any time instants $t_1, \ldots, t_k, s_1, \ldots, s_l \in \mathbb{R}$, the vector $[X(t_1), \ldots, X(t_k), Y(s_1), \ldots, Y(s_l)]^{\mathrm{T}}$ has a multivariate normal distribution.

(iv)″ There exists a positive constant $K_4 > 0$ such that for all $T > 0$

$$\sup_{t\in\left[-\frac{T}{2},\frac{T}{2}\right]} \int_{-\frac{T}{2}}^{\frac{T}{2}}\int_{-\frac{T}{2}}^{\frac{T}{2}}\int_{-\frac{T}{2}}^{\frac{T}{2}} \left|\mathrm{cum}\left(Y(t), \overline{X(s)}, \overline{Y(u)}, X(v)\right)\right| \mathrm{d}s\,\mathrm{d}u\,\mathrm{d}v \leq K_4.$$

From (iv)′, it follows that all cumulants of order higher than two are zero, simplifying the proof of Theorem 2.2. Assumption (iv)″ facilitates the proof of Theorem 2.2 compared to the proof conducted under condition (iv) or (iv)′. Since our results can be applicable to communication (see Section 1.4), it should be noted that the cumulants of communication signals can often be calculated analytically, and their summability can be proven, not just assumed [61, 62].

2.2.2 Unknown support line case

In the previous subsection, we assumed that the slope α and intercept β of the support line are known. However, this scenario has limited practical applicability in many real-world data applications (see, for example, [63]). Therefore, in this subsection, we consider the estimation of the spectral density corresponding to unknown support lines, assuming that the estimation of the support lines is feasible. Our approach consists of replacing the unknown slope α and the intercept β with their estimators. By $\widehat{\alpha}_T$ and $\widehat{\beta}_T$ we denote the estimators of α and β, respectively. Then we propose the

periodogram frequency-smoothed along the estimated support line $\nu = \widehat{\alpha}_T\omega + \widehat{\beta}_T$ as an estimator for $f^{XY}_{\alpha,\beta}(\omega)$. That is,

$$\widehat{f}^{XY}_{\widehat{\alpha}_T,\widehat{\beta}_T}(\omega) = \frac{1}{\mathcal{E}\left(\widehat{\alpha}_T\right)} \int\limits_{\mathbb{R}} I^{XY}_T\left(\mu, \widehat{\alpha}_T\mu + \widehat{\beta}_T\right) \tfrac{1}{h_T} q\left(\tfrac{\omega-\mu}{h_T}\right) \mathrm{d}\mu.$$

To obtain mean-square consistent of the above estimator we consider Assumption 2.1 with the following additional assumptions.

Assumption 2.2. Consider the following assumptions.

(i) The function w is a rectangular function (see Table 2.1).

(ii) Both processes $\{X(t), t \in \mathbb{R}\}$ and $\{Y(t), t \in \mathbb{R}\}$ are uniformly bounded, i.e., there exist positive constants $M_X, M_Y > 0$ such that $|X(t)| \leq M_X$ and $|Y(t)| \leq M_Y$ a.s. for all $t \in \mathbb{R}$.

(iii) Condition (iii) in Assumption 2.1 holds. The inverse Fourier transform $Q(t) = \int_{\mathbb{R}} q(\nu) e^{i2\pi\nu t}\,\mathrm{d}\nu$ of the window function q belongs to $L^1(\mathbb{R})$ and its derivative Q' exists and $Q' \in L^1(\mathbb{R})$.

(iv) The estimators satisfy $\lim\limits_{T\to\infty} T^r\,\mathbb{E}\left|\widehat{\alpha}_T - \alpha\right|^2 = 0$ and $\lim\limits_{T\to\infty} T^r\,\mathbb{E}\left|\widehat{\beta}_T - \beta\right|^2 = 0$, with some $r > 0$. Moreover, $\lim\limits_{T\to\infty} \widehat{\alpha}_T = \alpha$ a.s.

The assumption (i) facilitates the proof. The relaxation of this assumption is addressed in Remark 2.3. The assumption (ii) is generally satisfied by most signals used in applications such as communications, radar, sonar, and telemetry, as discussed in [62, Chapter 7]. In addition, measurements in fields such as acoustics, mechanics, econometrics, biology, and hydrology are typically uniformly bounded, as discussed in [62, Chapter 10]. The assumption (iii) holds for various windows, including the triangular window. An example illustrating where condition (iv) is satisfied is provided in Section 2.2.3.

In the following, we demonstrate the mean-square consistency of the normalized frequency-smoothed periodogram along the estimated support line.

Theorem 2.3. *Let Assumption 2.1 and Assumption 2.2 hold. Let $(\alpha, \beta) \in \mathcal{K}^{XY}$ be fixed. Then for every $\omega \in \mathbb{R}$ such that $\alpha\omega + \beta \neq \alpha'\omega + \beta'$, for all $(\alpha', \beta') \in \mathcal{K}^{XY} \setminus \{(\alpha, \beta)\}$, we have*

$$\lim_{T\to\infty} \mathbb{E}\left|\widehat{f}^{XY}_{\widehat{\alpha}_T,\widehat{\beta}_T}(\omega) - f^{XY}_{\alpha,\beta}(\omega)\right|^2 = 0,$$

with $h_T = \mathcal{O}(T^{-\kappa})$, $\kappa \in \left(0, \frac{r-2}{2}\right]$ and $r > 2$.

Proof. See Section 2.4. □

Remark 2.3. The proof of Theorem 2.3 presented in Section 2.4 is performed for the most general case of a window w satisfying the condition (ii) of Assumption 2.1. The rectangular window w is considered only where the convergence in the second moment of $\frac{1}{\mathcal{E}(\alpha)} - \frac{1}{\mathcal{E}(\widehat{\alpha}_T)}$ to zero is proven. To obtain this convergence, instead of the rectangular data-tapering window w (condition (i) in Assumption 2.2), one can impose the following assumptions on w, specifically on the corresponding

normalizing factor $\mathcal{E}(\alpha)$. Assume that there exists a positive constant $c > 0$ such that $\mathcal{E}(\alpha) > c$ for all $\alpha \in \mathbb{R}$, and $\mathcal{E}(\alpha)$ is a Lipschitz function with constant $L > 0$. These assumptions hold, for instance, for the Hann window. Then

$$\mathbb{E}\left|\frac{1}{\mathcal{E}(\alpha)} - \frac{1}{\mathcal{E}(\widehat{\alpha}_T)}\right|^2 = \mathbb{E}\left|\frac{\mathcal{E}(\widehat{\alpha}_T) - \mathcal{E}(\alpha)}{\mathcal{E}(\alpha)\,\mathcal{E}(\widehat{\alpha}_T)}\right|^2 < c^{-4}\,\mathbb{E}\,|\mathcal{E}(\widehat{\alpha}_T) - \mathcal{E}(\alpha)|^2 \le Lc^{-4}\,\mathbb{E}\,|\widehat{\alpha}_T - \alpha|^2\,.$$

In this case, we do not have to assume that the estimator $\widehat{\alpha}_T$ converges almost surely to α.

The natural question arises whether there exist support line estimators that satisfy condition (iv) in Assumption 2.2. The following subsection presents a method for estimating support lines in some specific model.

2.2.3 Example of support lines estimation in specific model

In this subsection, we provide an estimation procedure for the support line parameters in the model presented in Example 1.3. Namely, we observe two processes

$$X_j(t) = c_j Z(s_j(t - \tau_j))e^{i2\pi\eta_j t}, \quad j = 1, 2,$$

for $t \in [-\frac{T}{2}, \frac{T}{2}]$. We assume that a process $\{Z(t), t \in \mathbb{R}\}$ is an unobserved harmonizable APC process with the following autocovariance and conjugate autocovariance functions

$$R_{ZZ}(t, t+\tau) = \sum_{\lambda\in\Lambda} a_{ZZ}(\lambda, \tau)e^{i2\pi\lambda t}, \quad R_{Z\overline{Z}}(t, t+\tau) = \sum_{\gamma\in\Gamma} a_{Z\overline{Z}}(\gamma, \tau)e^{i2\pi\gamma t},$$

where Λ and Γ are a known countable set. The parameters $c_1, c_2, s_1, s_2, \tau_1, \tau_2, \eta_1, \eta_2$ are unknown.

As stated in Example 1.3, the autocovariance function of $X_j(t)$ can be written in terms of Fourier representation. That is,

$$R_{X_jX_j}(t, t+\tau) = \sum_{\lambda_j\in\Lambda_j} a_{X_jX_j}(\lambda_j, \tau)e^{i2\pi\lambda_j t},$$

where $\Lambda_j = \{s_j\lambda : \lambda \in \Lambda\}$. Similarly, one can show that

$$R_{X_j\overline{X_j}}(t, t+\tau) = \sum_{\gamma_j\in\Gamma_j} a_{X_j\overline{X_j}}(\gamma_j, \tau)e^{i2\pi\gamma_j t},$$

where $\Gamma_j = \{s_j\gamma + 2\eta_j : \gamma \in \Gamma\}$. In Example 1.3, we also show that spectral measure $F^{X_1X_2}$ is concentrated on the union of lines

$$\bigcup_{\lambda\in\Lambda}\left\{(\omega, \nu) \in \mathbb{R}^2 : \nu = \frac{s_k}{s_j}(\omega - \eta_j) + \eta_k - s_k\lambda\right\}.$$

Note that $s_j = \frac{\lambda_j}{\lambda}$ and $\eta_j = \frac{1}{2}(\gamma_j - s_j\gamma)$. By $\lambda_j = s_j\lambda$ and $\gamma_j = s_j\gamma + 2\eta_j$ we denote the frequencies corresponding to specific cyclic frequencies $\lambda \in \Lambda$ and $\gamma \in \Gamma$, respectively. Then slope α and intercept β of support lines can we written as follows

$$\alpha = \frac{s_k}{s_j} = \frac{\lambda_k}{\lambda_j}, \quad \beta = -\frac{s_k}{s_j}\eta_j + \eta_k - s_k\lambda = \frac{1}{2}\left(\gamma_k - \frac{\lambda_k}{\lambda_j}\gamma_j\right) - \lambda_k.$$

Since processes $X_1(t)$ and $X_2(t)$ are observed, one can estimate their cyclic frequencies λ_j and γ_j, allowing for the estimation of support line parameters. By $\widehat{\lambda}_j$ and $\widehat{\gamma}_j$ we denote estimators of λ and γ, respectively. Then $\widehat{s}_j = \frac{\widehat{\lambda}_j}{\lambda}$ and $\widehat{\nu}_j = \frac{1}{2}(\widehat{\gamma}_j - \widehat{s}_j\gamma)$ and the estimators of α and β can be obtained by the following formulas

$$\widehat{\alpha}_T = \frac{\widehat{\lambda}_k}{\widehat{\lambda}_j}, \quad \widehat{\beta}_T = \frac{1}{2}\left(\widehat{\gamma}_k - \frac{\widehat{\lambda}_k}{\widehat{\lambda}_j}\widehat{\gamma}_j\right) - \widehat{\lambda}_k. \tag{2.3}$$

In the following, we establish the asymptotic properties of $\widehat{\alpha}_T$ and $\widehat{\beta}_T$.

Proposition 2.2. *Let $\widehat{\lambda}_j$ and $\widehat{\gamma}_j$ be estimators of $\lambda_j \neq 0$ and γ_j, respectively, for $j = 1, 2$. Assume that there exist positive constants m_j, M_j such that $0 < m_j \leq \widehat{\lambda}_j \leq M_j$ a.s., and*

$$\lim_{T\to\infty} T^r\,\mathbb{E}\left|\widehat{\lambda}_j - \lambda_j\right|^2 = \lim_{T\to\infty} T^r\,\mathbb{E}\left|\widehat{\gamma}_j - \gamma_j\right|^2 = 0,$$

with some $r > 0$, and $\lim_{T\to\infty} \widehat{\lambda}_j = \lambda_j$ a.s. Then the estimators of α and β given by (2.3) satisfy the condition (iv) of Assumption 2.2.

Proof. See Section 2.4. □

Now, we briefly present the cycle frequency estimation proposed in [13, 14]. Let $\lambda^* \in \Lambda$ be the known frequency that corresponds to the strongest cyclic characteristic of $Z(t)$. For most communication signals, λ^* is the smallest non-negative cycle frequency. Assume that there exists a known compact interval denoted by $C(\lambda^*, \delta_{\lambda^*})$ that contains λ^* with width δ_{λ^*} such that it contains only one cycle frequency of $X_j(t)$ denoted by $\lambda_j^* = s_j\lambda^* \in \Lambda_j$. In the problem of locating a moving source, it can be shown that the width δ_{λ^*} is proportional to the maximum magnitude of the relative radial speeds [63]. Then the estimator of λ_j^* has the form

$$\widehat{\lambda}_j^* = \operatorname*{argmax}_{\mu\in C(\lambda^*,\delta\lambda^*)} \int_{\mathcal{T}_j} \left|\widehat{a}_{X_jX_j}(\mu,\tau)\right|^2 \mathrm{d}\tau, \tag{2.4}$$

where the set $\mathcal{T}_j$ is such that $a_{X_jX_j}(\lambda_j^*, \tau) \neq 0$ for $\tau \in \mathcal{T}_j$. By $\widehat{a}_{X_jX_j}(\mu,\tau)$ we denote an estimator of $a_{X_jX_j}(\mu,\tau)$ obtained by

$$\widehat{a}_{X_jX_j}(\mu,\tau) = \frac{1}{T}\int_{-\frac{T}{2}}^{\frac{T}{2}} X_j(t+\tau)\,\overline{X_j(t)}\,\mathbb{1}_{\left[-\frac{T}{2},\frac{T}{2}\right]}(t+\tau)\,e^{-i2\pi\mu t}\,\mathrm{d}t.$$

The estimator of γ_j is defined analogously starting from $\widehat{a}_{X_j\overline{X_j}}(\mu,\tau)$. Another method of estimating cycle frequency is presented in [19].

Note that the estimator $\widehat{\lambda}_j$ is bounded, since we are looking for the cycle frequency λ_j within a certain compact interval. Moreover, in [13, 14] it is shown that under the assumption of summability of cumulants of the process, the estimator $\widehat{\lambda}_j$ of the cycle frequency λ_j satisfies $\lim_{T\to\infty} T^3\mathbb{E}\left|\widehat{\lambda}_j - \lambda_j\right|^2 = \sigma^2_{\lambda_j}$ and $\lim_{T\to\infty} T\left|\widehat{\lambda}_j - \lambda_j\right| = 0$ a.s. These assumptions hold and are verified, for example, for communication signals. Consequently, the estimator (2.4) satisfies the assumptions of Proposition 2.2 with all $r \leq 3$.

The above estimation procedure of α and β has been discussed in [63], but without any theoretical results.

2.3 Asymptotic distribution of the rescaled spectral estimators

The next asymptotic property of the normalized periodogram frequency-smoothed along the line that we present is its asymptotic normality. Moreover, we establish the asymptotic distribution of the rescaled spectral coherence estimator. In this section, we concentrate on the scenario in which the support lines are known. The results discussed here are based on those presented in [29]. To be consistent with the previous section, we assume that the observation interval of $X(t)$ and $Y(t)$ is $\left[-\frac{T}{2}, \frac{T}{2}\right]$. However, in [29], we address a more general form of the observation interval. The general case, essential for the subsampling procedure, is explored in Chapter 3. Therefore, all proofs of the theorems outlined in this section can be found in Chapter 3.

2.3.1 Asymptotic distribution of the rescaled spectral density estimator

To obtain an asymptotic normality of the normalized periodogram frequency-smoothed along the line, we consider Assumption 2.1 and the following additional conditions.

Assumption 2.3. Consider the following assumptions.

(i) There exists a positive constant $K_W > 0$ such that $\sup_{x\in\mathbb{R}} |xW(x)| = K_W$.

(ii) For all $(\alpha, \beta) \in \mathcal{K}^{XY}$, there exists a first derivative $f^{XY\prime}_{\alpha,\beta}$ that belongs to $L^2(\mathbb{R}) \cap L^\infty(\mathbb{R})$.

(iii) For any $r \in \mathbb{N}$ and for any $\boldsymbol{V} = (V_1, \ldots, V_r)$, with $V_1, \ldots, V_r \in \{X, Y, \overline{X}, \overline{Y}\}$, we have

$$\operatorname{cum}(V_1(t_1), \ldots, V_r(t_r)) = \sum_{k=(\alpha_1,\ldots,\alpha_{r-1},\beta)\in\mathcal{K}^{\boldsymbol{V}}} \int_{\mathbb{R}^{r-1}} \cdots \int f_k^{\boldsymbol{V}}(\eta_1, \ldots \eta_{r-1}) \times e^{i2\pi\left(\eta_1 t_1 + \ldots + \eta_{r-1} t_{r-1} + \Phi_k^{\boldsymbol{V}}(\eta_1,\ldots\eta_{r-1}) t_r\right)} \, \mathrm{d}\eta_1 \ldots \mathrm{d}\eta_{r-1},$$

where a set $\mathcal{K}^{\boldsymbol{V}}$ is a finite in $\mathbb{R}^r$, and $\Phi_k^{\boldsymbol{V}}(\eta_1, \ldots \eta_{r-1}) = \sum_{j=1}^{r-1} \alpha_j \eta_j + \beta$, with $\alpha_j > 0$, $j = 1, 2 \ldots, r-1$. The functions $f_k^{\boldsymbol{V}}(\eta_1, \ldots \eta_{r-1})$ are almost everywhere continuous and belong to $L^1(\mathbb{R}^{r-1}) \cap L^\infty(\mathbb{R}^{r-1})$.

The assumption (i) is significantly less restrictive compared to the condition stated in Theorem 4.7.11 in [61], where it is assumed that the function $\mathbb{R} \ni x \mapsto x^2 W(x) \in \mathbb{R}$ belongs to $L^1(\mathbb{R})$. This condition is not satisfied for many popular window functions, including those listed in Table 2.1. In contrast, our assumption is weaker and is satisfied by the windows listed in Table 2.1 and many others. By the assumption (ii) we impose some regularity of the spectral density functions. This condition is required to obtain the convergence rate of the bias of $\widehat{f}^{XY}_{\alpha,\beta}(\omega)$. The assumption (iii) refers to some regularity of higher-order spectral densities (see Section 4.2.3 in [61]). It is satisfied by many signals, e.g. in telecommunications, which are modifications of APC processes.

First, we present some asymptotic properties of the estimator $\widehat{f}^{XY}_{\alpha,\beta}(\omega)$. Specifically, we derive the convergence rate of the bias of this estimator and show that its joint cumulants of higher order than two are asymptotically zero.

Theorem 2.4. *Let Assumption 2.1, and the conditions (i) and (ii) in Assumption 2.3 hold. Let* $(\alpha,\beta)\in\mathcal{K}^{XY}$ *be fixed. Then for every* $\omega\in\mathbb{R}$ *such that* $\alpha\omega+\beta\neq\alpha'\omega+\beta'$*, for all* $(\alpha',\beta')\in\mathcal{K}^{XY}\setminus\{(\alpha,\beta)\}$*, we have*

$$\lim_{T\to\infty}\sqrt{Th_T}\,\mathbb{E}\left(\widehat{f}^{XY}_{\alpha,\beta}(\omega)-f^{XY}_{\alpha,\beta}(\omega)\right)=0,$$

provided that $h_T=\mathcal{O}(T^{-\kappa})$*,* $\kappa\in\left(\frac{1}{3},1\right)$*.*

Proof. This result is a special case of Theorem 3.2 given in Chapter 3. □

Theorem 2.5. *Fix* $P>2$*. Let Assumption 2.1, and (i) and (iii) in Assumption 2.3 hold. Let* $(\alpha_1,\beta_1),\ldots,(\alpha_P,\beta_P)\in\mathcal{K}^{XY}$ *be fixed. Then for* $\omega_1,\ldots,\omega_P\in\mathbb{R}$*, excluding points of intersection of support lines, we have*

$$\lim_{T\to\infty}(Th_T)^{P/2}\operatorname{cum}\left(\widehat{f}^{XY}_{\alpha_1,\beta_1}(\omega_1)^{[*]},\ldots,\widehat{f}^{XY}_{\alpha_P,\beta_P}(\omega_P)^{[*]}\right)=0.$$

By $z^{[*]}$ *we denote an optional complex conjugate of* $z\in\mathbb{C}$*, i.e.,* $z^{[*]}\in\{z,\overline{z}\}$*.*

Proof. This result is a special case of Theorem 3.4 given in Chapter 3. □

Remark 2.4. To prove Theorem 2.5, in (iii) in Assumption 2.3, we can restrict to $r\in[2,2P]\cap\mathbb{N}$. Namely, to demonstrate the convergence of the P-th order cumulants of the spectral density estimator to zero, it is sufficient to assume only regularity of the higher-order spectral densities up to order $2P$.

Below we present the asymptotic normality of the normalized periodogram frequency-smoothed along the support line. For this purpose, we treat the complex number $z\in\mathbb{C}$, as a two-dimensional vector $[\operatorname{Re}(z),\operatorname{Im}(z)]^{\mathrm{T}}\in\mathbb{R}^2$.

Theorem 2.6. *Let Assumption 2.1 and Assumption 2.3 hold. Let* $(\alpha,\beta)\in\mathcal{K}^{XY}$ *be fixed. Then for every* $\omega\in\mathbb{R}$ *such that* $\alpha\omega+\beta\neq\alpha'\omega+\beta'$*, for all* $(\alpha',\beta')\in\mathcal{K}^{XY}\setminus\{(\alpha,\beta)\}$*, we have*

$$\sqrt{Th_T}\,\left(\widehat{f}^{XY}_{\alpha,\beta}(\omega)-f^{XY}_{\alpha,\beta}(\omega)\right)\xrightarrow{d}\mathcal{N}_2(\mathbf{0},\mathbf{\Sigma}(\omega;\alpha,\beta)),$$

provided that $h_T=\mathcal{O}(T^{-\kappa})$*,* $\kappa\in\left(\frac{1}{3},1\right)$*. The covariance matrix* $\mathbf{\Sigma}(\omega;\alpha,\beta)$ *is given by*

$$\mathbf{\Sigma}(\omega;\alpha,\beta)=\frac{1}{2}\begin{bmatrix}\operatorname{Re}(\sigma^2)+\operatorname{Re}(\sigma_c^2) & \operatorname{Im}(\sigma^2)-\operatorname{Im}(\sigma_c^2)\\ \operatorname{Im}(\sigma^2)-\operatorname{Im}(\sigma_c^2) & \operatorname{Re}(\sigma_c^2)-\operatorname{Re}(\sigma^2)\end{bmatrix},\tag{2.5}$$

where

$$\sigma^2=\sigma^2(\omega;\alpha,\beta)=\lim_{T\to\infty}Th_T\operatorname{Var}\left(\widehat{f}^{XY}_{\alpha,\beta}(\omega)\right),$$
$$\sigma_c^2=\sigma_c^2(\omega;\alpha,\beta)=\lim_{T\to\infty}Th_T\operatorname{Cov}\left(\widehat{f}^{XY}_{\alpha,\beta}(\omega),\overline{\widehat{f}^{XY}_{\alpha,\beta}(\omega)}\right).$$

Proof. This result is a special case of Theorem 3.5 given in Chapter 3. □

Using the continuous mapping theorem and the delta method, we can derive the asymptotic distribution of the rescaled magnitude of the spectral density estimator.

Corollary 2.2. *Let Assumption 2.1 and Assumption 2.3 hold. Let* $(\alpha,\beta)\in\mathcal{K}^{XY}$ *be fixed. Let* $\omega\in\mathbb{R}$ *such that* $\alpha\omega+\beta\neq\alpha'\omega+\beta'$*, for all* $(\alpha',\beta')\in\mathcal{K}^{XY}\setminus\{(\alpha,\beta)\}$*. Assume that* $\det(\mathbf{\Sigma}(\omega;\alpha,\beta))>0$*, where* $\mathbf{\Sigma}(\omega;\alpha,\beta)$ *is given by* (2.5)*. Then*

$$\sqrt{Th_T}\left(\left|\widehat{f}^{XY}_{\alpha,\beta}(\omega)\right|-\left|f^{XY}_{\alpha,\beta}(\omega)\right|\right)\xrightarrow{d}J^{|f^{XY}_{\alpha,\beta}(\omega)|},$$

where

$$J^{|f^{XY}_{\alpha,\beta}(\omega)|}=\begin{cases}\mathcal{L}\left(\sqrt{U_1^2+U_2^2}\right), & \text{if } f^{XY}_{\alpha,\beta}(\omega)=0,\\ \mathcal{N}_1(\mathbf{0},\boldsymbol{A}_1\mathbf{\Sigma}(\omega;\alpha,\beta)\boldsymbol{A}_1^{\mathrm{T}}), & \text{if } f^{XY}_{\alpha,\beta}(\omega)\neq 0,\end{cases}$$

and the random vector $[U_1,U_2]^{\mathrm{T}}$ *has a two-dimensional normal distribution* $\mathcal{N}_2(\mathbf{0},\mathbf{\Sigma}(\omega;\alpha,\beta))$*, and the vector* $\boldsymbol{A}_1\in\mathbb{R}^{1\times 2}$ *has the form*

$$\boldsymbol{A}_1=\frac{1}{|f^{XY}_{\alpha,\beta}(\omega)|}[\mathrm{Re}\left(f^{XY}_{\alpha,\beta}(\omega)\right),\mathrm{Im}\left(f^{XY}_{\alpha,\beta}(\omega)\right)].$$

Proof. This result is a special case of Corollary 3.1 given in Chapter 3. □

In the next subsection, we introduce the concept of spectral coherence and define its estimator. Then, using Theorem 2.6, we determine the asymptotic distribution of the rescaled estimator of the spectral coherence.

2.3.2 Asymptotic distribution of the rescaled spectral coherence estimator

As noted in Chapter 1, the spectral measure, and consequently the spectral density, correspond to the covariance in the frequency domain. In this subsection, we introduce the spectral coherence that can be treated as the spectral counterpart of the correlation [67]. Building on the concept of spectral coherence for cyclic frequencies λ in the context of harmonizable APC processes (see e.g. [62, eq. (8.116)]), we define the spectral coherence function along the support line $\left\{(\omega,\nu)\in\mathbb{R}^2:\nu=\alpha\omega+\beta\right\}$ as follows

$$\gamma^{XY}_{\alpha,\beta}(\omega)=\frac{f^{XY}_{\alpha,\beta}(\omega)}{\sqrt{f^{XX}_{1,0}(\omega)f^{YY}_{1,0}(\alpha\omega+\beta)}},\quad\omega\in\mathbb{R}.$$

Note that $\gamma^{XX}_{1,0}(\omega)=1$ for all $\omega\in\mathbb{R}$.

Based on the spectral density estimator (2.1), we propose the estimator of the spectral coherence function. Namely, for fixed $\omega\in\mathbb{R}$, the spectral coherence $\gamma^{XY}_{\alpha,\beta}(\omega)$ can be estimated by

$$\widehat{\gamma}^{XY}_{\alpha,\beta}(\omega)=\frac{\widehat{f}^{XY}_{\alpha,\beta}(\omega)}{\sqrt{\widehat{f}^{XX}_{1,0}(\omega)\widehat{f}^{YY}_{1,0}(\alpha\omega+\beta)}}.\tag{2.6}$$

In the following, we can establish the asymptotic distribution of the rescaled estimator $\widehat{\gamma}^{XY}_{\alpha,\beta}(\omega)$.

Theorem 2.7. *Let Assumption 2.1 and Assumption 2.3 hold. Let* $(\alpha,\beta)\in\mathcal{K}^{XY}$ *be fixed. Let* $\omega\in\mathbb{R}$ *be a point that does not lie at the intersection of the support lines of the spectral measures* F^{XY}*,* F^{XX} *and* F^{YY}*. Assume* $\det(\mathbf{\Lambda}(\omega,\alpha\omega+\beta))>0$*, where* $\mathbf{\Lambda}(\omega,\alpha\omega+\beta)=\boldsymbol{D}_0(\omega,\alpha\omega+\beta;\alpha,\beta)$ *is an*

asymptotic covariance matrix from Lemma 3.1. Moreover, there exist first derivatives $f_{1,0}^{XX\prime}$, $f_{1,0}^{YY\prime}$ *that belong to* $L^2(\mathbb{R}) \cap L^\infty(\mathbb{R})$. *Then*

$$\sqrt{Th_T}\left(\left|\widehat{\gamma}_{\alpha,\beta}^{XY}(\omega)\right| - \left|\gamma_{\alpha,\beta}^{XY}(\omega)\right|\right) \xrightarrow{d} J^{|\gamma_{\alpha,\beta}^{XY}(\omega)|},$$

where

$$J^{|\gamma_{\alpha,\beta}^{XY}(\lambda)|} = \begin{cases} \mathcal{L}\left(\frac{\sqrt{U_1^2+U_2^2}}{\sqrt{f_{1,0}^{XX}(\omega) f_{1,0}^{YY}(\alpha\omega+\beta)}}\right), & \text{if } f_{\alpha,\beta}^{XY}(\omega) = 0, \\ \mathcal{N}_1(\mathbf{0}, \boldsymbol{A}_2 \boldsymbol{\Lambda}(\omega, \alpha\omega+\beta)\boldsymbol{A}_2^{\mathrm{T}}), & \text{if } f_{\alpha,\beta}^{XY}(\omega) \neq 0, \end{cases}$$

the random vector $[U_1, U_2]^{\mathrm{T}}$ *has a two-dimensional normal distribution* $\mathcal{N}_2(\mathbf{0}, \boldsymbol{\Lambda}(\omega, \alpha\omega+\beta))$, *and the vector* $\boldsymbol{A}_2 \in \mathbb{R}^{1\times 2}$ *has the form*

$$\boldsymbol{A}_2 = \left|\gamma_{\alpha,\beta}^{XY}(\omega)\right| \left[\frac{\mathrm{Re}\left(f_{\alpha,\beta}^{XY}(\omega)\right)}{\left|f_{\alpha,\beta}^{XY}(\omega)\right|^2}, -\frac{1}{2f_{1,0}^{XX}(\omega)}, -\frac{1}{2f_{1,0}^{YY}(\alpha\omega+\beta)}, \frac{\mathrm{Im}\left(f_{\alpha,\beta}^{XY}(\omega)\right)}{\left|f_{\alpha,\beta}^{XY}(\omega)\right|^2}\right].$$

Proof. This result is a special case of Theorem 3.6 given in Chapter 3. □

2.4 Proofs of results presented in Chapter 2

This section contains proofs of the original results presented in this chapter.

Proof of Theorem 2.1. By (i) of Assumption 2.1, we have

$$\begin{aligned}
\mathbb{E}\left[\widetilde{f}_{\alpha,\beta}^{XY}(\omega)\right] &= \frac{1}{T}\int_{\mathbb{R}} \int_{-\frac{T}{2}}^{\frac{T}{2}} \int_{-\frac{T}{2}}^{\frac{T}{2}} \mathbb{E}\left[X(t)\,\overline{Y(t)}\right] w\left(\tfrac{t}{T}\right) w\left(\tfrac{s}{T}\right) e^{-i2\pi\mu t} e^{i2\pi(\alpha\mu+\beta)s} \tfrac{1}{h_T} q\left(\tfrac{\omega-\mu}{h_T}\right) \mathrm{d}t\,\mathrm{d}s\,\mathrm{d}\mu \\
&= \frac{1}{Th_T} \sum_{(\gamma,\delta)\in\mathcal{K}^{XY}} \int_{\mathbb{R}}\int_{\mathbb{R}} \int_{-\frac{T}{2}}^{\frac{T}{2}} \int_{-\frac{T}{2}}^{\frac{T}{2}} f_{\gamma,\delta}^{XY}(\nu)\, e^{i2\pi(\nu t-(\gamma\nu+\delta)s)}\, w\left(\tfrac{t}{T}\right) w\left(\tfrac{s}{T}\right) \\
&\qquad\qquad \times e^{-i2\pi\mu t}\, e^{i2\pi(\alpha\mu+\beta)s}\, q\left(\tfrac{\omega-\mu}{h_T}\right) \mathrm{d}t\,\mathrm{d}s\,\mathrm{d}\mu\,\mathrm{d}\nu \\
&= \frac{1}{Th_T} \sum_{(\gamma,\delta)\in\mathcal{K}^{XY}} \int_{\mathbb{R}}\int_{\mathbb{R}} f_{\gamma,\delta}^{XY}(\nu)\, q\left(\tfrac{\omega-\mu}{h_T}\right) \int_{-\frac{T}{2}}^{\frac{T}{2}} w\left(\tfrac{t}{T}\right) e^{i2\pi(\nu-\mu)t}\,\mathrm{d}t \\
&\qquad\qquad \times \int_{-\frac{T}{2}}^{\frac{T}{2}} w\left(\tfrac{s}{T}\right) e^{-i2\pi(\gamma\nu-\alpha\mu+\delta-\beta)s}\,\mathrm{d}s\,\mathrm{d}\mu\,\mathrm{d}\nu \\
&= \frac{T}{h_T} \sum_{(\gamma,\delta)\in\mathcal{K}^{XY}} \int_{\mathbb{R}}\int_{\mathbb{R}} f_{\gamma,\delta}^{XY}(\nu)\, q\left(\tfrac{\omega-\mu}{h_T}\right) W(T(\mu-\nu))\, W(T(\gamma\nu-\alpha\mu+\delta-\beta))\,\mathrm{d}\mu\,\mathrm{d}\nu.
\end{aligned}$$

The last equality follows from Lemma B.4. The interchange of integrals above is allowed by Fubini theorem since

$$\int_{\mathbb{R}}\int_{\mathbb{R}}\int_{-\frac{T}{2}}^{\frac{T}{2}}\int_{-\frac{T}{2}}^{\frac{T}{2}}\left|f^{XY}_{\gamma,\delta}(\nu)\,w\left(\tfrac{t}{T}\right)\,w\left(\tfrac{s}{T}\right)\,q\left(\tfrac{\omega-\mu}{h_T}\right)\right|\,\mathrm{d}t\,\mathrm{d}s\,\mathrm{d}\mu\,\mathrm{d}\nu$$

$$\leq T^2\|w\|^2_\infty\int_{\mathbb{R}}\left|f^{XY}_{\gamma,\delta}(\nu)\right|\,\mathrm{d}\nu\int_{\mathbb{R}}q\left(\tfrac{\omega-\mu}{h_T}\right)\,\mathrm{d}\mu=\frac{T^2}{h_T}\|w\|^2_\infty\int_{\mathbb{R}}\left|f^{XY}_{\gamma,\delta}(\nu)\right|\,\mathrm{d}\nu<\infty.$$

We consider the following changing the variables $\eta=T(\mu-\nu)$ and $\lambda=\frac{\omega-\mu}{h_T}$. Then

$$\mu=\omega-h_T\lambda,\quad \nu=\omega-h_T\lambda+\tfrac{\eta}{T},$$

$$T(\gamma\nu-\alpha\mu+\delta-\beta)=-\gamma\eta+\underbrace{T(\gamma-\alpha)(\omega-h_T\lambda)+T(\delta-\beta)}_{=\eta_T}.$$

Hence,

$$\mathbb{E}\left[\widetilde{f}^{XY}_{\alpha,\beta}(\omega)\right]=\sum_{(\gamma,\delta)\in\mathcal{K}^{XY}}\int_{\mathbb{R}}\int_{\mathbb{R}}f^{XY}_{\gamma,\delta}\left(\omega-h_T\lambda-\tfrac{\eta}{T}\right)\,q(\lambda)\,W(\eta)\,W(-\gamma\eta+\eta_T)\,\mathrm{d}\lambda\,\mathrm{d}\eta$$

$$=\sum_{(\gamma,\delta)\in\mathcal{K}^{XY}}E(\gamma,\delta).$$

Consider the limit of $E(\gamma,\delta)$ in two cases: $(\gamma,\delta)=(\alpha,\beta)$ and $(\gamma,\delta)\neq(\alpha,\beta)$.

Let us start with the term corresponding to $(\gamma,\delta)=(\alpha,\beta)$. In that case, we have $\eta_T=0$. Observe that the integrand function in $E(\alpha,\beta)$ is bounded by some integrable function that does not depend on T. That is,

$$\left|f^{XY}_{\gamma,\delta}\left(\omega-h_T\lambda-\tfrac{\eta}{T}\right)\,q(\lambda)\,W(\eta)\,W(-\gamma\eta)\right|\leq\left\|f^{XY}_{\gamma,\delta}\right\|_\infty\,|q(\lambda)|\,|W(\eta)\,W(-\gamma\eta)|=G(\lambda,\eta).$$

By Hölder inequality the function $G\in L^1(\mathbb{R}^2)$ since $W\in L^2(\mathbb{R})$. Therefore, by Lebesgue's dominated convergence theorem we obtain

$$\lim_{T\to\infty}E(\alpha,\beta)=f^{XY}_{\alpha,\beta}(\omega)\int_{\mathbb{R}}q(\lambda)\,\mathrm{d}\lambda\int_{\mathbb{R}}W(\eta)\,W(-\gamma\eta)\,\mathrm{d}\eta=f^{XY}_{\alpha,\beta}(\omega)\,\mathcal{E}(\alpha).$$

It remains to show that $E(\gamma,\delta)$, with $(\gamma,\delta)\neq(\alpha,\beta)$, converges to zero as $T\to\infty$. Note that the term $E(\gamma,\delta)$ can be bounded as follows

$$|E(\gamma,\delta)|\leq\left\|f^{XY}_{\gamma,\delta}\right\|_\infty\int_{\mathbb{R}}F_T(\lambda)\,\mathrm{d}\lambda,$$

where

$$F_T(\lambda)=q(\lambda)\int_{\mathbb{R}}|W(\eta)\,W(-\gamma\eta+\eta_T)|\,\mathrm{d}\eta.$$

From Hölder inequality we have

$$|F_T(\lambda)|\leq q(\lambda)\left(\int_{\mathbb{R}}|W(\eta)|^2\,\mathrm{d}\eta\int_{\mathbb{R}}|W(-\gamma\eta+\eta_T)|^2\,\mathrm{d}\eta\right)^{\frac{1}{2}}=q(\lambda)\,\gamma^{-\frac{1}{2}}\|W\|^2_2,$$

and hence the function $F_T(\lambda)$ is bounded by an integrable function and independent of T. Hence, by Lebesgue's dominated convergence theorem, we can interchange the order of the limit and the integral with respect to the variable λ. Finally, using Lemma B.5 we have $\lim_{T\to\infty} E(\gamma,\delta) = 0$, with $(\gamma,\delta) \neq (\alpha,\beta)$, which ends the proof. □

Below, we provide an alternative expression for the periodogram frequency-smoothed along the line. This expression is then used to prove Theorem 2.3.

Lemma 2.1. *Assume that $q, w \in L^\infty(\mathbb{R})$ with compact support $[-\frac{1}{2},\frac{1}{2}]$. Moreover, there exist positive constants $M_X, M_Y > 0$ such that $|X(t)| \leq M_X$ and $|Y(t)| \leq M_Y$ a.s. for all $t \in \mathbb{R}$. Then*

$$\widetilde{f}^{XY}_{\alpha,\beta}(\omega) = \frac{1}{T} \int\limits_{-\frac{T}{2}}^{\frac{T}{2}} \int\limits_{-\frac{T}{2}}^{\frac{T}{2}} X(t)\,\overline{Y(s)}\, w\left(\tfrac{t}{T}\right)\, w\left(\tfrac{s}{T}\right)\, Q(h_T(t-\alpha s))\, e^{-i2\pi(\omega t-(\alpha\omega+\beta)s)} \mathrm{d}t\,\mathrm{d}s,$$

where Q denotes the inverse Fourier transform q, i.e., $Q(t) = \int_{\mathbb{R}} q(\lambda)\, e^{i2\pi\lambda t}\,\mathrm{d}\lambda$.

Proof of Lemma 2.1. Applying the Fubini theorem, we have

$$\begin{aligned}\widetilde{f}^{XY}_{\alpha,\beta}(\omega) &= \frac{1}{T} \int\limits_{\mathbb{R}} \int\limits_{-\frac{T}{2}}^{\frac{T}{2}} \int\limits_{-\frac{T}{2}}^{\frac{T}{2}} X(t)\,\overline{Y(s)}\, w\left(\tfrac{t}{T}\right)\, w\left(\tfrac{s}{T}\right)\, e^{-i2\pi\mu t}\, e^{i2\pi(\alpha\mu+\beta)s}\, \tfrac{1}{h_T} q\left(\tfrac{\omega-\mu}{h_T}\right) \mathrm{d}t\,\mathrm{d}s\,\mathrm{d}\mu \\ &= \frac{1}{T} \int\limits_{-\frac{T}{2}}^{\frac{T}{2}} \int\limits_{-\frac{T}{2}}^{\frac{T}{2}} X(t)\,\overline{Y(s)}\, w\left(\tfrac{t}{T}\right)\, w\left(\tfrac{s}{T}\right)\, e^{i2\pi\beta s} \left(\int\limits_{\mathbb{R}} \tfrac{1}{h_T} q\left(\tfrac{\omega-\mu}{h_T}\right)\, e^{-i2\pi(t-\alpha s)\mu}\,\mathrm{d}\mu \right) \mathrm{d}t\,\mathrm{d}s.\end{aligned}$$

By changing the variables $\lambda = \frac{\omega-\mu}{h_T}$, we get

$$\begin{aligned}\int\limits_{\mathbb{R}} \tfrac{1}{h_T} q\left(\tfrac{\omega-\mu}{h_T}\right)\, e^{-i2\pi(t-\alpha s)\mu}\,\mathrm{d}\mu &= e^{-i2\pi(t-\alpha s)\omega} \int\limits_{\mathbb{R}} q(\lambda)\, e^{i2\pi(t-\alpha s)h_T\lambda}\,\mathrm{d}\lambda \\ &= e^{-i2\pi(t-\alpha s)\omega} Q(h_T(t-\alpha s)),\end{aligned}$$

which ends the proof. □

Proof of Theorem 2.3. Let us consider the following decomposition of the estimation error

$$\widehat{f}^{XY}_{\widehat{\alpha}_T,\widehat{\beta}_T}(\omega) - f^{XY}_{\alpha,\beta}(\omega) = R_1 + R_2 + R_3,$$

where

$$\begin{aligned}R_1 &= \frac{\widetilde{f}^{XY}_{\widehat{\alpha}_T,\widehat{\beta}_T}(\omega)}{\mathcal{E}(\widehat{\alpha}_T)} - \frac{\widetilde{f}^{XY}_{\widehat{\alpha}_T,\widehat{\beta}_T}(\omega)}{\mathcal{E}(\alpha)} = \widetilde{f}^{XY}_{\widehat{\alpha}_T,\widehat{\beta}_T}(\omega) \left(\frac{1}{\mathcal{E}(\widehat{\alpha}_T)} - \frac{1}{\mathcal{E}(\alpha)} \right), \\ R_2 &= \frac{\widetilde{f}^{XY}_{\widehat{\alpha}_T,\widehat{\beta}_T}(\omega)}{\mathcal{E}(\alpha)} - \frac{\widetilde{f}^{XY}_{\alpha,\beta}(\omega)}{\mathcal{E}(\alpha)} = \frac{1}{\mathcal{E}(\alpha)} \left(\widetilde{f}^{XY}_{\widehat{\alpha}_T,\widehat{\beta}_T}(\omega) - \widetilde{f}^{XY}_{\alpha,\beta}(\omega) \right), \\ R_3 &= \widehat{f}^{XY}_{\alpha,\beta}(\omega) - f^{XY}_{\alpha,\beta}(\omega).\end{aligned}$$

From Theorem 2.1 the term R_3 approaches zero as $T \to \infty$ in the second moment. In the sequel, we show the convergence in the second moment of R_1 and R_2.

Let us start with the term R_1. From Lemma 2.1 and by changing the variable $u = h_T(t - \alpha s)$, we obtain

$$\begin{aligned}\left|\widetilde{f}^{XY}_{\widehat{\alpha}_T,\widehat{\beta}_T}(\omega)\right| &\leq \frac{1}{T}\int\limits_{-\frac{T}{2}}^{\frac{T}{2}}\int\limits_{-\frac{T}{2}}^{\frac{T}{2}}\left|X(t)\,\overline{Y(s)}\,w\left(\tfrac{t}{T}\right)\,w\left(\tfrac{s}{T}\right)\,Q(h_T(t-\alpha s))\right|\mathrm{d}t\,\mathrm{d}s\\ &\leq \frac{\|w\|_\infty^2 M_X M_Y}{T}\int\limits_{-\frac{T}{2}}^{\frac{T}{2}}\int\limits_{\mathbb{R}}|Q(h_T(t-\alpha s))|\,\mathrm{d}t\,\mathrm{d}s \leq \frac{\|w\|_\infty^2 M_X M_Y}{T h_T}\int\limits_{-\frac{T}{2}}^{\frac{T}{2}}\int\limits_{\mathbb{R}}|Q(u)|\,\mathrm{d}u\,\mathrm{d}s\\ &= \frac{\|w\|_\infty^2 M_X M_Y \|Q\|_1}{h_T}.\end{aligned}$$

Hence, there exists some positive constant $C_1 > 0$ such that

$$\mathbb{E}|R_1|^2 \leq C_1\, T^{2\kappa}\,\mathbb{E}\left|\frac{1}{\mathcal{E}(\widehat{\alpha}_T)} - \frac{1}{\mathcal{E}(\alpha)}\right|^2.$$

For a rectangular function w we have $\mathcal{E}(\alpha) = \min\left(1, |\alpha|^{-1}\right)$ and $\widehat{\mathcal{E}}_T(\alpha) = \min\left(1, \left|\widehat{\alpha}\right|^{-1}\right)$ (see Table 2.1). Thus, we examine separately two cases: $|\alpha| \leq 1$ and $|\alpha| > 1$.

If $|\alpha| \leq 1$, the almost sure convergence of $\widehat{\alpha}_T$ to α implies the existence of $T_0 > 0$ such that $|\widehat{\alpha}_T| \leq 1$ a.s. for all $T \geq T_0$. Thus, $R_1 = 0$ almost surely for $T \geq T_0$.

If $|\alpha| > 1$, the almost sure convergence of $\widehat{\alpha}_T$ to α implies the existence of $T_0 > 0$ such that $|\widehat{\alpha}_T| > 1$ a.s. for all $T \geq T_0$. Thus, for $T \geq T_0$

$$\mathbb{E}|R_1|^2 \leq C_1\, T^{2\kappa}\,\mathbb{E}\left|\widehat{\alpha}_T - \alpha\right|^2. \tag{2.7}$$

Now, we consider the term R_2. From Lemma 2.1, we get

$$\begin{aligned}|R_2| \leq \frac{1}{\mathcal{E}(\alpha)T}\int\limits_{-\frac{T}{2}}^{\frac{T}{2}}\int\limits_{-\frac{T}{2}}^{\frac{T}{2}}\Big|X(t)\,\overline{Y(s)}\,w\left(\tfrac{t}{T}\right)\,w\left(\tfrac{s}{T}\right)\,e^{-i2\pi\omega t}\Big(&Q(h_T(t-\widehat{\alpha}_T s))\,e^{i2\pi(\widehat{\alpha}_T\omega+\widehat{\beta}_T)s}\\ &- Q(h_T(t-\alpha s))\,e^{i2\pi(\alpha\omega+\beta)s}\Big)\Big|\mathrm{d}t\,\mathrm{d}s\\ \leq \frac{M_X M_Y \|w\|_\infty^2}{\mathcal{E}(\alpha)T}\int\limits_{-\frac{T}{2}}^{\frac{T}{2}}\int\limits_{-\frac{T}{2}}^{\frac{T}{2}}&\left|Q(h_T(t-\widehat{\alpha}_T s))\,e^{i2\pi(\widehat{\alpha}_T\omega+\widehat{\beta}_T)s} - Q(h_T(t-\alpha s))\,e^{i2\pi(\alpha\omega+\beta)s}\right|\mathrm{d}t\,\mathrm{d}s.\end{aligned}$$

From the Euler's formula, for all $\omega_1, \omega_2 \in \mathbb{R}$ and $t \in \mathbb{R}$, we have

$$e^{i2\pi\omega_1 t} - e^{i2\pi\omega_2 t} = -2i\sin\left(\pi t(\omega_2 - \omega_1)\right)e^{i\pi(\omega_1+\omega_2)t},$$

and hence

$$\begin{aligned}
&\left|Q(h_T(t-\widehat{\alpha}_T s))\, e^{i2\pi(\widehat{\alpha}_T\omega+\widehat{\beta}_T)s} - Q(h_T(t-\alpha s))\, e^{i2\pi(\alpha\omega+\beta)s}\right| \\
&\quad \le \left|e^{i2\pi(\widehat{\alpha}_T\omega+\widehat{\beta}_T)s}\right| |Q(h_T(t-\widehat{\alpha}_T s)) - Q(h_T(t-\alpha s))| \\
&\quad + |Q(h_T(t-\alpha s))| \cdot \left|e^{i2\pi(\widehat{\alpha}_T\omega+\widehat{\beta}_T)s} - e^{i2\pi(\alpha\omega+\beta)s}\right| \\
&\quad = |Q(h_T(t-\widehat{\alpha}_T s)) - Q(h_T(t-\alpha s))| + 2|Q(h_T(t-\alpha s))| \cdot \left|\sin\left(\pi s((\widehat{\alpha}_T-\alpha)\omega + (\widehat{\beta}_T-\beta))\right)\right|.
\end{aligned}$$

Consequently, by inequality $(a+b)^2 \le 2(a^2+b^2)$ for $a, b \in \mathbb{R}$, we obtain

$$\mathbb{E}|R_2|^2 \le 2\frac{M_X M_Y \|w\|_\infty^2}{\mathcal{E}(\alpha)} \left(\mathbb{E}|R_{1,2}|^2 + \mathbb{E}|R_{2,2}|^2\right),$$

where

$$R_{2,1} = \frac{1}{T} \int\limits_{-\frac{T}{2}}^{\frac{T}{2}} \int\limits_{-\frac{T}{2}}^{\frac{T}{2}} |Q(h_T(t-\widehat{\alpha}_T s)) - Q(h_T(t-\alpha s))|\, \mathrm{d}t\, \mathrm{d}s,$$

and

$$R_{2,2} = \frac{2}{T} \int\limits_{-\frac{T}{2}}^{\frac{T}{2}} \int\limits_{-\frac{T}{2}}^{\frac{T}{2}} |Q(h_T(t-\alpha s))| \cdot \left|\sin\left(\pi s((\widehat{\alpha}_T-\alpha)\omega + (\widehat{\beta}_T-\beta))\right)\right| \mathrm{d}t\, \mathrm{d}s.$$

It remains to discuss the convergence of $R_{2,1}$ and $R_{2,2}$ in the second moment.

Consider $R_{2,1}$. By changing the variable $u = h_T(t-\alpha s)$ and using the first-order Taylor approximations, we have

$$\begin{aligned}
R_{2,1} &\le \frac{1}{Th_T} \int\limits_{-\frac{T}{2}}^{\frac{T}{2}} \int\limits_{\mathbb{R}} |Q(u + h_T(\alpha-\widehat{\alpha}_T)s) - Q(u)|\, \mathrm{d}u\, \mathrm{d}s \\
&= \frac{1}{Th_T} \int\limits_{-\frac{T}{2}}^{\frac{T}{2}} \int\limits_{\mathbb{R}} \left|Q'(u + \varrho h_T(\alpha-\widehat{\alpha}_T)s)\right| \cdot |h_T(\alpha-\widehat{\alpha}_T)s|\, \mathrm{d}u\, \mathrm{d}s \\
&= \frac{|\alpha-\widehat{\alpha}_T|}{T} \int\limits_{\mathbb{R}} |Q'(u)|\, \mathrm{d}u \int\limits_{-\frac{T}{2}}^{\frac{T}{2}} |s|\, \mathrm{d}s \\
&= \tfrac{1}{4}\|Q'\|_1\, T|\alpha-\widehat{\alpha}_T|,
\end{aligned}$$

where $\varrho \in [0,1]$ is some constant. Then there exists some positive constant $C_{2,1} > 0$ such that

$$\mathbb{E}|R_{2,1}|^2 \le C_{2,1}\, T^2\, \mathbb{E}\,|\alpha-\widehat{\alpha}_T|^2. \tag{2.8}$$

For $R_{2,2}$, by changing the variable $u = h_T(t - \alpha s)$, we obtain

$$\begin{aligned}
R_{2,2} &\leq \frac{2}{T} \int\limits_{-\frac{T}{2}}^{\frac{T}{2}} \int\limits_{\mathbb{R}} |Q(h_T(t-\alpha s))| \cdot \left|\sin\left(\pi s((\widehat{\alpha}_T - \alpha)\omega + (\widehat{\beta}_T - \beta))\right)\right| \mathrm{d}t \, \mathrm{d}s \\
&\leq \frac{2}{Th_T} \int\limits_{\mathbb{R}} |Q(u)| \, \mathrm{d}u \int\limits_{-\frac{T}{2}}^{\frac{T}{2}} \left|\sin\left(\pi s((\widehat{\alpha}_T - \alpha)\omega + (\widehat{\beta}_T - \beta))\right)\right| \, \mathrm{d}s \\
&\leq \frac{2\pi \|Q\|_1}{Th_T} \int\limits_{-\frac{T}{2}}^{\frac{T}{2}} |s| \left(|\widehat{\alpha}_T - \alpha| \, |\omega| + \left|\widehat{\beta}_T - \beta\right|\right) \mathrm{d}s \\
&\leq \frac{\pi \|Q\|_1}{2} T^{1+\kappa} \left(|\widehat{\alpha}_T - \alpha| \, |\omega| + \left|\widehat{\beta}_T - \beta\right|\right).
\end{aligned}$$

Therefore, there exists some positive constant $C_{2,2} > 0$ such that

$$\mathbb{E}|R_{2,2}|^2 \leq C_{2,2} \, T^{2(1+\kappa)} \left(|\omega|^2 \, \mathbb{E} \, |\widehat{\alpha}_T - \alpha|^2 + \mathbb{E} \left|\widehat{\beta}_T - \beta\right|^2\right). \tag{2.9}$$

Finally, combining inequities (2.7), (2.8) and (2.9), and by $\max\left(2\kappa, 2, 2(1+\kappa)\right) = 2(1+\kappa) \leq r$, for all $\kappa \in (0, \frac{r-2}{2}]$, we end the proof. □

Proof of Proposition 2.2. Let $k, j \in \{1, 2\}$, $k \neq j$. Note that

$$T^r \left|\frac{\widehat{\lambda}_j}{\widehat{\lambda}_k} - \frac{\lambda_j}{\lambda_k}\right|^2 = T^r \left|\frac{\widehat{\lambda}_j \, \lambda_k - \lambda_j \, \widehat{\lambda}_k}{\widehat{\lambda}_k \, \lambda_k}\right|^2 \leq 2T^r \left|\frac{\widehat{\lambda}_j - \lambda_j}{\widehat{\lambda}_k}\right|^2 + 2T^r \left|\frac{(\lambda_k - \widehat{\lambda}_k) \, \lambda_j}{\widehat{\lambda}_k \, \lambda_k}\right|^2.$$

From $\widehat{\lambda}_k \geq m_k$ a.s. and $\lim\limits_{T\to\infty} T^r \, \mathbb{E}|\widehat{\lambda}_k - \lambda_k|^2 = 0$, we have

$$\lim_{T\to\infty} T^r \, \mathbb{E} \left|\frac{\widehat{\lambda}_j}{\widehat{\lambda}_k} - \frac{\lambda_j}{\lambda_k}\right|^2 = 0. \tag{2.10}$$

In an analogous way, we obtain an almost sure convergence of the slope estimator.

Now, we show the convergence of $\widehat{\beta}_T$. We have

$$T^r \left|\frac{\widehat{\lambda}_2}{\widehat{\lambda}_1}\widehat{\gamma}_1 - \frac{\lambda_2}{\lambda_1}\gamma_1\right|^2 \leq 2T^r \, |\widehat{\gamma}_1 - \gamma_1|^2 \cdot \left|\frac{\widehat{\lambda}_2}{\widehat{\lambda}_1}\right|^2 + 2T^r \left|\frac{\widehat{\lambda}_2}{\widehat{\lambda}_1} - \frac{\lambda_2}{\lambda_1}\right|^2 \cdot |\gamma_1|^2$$

From (2.10) and the fact that $m_j \leq \widehat{\lambda}_j \leq M_j$ a.s. and $\lim\limits_{T\to\infty} T^r \, \mathbb{E}|\widehat{\gamma}_j - \gamma_j|^2 = 0$, for $j = 1, 2$, we obtain that

$$\lim_{T\to\infty} T^r \, \mathbb{E} \left|\frac{\widehat{\lambda}_2}{\widehat{\lambda}_1}\widehat{\gamma}_1 - \frac{\lambda_2}{\lambda_1}\gamma_1\right|^2 = 0,$$

and consequently, we obtain the convergence of $\widehat{\beta}_T$. □

CHAPTER 3

SUBSAMPLING PROCEDURE IN SPECTRAL ANALYSIS

In the previous chapter, we considered the point estimation of the spectral density and spectral coherence functions for harmonizable processes with spectral mass concentrated along lines. However, in practical applications, statistical inference goes beyond point estimation, including the construction of confidence intervals and hypothesis testing. For this purpose, one can use asymptotic distributions of rescaled estimators. Unfortunately, in that case, directly applying the asymptotic distribution is highly challenging because of the need to estimate the asymptotic covariance. The asymptotic covariance matrix of the rescaled estimator has a complex structure (see Theorem 2.2), making it almost impossible to estimate accurately. Therefore, in this chapter, we introduce a resampling method that allows us to obtain confidence intervals for parameters of interest and does not require the estimation of the covariance matrix. The proposed method is based on the subsampling method.

In Section 3.1, we recall the notation and outline the primary concept of the subsampling procedure for time series. In Section 3.2, we introduce our subsampling procedure tailored for continuous-time harmonizable processes. In Section 3.3, we define the subsampling estimators of spectral density and spectral coherence. Moreover, we derive their asymptotic properties. In Section 3.4, we establish the consistency theorem for the proposed subsampling procedure in spectral analysis. In Section 3.5, we discuss the application of the subsampling procedure in constructing confidence intervals for spectral characteristics. Finally, Section 3.6 includes proofs of the results.

All theorems, propositions, and corollaries in this chapter, except those in Section 3.1, are original contributions. These results can be found in [29].

3.1 Brief overview of the subsampling for time series

In this section, we briefly recall the classical subsampling approach introduced by Politis and Romano [73, 74].

Consider a time series $\{X(n),\, n \in \mathbb{N}\}$, and let $\theta \in \mathbb{R}$ be a parameter of interest. Fix $n \in \mathbb{N}$. We denote by $\widehat{\theta}_n = \widehat{\theta}_n(\boldsymbol{X}_n)$ an estimator of θ based on the sample $\boldsymbol{X}_n = (X(1), \ldots, X(n))$. To perform inference on θ, it is essential to derive or approximate the sampling distribution of $\widehat{\theta}_n$. Let J_n^θ be the sampling distribution of $\tau_n(\widehat{\theta}_n - \theta)$, where τ_n is a normalizing factor. Moreover, we consider the cumulative distribution function

$$J_n^\theta(x) = \mathbb{P}\left(\tau_n(\widehat{\theta}_n - \theta) \le x\right), \quad x \in \mathbb{R}.$$

The idea behind subsampling is to approximate the sampling distribution J_n^θ of statistics based on smaller data sets, referred to as subsamples. For time series, to mimic the time dependency, the data set is divided into overlapping blocks of size b. Denote by $\boldsymbol{X}_{s,b} = (X(s), \ldots, X(s+b-1))$, with $s = 1, 2, \ldots, n-b+1$, the subsample of length b from $\boldsymbol{X}_n$. By $\widehat{\theta}_{n,b,s} = \widehat{\theta}_b(\boldsymbol{X}_{s,b})$ we denote the subsampling estimator of θ based on the subsample $\boldsymbol{X}_{s,b}$. Let $J_{b,s}^\theta$ denote the sampling distribution of $\tau_b(\widehat{\theta}_{n,b,s} - \theta)$, where τ_b is some normalizing factor. Moreover, we consider the cumulative distribution function

$$J_{b,s}^\theta(x) = \mathbb{P}\left(\tau_b(\widehat{\theta}_{n,b,s} - \theta) \le x\right), \quad x \in \mathbb{R}.$$

Therefore,

$$L_{n,b}^\theta(x) = \tfrac{1}{n-b+1} \sum_{s=1}^{n-b+1} \mathbb{1}_{\left\{\tau_b(\widehat{\theta}_{n,b,s} - \widehat{\theta}_n) \le x\right\}}$$

is used to approximate $J_n^\theta(x)$ for $x \in \mathbb{R}$.

Note that the distribution $J_{b,s}^\theta$ may depend on the index s since time series $X(t)$ can be nonstationary. To ensure an appropriate approximation of $J_n^\theta(x)$ based on $L_{n,b}^\theta(x)$, the following assumption should be considered.

Assumption 3.1 ([72]). There exists a limiting law J^θ such that

(i) J_n^θ converges weakly to J^θ as $n \to \infty$.

(ii) For every continuity point x of $J^\theta(\cdot)$ and for any sequences n, b with $n, b \to \infty$ and $b/n \to 0$, we have

$$\frac{1}{n-b+1} \sum_{s=1}^{n-b+1} J_{b,s}^\theta(x) \to J^\theta(x).$$

In [72], the consistency of subsampling for nonstationary time series is established under the assumption of weak dependence. For this purpose, we introduce the concept of α-mixing.

Let $\{X(t),\, t \in \mathbb{T}\}$, where $\mathbb{T} = \mathbb{Z}$ or $\mathbb{T} = \mathbb{R}$. Then $\{X(t),\, t \in \mathbb{T}\}$ is called α-mixing if $\alpha_X(\tau) \to 0$ as $\tau \to \infty$, where

$$\alpha_X(\tau) = \sup_{t \in \mathbb{R}} \sup_{\substack{A \in \mathcal{F}_X(-\infty, t) \\ B \in \mathcal{F}_X(t+\tau, \infty)}} \left|\mathbb{P}(A \cap B) - \mathbb{P}(A)\,\mathbb{P}(B)\right|,$$

with $\mathcal{F}_X(a, b) = \sigma\left(\{X(t),\, a \le t \le b\}\right)$. The coefficient $\alpha_X(\tau)$ is a standard measure of weak dependence for stochastic processes. Namely, it measures the dependence between past and future information. If $\alpha_X(\tau) = 0$, then observations distant by at least τ time units are independent. For

more information on weak dependency, we refer the reader to [21]. Furthermore, in Appendix B, we recall two inequalities for bounding covariance using the α-mixing measure.

In the following, we present the theorem on the consistency of subsampling for nonstationary time series.

Theorem 3.1 ([72]). *Let $\{X(n),\, n \in \mathbb{N}\}$ be an α-mixing. Let Assumption 3.1 holds and that $\tau_b/\tau_n \to 0$, $b/n \to 0$, and $b \to \infty$ as $n \to \infty$. Then*

(i) If x is a continuity point of $J^\theta(\cdot)$, then $L^\theta_{n,b}(x) \to J^\theta(x)$ in probability.

(ii) If $J^\theta(\cdot)$ is continuous, then $\sup_{x\in\mathbb{R}} |L^\theta_{n,b}(x) - J^\theta(x)|$ in probability.

(iii) For $\rho \in (0,1)$, let $c^\theta_{n,b}(1-\rho) = \inf\{x : L^\theta_{n,b}(x) \geq 1-\rho\}$. Correspondingly, define $c^\theta(1-\rho) = \inf\{x : J^\theta(x) \geq 1-\rho\}$. If $J^\theta(\cdot)$ is continuous at $c^\theta(1-\rho)$, then

$$\mathbb{P}\left(\tau_n(\widehat{\theta}_n - \theta) \leq c^\theta_{n,b}(1-\rho)\right) \to 1-\rho \quad \text{as } n \to \infty.$$

Thus, the asymptotic coverage probability of the interval $\left[\widehat{\theta}_n - \tau_n^{-1} c^\theta_{n,b}(1-\rho), \infty\right)$ is the nominal level $1-\rho$.

Thus, the consistency of subsampling can be achieved under weak assumptions. Note that we do not need to know the form of the sampling distribution of the estimator to prove the consistency. Detailed discussion on subsampling can be found in [72].

In this section, we presented a subsampling for discrete-time stochastic processes. In our case, we consider continuous-time stochastic processes, and in the subsequent section we adapt the subsampling to this case.

3.2 Subsampling for continuous-time processes

In this section, we propose a continuous-time counterpart to the subsampling method introduced by Politis and Romano. Although general results on subsampling for continuous-time processes have been explored in [4], these results are not directly applicable to our specific problem. Our case requires significantly weaker assumptions. This issue is further discussed in Section 3.4.

Let $\{X(t),\, t \in \mathbb{R}\}$ and $\{Y(t),\, t \in \mathbb{R}\}$ be two zero-mean complex-valued harmonizable stochastic processes with cross-spectral measure supported on a countable union of lines. Fix $T > 0$. Let $\boldsymbol{X}_T = \left\{X(t),\, t \in \left[-\frac{T}{2}, \frac{T}{2}\right]\right\}$ and $\boldsymbol{Y}_T = \left\{Y(t),\, t \in \left[-\frac{T}{2}, \frac{T}{2}\right]\right\}$ be observed samples. We divide the samples into overlapping blocks of length b (where $0 < b < T$), with an overlap determined by the factor $\Delta > 0$. Assume that Δ is such that $q_T = \frac{T-b}{2\Delta}$ is an integer number. The resulting blocks are defined as $\boldsymbol{X}_{b,s\Delta} = \left\{X(t),\, t \in \left[s\Delta - \frac{b}{2}, s\Delta + \frac{b}{2}\right]\right\}$ and $\boldsymbol{Y}_{b,s\Delta} = \left\{Y(t),\, t \in \left[s\Delta - \frac{b}{2}, s\Delta + \frac{b}{2}\right]\right\}$ for $s = -q_T, -q_T+1 \ldots, q_T$. Figure 3.1 illustrates an example of this block division.

Let $\theta \in \mathbb{R}$ be a parameter of interest. By $\widehat{\theta}_T = \widehat{\theta}_T(\boldsymbol{X}_T, \boldsymbol{Y}_T)$ we denote the estimator of θ based on the sample $(\boldsymbol{X}_T, \boldsymbol{Y}_T)$, and by $\widehat{\theta}_{T,b,s\Delta} = \widehat{\theta}_b(\boldsymbol{X}_{b,s\Delta}, \boldsymbol{Y}_{b,s\Delta})$ its counterpart based on the subsample

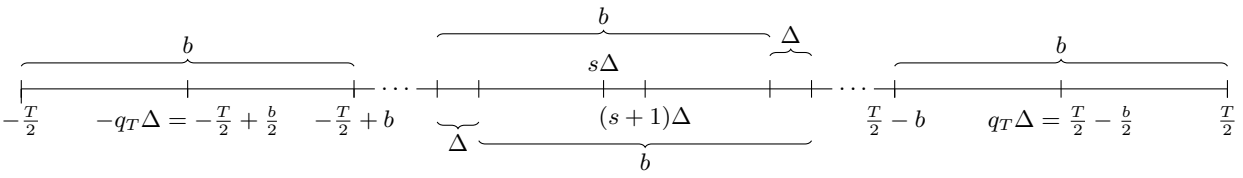

Figure 3.1: Splitting the observation interval $\left[-\frac{T}{2}, \frac{T}{2}\right]$ into overlapping blocks of size b with overlap factor Δ.

$(\boldsymbol{X}_{b,s\Delta}, \boldsymbol{Y}_{b,s\Delta})$. Our goal is to approximate the distribution of $\tau_T\big(\widehat{\theta}_T - \theta\big)$ using $\tau_b\big(\widehat{\theta}_{T,b,s\Delta} - \widehat{\theta}_T\big)$. For this purpose, we define

$$L^{\theta}_{T,b}(x) = \frac{1}{2l_T+1} \sum_{j=-l_T}^{l_T} \mathbb{I}_{\{\tau_b(\widehat{\theta}_{T,b,j\Delta} - \widehat{\theta}_T) \le x\}}, \quad x \in \mathbb{R},$$

where $2l_T + 1$ is the number of blocks considered in the subsampling. Then $L^{\theta}_{T,b}(x)$ approximates the cumulative distribution function of $\tau_T(\widehat{\theta}_T - \theta)$ at point $x \in \mathbb{R}$.

Our objective is to develop a consistent subsampling procedure that approximates the distributions of

$$\sqrt{Th_T}\left(\left|\widehat{f}^{XY}_{\alpha,\beta}(\omega)\right| - \left|f^{XY}_{\alpha,\beta}(\omega)\right|\right) \quad \text{and} \quad \sqrt{Th_T}\left(\left|\widehat{\gamma}^{XY}_{\alpha,\beta}(\omega)\right| - \left|\gamma^{XY}_{\alpha,\beta}(\omega)\right|\right).$$

for fixed $\omega \in \mathbb{R}$. Recall that the estimators $\widehat{f}^{XY}_{\alpha,\beta}(\omega)$ and $\widehat{\gamma}^{XY}_{\alpha,\beta}(\omega)$ are given by (2.1) and (2.6), respectively. We start by defining the subsampling counterparts of $\widehat{f}^{XY}_{\alpha,\beta}(\omega)$ and $\widehat{\gamma}^{XY}_{\alpha,\beta}(\omega)$ and analyzing their asymptotic properties.

3.3 Subsampling estimators and their properties

The purpose of this section is to define the subsampling estimator for the spectral density function and spectral coherence function. Specifically, these estimators are based on the subsamples $\left\{X(t),\, t \in \left[s\Delta - \frac{b}{2}, s\Delta + \frac{b}{2}\right]\right\}$ and $\left\{Y(t),\, t \in \left[s\Delta - \frac{b}{2}, s\Delta + \frac{b}{2}\right]\right\}$ for $s = -q_T, -q_T+1, \ldots, q_T$, where $q_T = \frac{T-b}{2\Delta}$. For generality, we consider estimators based on $\left\{X(t),\, t \in \left[c_T - \frac{d_T}{2}, c_T + \frac{d_T}{2}\right]\right\}$ and $\left\{Y(t),\, t \in \left[c_T - \frac{d_T}{2}, c_T + \frac{d_T}{2}\right]\right\}$. By d_T we denote the length of the time interval and c_T is the midpoint of the observation time. Note that in Chapter 2, we focused on the specific case where $d_T = T$ and $c_T = 0$ and in this section we generalize it. We impose the following conditions on c_T and d_T.

Assumption 3.2. $d_T \to \infty$ and $c_T/d_T \to \vartheta \in \mathbb{R}$ as $T \to \infty$.

We define the short-time Fourier Transform

$$D^X_{c_T,d_T}(\omega) = \int_{c_T - \frac{d_T}{2}}^{c_T + \frac{d_T}{2}} X(t)\, w\left(\tfrac{t-c_T}{d_T}\right) e^{-i2\pi\omega t}\, \mathrm{d}t, \qquad D^Y_{c_T,d_T}(\omega) = \int_{c_T - \frac{d_T}{2}}^{c_T + \frac{d_T}{2}} Y(t)\, w\left(\tfrac{t-c_T}{d_T}\right) e^{-i2\pi\omega t}\, \mathrm{d}t,$$

the bifrequency periodogram

$$I^{XY}_{c_T,d_T}(\omega,\nu) = \frac{1}{d_T} D^X_{c_T,d_T}(\omega)\, \overline{D^Y_{c_T,d_T}(\nu)},$$

and the normalized periodogram frequency-smoothed along this line $\{(\omega,\nu)\in\mathbb{R}^2 : \nu=\alpha\omega+\beta\}$

$$\widehat{f}^{XY}_{\alpha,\beta}(\omega)_{c_T,d_T}=\frac{\widetilde{f}^{XY}_{\alpha,\beta}(\omega)_{c_T,d_T}}{\mathcal{E}_{c_T/d_T}(\alpha)}, \tag{3.1}$$

where

$$\widetilde{f}^{XY}_{\alpha,\beta}(\omega)_{c_T,d_T}=\int_{\mathbb{R}} I^{XY}_{c_T,d_T}(\mu,\alpha\mu+\beta)\ \tfrac{1}{h_{d_T}}q\left(\tfrac{\omega-\mu}{h_{d_T}}\right)\mathrm{d}\mu,$$

and

$$\mathcal{E}_{\vartheta}(\alpha)=\int_{\mathbb{R}} W(\nu)\,W(-\alpha\nu)\,e^{i2\pi(\alpha-1)\vartheta\nu}\,\mathrm{d}\nu.$$

Note that in the general case, the normalizing factor $\mathcal{E}_{c_T/d_T}(\alpha)$ depends on the length of the observation d_T and the midpoint of the observation time c_T. Finally, based on the estimator (3.1), we define the estimator of the spectral coherence function $\gamma^{XY}_{\alpha,\beta}(\omega)$ for $\omega\in\mathbb{R}$. That is,

$$\widehat{\gamma}^{XY}_{\alpha,\beta}(\omega)_{c_T,d_T}=\frac{\widehat{f}^{XY}_{\alpha,\beta}(\omega)_{c_T,d_T}}{\sqrt{\widehat{f}^{XX}_{1,0}(\omega)_{c_T,d_T}\,\widehat{f}^{YY}_{1,0}(\alpha\omega+\beta)_{c_T,d_T}}}. \tag{3.2}$$

In contrast to the spectral density function estimator considered in Chapter 2, in this more general case, the normalizing factor $\mathcal{E}_{c_T/d_T}(\alpha)$ can be zero for some parameters α, c_T, d_T. The following result specifies a condition that ensures that the normalization factor is non-zero.

Proposition 3.1. *Assume that w is a non-negative function on the interval $\left(-\frac{1}{2},\frac{1}{2}\right)$ with compact support $\left[-\frac{1}{2},\frac{1}{2}\right]$. Then for all $\alpha>0$*

$$\mathcal{E}_{\vartheta}(\alpha)=\int_{\mathbb{R}} w(t)\,w(\alpha t+(\alpha-1)\vartheta)\,\mathrm{d}t.$$

For $\alpha\in(0,\infty)\setminus\{1\}$, the normalizing factor $\mathcal{E}_{\vartheta}(\alpha)$ is non-zero provided that $|\vartheta|\leq\frac{1}{2}\frac{\alpha+1}{|1-\alpha|}$. For $\alpha=1$, the normalizing factor $\mathcal{E}_{\vartheta}(\alpha)=\int_{\mathbb{R}} w^2(t)\,\mathrm{d}t$ is non-zero for any $\vartheta\in\mathbb{R}$.

Proof. See Section 3.6. □

We now present the asymptotic properties of $\widehat{f}^{XY}_{\alpha,\beta}(\omega)_{c_T,d_T}$ and $\widehat{\gamma}^{XY}_{\alpha,\beta}(\omega)_{c_T,d_T}$. The following properties extend those discussed in Section 2.3.

Theorem 3.2. *Let Assumption 2.1, Assumption 3.2, and (i), (ii) in Assumption 2.3 hold. Let $(\alpha,\beta)\in\mathcal{K}^{XY}$ be fixed. Then for every $\omega\in\mathbb{R}$ such that $\alpha\omega+\beta\neq\alpha'\omega+\beta'$, for all $(\alpha',\beta')\in\mathcal{K}^{XY}\setminus\{(\alpha,\beta)\}$, we have*

$$\lim_{T\to\infty}\sqrt{d_T h_{d_T}}\,\mathbb{E}\left(\widehat{f}^{XY}_{\alpha,\beta}(\omega)_{c_T,d_T}-f^{XY}_{\alpha,\beta}(\omega)\right)=0,$$

provided that $h_{d_T}=\mathcal{O}(d_T^{-\kappa})$, with $\kappa\in\left(\frac{1}{3},1\right)$, and $\mathcal{E}_{c_T/d_T}(\alpha)\neq 0$.

Proof. See Section 3.6. □

Theorem 3.3. *Let Assumption 2.1 and Assumption 3.2 hold. Let* $(\alpha_1,\beta_1),(\alpha_2,\beta_2)\in\mathcal{K}^{XY}$ *be fixed. Then for* $\omega_1,\omega_2\in\mathbb{R}$ *excluding points of intersection of support lines, we have*

$$\begin{aligned}\lim_{T\to\infty} d_T h_{d_T}\operatorname{Cov}\left(\widehat{f}^{XY}_{\alpha_1,\beta_1}(\omega_1)_{c_T,d_T},\widehat{f}^{XY}_{\alpha_2,\beta_2}(\omega_2)_{c_T,d_T}\right)&\\ =\sum_{(\gamma_1,\delta_1)\in\mathcal{K}^{YY}}\sum_{(\gamma_2,\delta_2)\in\mathcal{K}^{\overline{XX}}} f^{YY}_{\gamma_1,\delta_1}(\omega_1)\, f^{\overline{XX}}_{\gamma_2,\delta_2}(-\alpha_1\omega_1-\beta_1)\,\mathcal{Q}(\gamma_1)\,\frac{\mathcal{W}_\vartheta(\alpha_2\gamma_1,\gamma_2,\alpha_2)}{\mathcal{E}_\vartheta(\alpha_1)\,\mathcal{E}_\vartheta(\alpha_2)}&\\ \times\delta_{\alpha_2\gamma_1-\gamma_2\alpha_1}\,\delta_{\alpha_2\delta_1-\gamma_2\beta_1+\delta_2+\beta_2}\,\delta_{\gamma_1\omega_1+\delta_2-\omega_2}&\\ +\sum_{(\gamma_1,\delta_1)\in\mathcal{K}^{Y\overline{X}}}\sum_{(\gamma_2,\delta_2)\in\mathcal{K}^{\overline{X}Y}} f^{Y\overline{X}}_{\gamma_1,\delta_1}(\omega_1)\, f^{\overline{X}Y}_{\gamma_2,\delta_2}(-\alpha_1\omega_1-\beta_1)\,\mathcal{Q}(\gamma_1\alpha_1)\,\frac{\mathcal{W}_\vartheta(\alpha_2\gamma_2,\alpha_2,\gamma_1)}{\mathcal{E}_\vartheta(\alpha_1)\,\mathcal{E}_\vartheta(\alpha_2)}&\\ \times\delta_{\gamma_1-\alpha_2\gamma_2\alpha_1}\,\delta_{\alpha_2\delta_2+\beta_2+\delta_1-\alpha_2\gamma_2\beta_1}\,\delta_{\omega_2+\gamma_2(\alpha_1\omega_1+\beta_1)-\delta_2},&\end{aligned}$$

where

$$\mathcal{Q}(a)=\int_{\mathbb{R}} q(\lambda)q(a\lambda)\,\mathrm{d}\lambda,$$

$$\begin{aligned}\mathcal{W}_\vartheta(a_1,a_2,a_3)=\int_{\mathbb{R}}\int_{\mathbb{R}}\int_{\mathbb{R}} W(\eta_1)W(\eta_2)W(\eta_2)\,W(a_1\eta_1+a_2\eta_2+a_3\eta_3)&\\ \times e^{-i2\pi(\eta_1+\eta_2+\eta_3)\vartheta}\,e^{i2\pi(a_1\eta_1+a_2\eta_2+a_3\eta_3)\vartheta}\,\mathrm{d}\eta_1\,\mathrm{d}\eta_2\,\mathrm{d}\eta_3,&\end{aligned}$$

provided that $\mathcal{E}_{c_T/d_T}(\alpha_1)\neq 0$ *and* $\mathcal{E}_{c_T/d_T}(\alpha_2)\neq 0$.

Proof. See Section 3.6. □

Theorem 3.4. *Fix* $P>2$. *Let Assumption 2.1, Assumption 3.2, and (i), (iii) in Assumption 2.3 hold. Let* $(\alpha_1,\beta_1),\ldots,(\alpha_P,\beta_P)\in\mathcal{K}^{XY}$ *be fixed. Then for* $\omega_1,\ldots,\omega_P\in\mathbb{R}$, *excluding points of intersection of support lines, we have*

$$\lim_{T\to\infty}(d_T h_{d_T})^{P/2}\operatorname{cum}\left(\widehat{f}^{XY}_{\alpha_1,\beta_1}(\omega_1)^{[*]}_{c_T,d_T},\ldots,\widehat{f}^{XY}_{\alpha_P,\beta_P}(\omega_P)^{[*]}_{c_T,d_T}\right)=0,$$

provided that $\mathcal{E}_{c_T/d_T}(\alpha_j)\neq 0$ *for* $j=1,2,\ldots,P$.

Proof. See Section 3.6. □

Theorem 3.5. *Let Assumption 2.1, Assumption 2.3 and Assumption 3.2 hold. Let* $(\alpha,\beta)\in\mathcal{K}^{XY}$ *be fixed. Then for every* $\omega\in\mathbb{R}$ *such that* $\alpha\omega+\beta\neq\alpha'\omega+\beta'$, *for all* $(\alpha',\beta')\in\mathcal{K}^{XY}\setminus\{(\alpha,\beta)\}$, *we have*

$$\sqrt{d_T h_{d_T}}\left(\widehat{f}^{XY}_{\alpha,\beta}(\omega)_{c_T,d_T}-f^{XY}_{\alpha,\beta}(\omega)\right)\xrightarrow{d}\mathcal{N}_2(\mathbf{0},\mathbf{\Sigma}_\vartheta(\omega;\alpha,\beta)),$$

provided that $h_{d_T}=\mathcal{O}(d_T^{-\kappa})$, *with* $\kappa\in\left(\frac{1}{3},1\right)$, *and* $\mathcal{E}_{c_T/d_T}(\alpha)\neq 0$. *The covariance matrix* $\mathbf{\Sigma}_\vartheta(\omega;\alpha,\beta)$ *is given by*

$$\mathbf{\Sigma}_\vartheta(\omega;\alpha,\beta)=\frac{1}{2}\begin{bmatrix}\operatorname{Re}(\sigma^2_\vartheta)+\operatorname{Re}(\sigma^2_{\vartheta,c}) & \operatorname{Im}(\sigma^2_\vartheta)-\operatorname{Im}(\sigma^2_{\vartheta,c})\\ \operatorname{Im}(\sigma^2_\vartheta)-\operatorname{Im}(\sigma^2_{\vartheta,c}) & \operatorname{Re}(\sigma^2_{\vartheta,c})-\operatorname{Re}(\sigma^2_\vartheta)\end{bmatrix},\tag{3.3}$$

where

$$\begin{aligned}\sigma^2_\vartheta=\sigma^2_\vartheta(\omega;\alpha,\beta)&=\lim_{T\to\infty} d_T h_{d_T}\operatorname{Var}\left(\widehat{f}^{XY}_{\alpha,\beta}(\omega)_{c_T,d_T}\right),\\ \sigma^2_{\vartheta,c}=\sigma^2_{\vartheta,c}(\omega;\alpha,\beta)&=\lim_{T\to\infty} d_T h_{d_T}\operatorname{Cov}\left(\widehat{f}^{XY}_{\alpha,\beta}(\omega)_{c_T,d_T},\overline{\widehat{f}^{XY}_{\alpha,\beta}(\omega)_{c_T,d_T}}\right).\end{aligned}$$

Proof. See Section 3.6. □

Corollary 3.1. *Let Assumption 2.1, Assumption 2.3 and Assumption 3.2 hold. Let* $(\alpha,\beta)\in\mathcal{K}^{XY}$ *be fixed. Let* $\omega\in\mathbb{R}$ *such that* $\alpha\omega+\beta\neq\alpha'\omega+\beta'$, *for all* $(\alpha',\beta')\in\mathcal{K}^{XY}\setminus\{(\alpha,\beta)\}$. *Assume that* $\det(\mathbf{\Sigma}_\vartheta(\omega;\alpha,\beta))>0$, *where* $\mathbf{\Sigma}_\vartheta(\omega;\alpha,\beta)$ *is given by* (3.3). *Then*

$$\sqrt{d_Th_T}\left(\left|\widehat{f}^{XY}_{\alpha,\beta}(\omega)_{c_T,d_T}\right|-\left|f^{XY}_{\alpha,\beta}(\omega)\right|\right)\xrightarrow{d}J_\vartheta^{|f^{XY}_{\alpha,\beta}(\omega)|},$$

where

$$J_\vartheta^{|f^{XY}_{\alpha,\beta}(\omega)|}=\begin{cases}\mathcal{L}\left(\sqrt{U_1^2+U_2^2}\right), & \text{if } f^{XY}_{\alpha,\beta}(\omega)=0,\\ \mathcal{N}_1(\mathbf{0},\boldsymbol{A}_1\mathbf{\Sigma}_\vartheta(\omega;\alpha,\beta)\boldsymbol{A}_1^{\mathrm{T}}), & \text{if } f^{XY}_{\alpha,\beta}(\omega)\neq 0,\end{cases}$$

and the random vector $[U_1,U_2]^{\mathrm{T}}$ *has a two-dimensional normal distribution* $\mathcal{N}_2(\mathbf{0},\mathbf{\Sigma}_\vartheta(\omega;\alpha,\beta))$, *and the vector* $\boldsymbol{A}_1\in\mathbb{R}^{1\times 2}$ *has the form*

$$\boldsymbol{A}_1=\frac{1}{|f^{XY}_{\alpha,\beta}(\omega)|}[\mathrm{Re}\left(f^{XY}_{\alpha,\beta}(\omega)\right),\mathrm{Im}\left(f^{XY}_{\alpha,\beta}(\omega)\right)].$$

Proof. See Section 3.6. □

Theorem 3.6. *Let Assumption 2.1 and Assumption 2.3 hold. Let* $(\alpha,\beta)\in\mathcal{K}^{XY}$ *be fixed. Let* $\omega\in\mathbb{R}$ *be a point that does not lie at the intersection of the support lines of the spectral measures* F^{XY}, F^{XX} *and* F^{YY}. *Assume* $\det(\mathbf{\Lambda}_\vartheta(\omega,\alpha\omega+\beta))>0$, *where* $\mathbf{\Lambda}_\vartheta(\omega,\alpha\omega+\beta)=\boldsymbol{D}_\vartheta(\omega,\alpha\omega+\beta;\alpha,\beta)$ *is an asymptotic covariance matrix from Lemma 3.1. Moreover, there exist first derivatives* $f^{XX\prime}_{1,0}$, $f^{YY\prime}_{1,0}$ *that belong to* $L^2(\mathbb{R})\cap L^\infty(\mathbb{R})$. *Then*

$$\sqrt{d_Th_T}\left(\left|\widehat{\gamma}^{XY}_{\alpha,\beta}(\omega)_{c_T,d_T}\right|-\left|\gamma^{XY}_{\alpha,\beta}(\omega)\right|\right)\xrightarrow{d}J_\vartheta^{|\gamma^{XY}_{\alpha,\beta}(\omega)|},$$

where

$$J_\vartheta^{|\gamma^{XY}_{\alpha,\beta}(\lambda)|}=\begin{cases}\mathcal{L}\left(\frac{\sqrt{U_1^2+U_2^2}}{\sqrt{f^{XX}_{1,0}(\omega)f^{YY}_{1,0}(\alpha\omega+\beta)}}\right), & \text{if } f^{XY}_{\alpha,\beta}(\omega)=0,\\ \mathcal{N}_1(\mathbf{0},\boldsymbol{A}_2\mathbf{\Lambda}_\vartheta(\omega,\alpha\omega+\beta)\boldsymbol{A}_2^{\mathrm{T}}), & \text{if } f^{XY}_{\alpha,\beta}(\omega)\neq 0,\end{cases}$$

the random vector $[U_1,U_2]^{\mathrm{T}}$ *has a two-dimensional normal distribution* $\mathcal{N}_2(\mathbf{0},\mathbf{\Lambda}_\vartheta(\omega,\alpha\omega+\beta))$, *and the vector* $\boldsymbol{A}_2\in\mathbb{R}^{1\times 2}$ *has the form*

$$\boldsymbol{A}_2=\left|\gamma^{XY}_{\alpha,\beta}(\omega)\right|\left[\frac{\mathrm{Re}\left(f^{XY}_{\alpha,\beta}(\omega)\right)}{\left|f^{XY}_{\alpha,\beta}(\omega)\right|^2},-\frac{1}{2f^{XX}_{1,0}(\omega)},-\frac{1}{2f^{YY}_{1,0}(\alpha\omega+\beta)},\frac{\mathrm{Im}\left(f^{XY}_{\alpha,\beta}(\omega)\right)}{\left|f^{XY}_{\alpha,\beta}(\omega)\right|^2}\right].$$

Proof. See Section 3.6. □

3.4 Consistency of subsampling procedure

In this section, our aim is to establish the consistency of the subsampling procedure for spectral characteristics. Recall that we focus on two cases:

Case 1. The magnitude of the spectral density function corresponding to the line $\{(\omega,\nu)\in\mathbb{R}:\nu=\alpha\omega+\beta\}$, i.e., for the fixed point $\omega\in\mathbb{R}$, which is not the intersection point of the support lines, we consider

$$\theta=\left|f^{XY}_{\alpha,\beta}(\omega)\right|,\quad \widehat{\theta}_T=\left|\widehat{f}^{XY}_{\alpha,\beta}(\omega)\right|,\quad \widehat{\theta}_{T,b,\Delta s}=\left|\widehat{f}^{XY}_{\alpha,\beta}(\omega)_{s\Delta,b}\right|;$$

Case 2. The magnitude of the spectral coherence function corresponding to the line $\{(\omega,\nu)\in\mathbb{R}:\nu=\alpha\omega+\beta\}$, i.e., for the fixed point $\omega\in\mathbb{R}$, which is not the intersection point of the support lines, we consider

$$\theta=\left|\gamma^{XY}_{\alpha,\beta}(\omega)\right|,\quad \widehat{\theta}_T=\left|\widehat{\gamma}^{XY}_{\alpha,\beta}(\omega)\right|,\quad \widehat{\theta}_{T,b,\Delta s}=\left|\widehat{\gamma}^{XY}_{\alpha,\beta}(\omega)_{s\Delta,b}\right|.$$

We exclude intersection points because we do not have asymptotic properties for them.

First, note that the subsampling estimators in both cases are not always well-defined for certain subsamples. As stated in Proposition 3.1, the normalizing factor $\mathcal{E}_{s\Delta/b}(\alpha)\neq 0$ for $\alpha\neq 1$, if

$$\left|\frac{s\Delta}{b}\right|\leq\frac{1}{2}\frac{\alpha+1}{|\alpha-1|}.$$

The above inequality is equivalent to

$$-\frac{b}{2\Delta}\frac{\alpha+1}{|\alpha-1|}\leq s\leq\frac{b}{2\Delta}\frac{\alpha+1}{|\alpha-1|}.$$

To ensure well-defined estimators, we have to restrict the set of subsamples to those for which the normalizing factor is non-zero, in order to avoid division by zero. That is subsamples indexed by $s=-l_T,-l_T+1,\ldots,l_T$, where

$$l_T=\begin{cases}\frac{T-b}{2\Delta}, & \alpha=1,\\ \left\lfloor\frac{b}{2\Delta}\frac{1+\alpha}{|\alpha-1|}\right\rfloor, & \alpha\neq 1.\end{cases}\tag{3.4}$$

Note that for $\alpha\neq 1$ the number of subsamples for which the subsampling estimator is well defined is $2l_T+1$. This quantity grows significantly slower than the total number of subsamples $2q_T+1$, as $T\to\infty$ and $b=o(T)$. This is a crucial difference compared to subsampling in spectral analysis for APC processes ($\alpha=1$), where we can select all available blocks (see [51]).

To obtain consistency of subsampling for time series using Theorem 3.1, it should be assumed that the time series is α-mixing. However, in our case, this assumption does not hold. For example, let $X(t)$ be a stationary process with an autocovariance function $\gamma_X(\tau)$ taking the maximum value at $\tau=0$, decreasing as a function of $|\tau|$ and $\lim_{|\tau|\to\infty}\gamma_X(\tau)=0$. Moreover, assume that $\sup_{t\in\mathbb{R}}\mathbb{E}|X(t)|^{2+\delta}<\infty$ for some $\delta>0$. Define $Y(t)=X(st)$ with $s>0$. Such processes are a special case of those presented in Example 1.3. Note that

$$\mathrm{Cov}(X(t),Y(t+\tau))=\gamma_X(s(t+\tau)-t).$$

The covariance can be bounded from above by an α-mixing measure between two σ-fields (see Lemma B.2). That is,

$$\begin{aligned} 0 < |\gamma_X(0)| &= \sup_{t\in\mathbb{R}} |\mathrm{Cov}(X(t), Y(t+\tau))| \\ &\leq 8 \sup_{t\in\mathbb{R}} \left[\left(\mathbb{E}|X(t)|^{2+\delta} \right)^{\frac{1}{2+\delta}} \left(\mathbb{E}|Y(t+\tau)|^{2+\delta} \right)^{\frac{1}{2+\delta}} \alpha_{XY}^{\frac{\delta}{2+\delta}}(|\tau|) \right] \\ &\leq 8 \left(\sup_{t\in\mathbb{R}} \mathbb{E}|X(t)|^{2+\delta} \right)^{\frac{2}{2+\delta}} \alpha_{XY}^{\frac{\delta}{2+\delta}}(|\tau|), \end{aligned}$$

where

$$\alpha_{XY}(\tau) = \sup_{t\in\mathbb{R}} \alpha\left(\mathcal{F}_{XY}(-\infty, t), \mathcal{F}_{XY}(t+\tau, +\infty)\right),$$

with $\mathcal{F}_{XY}(a,b) = \sigma\left(\{X(t),\, a \leq t \leq b\}, \{Y(t),\, a \leq t \leq b\}\right)$. For the definition of function $\alpha(\cdot,\cdot)$ see (B.2). The α-mixing function α_{XY} is bounded from below by a positive constant and consequently cannot converge to zero. Thus, a milder assumption of weak dependency should be made.

Assumption 3.3. Consider the following assumptions.

(i) Assume that there exists a function $h(t,\tau)$ such that for all $t \in \mathbb{R}$ is a decreasing function of $|\tau|$, with $\sup_{t\in\mathbb{R}} \int_{\mathbb{R}} h(t,\tau)\,\mathrm{d}\tau = M$ for some positive constant M. Moreover, for $t, \tau \in \mathbb{R}$

$$\alpha\left(\mathcal{F}_{XY}(-\infty, t), \mathcal{F}_{XY}(t+\tau, +\infty)\right) \leq h(t,\tau) \leq \frac{1}{4}.$$

(ii) $b = \mathcal{O}(T^p)$ and $\Delta = \mathcal{O}(T^{-q})$, with $p, q \in (0,1)$. Moreover, $\frac{bh_b}{Th_T} \to 0$ as $T \to \infty$.

(iii) The asymptotic distributions of $\sqrt{bh_b}\big(\widehat{\theta}_{T,b,s\Delta} - \theta\big)$ do not depend on $s = -l_T, -l_T+1, \ldots, l_T$

The condition (i) is introduced to address the limitations of the α-mixing assumption that appears in Theorem 3.1. The condition (ii) imposes the convergence rates of the subsample size b and the overlapping factor Δ. The condition (iii) is used to address the issue of varying asymptotic distributions across different subsamples. For example, using a rectangular window function as a data-tapering window, the asymptotic distributions of the subsampling estimators are the same across all subsamples. In particular, Assumption 3.1, assumed in Theorem 3.1, is satisfied.

Proposition 3.2. *For Case 1, assume the same conditions as in Corollary 3.1. For Case 2, assume the same conditions as in Theorem 3.6. Then using the rectangular window function as a data-tapering window w, the asymptotic distributions of $\sqrt{bh_b}(\widehat{\theta}_{T,s\Delta,b} - \theta)$ do not depend on $s = -l_T, -l_T+1, \ldots, l_T$, provided that*

$$l_T = \begin{cases} \frac{T-b}{2\Delta}, & \alpha = 1, \\ \left\lfloor \frac{b}{2\Delta} \right\rfloor, & \alpha \neq 1. \end{cases} \tag{3.5}$$

.

Note that the value of l_T given by (3.5), for fixed $\alpha \neq 1$, is smaller than that in (3.4), however, asymptotically, they behave in the same way.

In the following, we provide an example of processes that satisfy the condition (i). Specifically, the processes in Example 1.3 fulfill this assumption.

Proposition 3.3. *Let $Z(t)$ be an α-mixing process. Let $L, K \in \mathbb{N}$. Consider two processes*

$$X(t) = g_1(Z(s_1 t), \ldots, Z(s_K t)), \quad Y(t) = g_2(Z(r_1 t), \ldots, Z(r_L t)),$$

where $g_1 : \mathbb{R}^K \mapsto \mathbb{R}$ and $g_2 : \mathbb{R}^L \mapsto \mathbb{R}$ are deterministic and Borel measurable functions, and $s_1, \ldots, s_K > 0$, $r_1, \ldots, r_L > 0$. Assume that there exists some $\delta > 0$ such that $\sup_{t\in\mathbb{R}} \mathbb{E}|Z(t)|^{2+\delta} < \infty$ and $\int_{\mathbb{R}} \alpha_Z^{\delta/(2+\delta)}(\tau)\, \mathrm{d}\tau < \infty$. Then the processes $X(t)$ and $Y(t)$ satisfy the condition (i) of Assumption 3.3.

Proof. See Section 3.6. □

The following result states the consistency of subsampling for both the spectral density estimator and the coherence estimator.

Theorem 3.7. *For Case 1, assume the same conditions as in Corollary 3.1. For Case 2, assume the same conditions as in Theorem 3.6. Assume that l_T is given by* (3.5)*. In both cases, under Assumption 3.3, we have that*

(i) If x is a continuity point of $J^\theta(\cdot)$, then $L^\theta_{T,b}(x) \to J^\theta(x)$ in probability.

(ii) If $J^\theta(\cdot,)$ is continuous, then $\sup_{x\in\mathbb{R}} \left|L^\theta_{T,b}(x) - J^\theta(x)\right| \to 0$ in probability.

(iii) For $\rho \in (0,1)$, let $c^\theta_{T,b}(1-\rho) = \inf\{x : L^\theta_{T,b}(x) \geq 1-\rho\}$. Correspondingly, define $c^\theta(1-\rho) = \inf\{x : J^\theta(x) \geq 1-\rho\}$. If $J^\theta(\cdot)$ is continuous at $c^\theta(1-\rho)$, then

$$\mathbb{P}\left(\sqrt{Th_T}\left(\widehat{\theta}_T - \theta\right) \leq c^\theta_{T,b}(1-\rho)\right) \longrightarrow 1-\rho, \quad \text{as} \quad T \to \infty.$$

Proof. See Section 3.6. □

Remark 3.1. From the proof of Theorem 3.7, one can conclude that for $\alpha \neq 1$, subsampling converges more slowly than for $\alpha = 1$. This is due to the fact that the number of overlapping blocks $2l_T + 1$, given by (3.5), increases slower to infinity for $\alpha \neq 1$ than for $\alpha = 1$.

Using Theorem 3.7, one can construct, for example, equal-tailed confidence intervals, which are usually asymmetric. In our case, the limiting distribution of J^θ_T is symmetric. Therefore, a two-sided symmetric confidence interval may be a more appropriate choice. To achieve this, our objective is to estimate the two-sided distribution of $\sqrt{Th_T}|\widehat{\theta}_T - \theta|$ denoted by $J^\theta_{T,|\cdot|}$. Its subsampling approximation is given by

$$L^\theta_{T,b,|\cdot|}(x) = \frac{1}{2l_T+1} \sum_{j=-l_T}^{l_T} \mathbb{1}_{\{\sqrt{bh_b}|\widehat{\theta}_{T,b,j\Delta} - \widehat{\theta}_T| \leq x\}}, \quad x \in \mathbb{R},$$

see [72, p. 72–73]. By $J^\theta_{|\cdot|}$ we denote the law such that $J^\theta_{T,|\cdot|} \to J^\theta_{|\cdot|}$ as $T \to \infty$. Moreover, $J^\theta_{|\cdot|}(\cdot)$ is a cumulative distribution function $J^\theta_{|\cdot|}$. The following theorem states the validity of two-sided confidence intervals.

Corollary 3.2. *Under the conditions of Theorem 3.7, the following are satisfied. Then:*

(i) If x is a continuity point of $J^\theta_{|\cdot|}(\cdot)$, then $L^\theta_{T,b,|\cdot|}(x) \to J^\theta_{|\cdot|}(x)$ in probability.

(ii) If $J^{\theta}(\cdot)$ is continuous, then $\sup_{x\in\mathbb{R}} \left|L^{\theta}_{T,b,|\cdot|}(x) - J^{\theta}_{|\cdot|}(x)\right| \to 0$ *in probability.*

(iii) For $\rho \in (0,1)$, let $c^{\theta}_{T,b,|\cdot|}(1-\rho) = \inf\{x : L^{\theta}_{T,b,|\cdot|}(x) \geq 1-\rho\}$. *Correspondingly, define* $c^{\theta}_{|\cdot|}(1-\rho) = \inf\{x : J^{\theta}_{|\cdot|}(x) \geq 1-\rho\}$. *If $J^{\theta}_{|\cdot|}(\cdot)$ is continuous at $c^{\theta}_{|\cdot|}(1-\rho)$, then*

$$\mathbb{P}\left(\sqrt{Th_T}\left|\widehat{\theta}_T - \theta\right| \leq c^{\theta}_{T,b,|\cdot|}(1-\rho)\right) \longrightarrow 1-\rho, \quad as \quad T\to\infty.$$

Proof. See Section 3.6. □

In the next section, we discuss the construction of confidence intervals based on our subsampling procedure.

3.5 Subsampling-based confidence intervals

As noted, the asymptotic covariances of the rescaled estimators for the spectral density magnitude $|f^{XY}_{\alpha,\beta}(\omega)|$ and the spectral coherence magnitude $|\gamma^{XY}_{\alpha,\beta}(\omega)|$ have complicated formulas and are consequently difficult to estimate. Therefore, resampling methods can be employed to construct confidence intervals. This approach is commonly used for various frequency domain and time domain characteristics, for example, in the case of APC processes (see, e.g. [23, 27, 51]). Using Theorem 3.7 equal-tailed confidence interval at the $1-\rho$ confidence level for the parameter θ based on our subsampling procedure is given by

$$\left(\hat{\theta}_T - \frac{c^{\theta}_{T,b}\left(1-\frac{\rho}{2}\right)}{\sqrt{Th_T}}, \hat{\theta}_T - \frac{c^{\theta}_{T,b}\left(\frac{\rho}{2}\right)}{\sqrt{Th_T}}\right), \tag{3.6}$$

where $c^{\theta}_{T,b}(\cdot)$ is given in Theorem 3.7. Furthermore, applying Corollary 3.2, we can construct a two-sided symmetric confidence interval at the $1-\rho$ confidence level for the parameter θ based on our subsampling procedure. Specifically, we have

$$\left(\hat{\theta}_T - \frac{c^{\theta}_{T,b,|\cdot|}(1-\rho)}{\sqrt{Th_T}}, \hat{\theta}_T + \frac{c^{\theta}_{T,b,|\cdot|}(1-\rho)}{\sqrt{Th_T}}\right), \tag{3.7}$$

where $c^{\theta}_{T,b,|\cdot|}(\cdot)$ is given in Corollary 3.2.

3.6 Proofs of results presented in Chapter 3

This section contains proofs of the original results presented in this chapter.

Proof of Proposition 3.1. By $\mathcal{F}\{\cdot\}$ and $\mathcal{F}^{-1}\{\cdot\}$, we denote the Fourier transform and the inverse Fourier transform operators, respectively. Note that

$$W(\nu) = \int_{\mathbb{R}} w(t)\, e^{-i2\pi\nu t}\,\mathrm{d}t = \mathcal{F}\{w\}(\nu),$$

$$W(-\alpha\nu) = \int_{\mathbb{R}} w(t)\, e^{i2\pi\alpha\nu t}\,\mathrm{d}t = \frac{1}{\alpha}\int_{\mathbb{R}} w\left(-\frac{t}{\alpha}\right) e^{-i2\pi\nu t}\,\mathrm{d}t = \mathcal{F}\{w_\alpha\}(\nu),$$

where $w_\alpha(t) = \frac{1}{\alpha} w\left(-\frac{t}{\alpha}\right)$. By the convolution theorem, we get the following

$$\begin{aligned}\mathcal{E}_\vartheta(\alpha) &= \int_{\mathbb{R}} \mathcal{F}\{w\}(\nu) \cdot \mathcal{F}\{w_\alpha\}(\nu)\, e^{i2\pi(\alpha-1)\nu\vartheta}\,\mathrm{d}\nu = \int_{\mathbb{R}} \mathcal{F}\left\{w * w_\alpha\right\}(\nu)\, e^{i2\pi(\alpha-1)\nu\vartheta}\,\mathrm{d}\nu \\ &= \mathcal{F}^{-1}\left\{\mathcal{F}\{w * w_\alpha\}\right\}((\alpha-1)\vartheta) = \frac{1}{\alpha}\int_{\mathbb{R}} w(u)\, w\left(\frac{u-(\alpha-1)\vartheta}{\alpha}\right)\mathrm{d}u \\ &= \int_{\mathbb{R}} w(t)\, w(\alpha t + (\alpha-1)\vartheta))\,\mathrm{d}t.\end{aligned}$$

The last equality follows from the change of variables $t = \frac{u-(\alpha-1)\vartheta}{\alpha}$. The supports of functions $w(t)$ and $w(\alpha t+(\alpha-1)\vartheta)$ are given by the following inequalities, respectively, $|t| \le \frac{1}{2}$ and $|\alpha t+(\alpha-1)\vartheta| \le \frac{1}{2}$. Equivalently, for $\alpha > 0$

$$-\frac{1}{2} \le t \le \frac{1}{2}, \quad -\frac{1}{2\alpha} + \frac{1-\alpha}{\alpha}\vartheta \le t \le \frac{1}{2\alpha} + \frac{1-\alpha}{\alpha}\vartheta.$$

Therefore, the support of $w(t)\, w(\alpha t + (\alpha-1)\vartheta)$ has non-zero Lebesgue measure if

$$\left|\frac{1-\alpha}{\alpha}\vartheta\right| \le \frac{1}{2} + \frac{1}{2\alpha},$$

and equivalently,

$$|\vartheta| \le \frac{1}{2}\frac{\alpha+1}{|1-\alpha|}. \tag{3.8}$$

Thus, $\mathcal{E}_\vartheta(\alpha)$ is non-zero provided that (3.8) holds. □

Proof of Theorem 3.2. Using Lemma B.4 and similar steps as in the proof of Theorem 2.1, we have

$$\begin{aligned}\mathbb{E}\left[\widetilde{f}^{XY}_{\alpha,\beta}(\omega)_{c_T,d_T}\right] &= \frac{1}{d_T}\int_{\mathbb{R}}\int_{\mathbb{R}}\int_{\mathbb{R}} \mathbb{E}\left[X(t)\,\overline{Y(t)}\right]\, w\left(\tfrac{t-c_T}{d_T}\right)\, w\left(\tfrac{s-c_T}{d_T}\right) \\ &\qquad \times e^{-i2\pi\mu t}\, e^{i2\pi(\alpha\mu+\beta)s}\, \tfrac{1}{h_{d_T}} q\left(\tfrac{\omega-\mu}{h_{d_T}}\right)\,\mathrm{d}t\,\mathrm{d}s\,\mathrm{d}\mu \\ &= \frac{1}{d_T h_{d_T}} \sum_{(\gamma,\delta)\in\mathcal{K}^{XY}} \int_{\mathbb{R}}\int_{\mathbb{R}}\int_{\mathbb{R}}\int_{\mathbb{R}} f^{XY}_{\gamma,\delta}(\nu)\, e^{i2\pi(\nu t-(\gamma\nu+\delta)s)}\, w\left(\tfrac{t-c_T}{d_T}\right)\, w\left(\tfrac{s-c_T}{d_T}\right) \\ &\qquad \times e^{-i2\pi\mu t}\, e^{i2\pi(\alpha\mu+\beta)s}\, q\left(\tfrac{\omega-\mu}{h_{d_T}}\right)\,\mathrm{d}t\,\mathrm{d}s\,\mathrm{d}\mu\,\mathrm{d}\nu \\ &= \frac{1}{d_T h_{d_T}} \sum_{(\gamma,\delta)\in\mathcal{K}^{XY}} \int_{\mathbb{R}}\int_{\mathbb{R}} f^{XY}_{\gamma,\delta}(\nu)\, q\left(\tfrac{\omega-\mu}{h_{d_T}}\right) \int_{\mathbb{R}} w\left(\tfrac{t-c_T}{d_T}\right)\, e^{i2\pi(\nu-\mu)t)}\,\mathrm{d}t \\ &\qquad \times \int_{\mathbb{R}} w\left(\tfrac{s-c_T}{d_T}\right)\, e^{-i2\pi(\gamma\nu-\alpha\mu+\delta-\beta)s}\,\mathrm{d}s\,\mathrm{d}\mu\,\mathrm{d}\nu \\ &= \frac{d_T}{h_{d_T}} \sum_{(\gamma,\delta)\in\mathcal{K}^{XY}} \int_{\mathbb{R}}\int_{\mathbb{R}} f^{XY}_{\gamma,\delta}(\nu)\, q\left(\tfrac{\omega-\mu}{h_{d_T}}\right)\, W(d_T(\mu-\nu))\, W(d_T(\gamma\nu-\alpha\mu+\delta-\beta)) \\ &\qquad \times e^{-i2\pi(\mu-\nu)c_T}\, e^{-i2\pi(\gamma\nu+\delta-\alpha\mu-\beta)c_T}\,\mathrm{d}\mu\,\mathrm{d}\nu.\end{aligned}$$

We consider the following change the variables $\lambda = \frac{\omega-\mu}{h_{d_T}}$ and $\eta = d_T(\mu-\nu)$. Then

$$\mu = \omega - \lambda h_{d_T}, \quad \nu = \omega - \lambda h_{d_T} - \tfrac{\eta}{d_T}$$

$$d_T(\gamma\nu - \alpha\mu + \delta - \beta) = -\gamma\eta + \underbrace{d_T(\gamma-\alpha)(\omega - \lambda h_{d_T}) + d_T(\delta-\beta)}_{=\eta_{d_T}}.$$

Hence,

$$\begin{aligned}
&\mathbb{E}\left[\widetilde{f}^{XY}_{\alpha,\beta}(\omega)_{c_T,d_T}\right] = \\
&\quad= \sum_{(\gamma,\delta)\in\mathcal{K}^{XY}} \int_{\mathbb{R}}\int_{\mathbb{R}} f^{XY}_{\gamma,\delta}\big(\omega - \lambda h_{d_T} - \tfrac{\eta}{d_T}\big)\, q(\lambda)\, W(\eta)\, W(-\gamma\eta + \eta_{d_T})\, e^{-i2\pi\eta c_T/d_T}\, e^{-i2\pi(-\gamma\eta+\eta_{d_T})c_T/d_T} \\
&\quad= \sum_{(\gamma,\delta)\in\mathcal{K}^{XY}} E(\gamma,\delta).
\end{aligned}$$

Consider the limit of each $E(\gamma,\delta)$ in two cases: $(\gamma,\delta) = (\alpha,\beta)$ and $(\gamma,\delta) \neq (\alpha,\beta)$.

Let us start with the term corresponding to $(\gamma,\delta) = (\alpha,\beta)$. In that case, we have $\eta_T = 0$. Using twice the first-order Taylor approximations, we have

$$\begin{aligned}
f^{XY}_{\alpha,\beta}\big(\omega - \lambda h_{d_T} - \tfrac{\eta}{d_T}\big) &= f^{XY}_{\alpha,\beta}\big(\omega - \tfrac{\eta}{d_T}\big) - \lambda h_{d_T}\big(f^{XY}_{\alpha,\beta}\big)'\big(\omega - \tfrac{\eta}{d_T} - \widetilde{\varrho}\lambda h_{d_T}\big) \\
&= f^{XY}_{\alpha,\beta}(\omega) - \tfrac{\eta}{d_T}\big(f^{XY}_{\alpha,\beta}\big)'\big(\omega - \varrho\tfrac{\eta}{d_T}\big) - \lambda h_{d_T}\big(f^{XY}_{\alpha,\beta}\big)'\big(\omega - \tfrac{\eta}{d_T} - \widetilde{\varrho}\lambda h_{d_T}\big),
\end{aligned}$$

for some $\varrho, \widetilde{\varrho} \in [0,1]$. Thus $G(\alpha,\beta) = E_1 - E_2 - E_3$.

For E_1, we have

$$E_1 = \int_{\mathbb{R}}\int_{\mathbb{R}} f^{XY}_{\alpha,\beta}(\omega) q(\lambda) W(\eta) W(-\alpha\eta) e^{i2\pi(\alpha-1)\eta c_T/d_T}\,\mathrm{d}\lambda\,\mathrm{d}\mu = f^{XY}_{\alpha,\beta}(\omega)\,\mathcal{E}_{c_T/d_T}(\alpha).$$

By (ii) and (iii) from Assumption 2.1, (i) and (ii) from Assumption 2.3, and applying Hölder inequality, we obtain

$$\begin{aligned}
|E_2| &\le \frac{1}{d_T}\int_{\mathbb{R}} \Big|\big(f^{XY}_{\alpha,\beta}\big)'\big(\omega - \varrho\tfrac{\eta}{d_T}\big)\,\eta\, W(\eta)\, W(-\alpha\eta)\Big|\,\mathrm{d}\eta \int_{\mathbb{R}} q(\lambda)\,\mathrm{d}\lambda \\
&\le \frac{K_W}{d_T}\int_{\mathbb{R}} \Big|\big(f^{XY}_{\alpha,\beta}\big)'\big(\omega - \varrho\tfrac{\eta}{d_T}\big)\, W(-\alpha\eta)\Big|\,\mathrm{d}\eta \\
&\le \frac{K_W}{d_T}\left(\int_{\mathbb{R}} \Big|\big(f^{XY}_{\alpha,\beta}\big)'\big(\omega - \varrho\tfrac{\eta}{d_T}\big)\Big|^2\,\mathrm{d}\eta \int_{\mathbb{R}} |W(-\alpha\eta)|^2\,\mathrm{d}\eta\right)^{1/2} \\
&\frac{K_W}{\sqrt{\varrho d_T}}\left(\int_{\mathbb{R}} |\big(f^{XY}_{\alpha,\beta}\big)'(\eta)|^2\,\mathrm{d}\eta \int_{\mathbb{R}} |W(-\alpha\eta)|^2\,\mathrm{d}\eta\right)^{1/2} = C_1\, d_T^{\frac{1}{2}},
\end{aligned}$$

and

$$\begin{aligned}
|E_3| &\le h_{d_T}\int_{\mathbb{R}}\int_{\mathbb{R}} \Big|\lambda\big(f^{XY}_{\alpha,\beta}\big)'\big(\omega - \tfrac{\eta}{d_T} - \widetilde{\varrho}\lambda h_{d_T}\big)\, q(\lambda)\, W(\eta)\, W(-\alpha\eta)\Big|\,\mathrm{d}\eta\,\mathrm{d}\lambda \\
&\le h_{d_T}\left\|\big(f^{XY}_{\alpha,\beta}\big)'\right\|_\infty \int_{-1/2}^{1/2} |\lambda q(\lambda)|\,\mathrm{d}\lambda \int_{\mathbb{R}} |W(\eta)W(-\alpha\eta)|\,\mathrm{d}\eta = C_2\, d_T^{-\kappa},
\end{aligned}$$

with some constants $C_1, C_2 > 0$.

Now let us consider $E(\gamma,\delta)$, with $(\gamma,\delta)\neq(\alpha,\beta)$. Note that

$$|E(\gamma,\delta)| \leq \left\|f^{XY}_{\gamma,\delta}\right\|_\infty \int\limits_{\mathbb{R}} |q(\lambda)| \int\limits_{\mathbb{R}} |W(\eta)W(-\gamma\eta + d_T((\gamma-\alpha)(\omega-h_{d_T}\lambda)+\delta-\beta))|\,\mathrm{d}\eta\,\mathrm{d}\mu.$$

Define $W_{M_T}(\eta) = W(\eta)\mathbb{1}_{[-M_T/2,M_T/2]}(\eta)$ with $M_T = \mathcal{O}\Big(d_T^{\frac{2}{3}}\Big)$. Then by Lemma B.9, we have

$$\begin{aligned}\int\limits_{\mathbb{R}} &|W(\eta)W(-\gamma\eta + d_T((\gamma-\alpha)(\omega-h_{d_T}\mu)+\delta-\beta))|\,\mathrm{d}\eta \\ &= \int\limits_{\mathbb{R}} |\widetilde{W}_{M_T}(\eta)\widetilde{W}_{M_T}(-\gamma\eta+\eta_T)|\,\mathrm{d}\eta + \mathcal{O}\left(d_T^{-\frac{1}{3}}\right),\end{aligned}$$

where $\eta_T = d_T((\gamma-\alpha)(\lambda-h_{d_T}\mu)+\delta-\beta)$. Observe that the support of $W_{M_T}(\eta)$ and $W_{M_T}(-\gamma\eta+\eta_T)$ are given by the following inequalities, respectively,

$$-\frac{M_T}{2} \leq \eta \leq \frac{M_T}{2}, \quad -\frac{M_T}{2\gamma} + \frac{\eta_T}{\gamma} \leq \eta \leq \frac{M_T}{2\gamma} + \frac{\eta_T}{\gamma}.$$

Therefore, the support of $W_{M_T}(\eta)\,W_{M_T}(-\gamma\eta+\eta_T)$ has a zero Lebesgue measure if $|\eta_T| \geq \frac{M_T}{2}(1+\gamma)$, which is satisfied for sufficiently large T. Hence, for enough large T

$$\int\limits_{\mathbb{R}} |W(\eta)\,W(-\gamma\eta + d_T((\gamma-\alpha)(\omega-h_{d_T}\lambda)+\delta-\beta))|\,\mathrm{d}\eta = \mathcal{O}\left(d_T^{-\frac{1}{3}}\right).$$

To summarize, we obtain

$$\begin{aligned}\varepsilon_{c_T,d_T}(\omega) &= \sqrt{d_T h_T}\left|\mathbb{E}\left[\widehat{f}^{c_T,d_T}_{\alpha,\beta}(\omega)\right] - f_{\alpha,\beta}(\omega)\right| \\ &\leq \sqrt{d_T h_{d_T}}\left(\left|\frac{E(\alpha,\beta)}{\mathcal{E}_{c_T/d_T}(\alpha)} - f_{\alpha,\beta}(\omega)\right| + \sum_{(\gamma,\delta)\neq(\alpha,\beta)} \frac{|E(\gamma,\beta)|}{|\mathcal{E}_{c_T/d_T}(\alpha)|}\right) \\ &\leq \frac{\sqrt{d_T h_{d_T}}}{|\mathcal{E}_{c_T/d_T}(\alpha)|}\left(|E_2| + |E_3| + \sum_{(\gamma,\delta)\neq(\alpha,\beta)} |E(\gamma,\beta)|\right) \\ &\leq \frac{d_T^{\frac{1}{2}(1-\kappa)}}{|\mathcal{E}_{c_T/d_T}(\alpha)|}\left(C_1 d_T^{-\frac{1}{2}} + C_2 d_T^{-\kappa} + C_3 d_T^{-\frac{1}{3}}\right) \\ &= \frac{\left(C_1 d_T^{-\frac{1}{2}\kappa} + C_2 d_T^{\frac{1}{2}(1-3\kappa)} + C_3 d_T^{\frac{1}{6}(1-3\kappa)}\right)}{|\mathcal{E}_{c_T/d_T}(\alpha)|},\end{aligned}$$

for sufficiently large T. Moreover, by Lemma B.8, we get $\lim_{T\to\infty}\varepsilon_{c_T,d_T}(\omega) = 0$, provided that $\kappa > \frac{1}{3}$. □

Proof of Theorem 3.3. From the following properties of the cumulants

$$\begin{aligned}\mathrm{Cov}\big(Y(t_1)\overline{X(t_2)}, Y(t_3)\overline{X(t_4)}\big) &= \mathrm{cum}\big(Y(t_1), \overline{X(t_2)}, \overline{Y(t_3)}, X(t_4)\big) \\ &\quad + \mathbb{E}\big(Y(t_1)\overline{Y(t_3)}\big)\mathbb{E}\big(\overline{X(t_2)}X(t_4)\big) \\ &\quad + \mathbb{E}\big(Y(t_1)X(t_4)\big)\mathbb{E}\big(\overline{X(t_2)Y(t_3)}\big)\end{aligned}$$

we obtain

$$d_T h_{d_T} \operatorname{Cov}\left(\widetilde{f}^{XY}_{\alpha_1,\beta_1}(\omega_1)_{c_T,d_T}, \widetilde{f}^{XY}_{\alpha_2,\beta_2}(\omega_2)_{c_T,d_T})\right) = \mathcal{D}_1 + \mathcal{D}_2 + \mathcal{D}_3.$$

The first term $\mathcal{D}_1$ (related to the 4th-order cumulant) has the form

$$\begin{aligned}\mathcal{D}_1 = \frac{1}{d_T h_{d_T}} \int\limits_{\mathbb{R}}\int\limits_{\mathbb{R}}\int\limits_{\mathbb{R}}\int\limits_{\mathbb{R}}\int\limits_{\mathbb{R}}\int\limits_{\mathbb{R}} &\operatorname{cum}\big(Y(t_1), \overline{X(t_2)}, \overline{Y(t_3)}, X(t_4)\big)\\ &\times w\left(\tfrac{t_1-c_T}{d_T}\right) w\left(\tfrac{t_2-c_T}{d_T}\right) w\left(\tfrac{t_3-c_T}{d_T}\right) w\left(\tfrac{t_4-c_T}{d_T}\right)\\ &\times e^{-i2\pi\mu_1 t_1} e^{i2\pi(\alpha_1\mu_1+\beta_1)t_2} e^{i2\pi\mu_2 t_3} e^{-i2\pi(\alpha_2\mu_2+\beta_2)t_4}\\ &\times q\left(\tfrac{\omega_1-\mu_1}{h_{d_T}}\right) q\left(\tfrac{\omega_2-\mu_2}{h_{d_T}}\right) \mathrm{d}t_1\,\mathrm{d}t_2\,\mathrm{d}t_3\,\mathrm{d}t_4\,\mathrm{d}\mu_1\,\mathrm{d}\mu_2,\end{aligned}$$

and tends to zero as $T \to \infty$ (see the proof of Theorem 3.4, i.e. the convergence of the term $\mathcal{T}_{\boldsymbol{v}}$ with $\boldsymbol{v} = (v_1)$).

For the second term $\mathcal{D}_2$, we have

$$\begin{aligned}\mathcal{D}_2 &= \frac{1}{d_T h_{d_T}} \int\limits_{\mathbb{R}}\int\limits_{\mathbb{R}}\int\limits_{\mathbb{R}}\int\limits_{\mathbb{R}}\int\limits_{\mathbb{R}}\int\limits_{\mathbb{R}} \mathbb{E}\left(Y(t_1)\overline{Y(t_3)}\right) \mathbb{E}\left(\overline{X(t_2)}X(t_4)\right)\\ &\quad\times w\left(\tfrac{t_1-c_T}{d_T}\right) w\left(\tfrac{t_2-c_T}{d_T}\right) w\left(\tfrac{t_3-c_T}{d_T}\right) w\left(\tfrac{t_4-c_T}{d_T}\right)\\ &\quad\times e^{-i2\pi\mu_1 t_1} e^{i2\pi(\alpha_1\mu_1+\beta_1)t_2} e^{i2\pi\mu_2 t_3} e^{-i2\pi(\alpha_2\mu_2+\beta_2)t_4}\\ &\quad\times q\left(\tfrac{\omega_1-\mu_1}{h_{d_T}}\right) q\left(\tfrac{\omega_2-\mu_2}{h_{d_T}}\right) \mathrm{d}t_1\,\mathrm{d}t_2\,\mathrm{d}t_3\,\mathrm{d}t_4\,\mathrm{d}\mu_1\,\mathrm{d}\mu_2,\\ &= \frac{1}{d_T h_{d_T}} \int\limits_{\mathbb{R}}\int\limits_{\mathbb{R}} \sum_{(\gamma_1,\delta_1)\in\mathcal{K}^{YY}} \int\limits_{\mathbb{R}} f^{YY}_{\gamma_1,\delta_1}(\nu_1) \sum_{(\gamma_2,\delta_2)\in\mathcal{K}^{\overline{XX}}} \int\limits_{\mathbb{R}} f^{\overline{XX}}_{\gamma_2,\delta_2}(\nu_2)\\ &\quad\times \int\limits_{\mathbb{R}} w\left(\tfrac{t_1-c_T}{d_T}\right) e^{-i2\pi\mu_1 t_1} e^{i2\pi\nu_1 t_1}\,\mathrm{d}t_1\\ &\quad\times \int\limits_{\mathbb{R}} w\left(\tfrac{t_2-c_T}{d_T}\right) e^{i2\pi(\alpha_1\mu_1+\beta_1)t_2} e^{i2\pi\nu_2 t_2}\,\mathrm{d}t_2\\ &\quad\times \int\limits_{\mathbb{R}} w\left(\tfrac{t_3-c_T}{d_T}\right) e^{i2\pi\mu_2 t_3} e^{-i2\pi(\gamma_1\nu_1+\delta_1)t_3}\,\mathrm{d}t_3\\ &\quad\times \int\limits_{\mathbb{R}} w\left(\tfrac{t_4-c_T}{d_T}\right) e^{-i2\pi(\alpha_2\mu_2+\beta_2)t_4} e^{-i2\pi(\gamma_2\nu_2+\delta_2)t_4}\,\mathrm{d}t_4\\ &\quad\times q\left(\tfrac{\omega_1-\mu_1}{h_{d_T}}\right) q\left(\tfrac{\omega_2-\mu_2}{h_{d_T}}\right) \mathrm{d}\nu_1\,\mathrm{d}\nu_2\,\mathrm{d}\mu_1\,\mathrm{d}\mu_2,\end{aligned}$$

and by Lemma B.4 we get

$$\begin{aligned}\mathcal{D}_2 = \frac{1}{d_T h_{d_T}} \int\limits_{\mathbb{R}}\int\limits_{\mathbb{R}} &\sum_{(\gamma_1,\delta_1)\in\mathcal{K}^{YY}} \int\limits_{\mathbb{R}} f^{YY}_{\gamma_1,\delta_1}(\nu_1) \sum_{(\gamma_2,\delta_2)\in\mathcal{K}^{\overline{XX}}} \int\limits_{\mathbb{R}} f^{\overline{XX}}_{\gamma_2,\delta_2}(\nu_2)\\ &\times d_T W(d_T(\mu_1-\nu_1)) \times d_T W(-d_T(\nu_2+\alpha_1\mu_1+\beta_1))\\ &\times d_T W(d_T(\gamma_1\nu_1+\delta_1-\mu_2)) \times d_T W(d_T(\alpha_2\mu_2+\beta_2+\gamma_2\nu_2+\delta_2))\\ &\times e^{-i2\pi(\mu_1-\nu_1)c_T} e^{i2\pi(\nu_2+\alpha_1\mu_1+\beta_1)c_T}\\ &\times e^{-i2\pi(\gamma_1\nu_1+\delta_1-\mu_2)c_T} e^{-i2\pi(\alpha_2\mu_2+\beta_2+\gamma_2\nu_2+\delta_2)c_T}\\ &\times q\left(\tfrac{\omega_1-\mu_1}{h_{d_T}}\right) q\left(\tfrac{\omega_2-\mu_2}{h_{d_T}}\right) \mathrm{d}\nu_1\,\mathrm{d}\nu_2\,\mathrm{d}\mu_1\,\mathrm{d}\mu_2.\end{aligned}$$

Let us consider the following change the variables

$$\begin{aligned}\lambda_1 &= \tfrac{\omega_1-\mu_1}{h_{d_T}},\\ \eta_1 &= d_T(\mu_1-\nu_1),\\ \eta_2 &= -d_T(\nu_2+\alpha_1\mu_1+\beta_1),\\ \eta_3 &= d_T(\gamma_1\nu_1+\delta_1-\mu_2),\end{aligned}$$

Then

$$\begin{aligned}\mu_1 &= \omega_1-\lambda_1 h_{d_T},\\ \nu_1 &= \mu_1-\tfrac{\eta_1}{d_T}=\omega_1-\lambda_1 h_{d_T}-\tfrac{\eta_1}{d_T},\\ \mu_2 &= \gamma_1\nu_1+\delta_1-\frac{\eta_3}{d_T}=\gamma_1\omega_1-\gamma_1\lambda_1 h_{d_T}-\gamma_1\tfrac{\eta_1}{d_T}+\delta_1-\tfrac{\eta_3}{d_T},\\ \nu_2 &= -\alpha_1\mu_1-\beta_1-\tfrac{\eta_2}{d_T}=-\alpha_1\omega_1+\alpha_1\lambda_1 h_{d_T}-\beta_1-\tfrac{\eta_2}{d_T},\end{aligned}$$

and

$$\frac{\omega_2-\mu_2}{h_{d_T}}=\gamma_1\lambda_1+\frac{\eta_3+\gamma_1\eta_1}{d_T h_{d_T}}+\frac{\omega_2-(\gamma_1\omega_1+\delta_1)}{h_{d_T}}=\gamma_1\lambda_1+\frac{\eta_3+\gamma_1\eta_1}{d_T h_{d_T}}+\zeta_T,$$

$$\begin{aligned}d_T(\alpha_2\mu_2+\beta_2+\gamma_2\nu_2+\delta_2) &= -\alpha_2\gamma_1\eta_1-\alpha_2\eta_3-\gamma_2\eta_2+d_T(\alpha_2\delta_1+\beta_2-\gamma_2\beta_1+\delta_2)\\ &\quad+(\omega_1-\lambda_1 h_{d_T})(\alpha_2\gamma_1-\gamma_2\alpha_1)\\ &= -\alpha_2\gamma_1\eta_1-\alpha_2\eta_3-\gamma_2\eta_2+\xi_T(\lambda_1).\end{aligned}$$

Hence,

$$\begin{aligned}\mathcal{D}_2 &= \int_{\mathbb{R}}\int_{\mathbb{R}}\sum_{(\gamma_1,\delta_1)\in\mathcal{K}^{YY}}\int_{\mathbb{R}} f^{YY}_{\gamma_1,\delta_1}\left(\omega_1-\lambda_1 h_{d_T}-\tfrac{\eta_1}{d_T}\right)\\ &\quad\times\sum_{(\gamma_2,\delta_2)\in\mathcal{K}^{\overline{XX}}}\int_{\mathbb{R}} f^{\overline{XX}}_{\gamma_2,\delta_2}\left(-\alpha_1\omega_1-\beta_1+\alpha_1\lambda_1 h_{d_T}-\tfrac{\eta_2}{d_T}\right)\\ &\quad\times W(\eta_1)W(\eta_2)W(\eta_3)\,W(-\alpha_2\gamma_1\eta_1-\gamma_2\eta_2-\alpha_2\eta_3+\xi_T(\lambda_1))\\ &\quad\times e^{-i2\pi\eta_1 c_T/d_T}e^{-i2\pi\eta_2 c_T/d_T}e^{-i2\pi\eta_3 c_T/d_T}e^{i2\pi(\alpha_2\gamma_1\eta_1+\gamma_2\eta_2+\alpha_2\eta_3+\xi_T(\lambda_1))c_T/d_T}\\ &\quad\times q(\lambda_1)q\left(\gamma_1\lambda_1+\tfrac{\eta_3+\gamma_1\eta_1}{d_T h_{d_T}}+\zeta_T\right)\mathrm{d}\eta_1\,\mathrm{d}\eta_2\,\mathrm{d}\lambda_1\,\mathrm{d}\eta_3\\ &= \sum_{(\gamma_1,\delta_1)\in\mathcal{K}^{YY}}\sum_{(\gamma_2,\delta_2)\in\mathcal{K}^{\overline{XX}}} G(\gamma_1,\delta_1,\gamma_2,\delta_2).\end{aligned}$$

For $\alpha_2\gamma_1=\gamma_2\alpha_1$ and $\alpha_2\delta_1-\gamma_2\beta_1+\delta_2+\beta_2=0$ and $\omega_2=\gamma_1\omega_1+\delta_1$, we get $\xi_T(\lambda_1)=0$ and $\zeta_T=0$. Consequnelty,

$$\begin{aligned}G(\gamma_1,\delta_1,\gamma_2,\delta_2) &= \int_{\mathbb{R}}\int_{\mathbb{R}}\int_{\mathbb{R}}\int_{\mathbb{R}} f^{YY}_{\gamma_1,\delta_1}\left(\omega_1-\lambda_1 h_{d_T}-\tfrac{\eta_1}{d_T}\right) f^{\overline{XX}}_{\gamma_2,\delta_2}\left(-\alpha_1\omega_1-\beta_1+\alpha_1\lambda_1 h_{d_T}-\tfrac{\eta_2}{d_T}\right)\\ &\quad\times W(\eta_1)W(\eta_2)W(\eta_3)\,W(-\alpha_2\gamma_1\eta_1-\gamma_2\eta_2-\alpha_2\eta_3)\\ &\quad\times e^{-i2\pi\eta_1 c_T/d_T}e^{-i2\pi\eta_2 c_T/d_T}e^{-i2\pi\eta_3 c_T/d_T}e^{i2\pi(\alpha_2\gamma_1\eta_1+\gamma_2\eta_2+\alpha_2\eta_3)c_T/d_T}\\ &\quad\times q(\lambda_1)q\left(\gamma_1\lambda_1+\tfrac{\eta_3+\gamma_1\eta_1}{d_T h_{d_T}}\right)\mathrm{d}\eta_1\,\mathrm{d}\eta_2\,\mathrm{d}\lambda_1\,\mathrm{d}\eta_3\\ &= \int_{\mathbb{R}}\int_{\mathbb{R}}\int_{\mathbb{R}}\int_{\mathbb{R}} g(\eta_1,\eta_2,\lambda_1,\eta_3)\,\mathrm{d}\eta_1\,\mathrm{d}\eta_2\,\mathrm{d}\lambda_1\,\mathrm{d}\eta_3,\end{aligned}$$

and the integrand function $g(\eta_1, \eta_2, \lambda_1, \eta_3)$ is bounded by the integrable function which does not depend on T. Namely,

$$|g(\eta_1, \eta_2, \lambda_1, \eta_3)| \leq \left\| f^{YY}_{\gamma_1,\delta_1} \right\|_\infty \left\| f^{\overline{XX}}_{\gamma_2,\delta_2} \right\|_\infty \|q\|_\infty \, q(\lambda_1) \, |W(\eta_1) \, W(\eta_2) \, W(\eta_3) \, W(-\alpha_2\gamma_1\eta_1 - \gamma_2\eta_2 - \alpha_2\eta_3)|.$$

and by Lemma B.10 the right-hand side of the above inequality is integrable on $\mathbb{R}^4$. Thus, by Lebesgue's dominated convergence theorem

$$\begin{aligned}\lim_{T\to\infty} G(\gamma_1, \delta_1, \gamma_2, \delta_2) = f^{YY}_{\gamma_1,\delta_1}(\omega_1) \, f^{\overline{XX}}_{\gamma_2,\delta_2}(-\alpha_1\omega_1 - \beta_1) \int_{\mathbb{R}} q(\lambda_1) q(\gamma_1\lambda_1) \, \mathrm{d}\lambda_1 \\ \times \int_{\mathbb{R}}\int_{\mathbb{R}}\int_{\mathbb{R}} W(\eta_1)W(\eta_2)W(\eta_3) \, W(-\alpha_2\gamma_1\eta_1 - \gamma_2\eta_2 - \alpha_2\eta_3) \\ \times e^{-i2\pi(\eta_1+\eta_2+\eta_3)\vartheta} \, e^{i2\pi(\alpha_2\gamma_1\eta_1+\gamma_2\eta_2+\alpha_2\eta_3)\vartheta} \, \mathrm{d}\eta_1 \, \mathrm{d}\eta_2 \, \mathrm{d}\eta_3.\end{aligned}$$

It remains ti show that $G(\gamma_1, \delta_1, \gamma_2, \delta_2)$, for other parameters $\gamma_1, \delta_1, \gamma_2, \delta_2$, converges to zero as $T \to \infty$. Note that

$$|G(\gamma_1, \delta_1, \gamma_2, \delta_2)| \leq \left\| f^{YY}_{\gamma_1,\delta_1} \right\|_\infty \left\| f^{\overline{XX}}_{\gamma_2,\delta_2} \right\|_\infty \|q\|_\infty \int_{\mathbb{R}} F_T(\lambda_1) \mathrm{d}\lambda_1,$$

where

$$F_T(\lambda_1) = q(\lambda_1) \int_{\mathbb{R}}\int_{\mathbb{R}}\int_{\mathbb{R}} W(\eta_1) \, W(\eta_2) \, W(\eta_3) \, W(-\alpha_2\gamma_1\eta_1 - \gamma_2\eta_2 - \alpha_2\eta_3 + \xi_T)| \, \mathrm{d}\eta_1 \, \mathrm{d}\eta_2 \, \mathrm{d}\eta_3.$$

Similarly as for the factor $E(\gamma, \delta)$, with $(\gamma, \delta) \neq (\alpha, \beta)$ in the proof of Theorem 2.1, from Hölder inequity we have that $F_T(\lambda_1)$ is bounded by an integrable function and independent of T. Therefore, we can interchange the order of the limit and the integral with respect to λ_1. By Lemma B.6 we obtain that the terms $G(\gamma_1, \delta_1, \gamma_2, \delta_2)$ tends to zero as $T \to \infty$.

For the third term $\mathcal{D}_3$, the proof of its convergence is similar to the case $\mathcal{D}_2$, and only a sketch of the proof is presented. Note that the term $\mathcal{D}_3$ can be rewritten as

$$
\begin{aligned}
\mathcal{D}_3 = \frac{1}{d_T h_{d_T}} & \int_{\mathbb{R}}\int_{\mathbb{R}}\int_{\mathbb{R}}\int_{\mathbb{R}}\int_{\mathbb{R}}\int_{\mathbb{R}} \mathbb{E}\left(Y(t_1)X(t_4)\right)\, \mathbb{E}\left(\overline{X(t_2)Y(t_3)}\right) \\
& \times w\left(\tfrac{t_1-c_T}{d_T}\right)\, w\left(\tfrac{t_2-c_T}{d_T}\right)\, w\left(\tfrac{t_3-c_T}{d_T}\right)\, w\left(\tfrac{t_4-c_T}{d_T}\right) \\
& \times e^{-i2\pi\mu_1 t_1} e^{i2\pi(\alpha_1\mu_1+\beta_1)t_2} e^{i2\pi\mu_2 t_3} e^{-i2\pi(\alpha_2\mu_2+\beta_2)t_4} \\
& \times q\left(\tfrac{\omega_1-\mu_1}{h_{d_T}}\right) q\left(\tfrac{\omega_2-\mu_2}{h_{d_T}}\right)\, \mathrm{d}t_1\, \mathrm{d}t_2\, \mathrm{d}t_3\, \mathrm{d}t_4\, \mathrm{d}\mu_1\, \mathrm{d}\mu_2, \\
= \frac{1}{d_T h_{d_T}} & \int_{\mathbb{R}}\int_{\mathbb{R}} \sum_{(\gamma_1,\delta_1)\in\mathcal{K}^{Y\overline{X}}} \int_{\mathbb{R}} f^{Y\overline{X}}_{\gamma_1,\delta_1}(\nu_1) \sum_{(\gamma_2,\delta_2)\in\mathcal{K}^{\overline{X}Y}} \int_{\mathbb{R}} f^{\overline{X}Y}_{\gamma_2,\delta_2}(\nu_2) \\
& \times \int_{\mathbb{R}} w\left(\tfrac{t_1-c_T}{d_T}\right)\, e^{-i2\pi\mu_1 t_1} e^{i2\pi\nu_1 t_1}\, \mathrm{d}t_1 \\
& \times \int_{\mathbb{R}} w\left(\tfrac{t_2-c_T}{d_T}\right)\, e^{i2\pi(\alpha_1\mu_1+\beta_1)t_2} e^{i2\pi\nu_2 t_2}\, \mathrm{d}t_2 \\
& \times \int_{\mathbb{R}} w\left(\tfrac{t_3-c_T}{d_T}\right)\, e^{i2\pi\mu_2 t_3} e^{-i2\pi(\gamma_2\nu_2+\delta_2)t_3}\, \mathrm{d}t_3 \\
& \times \int_{\mathbb{R}} w\left(\tfrac{t_4-c_T}{d_T}\right)\, e^{-i2\pi(\alpha_2\mu_2+\beta_2)t_4} e^{-i2\pi(\gamma_1\nu_1+\delta_1)t_4}\, \mathrm{d}t_4 \\
& \times q\left(\tfrac{\omega_1-\mu_1}{h_{d_T}}\right) q\left(\tfrac{\omega_2-\mu_2}{h_{d_T}}\right)\, \mathrm{d}\nu_1\, \mathrm{d}\nu_2\, \mathrm{d}\mu_1\, \mathrm{d}\mu_2 \\
= \frac{1}{d_T h_{d_T}} & \int_{\mathbb{R}}\int_{\mathbb{R}} \sum_{(\gamma_1,\delta_1)\in\mathcal{K}^{Y\overline{X}}} \int_{\mathbb{R}} f^{Y\overline{X}}_{\gamma_1,\delta_1}(\nu_1) \sum_{(\gamma_2,\delta_2)\in\mathcal{K}^{\overline{X}Y}} \int_{\mathbb{R}} f^{\overline{X}Y}_{\gamma_2,\delta_2}(\nu_2) \\
& \times d_T W(d_T(\mu_1-\nu_1)) \times d_T W(-d_T(\nu_2+\alpha_1\mu_1+\beta_1)) \\
& \times d_T W(d_T(\gamma_2\nu_2+\delta_2-\mu_2)) \times d_T W(d_T(\alpha_2\mu_2+\beta_2+\gamma_1\nu_1+\delta_1)) \\
& \times e^{-i2\pi(\mu_1-\nu_1)c_T} e^{i2\pi(\nu_2+\alpha_1\mu_1+\beta_1)c_T} \\
& \times e^{-i2\pi(\gamma_2\nu_2+\delta_2-\mu_2)c_T} e^{-i2\pi(\alpha_2\mu_2+\beta_2+\gamma_1\nu_1+\delta_1)c_T} \\
& \times q\left(\tfrac{\omega_1-\mu_1}{h_{d_T}}\right) q\left(\tfrac{\omega_2-\mu_2}{h_{d_T}}\right)\, \mathrm{d}\nu_1\, \mathrm{d}\nu_2\, \mathrm{d}\mu_1\, \mathrm{d}\mu_2.
\end{aligned}
$$

Let us consider the following change the variables

$$
\begin{aligned}
\lambda_1 &= \tfrac{\omega_1-\mu_1}{h_{d_T}}, \\
\eta_1 &= d_T(\mu_1-\nu_1), \\
\eta_2 &= -d_T(\nu_2+\alpha_1\mu_1+\beta_1), \\
\eta_3 &= d_T(\gamma_2\nu_2+\delta_2-\mu_2),
\end{aligned}
$$

Then

$$
\begin{aligned}
\mu_1 &= \omega_1 - \lambda_1 h_{d_T}, \\
\nu_1 &= \omega_1 - \lambda_1 h_{d_T} - \tfrac{\eta_1}{d_T}, \\
\mu_2 &= -\gamma_2\alpha_1\omega_1 + \gamma_2\alpha_1\lambda_1 h_{d_T} - \gamma_2\beta_1 - \gamma_2\tfrac{\eta_2}{d_T} + \delta_2 - \tfrac{\eta_3}{d_T}, \\
\nu_2 &= -\alpha_1\omega_1 + \alpha_1\lambda_1 h_{d_T} - \beta_1 - \tfrac{\eta_2}{d_T},
\end{aligned}
$$

and

$$\begin{aligned}\frac{\omega_2-\mu_2}{h_{d_T}} &= -\gamma_1\alpha_1\lambda_1 + \frac{\eta_3+\gamma_2\eta_2}{d_T h_{d_T}} + \frac{\omega_2+\gamma_2(\alpha_1\omega_1+\beta_1)-\delta_2}{h_{d_T}} \\ &= -\gamma_1\alpha_1\lambda_1 + \frac{\eta_3+\gamma_2\eta_2}{d_T h_{d_T}} + \zeta_T,\end{aligned}$$

and

$$\begin{aligned}d_T(\alpha_2\mu_2+\beta_2+\gamma_1\nu_1+\delta_1) &= -\alpha_2\gamma_2\eta_2 - \alpha_2\eta_3 - \gamma_1\eta_1 + (\gamma_1-\alpha_2\gamma_2\alpha_1)(\omega_1-\lambda_1 h_{d_T}) \\ &\quad + d_T(\alpha_2\delta_2+\beta_2+\delta_1-\alpha_2\gamma_2\beta_1) \\ &= -\alpha_2\gamma_2\eta_2 - \alpha_2\eta_3 - \gamma_1\eta_1 + \xi_T(\lambda_1).\end{aligned}$$

Hence,

$$\begin{aligned}\mathcal{D}_3 = \int_{\mathbb{R}}\int_{\mathbb{R}} &\sum_{(\gamma_1,\delta_1)\in\mathcal{K}^{Y\overline{X}}} \int_{\mathbb{R}} f^{Y\overline{X}}_{\gamma_1,\delta_1}(\omega_1-\lambda_1 h_{d_T}-\tfrac{\eta_1}{d_T}) \\ &\times \sum_{(\gamma_2,\delta_2)\in\mathcal{K}^{\overline{X}Y}} \int_{\mathbb{R}} f^{\overline{X}Y}_{\gamma_2,\delta_2}(-\alpha_1\omega_1-\beta_1+\alpha_1\lambda_1 h_{d_T}-\tfrac{\eta_2}{d_T}) \\ &\times W(\eta_1)\,W(\eta_2)\,W(\eta_3)\,W(-\alpha_2\gamma_2\eta_2-\alpha_2\eta_3-\gamma_1\eta_1+\xi_T(\lambda_1)) \\ &\times e^{-i2\pi\eta_1 c_T/d_T}\,e^{i2\pi\eta_2 c_T/d_T}\,e^{-i2\pi\mu_2 c_T/d_T}\,e^{-i2\pi(-\alpha_2\gamma_2\eta_2-\alpha_2\eta_3-\gamma_1\eta_1+\xi_T(\lambda_1))c_T/d_T} \\ &\times q\,(\lambda_1)\,q\left(-\gamma_1\alpha_1\lambda_1+\tfrac{\eta_3+\gamma_2\eta_2}{d_T h_{d_T}}+\zeta_T\right)\,\mathrm{d}\eta_1\,\mathrm{d}\eta_2\,\mathrm{d}\lambda_1\,\mathrm{d}\eta_3.\end{aligned}$$

To obtain the convergence of $\mathcal{D}_3$ one has to consider two cases: (i) $\gamma_1=\alpha_2\gamma_2\alpha_1$ and $\alpha_2\delta_2+\beta_2+\delta_1-\alpha_2\gamma_2\beta_1=0$ and $\omega_2+\gamma_2(\alpha_1\omega_1+\beta_1)-\delta_2=0$ (ii) otherwise. The remaining part of the proof is the same as for the term $\mathcal{D}_2$.

Finally, we apply Lemma B.8 to end the proof. □

Proof of Theorem 3.4. Let us consider the cumulants without complex conjugation, i.e.

$$\operatorname{cum}\left(\widehat{f}^{XY}_{\alpha_1,\beta_1}(\omega_1)_{c_T,d_T},\ldots,\widehat{f}^{XY}_{\alpha_P,\beta_P}(\omega_P)_{c_T,d_T}\right).$$

The proofs for the other cases proceed with minor obvious changes. Note that

$$\begin{aligned}&\operatorname{cum}\left(\widetilde{f}^{XY}_{\alpha_1,\beta_1}(\omega_1)_{c_T,d_T},\ldots,\widetilde{f}^{XY}_{\alpha_P,\beta_P}(\omega_P)_{c_T,d_T}\right) \\ &\quad= \frac{1}{d_T^P h_{d_T}^P}\int_{\mathbb{R}^P}\cdots\int\int_{\mathbb{R}^{2P}}\cdots\int \operatorname{cum}\left(X(t_{1,1})\overline{Y(t_{1,2})},\ldots,X(t_{P,1})\overline{Y(t_{P,2})}\right) \\ &\qquad\times\prod_{j=1}^{P} w\left(\tfrac{t_{j,1}-c_T}{d_T}\right)e^{-i2\pi\mu_j t_{j,1}}\prod_{j=1}^{P} w\left(\tfrac{t_{j,2}-c_T}{d_T}\right)e^{i2\pi(\alpha_j\mu_j+\beta_j)t_{j,2}} \\ &\qquad\times\prod_{j=1}^{P} q\left(\tfrac{\omega_j-\mu_j}{h_{d_T}}\right)\,\mathrm{d}t_{1,1}\ldots\,\mathrm{d}t_{P,2}\,\mathrm{d}\mu_1\,\ldots\,\mathrm{d}\mu_P.\end{aligned}$$

From Lemma B.1, we have

$$\operatorname{cum}\left(X(t_{1,1})\overline{Y(t_{1,2})},\ldots,X(t_{P,1})\overline{Y(t_{P,2})}\right) = \sum_{\boldsymbol{v}=(v_1,\ldots,v_L)} \mathcal{C}_{v_1}\ldots\mathcal{C}_{v_L},$$

where the summation is over all indecomposable partitions $\boldsymbol{v}$ of the table

$$\begin{matrix}(1,1) & (1,2)\\ (2,1) & (2,2)\\ \vdots & \vdots\\ (P,1) & (P,2)\end{matrix}$$

and

$$\mathcal{C}_{v_m} = \operatorname{cum}\left(V_r(t_{j,r}), (j,r) \in v_m\right),$$

with

$$V_r(t_{j,r}) = \begin{cases} X(t_{j,1}), & r = 1,\\ \overline{Y(t_{j,2})}, & r = 2.\end{cases}$$

Therefore,

$$\operatorname{cum}\left(\widetilde{f}^{XY}_{\alpha_1,\beta_1}(\omega_1)_{c_T,d_T}, \ldots, \widetilde{f}^{XY}_{\alpha_P,\beta_P}(\omega_P)_{c_T,d_T}\right) = \sum_{\boldsymbol{v}=(v_1,\ldots,v_L)} \mathcal{T}_{\boldsymbol{v}},$$

where

$$\mathcal{T}_{\boldsymbol{v}} = \frac{1}{d_T^P h_{d_T}^P} \int_{\mathbb{R}^P} \cdots \int \int_{\mathbb{R}^{2P}} \cdots \int \mathcal{C}_{v_1} \ldots \mathcal{C}_{v_L} \prod_{j=1}^{P} w\left(\tfrac{t_{j,1}-c_T}{d_T}\right) e^{-i2\pi\mu_j t_{j,1}} \prod_{j=1}^{P} w\left(\tfrac{t_{j,2}-c_T}{d_T}\right) e^{i2\pi(\alpha_j\mu_j+\beta_j)t_{j,2}} \times \prod_{j=1}^{P} q\left(\tfrac{\omega_j-\mu_j}{h_{d_T}}\right) \mathrm{d}t_{1,1} \ldots \mathrm{d}t_{P,2}\, \mathrm{d}\mu_1, \ldots \mathrm{d}\mu_P.$$

We consider $\mathcal{T}_{\boldsymbol{v}}$ for two cases:

(i) $\boldsymbol{v} = (v_1)$,

(ii) $\boldsymbol{v} = (v_1, \ldots, v_L)$ for $L > 1$.

First, let us show the convergence in the first case, i.e. for $\mathcal{T}_{\boldsymbol{v}}$ with $\boldsymbol{v} = (v_1)$. This case is performed for $P \geq 2$, also to obtain the convergence of $\mathcal{D}_1$ in the proof of Theorems 2.2 and 3.3.

Denote $\boldsymbol{V}_{2P} = (\underbrace{X, \overline{Y}, \ldots, X, \overline{Y}}_{2P})$. Then by (iii) of Assumption 2.3

$$
\begin{aligned}
\mathcal{T}_{\boldsymbol{v}} &= \frac{1}{d_T^P h_{d_T}^P} \int_{\mathbb{R}^P} \cdots \int \int_{\mathbb{R}^{2P}} \cdots \int \operatorname{cum}\left(X(t_{1,1}), \overline{Y(t_{1,2})}, \ldots, X(t_{P,1}), \overline{Y(t_{P,2})}\right) \\
&\quad \times \prod_{j=1}^{P} w\left(\tfrac{t_{j,1}-c_T}{d_T}\right) e^{-i2\pi\mu_j t_{j,1}} \prod_{j=1}^{P} w\left(\tfrac{t_{j,2}-c_T}{d_T}\right) e^{i2\pi(\alpha_j\mu_j+\beta_j)t_{j,2}} \\
&\quad \times \prod_{j=1}^{P} q\left(\tfrac{\omega_j-\mu_j}{h_{d_T}}\right) \mathrm{d}t_{1,1} \ldots \mathrm{d}t_{P,2}\, \mathrm{d}\mu_1 \ldots \mathrm{d}\mu_P \\
&= \frac{1}{d_T^P h_{d_T}^P} \int_{\mathbb{R}^P} \cdots \int \int_{\mathbb{R}^{2P}} \cdots \int \sum_{k\in\mathcal{K}^{\boldsymbol{V}_{2P}}} \int_{\mathbb{R}^{2P-1}} \cdots \int f_k^{\boldsymbol{V}_{2P}}(\nu_{1,1}, \nu_{1,2}, \nu_{2,1}, \ldots, \nu_{P-1,2}, \nu_{P,1}) \\
&\quad \times e^{i2\pi\left(\nu_{1,1}t_{1,1}+\ldots+\nu_{P,1}t_{P,1}+\Phi_k^{\boldsymbol{V}_{2P}}(\nu_{1,1},\nu_{1,2},\nu_{2,1},\ldots,\nu_{P-1,2},\nu_{P,1})t_{P,2}\right)} \mathrm{d}\nu_{1,1} \ldots \mathrm{d}\nu_{P,1} \\
&\quad \times \prod_{j=1}^{P} w\left(\tfrac{t_{j,1}-c_T}{d_T}\right) e^{-i2\pi\mu_j t_{j,1}} \prod_{j=1}^{P} w\left(\tfrac{t_{j,2}-c_T}{d_T}\right) e^{i2\pi(\alpha_j\mu_j+\beta_j)t_{j,2}} \\
&\quad \times \prod_{j=1}^{P} q\left(\tfrac{\omega_j-\mu_j}{h_{d_T}}\right) \mathrm{d}t_{1,1} \ldots \mathrm{d}t_{P,2}\, \mathrm{d}\mu_1 \ldots \mathrm{d}\mu_P \\
&= \frac{1}{d_T^P h_{d_T}^P} \sum_{k\in\mathcal{K}^{\boldsymbol{V}_{2P}}} \int_{\mathbb{R}^P} \cdots \int \int_{\mathbb{R}^{2P-1}} \cdots \int f_k^{\boldsymbol{V}_{2P}}(\nu_{1,1}, \nu_{1,2}, \nu_{2,1}, \ldots, \nu_{P-1,2}, \nu_{P,1}) \\
&\quad \times \prod_{j=1}^{P} \int_{\mathbb{R}} w\left(\tfrac{t_{j,1}-c_T}{d_T}\right) e^{-i2\pi(\mu_j-\nu_{j,1})t_{j,1}} \mathrm{d}t_{j,1} \\
&\quad \times \prod_{j=1}^{P-1} \int_{\mathbb{R}} w\left(\tfrac{t_{j,2}-c_T}{d_T}\right) e^{i2\pi(\nu_{j,2}+\alpha_j\mu_j+\beta_j)t_{j,2}} \mathrm{d}t_{j,2} \\
&\quad \times \int_{\mathbb{R}} w\left(\tfrac{t_{P,2}-c_T}{d_T}\right) e^{i2\pi(\alpha_P\mu_P+\beta_P+\Phi_k^{\boldsymbol{V}_{2P}}(\nu_{1,1},\nu_{1,2},\nu_{2,1},\ldots,\nu_{P-1,2},\nu_{P,1}))t_{P,2}} \mathrm{d}t_{P,2} \\
&\quad \times \prod_{j=1}^{P} q\left(\tfrac{\omega_j-\mu_j}{h_{d_T}}\right) \mathrm{d}\nu_{1,1}\, \mathrm{d}\nu_{1,2}\, \mathrm{d}\nu_{2,1} \ldots \mathrm{d}\nu_{P-1,2}\, \mathrm{d}\nu_{P,1}\, \mathrm{d}\mu_1 \ldots \mathrm{d}\mu_P.
\end{aligned}
$$

Thus, by Lemma B.4

$$
\begin{aligned}
|\mathcal{T}_{\boldsymbol{v}}| \le \frac{1}{d_T^P} \sum_{k\in\mathcal{K}^{\boldsymbol{V}_{2P}}} \left\|f_k^{\boldsymbol{V}_{2P}}\right\|_\infty \int_{\mathbb{R}^{2P-1}} \cdots \int \int_{\mathbb{R}^P} \cdots \int \prod_{j=1}^{P} \left|q\left(\tfrac{\omega_j-\mu_j}{h_{d_T}}\right)\right| \\
\times \prod_{j=1}^{P} d_T \left|W(d_T(\mu_j-\nu_{j,1}))\right| \times \prod_{j=1}^{P-1} d_T \left|W(-d_T(\nu_{j,2}+\alpha_j\mu_j+\beta_j)\right| \\
\times d_T \left|W\left(d_T\left(\alpha_P\mu_P+\beta_P+\Phi_k^{\boldsymbol{V}_{2P}}(\nu_{1,1},\nu_{1,2},\nu_{2,1},\ldots,\nu_{P-1,2},\nu_{P,1})\right)\right)\right| \\
\mathrm{d}\nu_{1,1}\, \mathrm{d}\nu_{1,2}\, \mathrm{d}\nu_{2,1} \ldots \mathrm{d}\nu_{P-1,2}\, \mathrm{d}\nu_{P,1}\, \mathrm{d}\mu_1 \ldots \mathrm{d}\mu_P.
\end{aligned}
$$

Our goal is to apply Lemma B.10. To do this, first, we consider the following change of variables

$$
\begin{aligned}
&\lambda_j = \tfrac{\omega_j-\mu_j}{h_{d_T}}, && j = 1, 2, \ldots, P, \\
&\eta_{2j-1} = d_T(\mu_j-\nu_{j,1}), && j = 1, 2, \ldots, P, \\
&\eta_{2j} = -d_T(\nu_{j,2}+\alpha_j\mu_j+\beta_j), && j = 1, 2, \ldots, P-1.
\end{aligned}
$$

Then

$$\begin{aligned}
\mu_j &= \omega_j - \lambda_j h_{d_T}, && j = 1, 2, \ldots, P,\\
\nu_{j,1} &= \omega_j - \lambda_j h_{d_T} - \tfrac{\eta_{2j-1}}{d_T}, && j = 1, 2, \ldots, P,\\
\nu_{2,j} &= -\alpha_j\omega_j + \alpha_j\lambda_j h_{d_T} - \beta_j - \tfrac{\eta_{2j}}{d_T}, && j = 1, 2, \ldots, P-1.
\end{aligned}$$

Hence,

$$\begin{aligned}
|\mathcal{T}_{\boldsymbol{v}}| \leq \frac{1}{d_T^{P-1}} \sum_{k=(\gamma_1,\ldots,\gamma_{2P-1},\delta)\in\mathcal{K}^{\boldsymbol{V}_{2P}}} \left\| f_k^{\boldsymbol{V}_{2P}} \right\|_\infty \int_{\mathbb{R}^P} \cdots \int \int_{\mathbb{R}^{2P-1}} \cdots \int \prod_{j=1}^{P} |q(\lambda_j)| \prod_{j=1}^{2P-1} |W(\eta_j)|\\
\times |W(\Upsilon(\lambda_1, \ldots, \lambda_P, \eta_1, \ldots, \eta_{2P-1}))| \, \mathrm{d}\lambda_1 \ldots \mathrm{d}\lambda_P \, \mathrm{d}\eta_1 \ldots \mathrm{d}\eta_{2P-1},
\end{aligned}$$

where $\Upsilon(\lambda_1, \ldots, \lambda_P, \eta_1, \ldots, \eta_{2P-1})$ is a linear combination of $\eta_1, \ldots, \eta_{2P-1}$, i.e.,

$$\begin{aligned}
\Upsilon(\lambda_1, \ldots, \lambda_P, \eta_1, \ldots, \eta_{2P-1}) &= d_T\alpha_P(\omega_j - \lambda_j h_{d_T}) + d_T\beta_P + d_T \sum_{j=1}^{P-1} \gamma_{2j-1} \left(\omega_j - \lambda_j h_{d_T} - \tfrac{\eta_{2j-1}}{d_T}\right)\\
&\quad + d_T \sum_{j=1}^{P} \gamma_{2j} \left(-\alpha_j\omega_j + \alpha_j\lambda_j h_{d_T} - \beta_j - \tfrac{\eta_{2j}}{d_T}\right) + d_T\delta\\
&= -\sum_{j=1}^{2P-1} \gamma_j\eta_j + \xi_T(\lambda_1, \ldots, \lambda_P),
\end{aligned}$$

and $\xi_T(\lambda_1, \ldots, \lambda_P)$ does not depend on $\eta_1, \ldots, \eta_{2P-1}$. Finally, by Lemma B.10, we obtain that $|\mathcal{T}_{\boldsymbol{v}}| = \mathcal{O}(d_T^{-P+1})$ and

$$(d_T h_{d_T})^{P/2} |\mathcal{T}_{\boldsymbol{v}}| = \mathcal{O}\left(h_{d_T}^{P/2} d_T^{-P/2+1}\right) = \mathcal{O}\left(d_T^{-\kappa P/2 - P/2 + 1}\right).$$

Thus, for $P \geq 2$ the above term tends to zero since $-\kappa P/2 - P/2 + 1 < 0$, ant it is equivalent to $\kappa > \frac{2-P}{P}$, which is true for $\kappa \in (0, 1)$.

Now, let us show the convergence for $\mathcal{T}_{\boldsymbol{v}}$ with $\boldsymbol{v} = (v_1, \ldots, v_L)$ and $L > 1$. Without loss of generality, assume that v_n and v_{n+1} hook for $n = 1, 2, \ldots, L-1$. That is, for $n = 1, 2, \ldots, L-1$, there exist $(J_n, r_n) \in v_n$ and $(J'_{n+1}, r'_{n+1}) \in v_{n+1}$ such that $J_n = J'_{n+1}$ and $r_n \neq r'_{n+1}$. Moreover, we can assume that $(P, 2) \in v_L$ and denote $J_L = P$, $r_L = 2$.

By (iii) of Assumption 2.3, we have

$$\mathcal{C}_{v_m} = \sum_{k_m \in \mathcal{K}^{\boldsymbol{V}(v_m)}} \int_{\mathbb{R}^{l_m - 1}} \cdots \int f_{k_m}^{\boldsymbol{V}(v_m)}(\boldsymbol{\nu}'_{v_m}) \, e^{i2\pi\left(\sum_{(j,r)\in v'_m} \nu_{j,r} t_{j,r} + \Phi_{k_m}^{\boldsymbol{V}(v_m)}(\boldsymbol{\nu}'_{v_m}) t_{J_m, r_m}\right)} \, \mathrm{d}\boldsymbol{\nu}'_{v_m},$$

where $\boldsymbol{V}(v_m) = (V_j, (j, r) \in v_m)$, $v'_m = v_m \setminus \{(J_m, r_m)\}$, $\boldsymbol{\eta}'_{v_m} = (\eta_{j,r}, (j, r) \in v'_m)$, and

$$\Phi_{k_m}^{\boldsymbol{V}(v_m)}(\boldsymbol{\nu}'_{v_m}) = \sum_{(j,r)\in v'_m} \gamma_{j,r}\nu_{j,r} + \delta_{v_m}.$$

Moreover, by $f_{k_m}^{\boldsymbol{V}(v_m)}$ and $\mathcal{K}^{\boldsymbol{V}(v_m)}$ we denote, respectively, spectral cumulant functions and set of support lines corresponding to cumulant $\mathcal{C}_{v_m}$.

Note that

$$\begin{aligned}\mathcal{T}_{\boldsymbol{v}} = \frac{1}{d_T^P h_{d_T}^P} \int_{\mathbb{R}^P} \cdots \int \int_{\mathbb{R}^{2P}} \cdots \int \prod_{m=1}^{L} \sum_{k_m \in \mathcal{K}^{\boldsymbol{V}(v_m)}} \int_{\mathbb{R}^{|v_m|-1}} \cdots \int f_{k_m}^{\boldsymbol{V}(v_m)}(\boldsymbol{\eta}'_{v_m}) \\ \times \prod_{m=1}^{L} e^{i2\pi\left(\sum_{(j,r)\in v'_m} \nu_{j,r} t_{j,r} + \Phi_{k_m}^{\boldsymbol{V}(v_m)}(\boldsymbol{\nu}'_{v_m}) t_{J_m,r_m}\right)} \, \mathrm{d}\boldsymbol{\nu}'_{v_m} \\ \times \prod_{j=1}^{P} w\left(\tfrac{t_{j,1}-c_T}{d_T}\right) e^{-i2\pi\mu_j t_{j,1}} \prod_{j=1}^{P} w\left(\tfrac{t_{j,2}-c_T}{d_T}\right) e^{i2\pi(\alpha_j\mu_j+\beta_j)t_{j,2}} \\ \times \prod_{j=1}^{P} q\left(\tfrac{\omega_j-\mu_j}{h_{d_T}}\right) \mathrm{d}t_{1,1} \ldots \mathrm{d}t_{P,2} \, \mathrm{d}\mu_1, \ldots \mathrm{d}\mu_P.\end{aligned}$$

Denote

$$\alpha_{j,r} = \begin{cases} -1, & r = 1, \\ \alpha_j, & r = 2, \end{cases} \qquad \beta_{j,r} = \begin{cases} 0, & r = 1, \\ \beta_j, & r = 2, \end{cases}$$

and $1 \oplus 1 = 2$ and $2 \oplus 1 = 1$. Hence,

$$\begin{aligned}\mathcal{T}_{\boldsymbol{v}} = \frac{1}{d_T^P h_{d_T}^P} \sum_{k_1 \in \mathcal{K}^{\boldsymbol{V}(v_1)}} \cdots \sum_{k_L \in \mathcal{K}^{\boldsymbol{V}(v_L)}} \int_{\mathbb{R}^P} \cdots \int \int_{\mathbb{R}^{2P-L}} \cdots \int \prod_{m=1}^{L} f_{k_m}^{\boldsymbol{V}(v_m)}(\boldsymbol{\nu}'_{v_m}) \prod_{j=1}^{P} q\left(\tfrac{\omega_j-\mu_j}{h_{d_T}}\right) \\ \times \prod_{m=1}^{L} \left(\int_{\mathbb{R}} w\left(\tfrac{t_{J_m,r_m}-c_T}{d_T}\right) e^{i2\pi(\alpha_{J_m,r_m}\mu_{J_m}+\beta_{J_m,r_m}+\Phi_{k_m}^{\boldsymbol{V}(v_m)}(\boldsymbol{\nu}'_{v_m}))t_{J_m,r_m}} \, \mathrm{d}t_{J_m,r_m} \right) \\ \times \prod_{m=1}^{L} \prod_{(j,r)\in v'_m} \left(\int_{\mathbb{R}} w\left(\tfrac{t_{j,r}-c_T}{d_T}\right) e^{i2\pi(\alpha_{j,r}\mu_j+\beta_{j,r}+\nu_{j,r})t_{j,r}} \, \mathrm{d}t_{j,r} \right) \mathrm{d}\boldsymbol{\nu}'_{v_1} \ldots \boldsymbol{\nu}'_{v_L} \mathrm{d}\mu_1 \ldots \mathrm{d}\mu_P.\end{aligned}$$

Applying Lemma B.4, we get

$$\begin{aligned}|\mathcal{T}_{\boldsymbol{v}}| \le \frac{1}{d_T^P h_{d_T}^P} \sum_{k_1 \in \mathcal{K}^{\boldsymbol{V}(v_1)}} \cdots \sum_{k_L \in \mathcal{K}^{\boldsymbol{V}(v_L)}} \prod_{m=1}^{L} \left\| f_{k_m}^{\boldsymbol{V}(v_L)} \right\|_\infty \int_{\mathbb{R}^P} \cdots \int \int_{\mathbb{R}^{2P-L}} \cdots \int \prod_{j=1}^{P} q\left(\tfrac{\omega_j-\mu_j}{h_{d_T}}\right) \\ \times \prod_{m=1}^{L} d_T \left| W\left(-d_T\left(\alpha_{J_m,r_m}\mu_{J_m} + \beta_{J_m,r_m} + \Phi_{k_m}^{\boldsymbol{V}(v_m)}(\boldsymbol{\nu}'_{v_m})\right)\right)\right| \\ \times \prod_{m=1}^{L} \prod_{(j,r)\in v'_m} d_T \left| W(-d_T(\alpha_{j,r}\mu_j + \beta_{j,r} + \nu_{j,r}))\right| \mathrm{d}\boldsymbol{\nu}'_{v_1} \ldots \mathrm{d}\boldsymbol{\nu}'_{v_L} \mathrm{d}\mu_1 \ldots \mathrm{d}\mu_P.\end{aligned}$$

By the following change the variables

$$\eta_{j,r} = -d_T(\alpha_{j,r}\mu_j + \beta_{j,r} + \nu_{j,r}), \qquad (j,r) \in v'_m, m = 1, 2, \ldots L,$$

we have

$$\nu_{j,r} = -\alpha_{j,r}\mu_j - \beta_{j,r} + \tfrac{\eta_{j,r}}{d_T}, \qquad (j,r) \in v'_m, m = 1, 2, \ldots L,$$

and

$$|\mathcal{T}_{\boldsymbol{v}}| \le \frac{1}{d_T^P h_{d_T}^P} \sum_{k_1 \in \mathcal{K}^{\boldsymbol{V}(v_1)}} \cdots \sum_{k_L \in \mathcal{K}^{\boldsymbol{V}(v_L)}} \prod_{m=1}^{L} \left\| f_{k_m}^{\boldsymbol{V}(v_m)} \right\|_\infty \int_{\mathbb{R}^P} \cdots \int \int_{\mathbb{R}^{2P-L}} \cdots \int \prod_{j=1}^{P} q\left(\tfrac{\omega_j - \mu_j}{h_{d_T}}\right)$$
$$\times \prod_{m=1}^{L} d_T \left| W\left(-d_T \alpha_{J_m, r_m} \mu_{J_m} + \Upsilon_m(\boldsymbol{\eta}'_{v_m}, \boldsymbol{\mu}'_{v_m})\right)\right|$$
$$\times \prod_{m=1}^{L} \prod_{(j,r) \in v'_m} |W(\eta_{j,r})| \, \mathrm{d}\boldsymbol{\eta}'_{v_1} \, \ldots \, \mathrm{d}\boldsymbol{\eta}'_{v_L} \, \mathrm{d}\mu_1, \ldots, \mathrm{d}\mu_P,$$

where for $m = 2, 3, \ldots, L$

$$\begin{aligned}
\Upsilon_m(\boldsymbol{\eta}'_{v_m}, \boldsymbol{\mu}'_{v_m}) &= -d_T \beta_{J_m, r_m} - d_T \sum_{(j,r) \in v'_m} \gamma_{j,r} \nu_{j,r} - d_T \delta_{v_m} \\
&= -d_T \beta_{J_m, r_m} - d_T \sum_{(j,r) \in v'_m} \gamma_{j,r} \left(\tfrac{\eta_{j,r}}{d_T} - \alpha_{j,r} \mu_j - \beta_{j,r} \right) - d_T \delta_{v_m} \\
&= -d_T \beta_{J_m, r_m} - \sum_{(j,r) \in v'_m} \gamma_{j,r} \eta_{j,r} + d_T \sum_{(j,r) \in v'_m} \gamma_{j,r} \alpha_{j,r} \mu_j + d_T \sum_{(j,r) \in v'_m} \gamma_{j,r} \beta_{j,r} - d_T \delta_m \\
&= - \sum_{(j,r) \in v'_m} \gamma_{j,r} \eta_{j,r} + d_T \alpha_{J_{m-1}, r_{m-1} \oplus 1} \mu_{J_{m-1}} + \xi_T^{(m)}(\boldsymbol{\mu}'_{v_m}),
\end{aligned} \tag{3.9}$$

and $\xi_T^{(m)}(\boldsymbol{\mu}'_{v_m})$ does not depend on $\boldsymbol{\eta}'_{v_m}$. The last equality in (3.9) follows from the fact that $(J_{m-1}, r_{m-1} \oplus 1) = (J'_m, r'_m)$ belongs to v'_m.

Now let us consider the following change the variables

$$\lambda_m = -d_T \alpha_{J_m, r_m} \mu_{J_m} + \Upsilon_m(\boldsymbol{\eta}'_{v_m}, \boldsymbol{\mu}'_{v_m}), \quad m = 1, 2, \ldots, L-1. \tag{3.10}$$

Then

$$\mu_{J_m} = \tfrac{\Upsilon_m(\boldsymbol{\eta}'_{v_m}, \boldsymbol{\mu}'_{v_m}) - \lambda_m}{d_T \alpha_{J_m, r_m}}, \quad m = 1, 2, \ldots, L-1,$$

and

$$\begin{aligned}
\Upsilon_L(\boldsymbol{\eta}'_{v_L}, \boldsymbol{\mu}'_{v_L}) &= \sum_{(j,r) \in v'_L} \gamma_{j,r} \eta_{j,r} + d_T \alpha_{J_{L-1}, r_{L-1} \oplus 1} \mu_{J_{L-1}} + \xi_T^{(L)}(\boldsymbol{\mu}'_{v_L}) \\
&= \sum_{(j,r) \in v'_L} \gamma_{j,r} \eta_{j,r} + \tfrac{\alpha_{J_{L-1}, r_{L-1} \oplus 1}}{\alpha_{J_{L-1}, r_{L-1}}} \left(\Upsilon_{L-1}(\boldsymbol{\eta}'_{v_{L-1}}, \boldsymbol{\mu}'_{v_{L-1}}) - \lambda_{L-1} \right) + \xi_T^{(L)}(\boldsymbol{\mu}'_{v_L}).
\end{aligned}$$

By recursively combining (3.9) and (3.10), we get

$$d_T \alpha_{J_L, r_L} \mu_{J_L} + \Upsilon_L(\boldsymbol{\eta}'_{v_L}, \boldsymbol{\mu}'_{v_L}) = \sum_{m=1}^{L} \sum_{(j,r) \in v'_m} a_{j,r} \eta_{j,r} + \sum_{m=1}^{L-1} b_m \lambda_{J_m} + \xi_T(\boldsymbol{\mu}'_{v_1}, \ldots, \boldsymbol{\mu}'_{v_L}, \mu_{J_L}),$$

with some constants $a_{j,r}$, $(j,r) \in v'_m, m = 1, 2, \ldots, L$, and constants b_m, $m = 1, 2 \ldots, L-1$, and $\xi_T(\boldsymbol{\mu}'_{v_1}, \ldots, \boldsymbol{\mu}'_{v_L}, \mu_{J_L})$ does not depend on $\boldsymbol{\eta}'_{v_1}, \ldots, \boldsymbol{\eta}'_{v_L}$. Therefore,

$$
\begin{aligned}
|\mathcal{T}_{\boldsymbol{v}}| \leq \frac{1}{d_T^{P-1} h_{d_T}^P} \sum_{k_1 \in \mathcal{K}^{\boldsymbol{V}(v_1)}} \cdots \sum_{k_L \in \mathcal{K}^{\boldsymbol{V}(v_L)}} \prod_{m=1}^{L} \left\| f_{k_m}^{\boldsymbol{V}(v_m)} \right\|_\infty \int_{\mathbb{R}^P} \cdots \int \int_{\mathbb{R}^{2P-L}} \cdots \int \\
\times \|q\|_\infty^{L-1} \, q\left(\tfrac{\omega_{J_L} - \mu_{J_L}}{h_{d_T}}\right) \prod_{m=1}^{L} \prod_{(j,r) \in v'_m} q\left(\tfrac{\omega_j - \mu_j}{h_{d_T}}\right) \\
\times \left| W\left(\sum_{m=1}^{L} \sum_{(j,r) \in v'_m} a_{j,r} \eta_{j,r} + \sum_{m=1}^{L-1} b_m \lambda_{L_m} + \xi_T(\boldsymbol{\mu}'_{v_1}, \ldots, \boldsymbol{\mu}'_{v_L}, \mu_{J_L}) \right) \right| \\
\times \prod_{m=1}^{L} \prod_{(j,r) \in v'_m} |W(\eta_{j,r})| \prod_{m=1}^{L-1} |W(\lambda_{L_m})| \\
\mathrm{d}\boldsymbol{\eta}'_{v_1} \ldots \mathrm{d}\boldsymbol{\eta}'_{v_L} \, \mathrm{d}\boldsymbol{\mu}'_{v_1}, \ldots, \mathrm{d}\boldsymbol{\mu}'_{v_L} \, \mathrm{d}\mu_{J_L} \, \mathrm{d}\lambda_{J_1} \ldots \mathrm{d}\lambda_{J_{L-1}}.
\end{aligned}
$$

From Lemma B.10, we have

$$
\begin{aligned}
\int_{\mathbb{R}^{L-1}} \cdots \int \int_{\mathbb{R}^{2P-L}} \cdots \int \left| W\left(\sum_{m=1}^{L} \sum_{(j,r) \in v'_m} a_{j,r} \eta_{j,r} + \sum_{m=1}^{L-1} b_m \lambda_{L_m} + \xi_T(\boldsymbol{\mu}'_{v_1}, \ldots, \boldsymbol{\mu}'_{v_L}) \right) \right| \prod_{m=1}^{L} \prod_{(j,r) \in v'_m} |W(\eta_{j,r})| \\
\times \prod_{m=1}^{L-1} |W(\lambda_{L_m})| \, \mathrm{d}\boldsymbol{\eta}'_{v_1} \ldots \mathrm{d}\boldsymbol{\eta}'_{v_L} \, \mathrm{d}\lambda_{J_1} \ldots \mathrm{d}\lambda_{J_{L-1}} \leq C,
\end{aligned}
$$

with some positive constant $C > 0$. By the above inequality and the following change the variables

$$
\lambda_j = \frac{\omega_j - \mu_j}{h_{d_T}} \qquad j \neq J_1, \ldots, J_{L-1},
$$

we obtain

$$
|\mathcal{T}_{\boldsymbol{v}}| \leq \frac{C \, \|q\|_\infty^{L-1}}{d_T^{P-1} h_{d_T}^{L-1}} \sum_{k_1 \in \mathcal{K}^{\boldsymbol{V}(v_1)}} \cdots \sum_{k_L \in \mathcal{K}^{\boldsymbol{V}(v_L)}} \prod_{m=1}^{L} \|f_{k_m}\|_\infty \int_{\mathbb{R}^{P-L+1}} \cdots \int q(\lambda_{J_L}) \prod_{m=1}^{L} \prod_{(j,r) \in v'_m} q(\lambda_j).
$$

Consequently,

$$
(d_T h_{d_T})^{P/2} |\mathcal{T}_{\boldsymbol{v}}| = \mathcal{O}\left(d_T^{-P/2+1} h_{d_T}^{P/2-L+1} \right),
$$

The above term converges to zero as $T \to \infty$ provided that $-P/2 + 1 - \kappa(P/2 - L + 1) < 0$ and it is fulfilled for all $\kappa \in (0, 1)$. Namely, the condition $-P/2 + 1 - \kappa(P/2 - L + 1) < 0$

- for $L = P/2 + 1$ is equivalent to $P > 2$,
- for $L < P/2 + 1$ is equivalent to

$$
1 > \kappa > \frac{-P/2 + 1}{P/2 - L + 1},
$$

and it is fulfilled for all $\kappa \in (0, 1)$ since $\frac{-P/2+1}{P/2-L+1} < 0$.

- for $P/2+1 < L \leq P$ is equivalent to

$$0 < \kappa < \frac{-P/2+1}{P/2-L+1}$$

and it is fulfilled for all $\kappa \in (0,1)$ since $\frac{-P/2+1}{P/2-L+1} \geq 1$.

The above and Lemma B.8 complete the proof. □

Proof of Theorem 3.5. Observe that

$$\sqrt{d_T h_{d_T}} \left(\widehat{f}^{XY}_{\alpha,\beta}(\omega)_{c_T,d_T} - f^{XY}_{\alpha,\beta}(\omega) \right) = \varepsilon_{c_T,d_T}(\omega) + U_{c_T,d_T}(\omega),$$

where $\varepsilon_{c_T,d_T}(\omega)$ is a bias term

$$\varepsilon_{c_T,d_T}(\omega) = \sqrt{d_T h_{d_T}} \mathbb{E} \left(\widehat{f}^{XY}_{\alpha,\beta}(\omega)_{c_T,d_T} - f^{XY}_{\alpha,\beta}(\omega) \right),$$

and

$$U_{c_T,d_T}(\omega) = \sqrt{d_T h_{d_T}} \left(\widehat{f}^{XY}_{\alpha,\beta}(\omega)_{c_T,d_T} - \mathbb{E}\left[\widehat{f}^{XY}_{\alpha,\beta}(\omega)_{c_T,d_T} \right] \right).$$

From Theorem 3.2, we know that $\varepsilon_{c_T,d_T}(\omega)$ converges to zero as $T \to \infty$. Therefore, it remains to prove that

$$\begin{bmatrix} \mathrm{Re}\left(U_{c_T,d_T}(\omega)\right) \\ \mathrm{Im}\left(U_{c_T,d_T}(\omega)\right) \end{bmatrix} \xrightarrow{d} \mathcal{N}_2(\mathbf{0}, \mathbf{\Sigma}_\vartheta(\omega;\alpha,\beta)).$$

Obviously, the first moment of $U_{c_T,d_T}(\omega)$ is zero. From Theorem 3.3, we get that its asymptotic covariance is finite. Now we focus on the higher-order asymptotic cumulants. For any constants $c_1,\ldots,c_P \in \mathbb{R}$ and $m_1,\ldots,m_P \in \mathbb{C}$, we have

$$\mathrm{cum}(c_1(Z_1-m_1),\ldots,c_P(Z_P-m_P)) = c_1\ldots c_P \,\mathrm{cum}(Z_1,\ldots,Z_P).$$

In addition, for $P>2$, from Theorem 3.4, we get that the P-th order joint cumulant

$$\mathrm{cum}\left(U^{[*]}_{c_T,d_T}(\omega),\ldots,(U^{[*]}_{c_T,d_T}(\omega) \right)$$

tends to zero. Following the discussion provided in Section A.3, we obtain the asymptotic normality of $U_{c_T,d_T}(\omega)$.

Finally, let us consider elements of

$$\begin{bmatrix} \mathrm{Cov}\Big(\mathrm{Re}\left(U_{c_T,d_T}(\omega)\right), \mathrm{Re}\left(U_{c_T,d_T}(\omega)\right) \Big) & \mathrm{Cov}\Big(\mathrm{Re}\left(U_{c_T,d_T}(\omega)\right), \mathrm{Im}\left(U_{c_T,d_T}(\omega)\right) \Big) \\ \mathrm{Cov}\Big(\mathrm{Im}\left(U_{c_T,d_T}(\omega)\right), \mathrm{Re}\left(U_{c_T,d_T}(\omega)\right) \Big) & \mathrm{Cov}\Big(\mathrm{Im}\left(U_{c_T,d_T}(\omega)\right), \mathrm{Im}\left(U_{c_T,d_T}(\omega)\right) \Big) \end{bmatrix}.$$

For a complex number $z \in \mathbb{C}$, we have

$$\mathrm{Re}(z) = \frac{z+\overline{z}}{2}, \qquad \mathrm{Im}(z) = \frac{z-\overline{z}}{2i}. \tag{3.11}$$

Thus, by (3.11), we obtain

$$\begin{aligned}
&\operatorname{Cov}\Big(\operatorname{Re}\left(U_{c_T,d_T}(\omega)\right), \operatorname{Re}\left(U_{c_T,d_T}(\omega)\right) \Big) \\
&\quad = \frac{d_T h_{d_T}}{4} \operatorname{Cov}\left(\widehat{f}^{XY}_{\alpha,\beta}(\omega)_{c_T,d_T} + \overline{\widehat{f}^{XY}_{\alpha,\beta}(\omega)_{c_T,d_T}}, \widehat{f}^{XY}_{\alpha,\beta}(\omega)_{c_T,d_T} + \overline{\widehat{f}^{XY}_{\alpha,\beta}(\omega)_{c_T,d_T}} \right), \\
&\operatorname{Cov}\Big(\operatorname{Re}\left(U_{c_T,d_T}(\omega)\right), \operatorname{Im}\left(U_{c_T,d_T}(\omega)\right) \Big) \\
&\quad = \frac{d_T h_{d_T}}{4i} \operatorname{Cov}\left(\widehat{f}^{XY}_{\alpha,\beta}(\omega)_{c_T,d_T} + \overline{\widehat{f}^{XY}_{\alpha,\beta}(\omega)_{c_T,d_T}}, \widehat{f}^{XY}_{\alpha,\beta}(\omega)_{c_T,d_T} - \overline{\widehat{f}^{XY}_{\alpha,\beta}(\omega)_{c_T,d_T}} \right), \\
&\operatorname{Cov}\Big(\operatorname{Im}\left(U_{c_T,d_T}(\omega)\right), \operatorname{Im}\left(U_{c_T,d_T}(\omega)\right) \Big) \\
&\quad = -\frac{d_T h_{d_T}}{4} \operatorname{Cov}\left(\widehat{f}^{XY}_{\alpha,\beta}(\omega)_{c_T,d_T} - \overline{\widehat{f}^{XY}_{\alpha,\beta}(\omega)_{c_T,d_T}}, \widehat{f}^{XY}_{\alpha,\beta}(\omega)_{c_T,d_T} - \overline{\widehat{f}^{XY}_{\alpha,\beta}(\omega)_{c_T,d_T}} \right).
\end{aligned}$$

Next, using bilinearity of covariance, Theorems 3.3 and (3.11), we get

$$\begin{aligned}
\lim_{T\to\infty} \operatorname{Cov}\Big(\operatorname{Re}\left(U_{c_T,d_T}(\omega)\right), \operatorname{Re}\left(U_{c_T,d_T}(\omega)\right) \Big) &= \frac{\operatorname{Re}(\sigma^2_\vartheta) + \operatorname{Re}(\sigma^2_{\vartheta,c})}{2}, \\
\lim_{T\to\infty} \operatorname{Cov}\Big(\operatorname{Re}\left(U_{c_T,d_T}(\omega)\right), \operatorname{Im}\left(U_{c_T,d_T}(\omega)\right) \Big) &= \frac{\operatorname{Im}(\sigma^2_\vartheta) - \operatorname{Im}(\sigma^2_{\vartheta,c})}{2}, \\
\lim_{T\to\infty} \operatorname{Cov}\Big(\operatorname{Im}\left(U_{c_T,d_T}(\omega)\right), \operatorname{Im}\left(U_{c_T,d_T}(\omega)\right) \Big) &= \frac{\operatorname{Re}(\sigma^2_{\vartheta,c}) - \operatorname{Re}(\sigma^2_\vartheta)}{2},
\end{aligned}$$

where

$$\begin{aligned}
\sigma^2_\vartheta = \sigma^2_\vartheta(\omega;\alpha,\beta) &= \lim_{T\to\infty} d_T h_{d_T} \operatorname{Cov}\left(\widehat{f}^{XY}_{\alpha,\beta}(\omega)_{c_T,d_T}, \widehat{f}^{XY}_{\alpha,\beta}(\omega)_{c_T,d_T} \right), \\
\sigma^2_{\vartheta,c} = \sigma^2_{\vartheta,c}(\omega;\alpha,\beta) &= \lim_{T\to\infty} d_T h_{d_T} \operatorname{Cov}\left(\widehat{f}^{XY}_{\alpha,\beta}(\omega)_{c_T,d_T}, \overline{\widehat{f}^{XY}_{\alpha,\beta}(\omega)_{c_T,d_T}} \right).
\end{aligned}$$

Observe that σ^2_ϑ is computed in Theorem 3.3 and $\sigma^2_{\vartheta,c}$ can be calculated analogously.

□

Proof of Corollary 2.2. We apply the reasoning presented in [51].

For the case where $f^{XY}_{\alpha,\beta}(\omega) = 0$, the thesis follows from the continuous mapping theorem, i.e.,

$$\sqrt{d_T h_{d_T}} \left| \widehat{f}^{XY}_{\alpha,\beta}(\omega)_{c_T,d_T} \right| \xrightarrow{d} \mathcal{L}\left(\sqrt{U_1^2 + U_2^2} \right),$$

where $\mathcal{L}\left([U_1, U_2]^{\mathrm{T}}\right) = \mathcal{N}_2(\mathbf{0}, \mathbf{\Sigma}_\vartheta(\omega;\alpha,\beta))$.

For the case $f^{XY}_{\alpha,\beta}(\omega) \neq 0$, we apply the delta method for the convergence in Theorem 3.5 and for the function $g(x,y) = \sqrt{x^2+y^2}$ which is differentiable at

$$\left(\operatorname{Re}\left(f^{X,Y}_{\alpha,\beta}(\omega) \right), \operatorname{Im}\left(f^{XY}_{\alpha,\beta}(\omega) \right) \right).$$

Note that $\boldsymbol{A}_1 \mathbf{\Sigma}_\vartheta(\omega;\alpha,\beta) \boldsymbol{A}_1^{\mathrm{T}} > 0$ if $\det(\mathbf{\Sigma}_\vartheta(\omega;\alpha,\beta)) \neq 0$. □

Lemma 3.1. *Let Assumption 2.1 and Assumption 2.3 hold. Let $(\alpha,\beta) \in \mathcal{K}^{XY}$ be fixed. Let $\omega \in \mathbb{R}$ be a point that does not lie at the intersection of the support lines of the spectral measures F^{XY}, F^{XX} and F^{YY}. Moreover, there exist first derivatives $f^{XX\prime}_{1,0}$, $f^{YY\prime}_{1,0}$ that belong to $L^2(\mathbb{R}) \cap L^\infty(\mathbb{R})$.*

Then

$$\sqrt{d_T h_{d_T}}\left(\begin{bmatrix} \mathrm{Re}(\widehat{f}^{XY}_{\alpha,\beta}(\omega)_{c_T,d_T}) \\ \widehat{f}^{XX}_{0,1}(\omega)_{c_T,d_T} \\ \widehat{f}^{YY}_{0,1}(\nu)_{c_T,d_T} \\ \mathrm{Im}(\widehat{f}^{XY}_{\alpha,\beta}(\omega)_{c_T,d_T}) \end{bmatrix} - \begin{bmatrix} \mathrm{Re}(f^{XY}_{\alpha,\beta}(\omega)) \\ f^{XX}_{1,0}(\omega) \\ f^{YY}_{1,0}(\nu) \\ \mathrm{Im}(f^{XY}_{\alpha,\beta}(\omega)) \end{bmatrix}\right) \xrightarrow{d} \mathcal{N}_4(0, \boldsymbol{D}_\vartheta(\omega,\nu;\alpha,\beta)),$$

where elements of $\boldsymbol{D}_\vartheta(\omega,\nu;\alpha,\beta)$ *can be computed by Theorem 3.3.*

Proof of Lemma 3.1. It is a natural generalization of Theorem 3.5 to the multidimensional case, and the proof is analogous. □

Proof of Theorem 3.6. We apply the reasoning presented in [51].

For the case where $f^{XY}_{\alpha,\beta}(\omega) = 0$, the thesis follows from the continuous mapping theorem, the consistency of the cross-periodogram frequency-smoothed along the line, and Slutsky's lemma. Namely,

$$\sqrt{d_T h_{d_T}}\left|\widehat{\gamma}^{XY}_{\alpha,\beta}(\omega)_{c_T,d_T}\right| = \frac{\sqrt{d_T h_{d_T}}\left|\widehat{f}^{XY}_{\alpha,\beta}(\omega)_{c_T,d_T}\right|}{\sqrt{\widehat{f}^{XX}_{0,1}(\omega)_{c_T,d_T}\widehat{f}^{YY}_{0,1}(\alpha\omega+\beta)_{c_T,d_T}}} \xrightarrow{d} \mathcal{L}\left(\frac{\sqrt{U_1^2+U_2^2}}{f^{XX}_{1,0}(\omega)f^{YY}_{1,0}(\alpha\omega+\beta)}\right),$$

where $\mathcal{L}\left([U_1,U_2]^{\mathrm{T}}\right) = \mathcal{N}_2(\mathbf{0}, \boldsymbol{\Lambda}_\vartheta(\omega,\alpha\omega+\beta))$.

For the case $f^{XY}_{\alpha,\beta}(\omega) \neq 0$, we apply the delta method to convergence in Lemma 3.1 and for the function

$$g(x,y,z,t) = \frac{\sqrt{x^2+y^2}}{\sqrt{zt}},$$

which is differentiable at

$$\left(\mathrm{Re}\left(f^{XY}_{\alpha,\beta}(\omega)\right), f^{XX}_{1,0}(\omega), f^{YY}_{1,0}(\alpha\omega+\beta), \mathrm{Im}\left(f^{XY}_{\alpha,\beta}(\omega)\right)\right).$$

Note that $\boldsymbol{A}_2\boldsymbol{\Lambda}_\vartheta(\omega,\alpha\omega+\beta)\boldsymbol{A}_2^{\mathrm{T}} > 0$ if $\det(\boldsymbol{\Lambda}_\vartheta(\omega,\alpha\omega+\beta)) \neq 0$. □

Proof of Proposition 3.2. Observe that dependence of the asymptotic distributions on the parameter $\lim\limits_{T\to\infty}\frac{s\Delta}{b} = \vartheta$ appears only in the asymptotic covariance matrix, and precisely in the following factors

$$\mathcal{E}_\vartheta(a) = \int_{\mathbb{R}} W(\eta)W(-a\eta)e^{i2\pi(a-1)\eta\vartheta}\mathrm{d}\eta,$$

and

$$\mathcal{W}_\vartheta(a_1,a_2,a_3) = \int\limits_{\mathbb{R}}\int\limits_{\mathbb{R}}\int\limits_{\mathbb{R}} W(\eta_1)W(\eta_2)W(\eta_2)\,W(a_1\eta_1+a_2\eta_2+a_3\eta_3) \times e^{-i2\pi(\eta_1+\eta_2+\eta_3)\vartheta}\,e^{i2\pi(a_1\eta_1+a_2\eta_2+a_3\eta_3)\vartheta}\,\mathrm{d}\eta_1\,\mathrm{d}\eta_2\,\mathrm{d}\eta_3.$$

Thus, it is sufficient to show that $\mathcal{E}_\vartheta(a)$ and $\mathcal{W}_\vartheta(a,b,c)$ do not depend on ϑ. For $a=1$, the proof is straightforward. For $a \neq 1$, we have $|\vartheta| \leq \frac{1}{2}$, since $\left|\frac{s\Delta}{b}\right| \leq \frac{1}{2}$ for $s = -l_T, -l_T+1, \ldots, l_T$.

From Proposition 3.1, the normalizing factor takes the form

$$\mathcal{E}_\vartheta(a) = \left\|\left[-\tfrac{1}{2},\tfrac{1}{2}\right] \cap \left[-\tfrac{1}{2a}+\tfrac{(1-a)\vartheta}{a}, \tfrac{1}{2a}+\tfrac{(1-a)\vartheta}{a}\right]\right\|,$$

where $\|\cdot\|$ denotes the Lebsegue measure on $\mathbb{R}$. Note that

$$\mathcal{E}_\vartheta(a) = \|[h_{\text{low}}(1), h_{\text{up}}(1)] \cap [h_{\text{low}}(a), h_{\text{up}}(a)]\|,$$

where $h_{\text{low}}(x) = -\frac{1}{2x} + \frac{\vartheta(1-x)}{x}$ and $h_{\text{up}}(x) = \frac{1}{2x} + \frac{\vartheta(1-x)}{x}$. For $x > 0$ and $|\vartheta| \leq \frac{1}{2}$, the function $h_{\text{low}}(x)$ is increasing and $h_{\text{up}}(x)$ is decreasing. Then

$$\mathcal{E}_\vartheta(a) = \|[h_{\text{low}}(\max(1,a)), h_{\text{up}}(\max(1,a))]\| = |h_{\text{up}}(\max(1,a)) - h_{\text{low}}(\max(1,a))| = \frac{1}{\max(1,a)}.$$

As for $\mathcal{E}_\vartheta(a)$, we can show

$$\mathcal{W}_\vartheta(a_1,a_2,a_3) = \int_{\mathbb{R}} w(a_1x + \vartheta(a_1-1))\, w(a_2x + \vartheta(a_2-1))\, w(a_3x + \vartheta(a_3-1))\, w(x)\,\mathrm{d}x,$$

and hence

$$\begin{aligned}\mathcal{W}_\vartheta(a_1,a_2,a_3) &= \|[h_{\text{low}}(\max(1,a_1,a_2,a_3)), h_{\text{up}}(\max(a_1,a_2,a_3))]\| \\ &= |h_{\text{up}}(\max(a_1,a_2,a_3)) - h_{\text{low}}(\max(1,a_1,a_2,a_3))| \\ &= \frac{1}{\max(1,a_1,a_2,a_3)}.\end{aligned}$$

□

Proof of Proposition 3.3. Note that

$$\begin{aligned}\mathcal{F}_{XY}(a,b) &= \sigma\left(\{X(t) : a \leq t \leq b\}, \{Y(t) : a \leq t \leq b\}\right) \\ &\subset \sigma\left(\left\{Z(t) : t \in \bigcup_{k=1}^{K}[s_k a, s_k b)] \cup \bigcup_{l=1}^{L}[r_l a, r_l b]\right\}\right) \\ &\subset \sigma\left(\{Z(t) : t \in [\min\{s_1,\ldots,s_K,r_1,\ldots,r_L\}a, \max\{s_1,\ldots,s_K,r_1,\ldots,r_L\}b]\}\right) \\ &= \mathcal{F}_Z(\underline{q}a, \bar{q}b),\end{aligned}$$

where

$$\underline{q} = \min\{s_1,\ldots,s_K,r_1,\ldots,r_L\}, \qquad \bar{q} = \max\{s_1,\ldots,s_K,r_1,\ldots,r_L\}.$$

Finally, using Lemma B.2, we have for $t, \tau \in \mathbb{R}$

$$\begin{aligned}\alpha\left(\mathcal{F}_{XY}(-\infty,t), \mathcal{F}_{XY}(t+\tau,+\infty)\right) &\leq \alpha\left(\mathcal{F}_Z(-\infty,\bar{q}t), \mathcal{F}_Z(\underline{q}(t+\tau),\infty)\right) \\ &\leq 8\left(\sup_{u\in\mathbb{R}}\|Z(u)\|_{2+\delta}\right)^{\frac{2}{2+\delta}} \alpha_Z^{\frac{\delta}{2+\delta}}((\underline{q}-\bar{q})t + \bar{q}\tau) = h(t,\tau),\end{aligned}$$

and

$$\int_{\mathbb{R}} \alpha_Z^{\frac{\delta}{2+\delta}}((\underline{q}-\bar{q})t + \bar{q}\tau)\,\mathrm{d}\tau = \frac{1}{\bar{q}}\int_{\mathbb{R}} \alpha_Z^{\frac{\delta}{2+\delta}}(\tau)\,\mathrm{d}\tau < \infty.$$

□

Proof of Theorem 3.7. The proof is similar to the proof of Theorem 4.2.1 in [72]. However, it requires some key changes. Proof of *(i)*: Define

$$U_{T,b}^{\theta}(x) = \frac{1}{2l_T+1}\sum_{j=-l_T}^{l_T} \mathbb{1}_{\{\sqrt{bh_b}(\widehat{\theta}_{T,b,\Delta j}-\theta)\leq x\}}.$$

Observe that

$$L_{T,b}^{\theta}(x) = \frac{1}{2l_T+1} \sum_{j=-l_T}^{l_T} \mathbb{1}_{\{\sqrt{bh_b}(\widehat{\theta}_{T,b,\Delta_j}-\theta)+\sqrt{bh_b}(\theta-\widehat{\theta}_T)\leq x\}}.$$

Then for every $\varepsilon > 0$, we have

$$U_{T,b}^{\theta}(x-\varepsilon)\mathbb{1}_{E_{T,b}} \leq L_{T,b}^{\theta}(x)\mathbb{1}_{E_{T,b}} \leq U_{T,b}^{\theta}(x+\varepsilon),$$

where

$$E_{T,b} = \left\{ \sqrt{bh_b} \left(\theta - \widehat{\theta}_T \right) \leq x \right\}.$$

The probability of the set $E_{T,b}$ tends to one, and hence

$$U_{T,b}^{\theta}(x-\varepsilon) \leq L_{T,b}^{\theta}(x) \leq U_{T,b}^{\theta}(x+\varepsilon)$$

with probability tending to one. If $x \pm \varepsilon$ are continuity points of $J^{\theta}(x)$, then $U_{T,b}(x \pm \varepsilon)$ tending to $J^{\theta}(x \pm \varepsilon)$ in probability implies that

$$J^{\theta}(x-\varepsilon) - \varepsilon \leq L_{T,b}^{\theta}(x) \leq J^{\theta}(x+\varepsilon) + \varepsilon$$

with probability tending to one. To obtain $L_{T,b}^{\theta}(x) \to J^{\theta}(x)$ in probability, we take $\varepsilon \to 0$ such that $x \pm \varepsilon$ are continuity points of $J^{\theta}(x)$. Therefore, it is sufficient to show that $U_{T,b}^{\theta}(x)$ converges in probability to $J^{\theta}(x)$ for every continuity point x of $J^{\theta}(x)$.

Observe that

$$\mathbb{E}\left[U_{T,b}^{\theta}(x)\right] = \frac{1}{2l_T+1} \sum_{j=-l_T}^{l_T} J_{T,b,\Delta_j}^{\theta}(x),$$

where $J_{T,b,\Delta_j}^{\theta}(x)$ is the cumulative distribution function of $J_{T,b,\Delta_j}^{\theta}$. We know that $J_{T,b,\Delta_j}^{\theta}(x)$ converges to $J^{\theta}(x)$ as $T \to \infty$. Consequently, $\mathbb{E}\left[U_{T,b}^{\theta}(x)\right]$ converges to $J^{\theta}(x)$ and it remains to show that $\operatorname{Var}\left(U_T^{\theta}(x)\right)$ tends to zero as $T \to \infty$. Let

$$I_{b,j} = \mathbb{1}_{\{\sqrt{bh_b}(\widehat{\theta}_{T,b,\Delta_j}-\theta)\leq x\}},$$

and

$$A_{l_T,\tau} = \frac{1}{2l_T+1} \sum_{j=0}^{l_T-\tau} \operatorname{Cov}\left(I_{b,j}, I_{b,j+\tau}\right).$$

Thus,

$$\begin{aligned}\operatorname{Var}\left(U_{T,b}^{\theta}(x)\right) &= \frac{1}{(2l_T+1)^2} \sum_{j=-l_T}^{l_T} \sum_{k=-l_T}^{l_T} \operatorname{Cov}\left(I_{b,j}, I_{b,k}\right) = \frac{1}{(2l_T+1)^2} \sum_{j=-l_T}^{l_T} \sum_{\tau=-l_T-j}^{l_T-j} \operatorname{Cov}\left(I_{b,j}, I_{b,j+\tau}\right) \\ &= \frac{1}{2l_T+1} \sum_{\tau=0}^{2l_T+1} A_{l_T,\tau} = \frac{1}{2l_T+1} \left(A_{l_T,0} + \sum_{\tau=1}^{b-1} A_{l_T,\tau} + \sum_{\tau=b}^{2l_T+1} A_{l_T,\tau} \right) = V_1 + V_2,\end{aligned}$$

where

$$V_1 = \frac{1}{2l_T+1} \left(A_{l_T,0} + \sum_{\tau=1}^{b-1} A_{l_T,\tau} \right), \qquad V_2 = \frac{1}{2l_T+1} \sum_{\tau=b}^{2l_T+1} A_{l_T,\tau}.$$

One can easily notice that $|V_1| = \mathcal{O}\left(\frac{b}{l_T}\right)$ and it converges to zero as $T \to \infty$. For V_2, we use Lemma B.3 and the condition (i) of Assumption 3.3. Then for $\tau \geq b$

$$|\mathrm{Cov}\,(I_{b,j}, I_{b,j+\tau})| \leq 4\alpha\left(\mathcal{F}^{XY}_{(-\infty,j\Delta+b/2)}, \mathcal{F}^{XY}_{((j+\tau)\Delta-b/2,+\infty)}\right) \leq 4h(j\Delta + b/2, \tau\Delta - b),$$

and hence

$$\begin{aligned}
|V_2| &\leq \frac{4}{(2l_T+1)^2}\sum_{\tau=b}^{2l_T+1}\sum_{j=0}^{l_T-\tau} h(j\Delta + b/2, \tau\Delta - b) = \frac{4}{(2l_T+1)^2}\sum_{j=0}^{l_T-b}\sum_{\tau=b}^{l_T-j} h(j\Delta + b/2, \tau\Delta - b) \\
&\leq \frac{4}{(2l_T+1)^2}\sum_{j=0}^{l_T-b}\sum_{\tau=b}^{\infty} h(j\Delta + b/2, \tau\Delta - b) \\
&\leq \frac{4}{(2l_T+1)^2}\sum_{j=0}^{l_T-b}\left(h(j\Delta + b/2, b(\Delta-1)) + \int_b^{\infty} h(j\Delta + b/2, \tau\Delta - b)\,\mathrm{d}\tau\right).
\end{aligned}$$

Finally, by the change of the variable $u = \Delta\tau - b$, we get

$$|V_2| \leq \frac{4}{(2l_T+1)^2}\sum_{j=0}^{l_T-b}\left(h(j\Delta + b, -b) + \frac{1}{\Delta}\int_{b(\Delta-1)}^{\infty} h(j\Delta + b, u)\,\mathrm{d}u\right),$$

and hence

$$|V_2| \leq \frac{4(l_T-b)}{(2l_T+1)^2}\left(\frac{1}{4} + \frac{M}{\Delta}\right),$$

and V_2 converges to zero as $T \to \infty$.

Proof of *(ii)*: By the Heine definition of the limit of a function, $\sup_{x\in\mathbb{R}}\left|L^{\theta}_{T,b}(x) - J^{\theta}(x)\right| \to 0$ in probability if for every sequence $\{T_n\}$, such that $T_n \to \infty$ as $n \to \infty$, the sequence $\sup_{x\in\mathbb{R}}\left|L^{\theta}_{T_n,b_n}(x) - J^{\theta}(x)\right|$ tends to zero in probability as $n \to \infty$, where $b_n = \mathcal{O}(T_n^p)$. Finally, similarly as in Theorem 3.2.1 in [72] one can prove that $\sup_{x\in\mathbb{R}}\left|L^{\theta}_{T_n,b_n}(x) - J^{\theta}(x)\right| \to 0$ in probability as $n \to \infty$.

The proof of *(iii)* follows from the Heine definition of the limit of a function and the same reasoning as used in Theorem 3.2.1 in [72]. □

Proof of Corollary 3.2. It follows immediately from Theorem 3.7 and the continuous mapping theorem. □

CHAPTER 4

SIMULATION STUDY

In this chapter, we conduct simulation studies to illustrate our theoretical findings presented in Chapters 2 and 3. In Section 4.1, we introduce the models used in simulation studies. In Section 4.2, we present the simulation results examining the mean-square consistency of the normalized frequency-smoothed periodogram along the line, addressing both the cases when the line is known and when it is unknown. In Section 4.3, we analyze the performance of subsampling-based confidence intervals for the spectral density and spectral coherence functions.

4.1 Models used in the simulation study

Let $Z(t)$ be the Ornstein-Uhlenbeck processes defined by the following stochastic differential equation

$$\mathrm{d}Z(t) = -Z(t)\,\mathrm{d}t + \mathrm{d}W(t), \quad t \in \mathbb{R}, \tag{4.1}$$

where $\{W(t),\, t \in \mathbb{R}\}$ denotes the Wiener process, see [40, Chapter 6]. It can be shown that $Z(t)$ is a stationary process. Its mean function is $\mu_Z(t) = 0$ and its autocovariance function is $\gamma_Z(\tau) = \frac{1}{2}e^{-|\tau|}$. Consequently, its spectral density function has the form $\phi_Z(\omega) = \frac{1}{1+4\pi^2\omega^2}$. Furthermore, in [4] it is shown that $Z(t)$ is geometrically α-mixing.

We perform simulation studies using the following models.

M1 : A process $X(t)$ given by $X(t) = Z(t) + Z(st)\cos(2\pi\lambda t)$ with $s = \frac{1}{2}$ and $\lambda = \frac{1}{4}$.

M2 : A process $X(t)$ given by $X(t) = Z(t) + Z(st)\cos(2\pi\lambda t)$ with $s = \frac{1}{4}$ and $\lambda = \frac{1}{4}$.

M3 : Two processes $X_1(t)$ and $X_2(t)$ given by $X_1(t) = Y(s_1 t)e^{i2\pi\eta_1 t}$ and $X_2(t) = Y(s_2 t)e^{i2\pi\eta_2 t}$, where $Y(t) = Z(t)\cos(\pi\psi t)$, with $s_1 = \frac{1}{2}$, $s_2 = \frac{1}{4}$, $\eta_1 = \frac{1}{100}$, $\eta_2 = \frac{1}{50}$, $\psi = \frac{4}{3}$.

The models **M1** and **M2** differ in the parameter s, which affects the slope of the support lines. For the spectral properties of models **M1** and **M2**, we refer to Example 1.2. The model **M3** is discussed in Example 1.3, while the properties of $Y(t)$ can be found in Example 1.1.

To perform simulations for models **M1**–**M3**, first, we need to generate $Z(t)$ and $Z(st)$ with $s^{-1} \in \mathbb{N}$. Since $Z(t)$ is a solution of the stochastic differential equation (4.1) we can use the Euler-Maruyama scheme [57, Section 2.7] to generate it. Let $N \in \mathbb{N}$ be a number of samples and $\delta > 0$ be a discretization step. The observation interval is $\left[-\frac{T}{2}, \frac{T}{2}\right]$ with $T = (N-1)\delta > 0$. First, we approximate $\tilde{Z}(t) = Z(st)$ at points $t = -\frac{T}{2} + sn\delta$ using $\widetilde{Z}_n$ given by

$$\begin{cases} \widetilde{Z}_n = (1-\delta)\widetilde{Z}_{n-1} + \sqrt{\delta}\varepsilon_n, \quad n = 1, 2, \ldots, s(N-1), \\ \widetilde{Z}_0 \sim N(0, \frac{1}{2}), \end{cases}$$

where $\varepsilon_1, \ldots, \varepsilon_{s(N-1)}$ are independent random variables with the standard normal distribution $\mathcal{N}(0,1)$. Then $Z(t)$ is simulated as $\widetilde{Z}_{s^{-1}n}$.

In Figure 4.1, we present a single trajectory of the processes considered in models **M1** and **M2**. Both trajectories are derived from the same underlying trajectory $Z(t)$, which is also shown in the graphs. Figure 4.2 illustrates a single trajectory of the real part of the processes $X_1(t)$ and $X_2(t)$ considered in the model **M3** along with the trajectory of $Y(t)$.

4.2 Validation of mean-square consistency

In this section, we analyze the mean-square consistency of the frequency-smoothed periodogram through a simulation study. We begin by examining the scenario in which the support lines are known, considering models **M1** and **M2**. Then, we investigate the case where the support lines are estimated, considering model **M3**.

4.2.1 Known support line case

For both models **M1** and **M2**, we set the discretization step $\delta = \frac{1}{32}$, and the number of samples N takes values in $\{1024, 2048, 4096, 8192, 16384\}$. The length of the observation interval is given by $T = (N-1)\delta$. As the data-tapering window w we consider the rectangular window function, while the frequency-smoothing window q is the Hann window (see Table 2.1). The frequency-smoothing bandwidth is set to $h_T = \frac{1}{16}T^{-2/5}$. The frequencies at which the spectral density functions are estimated are given by $\omega_j^N = -\frac{1}{2\delta} + \frac{j}{(N-1)\delta}$ for $j = 0, 1, \ldots, N-1$. Note that $\omega_j^N \in \left[-\frac{1}{2\delta}, \frac{1}{2\delta}\right]$ for $j = 0, 1, \ldots, N-1$.

We consider the estimation of the spectral density functions $f^{XX}_{\alpha,\beta}(\omega)$, where α and β denote the slope and intercept of the support line, respectively. We focus on the following support lines:

L1 : $\{(\omega, \nu) \in \mathbb{R}^2 : \nu = \omega\}$,

L2 : $\{(\omega, \nu) \in \mathbb{R}^2 : \nu = s\omega + \lambda\}$,

L3 : $\{(\omega, \nu) \in \mathbb{R}^2 : \nu = s^{-1}(\omega + \lambda)\}$,

L4 : $\{(\omega, \nu) \in \mathbb{R}^2 : \nu = \omega + 2\lambda\}$,

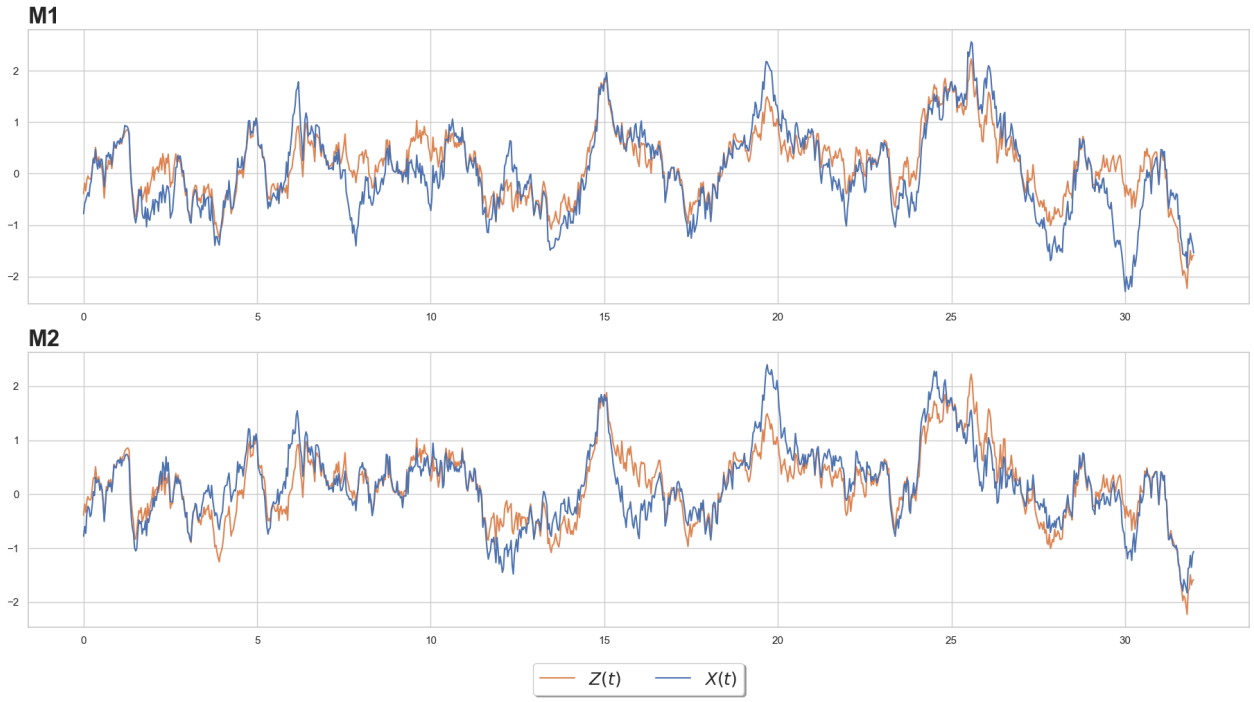

Figure 4.1: Blue line: single trajectory of the processes $X(t)$, $t \in \left[0, \frac{T}{2}\right]$, with $\delta = \frac{1}{32}$ and $N = 2048$. Orange line: single trajectory of the underlying trajectory $Z(t)$, $t \in \left[0, \frac{T}{2}\right]$, with $\delta = \frac{1}{32}$ and $N = 2048$. The top panel corresponds to model **M1**, and the bottom panel corresponds to model **M2**.

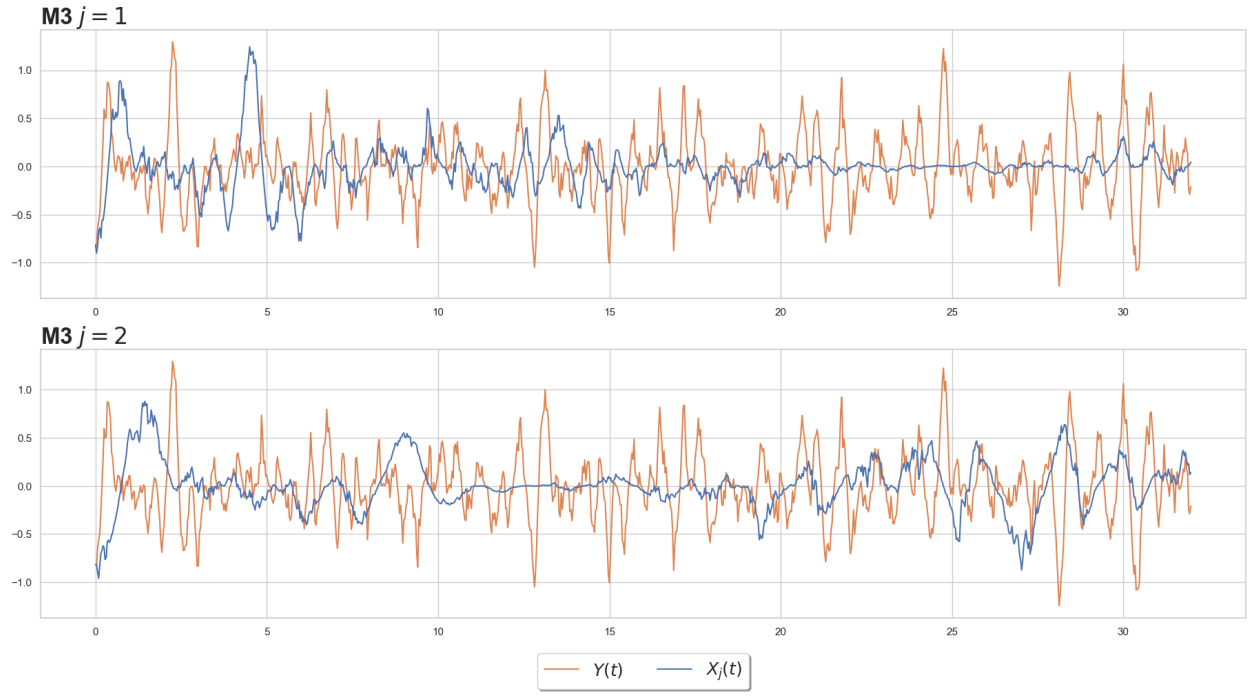

Figure 4.2: Blue line: single trajectory of the real part of $X_j(t)$ for $t \in \left[0, \frac{T}{2}\right]$, with $\delta = \frac{1}{32}$ and $N = 2048$, considered in the model **M3**. Orange line: single trajectory of the underlying trajectory $Y(t)$, $t \in \left[0, \frac{T}{2}\right]$, with $\delta = \frac{1}{32}$ and $N = 2048$. The top panel corresponds to the case $j = 1$, and the bottom panel corresponds to the case $j = 2$.

where the values of λ and s are given in **M1** and **M2** (see Section 4.1).

To evaluate the performance of the frequency-smoothed periodogram $\widehat{f}^{XX}_{\alpha,\beta}(\omega)$ for a fixed $\omega \in \mathbb{R}$, we examine its expected value and standard deviation, denoted by

$$\mathrm{E}(T;\omega) = \mathbb{E}\left(\widehat{f}^{XX}_{\alpha,\beta}(\omega)\right),$$
$$\mathrm{STD}(T;\omega) = \left(\mathrm{Var}\left(\widehat{f}^{XX}_{\alpha,\beta}(\omega)\right)\right)^{\frac{1}{2}}.$$

Recall that T denotes the length of the observation interval of $X(t)$. In other words, $\widehat{f}^{XX}_{\alpha,\beta}(\omega)$ is calculated based on the sample observed over an interval of length T. Moreover, we investigate the mean-squared error averaged over frequencies. Note that as T increases, the number of considered frequencies ω_j^N also increases. To ensure a consistent measure of accuracy for different values of T, we consider the same set of frequencies for each T. Specifically, we choose the frequencies ω_j^{1024} for $j = 0, 1, \ldots, 1023$. We define

$$\mathrm{MSE}_{\mathrm{mean}}(T) = \tfrac{1}{1024}\sum_{j=0}^{1023}\mathbb{E}\left|\widehat{f}^{XX}_{\alpha,\beta}(\omega_j^{1024}) - f^{XX}_{\alpha,\beta}(\omega_j^{1024})\right|^2.$$

By Monte Carlo simulation (using $M = 500$ Monte Carlo trials), we obtain estimates of $\mathrm{E}(T;\omega)$, $\mathrm{STD}(T;\omega)$ and $\mathrm{MSE}_{\mathrm{mean}}(T)$. Their estimates are denoted by $\widehat{\mathrm{E}}(T;\omega)$, $\widehat{\mathrm{STD}}(T;\omega)$ and $\widehat{\mathrm{MSE}}_{\mathrm{mean}}(T)$, respectively.

Note that the considered spectral density functions are real-valued (see Example 1.2) and hence, for simplicity of presentation, we decided to omit the estimation results for their imaginary parts. In Figures 4.3 and 4.5 we present the results for models **M1** and **M2**, respectively, focusing on the estimated expectation $\widehat{\mathrm{E}}(T;\omega)$ and the estimated standard deviation $\widehat{\mathrm{STD}}(T;\omega)$. Specifically, the figures display $\widehat{\mathrm{E}}(T;\omega)$ as a blue dashed line, along with the range $\widehat{\mathrm{E}}(T;\omega) \pm \widehat{\mathrm{STD}}(T;\omega)$, represented by a blue shaded area. Additionally, the theoretical values of the spectral density function are shown as a green solid line. Each column in the figures corresponds to a different support line **L1**–**L4**, while each row represents the results for a different value of N (consequently a different value of T). For clarity, we restrict the simulation results to frequencies within the range around the maximum values of the spectral density functions, that is, to the interval $[-0.5, 0.5]$. It is evident that for any line, as T increases, the estimated expected values $\widehat{\mathrm{E}}(T;\omega)$ progressively approach the true values. In addition, the range covered by one standard deviation $\widehat{\mathrm{STD}}(T;\omega)$ decreases. It indicates a reduction in the mean-squared error of the estimator. To visualize this trend, Figures 4.4 and 4.6 (corresponding to models **M1** and **M2**, respectively) show the estimated averaged mean-squared error $\widehat{\mathrm{MSE}}_{\mathrm{mean}}(T)$. This analysis further illustrates the decrease in the mean-squared error of the frequency-smoothed periodogram along the known support line as T increases, demonstrating consistency with the theoretical results (see Corollary 2.1).

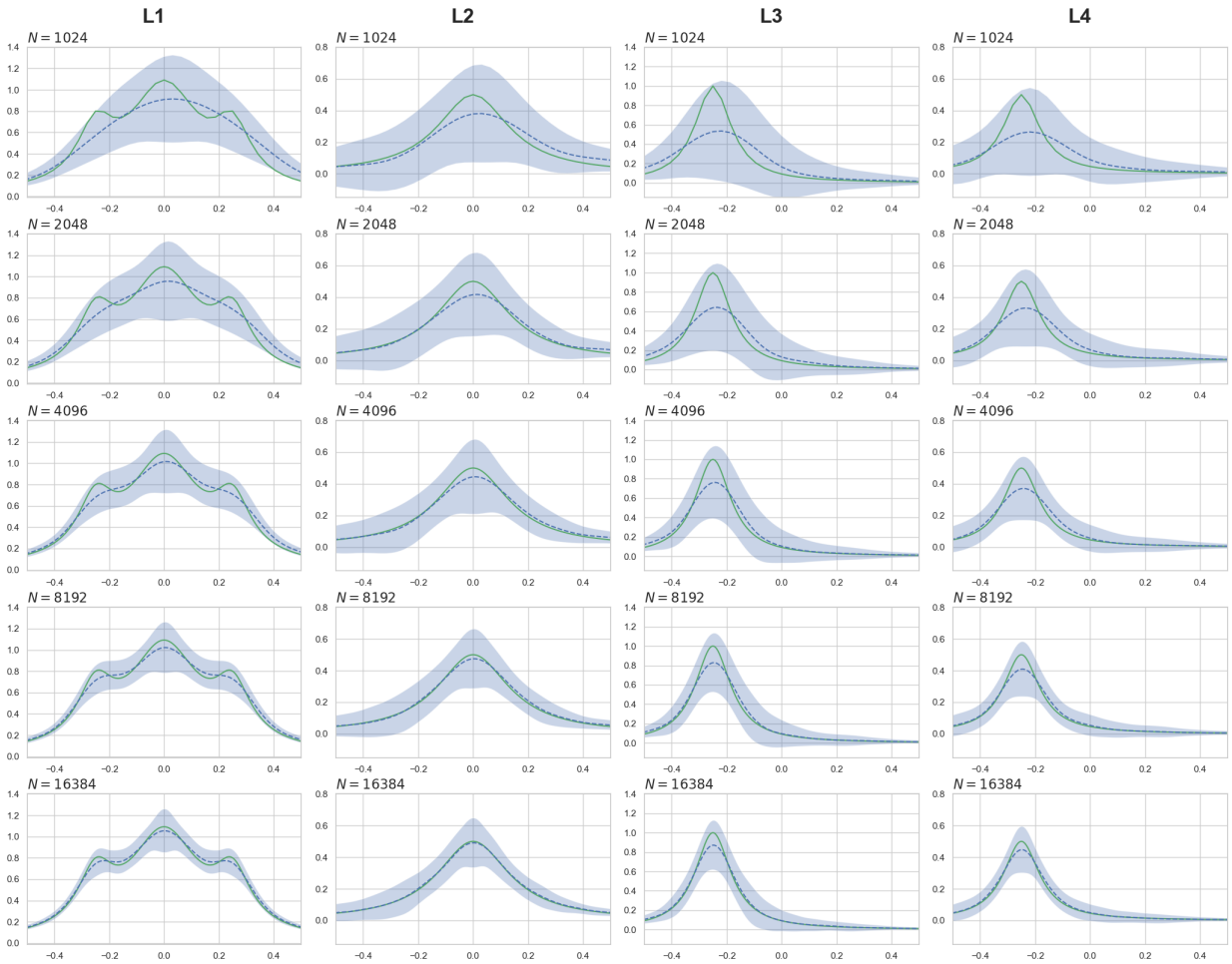

Figure 4.3: Results for **M1** (the case of a known line). Green solid line: the theoretical values of the spectral density function. Blue dashed line: the estimated expectation $\widehat{\mathrm{E}}(T;\omega_j^N)$. Shaded blue area: the region within one standard deviation $\widehat{\mathrm{STD}}(T;\omega_j^N)$. Each row represents a specific value of N. The subsequent columns (from the left) correspond respectively to lines **L1**–**L4**.

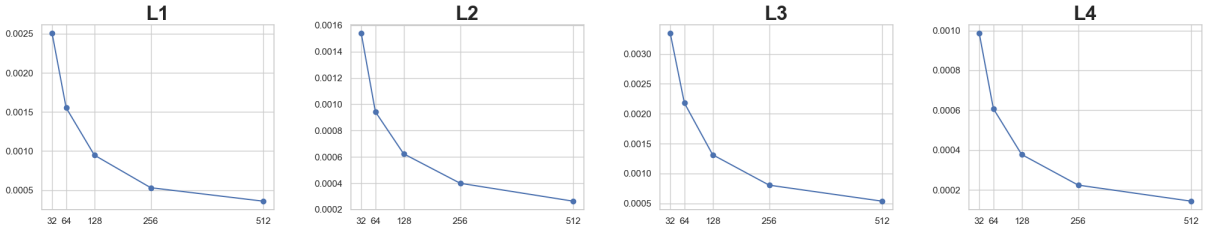

Figure 4.4: Results for **M1** (the case of a known line). The estimated average mean-squared error $\widehat{\mathrm{MSE}}_{\mathrm{mean}}(T)$ as a function of T. The subsequent columns (from the left) correspond respectively to lines **L1**–**L4**.

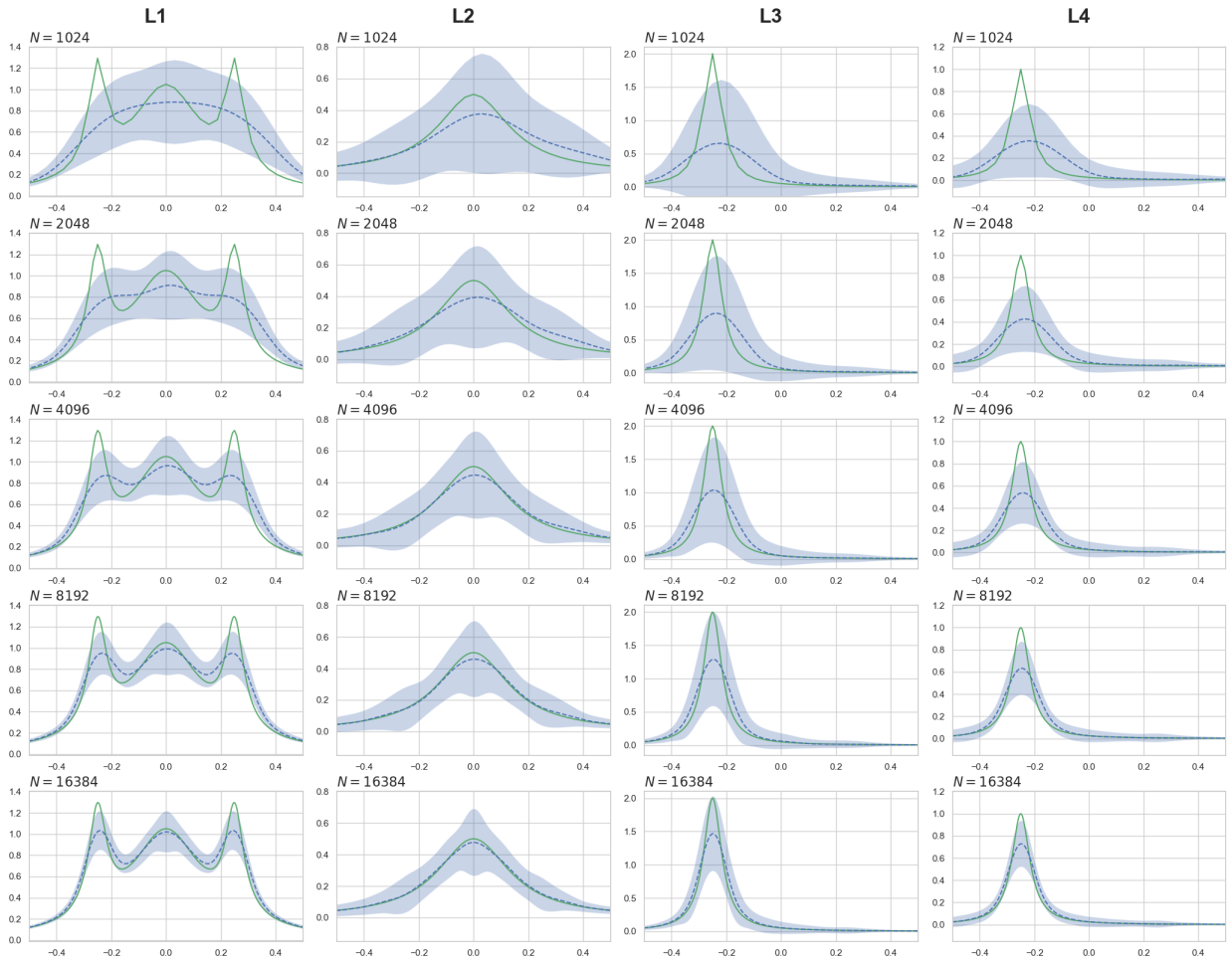

Figure 4.5: Results for **M2** (the case of a known line). Green solid line: the theoretical values of the spectral density function. Blue dashed line: the estimated expectation $\widehat{\mathrm{E}}(T;\omega_j^N)$. Shaded blue area: the region within one standard deviation $\widehat{\mathrm{STD}}(T;\omega_j^N)$. Each row represents a specific value of N. The subsequent columns (from the left) correspond respectively to lines **L1**–**L4**.

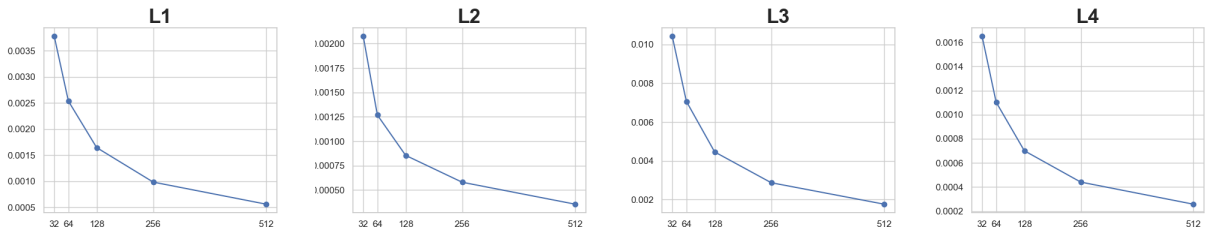

Figure 4.6: Results for **M2** (the case of a known line). The estimated average mean-squared error $\widehat{\mathrm{MSE}}_{\mathrm{mean}}(T)$ as a function of T. The subsequent columns (from the left) correspond respectively to lines **L1**–**L4**.

4.2.2 Unknown support line case

For the model **M3**, we set the discretization step $\delta = \frac{1}{32}$, and the number of samples N takes values in $\{1024, 2048, 4096, 8192, 16384\}$. The length of the observation interval is given by $T = (N-1)\delta$. As the data-tapering window w we consider the rectangular window function, while the frequency-smoothing window q is the Hann window (see Table 2.1). The frequency-smoothing bandwidth is set to $h_T = \frac{1}{80}T^{-1/3}$. The frequencies at which the spectral density functions are estimated are given by $\omega_j^N = -\frac{1}{2\delta} + \frac{j}{(N-1)\delta}$ for $j = 0, 1, \ldots, N-1$. Note that $\omega_j^N \in \left[-\frac{1}{2\delta}, \frac{1}{2\delta}\right]$ for $j = 0, 1, \ldots, N-1$.

We consider the estimation of the spectral density functions $f_{\alpha,\beta}^{X_1X_2}(\omega)$, where α and β denote the slope and intercept of the support line, respectively. We focus on the following support lines:

$$\textbf{L1} \ : \left\{(\omega, \nu) \in \mathbb{R}^2 \ : \ \nu = \tfrac{s_2}{s_1}(\omega - \eta_1) + \eta_2\right\},$$

$$\textbf{L2} \ : \left\{(\omega, \nu) \in \mathbb{R}^2 \ : \ \nu = \tfrac{s_2}{s_1}(\omega - \eta_1) + \eta_2 - s_1\lambda\right\},$$

where $\lambda = 2\psi$. We assume that λ is known and s_1, s_2, η_1, η_2 are unknown.

Let us demonstrate the estimation of the support line using the procedure outlined in Section 2.2.3. Specifically, we analyze the realization of $X_1(t)$ and $X_2(t)$ over an observation interval of length $T = 16383\delta$. The procedure assumes that the cycle autocovariance frequency and the cycle conjugate autocovariance frequency of $Y(t)$ are known. Both are equal to $\lambda = 2\psi$. The first step is to find the cyclic autocovariance frequency $\lambda_j = s_j\lambda$ of $X_j(t)$ and the cyclic conjugate autocovariance frequency $\gamma_j = s_j\gamma + 2\eta_j$ of $X_j(t)$, for $j = 1, 2$. Note that the value of $\lambda = 2.\overline{6}$ is chosen to make this problem more difficult, because the frequencies $\lambda_1, \lambda_2, \gamma_1, \gamma_2$ do not belong to the set of frequencies considered $\{\omega_j^N \ : \ j = 0, 1 \ldots, N-1\}$ and cannot be exactly represented on a computer. The digit with a horizontal line above represents an infinitely repeating digit in the repeating decimal.

Figure 4.7 presents the estimated magnitude of cyclic autocovariance functions and the estimated magnitude of cyclic conjugate autocovariance functions of $X_1(t)$ and $X_2(t)$ for a lag parameter $\tau = 0$. In addition, the identified frequencies $\lambda_1, \lambda_2, \gamma_1$ and γ_2 are marked with red 'x'. The shaded gray area in the top panel represents the frequency range in which the cycle frequencies are searched, that is, the range $[\lambda - 2, \lambda + 2]$. The bottom panel provides a zoomed-in view restricted to this range $[\lambda - 2, \lambda + 2]$. Having estimates of $\lambda_1, \lambda_2, \gamma_1$ and γ_2 we compute the estimates of the parameters s_1, s_2, η_1 and η_2, and consequently we can estimate the slopes and intercepts of **L1** and **L2**. The results are summarized in Table 4.1.

Now, we analyze the performance of the periodogram frequency-smoothed along the estimated support line. Note that the considered spectral density functions are real-valued (see Example 1.2) and hence, for simplicity of presentation, we decided to omit the estimation results for their imaginary parts. We follow the same approach as the Monte Carlo procedure described in the previous section. We use $M = 500$ Monte Carlo trails. We consider $\mathrm{E}(T;\omega)$, $\mathrm{STD}(T;\omega)$ and $\mathrm{MSE}_{\mathrm{mean}}(T)$ with $\widehat{f}_{\alpha,\beta}^{XY}(\omega)$ replaced by $\widehat{f}_{\widehat{\alpha},\widehat{\beta}}^{XY}(\omega)$. Here, $\widehat{\alpha}, \widehat{\beta}$ denote estimators of α, β, respectively. For each Monte Carlo trail, the estimation of line parameters follows the same method as applied above. Figure 4.8 displays the results in the same manner as Figures 4.3 and 4.5. For clarity, we restrict the simulation

results to frequencies within the range around the maximum values of the spectral density functions, that is, to the interval $[-1.5, 1.5]$. Note that the estimated expected values $\widehat{\mathrm{E}}(T;\omega)$ gradually converge to the theoretical values and the estimated standard deviation $\widehat{\mathrm{STD}}(T;\omega)$ decreases as T increases. Furthermore, Figure 4.9 shows the estimated averaged mean-squared errors $\widehat{\mathrm{MSE}}_{\mathrm{mean}}(T)$ in the same way as in Figures 4.4 and 4.6. This result illustrates that as T increases, the mean-squared error of the frequency-smoothed periodogram along the estimated support line decreases. It is consistent with Theorem 2.3.

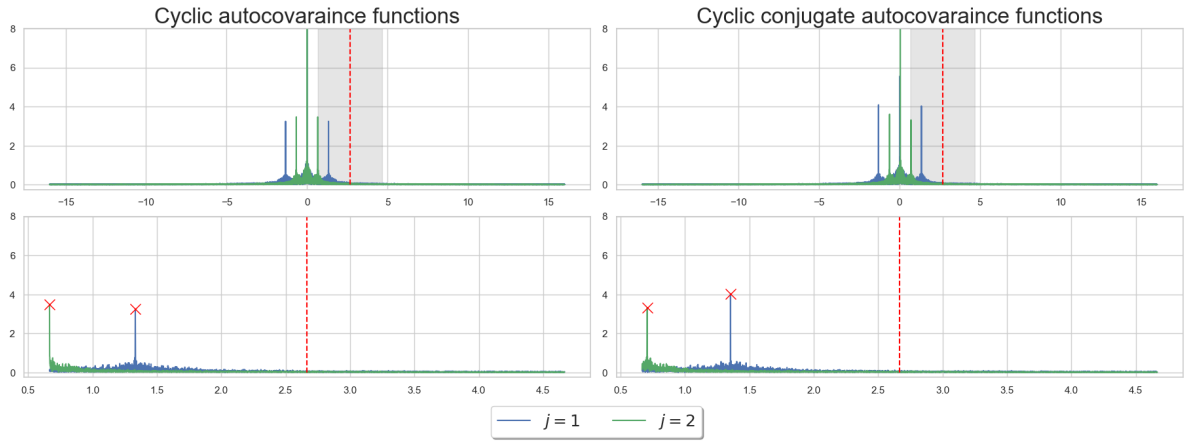

Figure 4.7: Identification of cycle frequencies. Blue line: the estimated magnitude of cyclic (conjugate) autocovariance functions of $X_1(t)$. Green line: the estimated magnitude of cyclic (conjugate) autocovariance functions of $X_2(t)$. Red dashed line: the frequency λ. Shaded gray area: the frequency range in which the cycle frequencies are searched, that is, the range $[\lambda - 2, \lambda + 2]$. Red markers 'x' highlight the maximum values of the cyclic functions. The left panels corresponds to the cyclic autocovariance, and and the right panels corresponds to the cyclic conjugate autocovariance function.

Parameter	**Description**	**Theoretical value**	**Estimate**
λ	cycle (conjugate) frequency of $Y(t)$	$2.\overline{6}$	–
λ_1	cycle frequency of $X_1(t)$	$1.\overline{3}$	1.3330078125
γ_1	cycle conjugate frequency of $X_1(t)$	$1.35\overline{3}$	1.353515625
λ_2	cycle frequency of $X_2(t)$	$0.\overline{6}$	0.6669921875
γ_2	cycle conjugate frequency of $X_2(t)$	$0.70\overline{6}$	0.70703125
s_1	time-scale factor in $X_1(t)$	0.5	0.4998779296875
s_2	time-scale factor in $X_2(t)$	0.25	0.2501220703125
η_1	frequency shift in $X_1(t)$	0.01	0.01025390625
η_2	frequency shift in $X_2(t)$	0.02	0.02001953125
–	slope of lines **L1** and **L2**	0.5	0.5003663003663004
–	intercept of **L1**	0.015	0.014888822115384615
–	intercept of **L2**	$-0.651\overline{6}$	−0.6521033653846153

Table 4.1: The theoretical and estimated values of the parameters in the model **M3**. The digit with a horizontal line above represents an infinitely repeating digit in the repeating decimal.

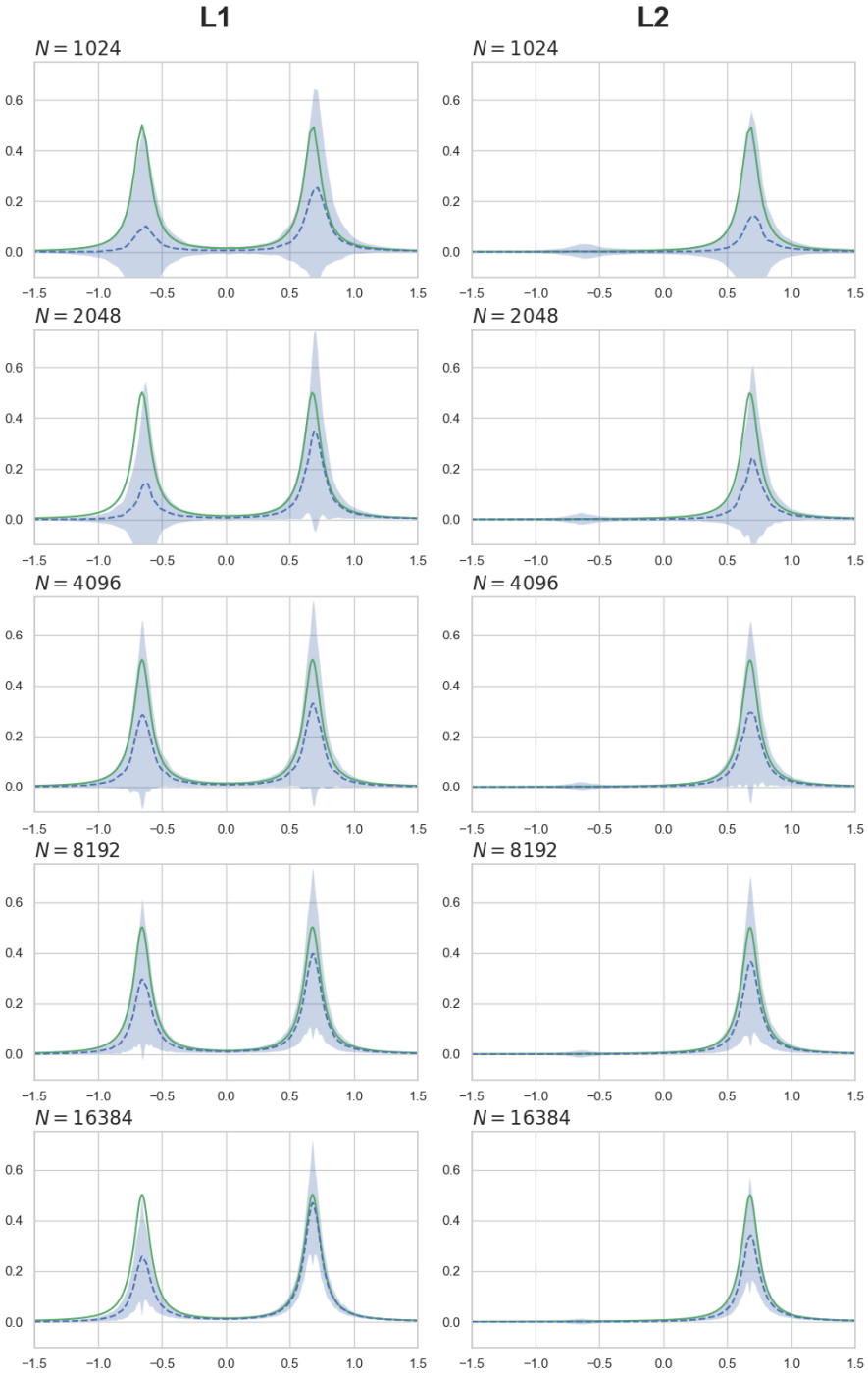

Figure 4.8: Results for **M3** (the case of an unknown line). Green solid line: the theoretical values of the spectral density function. Blue dashed line: the estimated expectation $\widehat{\mathrm{E}}(T;\omega_j^N)$. Shaded blue area: the region within one standard deviation $\widehat{\mathrm{STD}}(T;\omega_j^N)$. Each row represents a specific value of N. The subsequent columns (from the left) correspond respectively to lines **L1** and **L2**.

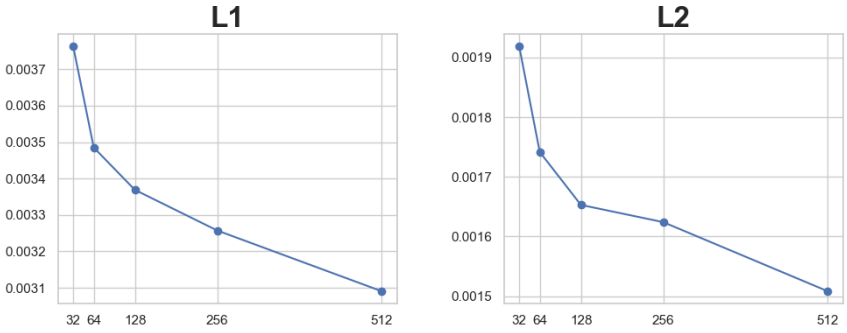

Figure 4.9: Results for **M3** (the case of an unknown line). The estimated average mean-squared error $\widehat{\mathrm{MSE}}_{\mathrm{mean}}(T)$ as a function of T. The subsequent columns (from the left) correspond respectively to lines **L1** and **L2**.

4.3 Validation of confidence intervals

In this section, we evaluate the performance of the confidence intervals proposed in Section 3.5.

For both models **M1** and **M2**, we set the discretization step $\delta = \frac{1}{32}$ and the number of samples $N = 16384$. The length of the observation interval is given by $T = (N-1)\delta$. As the data-tapering window w we consider the rectangular window function, while the frequency-smoothing window q is the Hann window (see Table 2.1). The frequency-smoothing bandwidth is set to $h_T = \frac{1}{16}T^{-2/5}$. The frequencies at which the spectral density functions are estimated are given by $\omega_j^N = -\frac{1}{2\delta} + \frac{j}{(N-1)\delta}$ for $j = 0, 1, \ldots, N-1$. Note that $\omega_j^N \in \left[-\frac{1}{2\delta}, \frac{1}{2\delta}\right]$ for $j = 0, 1, \ldots, N-1$.

We consider three types of confidence intervals of the magnitude of spectral density functions $\left|f^{XX}_{\alpha,\beta}(\omega)\right|$, and the spectral coherence functions $\left|\gamma^{XX}_{\alpha,\beta}(\omega)\right|$, where α and β denote the slope and intercept of the support line, respectively.

Let $\theta \in \mathbb{R}$ be a parameter of interest, and let $\widehat{\theta}_T$ be its estimator.

CI$_1$: Pointwise subsampling-based equal-tailed 95% confidence intervals given by (3.6).

CI$_2$: Pointwise symmetric subsampling-based 95% confidence intervals given by (3.7).

CI$_3$: Pointwise asymptotic equal-tailed 95% confidence interval, obtained using Corollary 2.2 and the Monte Carlo approach. That is,

$$\left(\widehat{\theta}_T - z(0.975)\,\frac{\widehat{\sigma}_{MC}}{\sqrt{Th_T}}, \widehat{\theta}_T - z(0.025)\,\frac{\widehat{\sigma}_{MC}}{\sqrt{Th_T}}\right),$$

where $z(\rho)$ is a ρ-quantile of the standard normal distribution. By $\widehat{\sigma}^2_{MC}$ we denote the estimator of $\mathbb{E}\left|\widehat{\theta}_T - \theta\right|^2$ obtained through Monte Carlo simulations with $M = 500$ runs.

The subsampling-based confidence intervals are constructed using the following parameters. The number of samples in each subsample is set to $N_b = 2048$. Then a block length is $b = (N_b - 1)\delta$. The frequency-smoothing bandwidth for a subsample estimator is $h_b = \frac{1}{16}b^{-2/5}$. It is important to note that the simulations are performed using parameters b, h_T and h_b that are not necessarily optimal.

Selecting optimal parameters is a challenging problem that remains unsolved in the literature for many classes of nonstationary processes, in particular, for processes under consideration.

Figures 4.10 and 4.11 display the confidence intervals for the spectral density functions of models **M1** and **M2**, respectively. The confidence intervals for the spectral coherence functions of models **M1** and **M2** are shown in Figures 4.12 and 4.13, respectively. As in Section 4.2.1, we display results for frequencies within the range around the maximum values of the spectral density functions. Note that the coherence functions and its estimator corresponding to a line **L1** are always equal to one.

Let us discuss the results for the magnitude of the spectral density functions $\left|f^{XX}_{\alpha,\beta}(\omega)\right|$. The confidence intervals $\mathbf{CI}_2$ and $\mathbf{CI}_3$ provide nearly the same coverage of theoretical values. The confidence intervals $\mathbf{CI}_1$ are the narrowest for most of the frequencies considered. Observe that both $\mathbf{CI}_2$ and $\mathbf{CI}_3$ are constructed to be symmetric and cover the theoretical values at more frequencies than $\mathbf{CI}_1$. This may be because the confidence interval $\mathbf{CI}_1$ fails to capture the symmetry of the asymptotic distribution. Another potential reason for this is the non-optimal choice of the parameter b. However, selecting the optimal parameter b is a challenging task. In particular, very few results regarding this problem are in the literature. To our knowledge, there are no such results for APC processes and their generalizations. The first and only existing result for bootstrap in the case of the overall mean and seasonal means for PC time series can be found in [3].

Finally, we examine the actual coverage probabilities (ACPs) for the confidence intervals $\mathbf{CI}_1$–$\mathbf{CI}_3$. We focus on the case of the magnitude of the spectral density functions. We compute ACPs by constructing confidence intervals $\mathbf{CI}_1$–$\mathbf{CI}_3$ for 500 different realizations of the processes considered in models **M1** and **M2**. For each case, we count the number of times that the constructed confidence intervals cover the theoretical value for each frequency. Figures 4.14 and 4.15 present the calculated ACPs for models **M1** and **M2**, respectively. In addition, each graph includes the shape of the spectral density, shown as a gray line. Note that the y-axis does not represent the actual values of these spectral densities. This visualization is intended to illustrate the behavior of the ACPs in relation to the spectral density, which is discussed in more detail later. The highest ACPs are achieved by $\mathbf{CI}_3$, followed by slightly lower values for $\mathbf{CI}_2$, and significantly lower ACPs for $\mathbf{CI}_1$. For most frequencies, the ACPs of $\mathbf{CI}_2$ and $\mathbf{CI}_3$ remain close to the dashed red line representing 95% level. Even in the worst cases for **M1**, the ACPs rarely drops below 80%. In contrast, $\mathbf{CI}_1$ shows its poorest performance in scenarios with slopes different than one (i.e., **L2** and **L3** for both models **M1** and **M2**), where ACPs fall below 60% for most frequencies. For the model **M1**, both the subsampling confidence intervals $\mathbf{CI}_1$ and $\mathbf{CI}_2$ exhibit lower ACPs at frequencies corresponding to local maxima in the spectral density. However, for **M2** and lines **L1**, **L3** and **L4** it can be noted also for $\mathbf{CI}_3$. For **M2**, the results are generally worse than for **M1**, but this may be attributed to the previously mentioned issue, namely the potentially non-optimal choice of parameters.

In summary, the best performance is achieved by $\mathbf{CI}_3$. However, as discussed in Chapter 3, constructing asymptotic confidence intervals can be challenging in practice. The subsampling confidence interval $\mathbf{CI}_2$ performs reasonably well, while $\mathbf{CI}_1$ consistently exhibits poor performance in all scenarios.

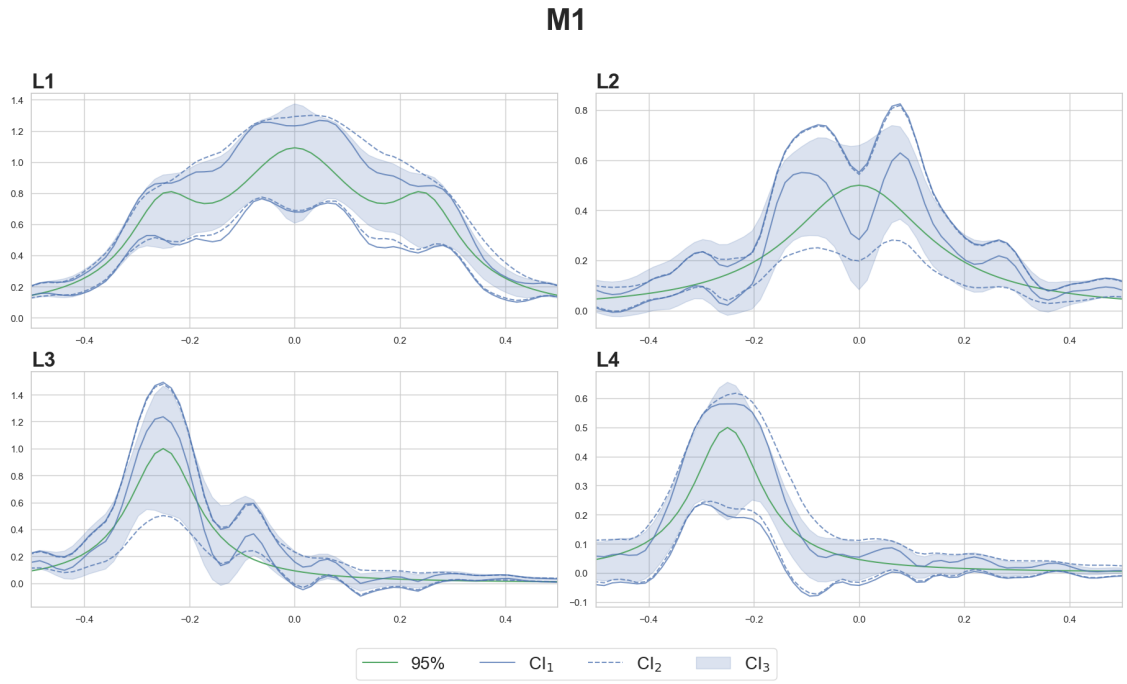

Figure 4.10: Results for **M1**. Confidence intervals for the magnitude of spectral density functions for lines **L1**–**L4**. Green solid line: theoretical values of the magnitude of the spectral density function. Blue solid line: bounds of confidence intervals $\mathbf{CI}_1$. Blue dashed line: bounds of confidence intervals $\mathbf{CI}_2$. Blue shaded area: bounds of confidence intervals $\mathbf{CI}_3$.

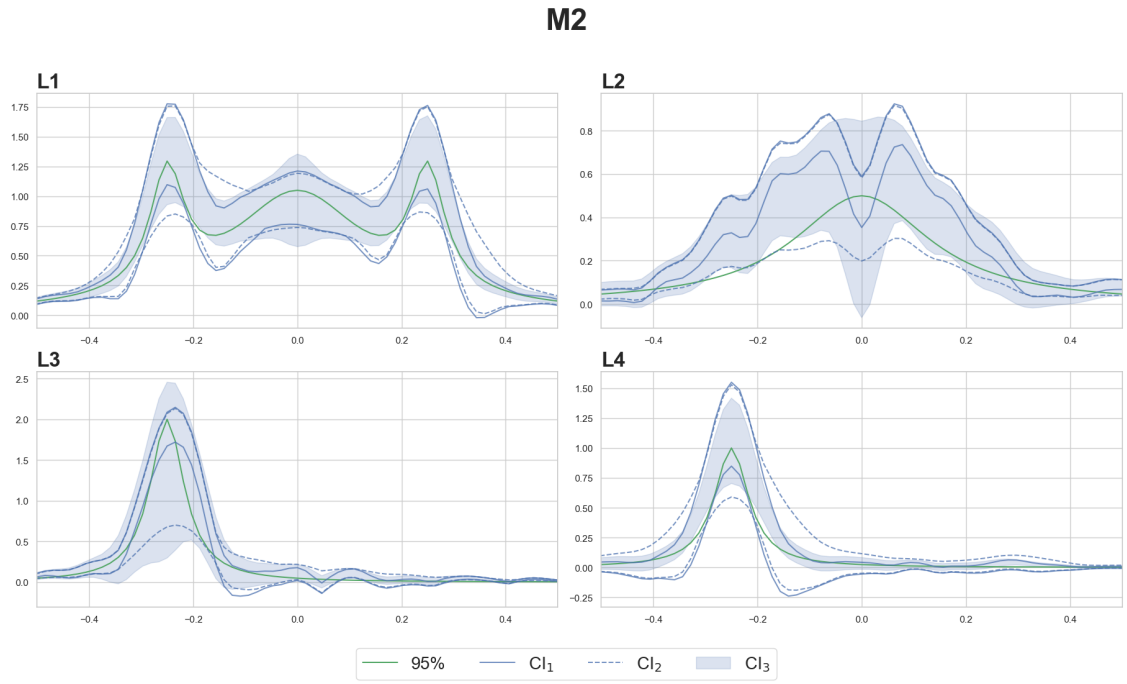

Figure 4.11: Results for **M2**. Confidence intervals for the magnitude of spectral density functions for lines **L1**–**L4**. Green solid line: theoretical values of the magnitude of the spectral density function. Blue solid line: bounds of confidence intervals $\mathbf{CI}_1$. Blue dashed line: bounds of confidence intervals $\mathbf{CI}_2$. Blue shaded area: bounds of confidence intervals $\mathbf{CI}_3$.

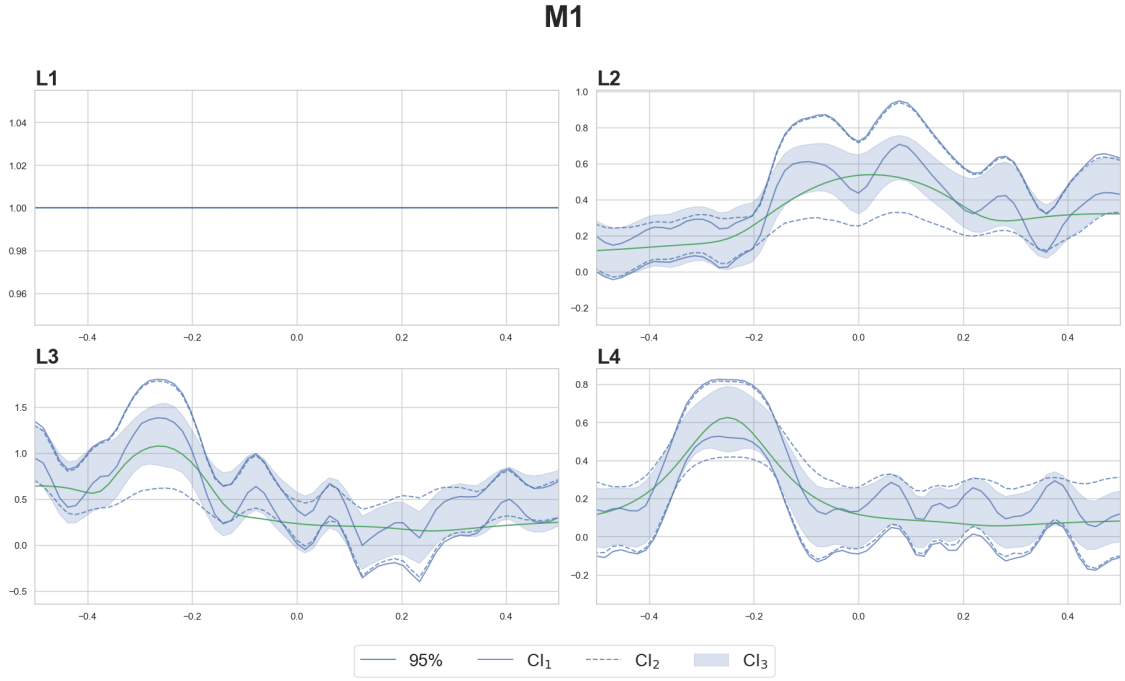

Figure 4.12: Results for **M1**. Confidence intervals for the magnitude of spectral coherence functions for lines **L1**–**L4**. Green solid line: theoretical values of the magnitude of the spectral coherence function. Blue solid line: bounds of confidence intervals $\mathbf{CI}_1$. Blue dashed line: bounds of confidence intervals $\mathbf{CI}_2$. Blue shaded area: bounds of confidence intervals $\mathbf{CI}_3$.

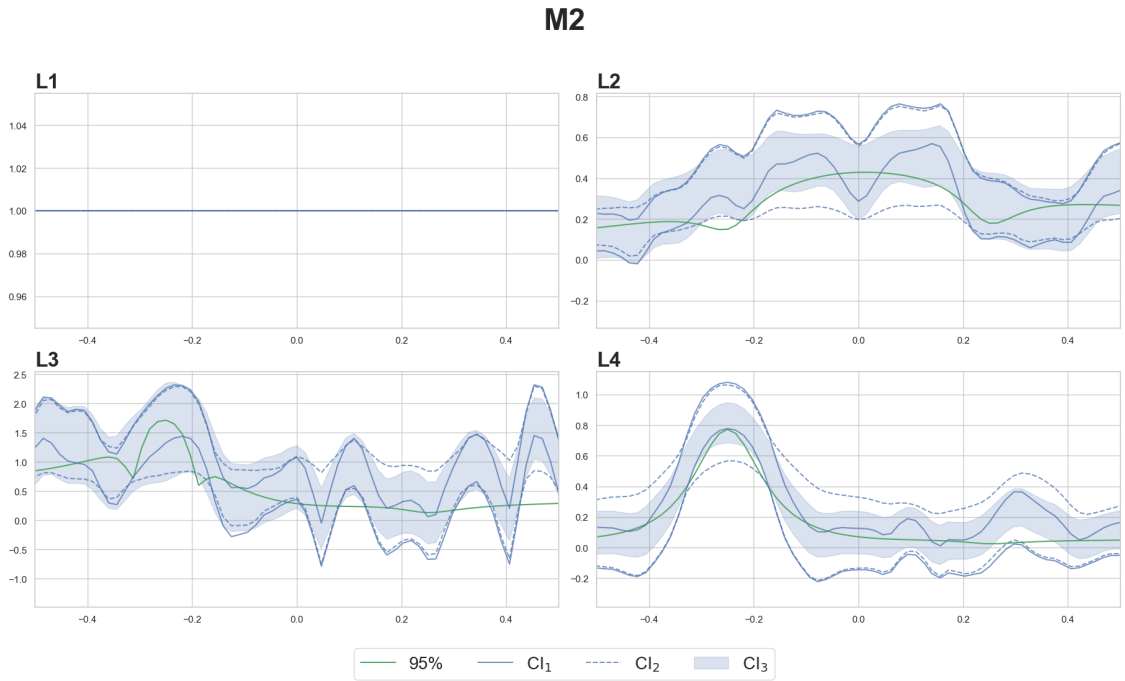

Figure 4.13: Results for **M2**. Confidence intervals for the magnitude of spectral coherence functions for lines **L1**–**L4**. Green solid line: theoretical values of the magnitude of the spectral coherence function. Blue solid line: bounds of confidence intervals $\mathbf{CI}_1$. Blue dashed line: bounds of confidence intervals $\mathbf{CI}_2$. Blue shaded area: bounds of confidence intervals $\mathbf{CI}_3$.

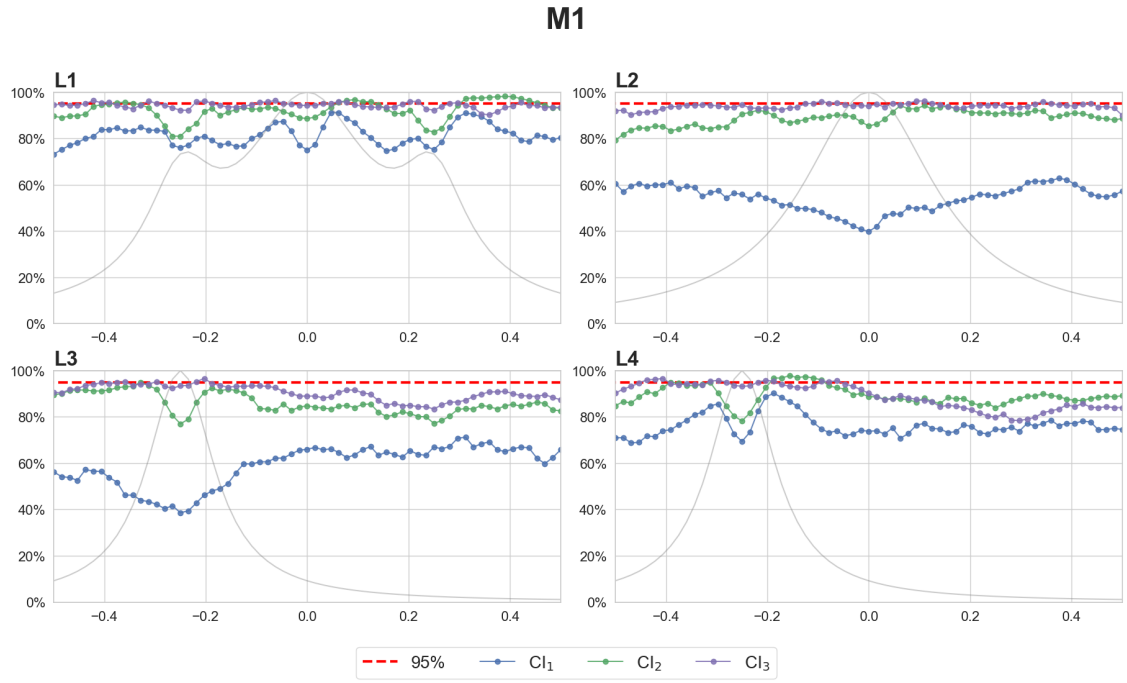

Figure 4.14: Results for **M1**. ACPs for confidence intervals for the magnitude of spectral density functions for lines **L1**–**L4**. Blue line: results for $\mathbf{CI}_1$. Green line: results for $\mathbf{CI}_2$. Violet line: results for $\mathbf{CI}_3$. Red dashed line: 95% level.

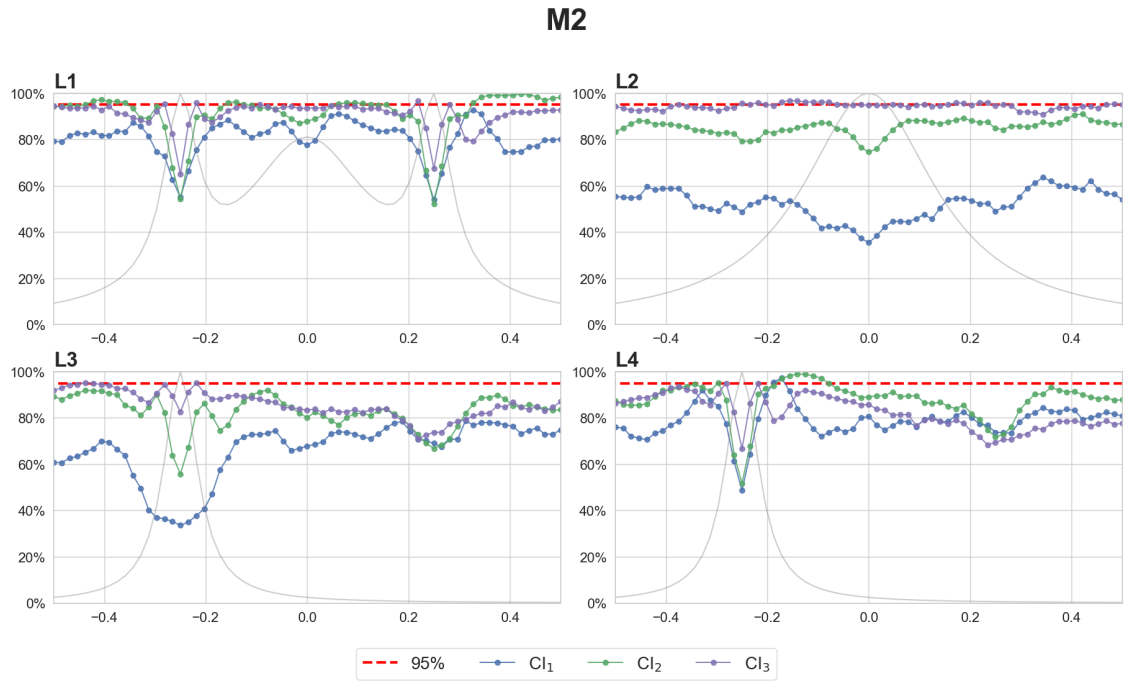

Figure 4.15: Results for **M2**. ACPs for confidence intervals for the magnitude of spectral density functions for lines **L1**–**L4**. Blue line: results for $\mathbf{CI}_1$. Green line: results for $\mathbf{CI}_2$. Violet line: results for $\mathbf{CI}_3$. Red dashed line: 95% level.

CHAPTER 5

ANALYSIS OF SIGNALS EXHIBITING IRREGULAR CYCLICITIES

The analysis of cyclic data plays a fundamental role in the study of stochastic processes. Various modeling approaches for such data have been proposed in the literature [2, 42, 43, 55, 62, 76], including PC and APC processes discussed in Section 1.2. However, a key challenge in modeling cyclic data is the natural irregularity observed in many real-world signals, particularly in biomedical applications. As a result, the study of processes that exhibit irregular cyclicity has gained increasing interest in recent years [15, 34, 48, 49, 63, 65].

In this chapter, we present some of our findings obtained in this field. However, since this topic lies outside the main scope of this thesis, we focus only on the main results. In Section 5.1, we discuss our results from [31], where we develop a statistical approach for ECG signals using an amplitude-modulated time-warping periodically correlated (AM-TW PC) model [64]. We propose two bootstrap procedures, based on the Circular Block Bootstrap [75], to perform statistical inference for ECG signals. In Section 5.2, we present our results from [26], where we introduce a new semiparametric continuous-time model for signals with irregular cyclicities and propose estimators for the first- and second-order characteristics.

5.1 Inference for signals exhibiting irregular statistical cyclicity with applications to electrocardiograms

In the literature, PC processes have been used to model ECG signals and have found applications in arrhythmia detection [38], heart and respiratory monitoring [45, 46], as well as in the separation of heart and lung sounds [35]. However, PC models assume a constant heart rate. This assumption is quite restrictive and generally only holds over very short time intervals, typically no longer than 10 seconds [64]. Consequently, the practical application of such models is limited, especially in long-term monitoring scenarios in which patients with potential cardiac conditions are observed over several hours. To address this limitation and capture irregular cyclicities in signals, Napolitano

proposed an AM-TW PC model in [64]. This model has been applied to the ECG analysis and was used to study a signal recorded over 800 seconds.

The statistical methods proposed in [34, 62, 64] for the AM-TW PC model provide only point estimates of certain characteristics. All existing approaches first require estimating the underlying PC process before estimating the specific characteristics of interest. However, these methods do not provide statistical inference tools such as hypothesis testing and confidence interval estimation. To overcome this limitation, we develop the bootstrap approach. In Section 5.1.1, we review the ECG model proposed by Napolitano. In Section 5.1.2, we propose two bootstrap methods that can be applied to the AM-TW PC model. In Section 5.1.3, we outline the application of our bootstrap approaches to ECG signals. In Section 5.1.4, we present the analysis of the ECG signal based on our bootstrap inference. Finally, Section 5.1.5 includes proofs of the theoretical results.

5.1.1 Amplitude-modulated time-warped periodically correlated processes

In our paper [30],we consider is the model of Napolitano [64]. In the sequel, we review this model and discuss the existing results.

Let T_0 be the average time to complete one ECG signal cycle and by λ_0 we denote the average heart rate. That is, $\lambda_0 = \frac{1}{T_0}$. In [64], the ECG signal $\{Y(t),\, t \in \mathbb{R}\}$ is proposed to be modeled using

$$Y(t) = A(t)\, X(t + \varepsilon(t)), \tag{5.1}$$

where $A(t) \neq 0$ and $\varepsilon(t)$ are deterministic functions. For a process $\{X(t),\, t \in \mathbb{R}\}$, we assume that it is an unobserved real-valued PC process with period T_0. Moreover, it can be decomposed into two components $X(t) = \mu_X(t) + X_r(t)$, where $\mu_X(t)$ is a periodic deterministic function with period T_0 and $X_r(t)$ is a zero-mean PC process with period T_0. The component $\mu_X(t)$ represents the mean function of $X(t)$, and $X_r(t)$ contains information about its periodic autocovariance function.

A process $\{Y(t),\, t \in \mathbb{R}\}$ given by (5.1) is called an amplitude-modulated time-warped periodically correlated (AM-TW PC) process. In [34, 62, 64], periodically correlated processes are referred to as cyclostationary processes. Consequently, processes of the form (5.1) are alternatively referred to as amplitude-modulated time-warped cyclostationary (AM-TW CS) processes.

Both functions $\varepsilon(t)$ and $A(t)$ represent fluctuations in the propagation of electrical waves throughout the heart. The time-warping function $\varepsilon(t)$ can specifically model the variability of heart rate over time, which can arise from various factors, including sensor movement during signal measurement, individual patient characteristics, arrhythmia, physical activity, or other irregular phenomena. In [64], certain conditions are assumed for the derivative of the time-warping function $\varepsilon(t)$, as a consequence of which the time-warping function changes slowly over time.

As noted in Section 1.2, the analysis of the PC process $X(t)$ can be performed using Fourier analysis of the mean function $\mu_X(t) = \mathbb{E}X(t)$ and the autocovariance function $R_{XX}(t, t+\tau) = \mathrm{Cov}(X(t), X(t+\tau))$. Therefore, assume that

$$\mu_X(t) = \sum_{k=-\infty}^{\infty} b\left(\tfrac{k}{T_0}\right) e^{\frac{i2\pi kt}{T_0}}, \quad R_{XX}(t, t+\tau) = \sum_{k=-\infty}^{\infty} a\left(\tfrac{k}{T_0}, \tau\right) e^{\frac{i2\pi kt}{T_0}},$$

where

$$b(\gamma) = \lim_{T\to\infty} \frac{1}{T} \int_{-\frac{T}{2}}^{\frac{T}{2}} \mu_X(t)\, e^{-i2\pi\gamma t}\, \mathrm{d}t, \quad a(\lambda,\tau) = \lim_{T\to\infty} \frac{1}{T} \int_{-\frac{T}{2}}^{\frac{T}{2}} R_{XX}(t,t+\tau)\, e^{-i2\pi\lambda t}\, \mathrm{d}t.$$

Consequnelty, the mean and autocovariance functions of $Y(t)$ have the following representation

$$\mu_Y(t) = \sum_{k=-\infty}^{\infty} \kappa\left(\tfrac{k}{T_0}, t\right) e^{\frac{i2\pi kt}{T_0}}, \quad R_{YY}(t,t+\tau) = \sum_{k=-\infty}^{\infty} \rho\left(\tfrac{k}{T_0}, t, \tau\right) e^{\frac{i2\pi kt}{T_0}},$$

where $\kappa(\gamma,t) = A(t)\, b(\gamma)\, e^{i2\pi\gamma\varepsilon(t)}$ and $\rho(\lambda,t,\tau) = A(t)\, A(t+\tau)\, a(\lambda, \tau+\varepsilon(t+\tau)-\varepsilon(t))\, e^{i2\pi\lambda\varepsilon(t)}$. Note that the functions $\kappa(\lambda,t)$ and $\rho(\lambda,t,\tau)$ depend on time t, which implies that $Y(t)$ is not PC.

Now, let us present the idea of statistical procedures for the model (5.1) proposed in [34, 62, 64]. The analysis of the AM-TW PC model involves estimating the time-warping function $\varepsilon(t)$ and the amplitude modulation function $A(t)$. Having estimates of $\varepsilon(t)$ and $A(t)$, we can reconstruct the underlying PC process $X(t)$. However, due to the complexity of these methods, we omit their description and refer the reader to [34, 62, 64], with additional details available in our paper [30]. Finally, Fourier analysis can be applied to the reconstructed process denoted by $\widehat{X}(t)$. Consequently, one can estimate the functions $b(\gamma)$ and $a(\lambda,\tau)$, using standard estimators developed for PC processes [42, 62]. However, in our model, the process $X(t)$ is unobservable. To address this, we substitute $X(t)$ with $\widehat{X}(t)$. Then, in our case the estimators of $b(\gamma)$ and $a(\lambda,\tau)$, $\tau \geq 0$, are

$$\begin{aligned} \widehat{b}(\gamma) &= \frac{1}{T} \int_0^T \widehat{X}(t)\, e^{-i2\pi\gamma t}\, \mathrm{d}t, \\ \widehat{a}(\lambda,\tau) &= \frac{1}{T} \int_0^{T-\tau} \big(\widehat{X}(t) - \widehat{\mu}_X(t)\big)\big(\widehat{X}(t+\tau) - \widehat{\mu}_X(t+\tau)\big)\, e^{-i2\pi\lambda t}\, \mathrm{d}t, \end{aligned} \tag{5.2}$$

where $\widehat{\mu}_X(t)$ is the estimator of $\mu_X(t)$. That is,

$$\widehat{\mu}_X(t) = \sum_{\gamma\in\widetilde{\Gamma}} \widehat{b}(\gamma)\, e^{i2\pi\gamma t},$$

and $\widetilde{\Gamma}$ is finite subset of the set Γ containing the frequencies at which the cyclic mean function is significantly non-zero, for example, determined by a statistical test (see, e.g., Section 5.1.3).

The main interest of our paper [31] is to provide statistical inference based on cyclic functions $b(\gamma)$ and $a(\lambda,\tau)$. This allows us to understand the structure of the underlying PC process $X(t)$ and how ECG signals relate to heart rhythm abnormalities. These functions are also essential for estimating related quantities like $\kappa(\gamma,t)$ and $\rho(\lambda,t,\tau)$. Our goal is to develop a framework for hypothesis testing and confidence interval construction for the underlying process $X(t)$. A key challenge is that the asymptotic covariance matrices of the rescaled estimators $\widehat{b}(\gamma)$ and $\widehat{a}(\lambda,\tau)$ depend on infinitely many unknown parameters, making statistical inference based on asymptotic distributions difficult in practice (see, e.g., Theorem 2.6 in [85]). In the next subsection, we introduce bootstrap methods to address this issue.

In the sequel, we assume that the underlying PC process $X(t)$ is directly observable. However, in the real-data application, we substitute $\widehat{X}(t)$ in place of $X(t)$. Our condition is necessary because there is strong evidence that the consistency of the estimators for the cyclic statistical functions $b(\gamma)$ and $a(\lambda, \tau)$, based on measurements from $\widehat{X}(t)$ cannot be established. Specifically, the estimators of $\widehat{A}(t)$ and $\widehat{\varepsilon}(t)$ proposed in the literature are, to date, biased (even asymptotically). We therefore treat our results as the upper bound of achievable performance. Since there is a lack of methods in the literature that provide theoretical guarantees in this context, we consider our work a step toward advancing the field. Our future research will focus on refining both the existing methods and the model to facilitate the derivation of theoretical results. In [31], we include an extensive simulation study to demonstrate the performance of our proposed bootstrap methods.

5.1.2 Bootstrap inference

Bootstrap is a very popular resampling approach used to approximate the sampling distribution of statistics, for example, to construct confidence intervals. The main idea of bootstrap for independent and identically distributed data is to construct bootstrap sample by drawing with replacement data point from the original data set. For dependent data, such as in our case, it is crucial to construct a bootstrap sample in a way to preserve the original dependence structure. For this propose, block bootstrap methods are used (see, e.g, [47]). Such methods involve splitting the data into blocks and then drawing them with replacement. The important and well-known block bootstrap method is the Circular Block Bootstrap (CBB) method, introduced by Politis and Romano [75]. The CBB method was designed for stationary data. However, it can be adapted for our nonstationay setting. For the convenience of the reader, we first recall the algorithm of the CBB approach.

Fix $n \in \mathbb{N}$. Let $(X_1, X_2, \ldots, X_n)$ be a sample from a time series $\{X_t,\, t \in \mathbb{Z}\}$. For $j = 1, 2, \ldots, n$ define the block of observations B_j of length $b \in \mathbb{N}$ $(0 < b < n)$ starting at X_j and given by

$$B_j = \begin{cases} (X_j, X_{j+1}, \ldots, X_{j+b-1}), & j = 1 \ldots, n-b+1, \\ (X_j, X_{j+1}, \ldots, X_n, X_1, \ldots, X_{b-n+j-1}), & j = n-b+2, \ldots, n. \end{cases}$$

The name "circular" derives from the fact that the data are wrapped around a circle, allowing the construction of additional blocks for $j = n-b+2, \ldots, n$. This approach was proposed to reduce the edge effect. That is, if we consider only the blocks for $j = 1 \ldots, n-b+1$, then the observations near the beginning and the end of the sample appear in fewer blocks, introducing the bias of the estimators. In the following, we present the usual CBB algorithm.

Algorithm.

1. Fix $b \in \mathbb{N}$ such that $0 < b < n$.

2. From $\{1, 2, \ldots, n\}$ choose randomly with replacement $l+1$ numbers $k_1, k_2, \ldots, k_{l+1}$ where l is the smallest integer such that $lb > n$. The probability of choosing any number is $\frac{1}{n}$. Then for $t = 1, 2, \ldots, l+1$ the bootstrap blocks are given by

$$B_{k_t} = (X_{k_t}, X_{k_t+1}, \ldots, X_{k_t+b-1}) = (X_t^*, X_{t+1}^*, \ldots, X_{t+b-1}^*) = B_t^*.$$

3. Join the selected $l+1$, blocks $\mathcal{B}^* = (B_1^*, B_2^*, \ldots, B_{l+1}^*)$. The bootstrap sample is obtained by taking the first n observations from $\mathcal{B}^*$, i.e., $(X_1^*, X_2^*, \ldots, X_n^*)$.

The CBB method cannot be applied directly to our case, as it is designed for discrete-time processes. Moreover, this approach does not preserve the periodic structure of the data. To overcome these limitations, we develop two bootstrap procedures based on the above algorithm.

Circular Extension of the Moving Block Bootstrap for the sampled process. The CBB method is primarily designed for stationary time series. For discrete-time PC time series, it provides consistent results only for the overall mean, defined as

$$\mu = \lim_{n\to\infty} \frac{1}{n} \sum_{k=1}^{n} \mathbb{E}X_k,$$

where $\{X_t,\, t \in \mathbb{Z}\}$ is a PC process [85]. In the nonstationary setting, in [23, 24] it is introduced the Circular Extension of the Moving Block Bootstrap (CEMBB), which retains information about the original time indices to construct consistent bootstrap estimators in the nonstationary case. However, the CEMBB method was developed for discrete-time models. Therefore, we generalize this approach to continuous-time processes $X(t)$.

Fix $T > 0$. Let $\{X(t),\, t \in [0,T]\}$ be an observed PC process with period T_0. By $h = \frac{T}{n-1}$ we denote the discretization size. We consider the sampled data $(X(0), X(h), \ldots, X((n-1)h))$. Note that if the ratio $\frac{h}{T_0}$ is a rational number, then the resulting discrete-time process is also PC, with period equal to the denominator of the ratio (assuming that the numerator and denominator are relatively prime), see [62, Section 3.6.2]. If the ratio is irrational, the sampled process becomes an APC process. Both PC and APC processes are nonstationary, and for such processes, the CEMBB algorithm can be appropriately applied [23, 24].

Below, we present the CEMBB algorithm for a sampled process.

Algorithm.

1. Define $U_j = (X(jh), j)$ for $j = 0, 1, \ldots, n-1$.

2. Do the CBB algorithm for the sample $(U_0, U_1, \ldots, U_{n-1})$ to obtain $(U_0^*, U_1^*, \ldots, U_{n-1}^*)$.

The major advantage of this method is its ability to keep the information about the original time index of each observation. The bootstrap estimators for cyclic mean functions $b(\gamma)$ and cyclic autocovariance functions $a(\lambda, \tau)$, $\tau \geq 0$, have the following form

$$\widehat{b}^*(\gamma) = \frac{1}{n} \sum_{k=0}^{n-1} X(k^*h)\, e^{-i2\pi\lambda k^*},$$

$$\widehat{a}^*(\lambda,\tau) = \frac{1}{n} \sum_{k=0}^{n-1-k_\tau} \left(X(k^*h) - \widehat{\mu}(k^*h)\right) \left(X(h(k^*+k_\tau)) - \widehat{\mu}(k^*+k_\tau)\right) e^{-i2\pi\lambda k^*},$$

where k_τ is the nearest integer to $\frac{\tau}{h}$ and $U_k^* = (X(k^*h), k^*)$ are the elements of the bootstrap sample. There is an implicit mapping from k to k^*, given by the CEMBB algorithm. Then we can write a summation of $\widehat{\mu}(k^*h)$ and $\widehat{\mu}(k^*+k_\tau)$ over $k = 0, \ldots, n-1-k_\tau$.

Let us formulate the bootstrap consistency theorem for $a(\lambda,\tau)$. Let $r\in\mathbb{N}$, $\boldsymbol{\tau}=(\tau_1,\dots,\tau_r)^{\mathrm{T}}\in\mathbb{R}^r$ be a vector of lag parameters and $\boldsymbol{\lambda}=(\lambda_1,\dots,\lambda_1)^{\mathrm{T}}\in\mathbb{R}^r$ be a vector of frequencies. We consider

$$a(\boldsymbol{\lambda},\boldsymbol{\tau})=[\operatorname{Re}a(\lambda_1,\tau_1),\operatorname{Im}a(\lambda_1,\tau_1),\dots,\operatorname{Re}a(\lambda_r,\tau_r),\operatorname{Im}a(\lambda_r,\tau_r)]^{\mathrm{T}}\in\mathbb{R}^{2r},$$

and analogously we define $\widehat{a}(\boldsymbol{\lambda},\boldsymbol{\tau})\in\mathbb{R}^{2r}$ and $\widehat{a}^*(\boldsymbol{\lambda},\boldsymbol{\tau})\in\mathbb{R}^{2r}$. For $\boldsymbol{x}=(x_1,\dots,x_{2r})\in\mathbb{R}^{2r}$ and $\boldsymbol{y}=(y_1,\dots,y_{2r})\in\mathbb{R}^{2r}$ we write $\boldsymbol{x}\le\boldsymbol{y}$, when $x_i\le y_j$ for $j=1,2,\dots,2r$.

Theorem 5.1. *Assume that $\{X(t),\,t\in\mathbb{R}\}$ is a α-mixing PC process such that*

(i) functions $\mathbb{E}[X(t)X(t+\tau_1)X(t+\tau_2)X(t+\tau_3)]$ and $\mathbb{E}[X(t)X(t+\tau_1)X(t+\tau_2)]$ are periodic in $t\in\mathbb{R}$ for any $\tau_1,\tau_2,\tau_3\in\mathbb{R}$;

(ii) the sets $\Gamma=\{\gamma\in\mathbb{R}:b(\gamma)\neq 0\}$ and $\Lambda=\bigcup_{\tau\in\mathbb{R}}\{\lambda\in\mathbb{R}:a(\lambda,\tau)\neq 0\}$ are finite;

(iii) $\sup_{t\in\mathbb{R}}\mathbb{E}|X(t)|^{8+2\delta}<\infty$ and $\int_{\mathbb{R}}\tau\alpha_X^{\frac{\delta}{4+\delta}}(\tau)\,\mathrm{d}\tau<\infty$ for some $\delta>0$;

(iv) $X(t)$ is strictly band-limited with bandwidth B satisfying $1>2Bh$;

(v) we have

$$\sqrt{nh}(\widehat{a}(\boldsymbol{\lambda},\boldsymbol{\tau})-a(\boldsymbol{\lambda},\boldsymbol{\tau}))\xrightarrow{d}\mathcal{N}_{2r}(0,\Sigma(\boldsymbol{\lambda},\boldsymbol{\tau})),$$

where $\det(\Sigma(\boldsymbol{\lambda},\boldsymbol{\tau})\neq 0$.

Then for $\boldsymbol{x}\in\mathbb{R}^{2r}$

$$\sup_{x\in\mathbb{R}}\left|\mathbb{P}^*\Big(\sqrt{nh}(\widehat{a}(\boldsymbol{\lambda},\boldsymbol{\tau})-a(\boldsymbol{\lambda},\boldsymbol{\tau}))\Big)\le\boldsymbol{x}\Big)-\mathbb{P}\Big(\sqrt{nh}(\widehat{a}^*(\boldsymbol{\lambda},\boldsymbol{\tau})-\mathbb{E}^*\widehat{a}^*(\boldsymbol{\lambda},\boldsymbol{\tau}))\Big)\le\boldsymbol{x}\Big)\right|\xrightarrow{\mathbb{P}}0,$$

as $b\to\infty$, $n\to\infty$ with $b/n\to 0$, where $\mathbb{P}^*$ and $\mathbb{E}^*$, respectively, denote the conditional probability and conditional expectation, given $(U_0^*,U_1^*,\dots,U_{n-1}^*)$.

Proof. See Section 5.1.5. □

Recall that the concept of α-mixing is introduced in Section 3.1. The condition *(iv)* means that the spectral density functions are supported within specific frequency ranges. This requirement is necessary to avoid aliasing. For further details, we refer the reader to [62, Section 3.6].

Analogously, we obtain results for cyclic mean functions $b(\gamma)$. In this case, the condition *(i)* is no longer required, and in the condition *(ii)*, the exponent $8+2\delta$ can be replaced with $4+\delta$.

Moreover, to construct the bootstrap simultaneous confidence intervals, we require the consistency of our bootstrap procedure for smooth functions of the estimator. This consistency can be achieved by following the same steps as in the proof of Theorem 4 in [23].

Circular Block Bootstrap for the averaged process. Selecting an appropriate block length is crucial to perform the block bootstrap method. This problem has been extensively studied for stationary processes [47, Chapter 7]. However, for nonstationary processes, there is a significant lack of results in this area. Recently, Bertail and Dudek [3] provided the first known result for PC time

series, focusing on the first-order characteristics in the time domain of a discrete-time PC process with a known integer-valued period. However, their result does not directly apply to our setting, which involves a continuous-time PC process whose period may not be an integer multiple of the discretization step. To overcome this limitation, we propose a bootstrap methodology suited for PC processes in continuous time. In addition, we are able to apply results of Berial and Dudek to determine the optimal block length, defined as the length that minimizes the mean-squared error of the bootstrap variance estimator, for characteristics in the frequency domain.

The core idea of our approach is to average the process over disjoint intervals equal to one period in length. This transformation produces a time series such that its mean function remains periodic and the autocovariance depends only on the lag, i.e., does not depend on time.

Fix $T > 0$. Let $\{X(t),\, t \in [0,T]\}$ be an observed PC process with period T_0. For simplicity, we introduce the bootstrap algorithm for the cyclic autocovariance function $a(\lambda,\tau)$ assuming that $\mathbb{E}X(t) = 0$. Fix $\tau \geq 0$ and $\lambda = \frac{p}{qT_0}$, where $p, q \in \mathbb{Z}$. Define $n = \lfloor \frac{T-\tau}{T_0} \rfloor$.

Algorithm.

1. For each $s = 1, 2, \ldots, n$ compute

$$Z_s(\lambda,\tau) = \frac{1}{T_0} \int_{(s-1)T_0}^{sT_0} X(t)\, X(t+\tau)\, e^{-i2\pi\lambda t}\, \mathrm{d}t. \tag{5.3}$$

2. Do the CBB for the sample $(Z_1(\lambda,\tau), Z_2(\lambda,\tau), \ldots, Z_n(\lambda,\tau))$ to obtain the bootstrap sample $(Z_1^*(\lambda,\tau), Z_2^*(\lambda,\tau), \ldots, Z_n^*(\lambda,\tau))$.

Observe that $a(\lambda,\tau)$ represents the overall mean of $Z_s(\lambda,\tau)$, while $\widehat{a}(\lambda,\tau)$ denotes its estimator. That is,

$$a(\lambda,\tau) = \lim_{n\to\infty} \frac{1}{k} \sum_{s=1}^{n} \mathbb{E}Z_s(\lambda,\tau) = \mu_{Z(\lambda,\tau)}, \qquad \widehat{a}(\lambda,\tau) = \frac{1}{n} \sum_{s=1}^{n} Z_s(\lambda,\tau) = \widehat{\mu}_{Z(\lambda,\tau)}.$$

Consequnelty, a bootstrap estimator of $a(\lambda,\tau)$ is given by

$$\widehat{a}^*(\lambda,\tau) = \frac{1}{n} \sum_{s=1}^{n} \widehat{Z}_s^*(\lambda,\tau) = \widehat{\mu}^*_{Z(\lambda,\tau)}.$$

Let us discuss the statistical properties of the resulting time series $\{Z_s(\lambda,\tau),\, s \in \mathbb{N}\}$.

Proposition 5.1. *Let $\lambda = \frac{p}{qT_0}$, where $p, q \in \mathbb{Z}$ are relatively prime. Assume that the process $X(t)$ is PC with period T_0 and its fourth moments are periodic with period T_0. Then the complex-valued process $\{Z_s(\lambda,\tau),\, s \in \mathbb{N}\}$ given by equation (5.3) has a periodic mean function with integer period q and its autocovariance function does not depend on time. For $q = 1$ the time series $Z_s(\lambda,\tau)$ is stationary.*

Proof. See Section 5.1.5. □

By properly averaging the process $X(t)$ as shown in (5.3), we obtain stationary or PC processes. This allows us to apply the bootstrap consistency results from [85], which we adapt to our settings.

Theorem 5.2. *Assume that* $\{X(t),\, t \in \mathbb{R}\}$ *is a zero-mean* α*-mixing PC process such that*

(i) functions $\mathbb{E}[X(t)X(t+\tau_1)X(t+\tau_2)X(t+\tau_3)]$ *are periodic in* $t \in \mathbb{R}$ *for any* $\tau_1, \tau_2, \tau_3 \in \mathbb{R}$*;*

(ii) the set $\Lambda = \bigcup_{\tau\in\mathbb{R}} \{\lambda \in \mathbb{R} : a(\lambda,\tau) \neq 0\}$ *is finite;*

(iii) $\sup_{t\in\mathbb{R}} \mathbb{E}|X(t)|^{8+2\delta} < \infty$ *and* $\int\limits_{\mathbb{R}} \tau \alpha_X^{\frac{\delta}{4+\delta}}(\tau)\,\mathrm{d} < \infty$ *for some* $\delta > 0$*;*

(iv) $\sqrt{n}(\widehat{a}(\lambda,\tau) - a(\lambda,\tau)) \xrightarrow{d} \mathcal{N}_2(0,\Sigma)$*, where* $\det(\Sigma) \neq 0$*.*

Then

$$\sup_{x\in\mathbb{R}} \left| \mathbb{P}^*\Big(\sqrt{n}\,\mathrm{Re}\left(\widehat{\mu}^*_{Z(\lambda,\tau)} - \mathbb{E}^*\widehat{\mu}^*_{Z(\lambda,\tau)}\right) \le x\Big) - \mathbb{P}\Big(\sqrt{n}\,\mathrm{Re}\left(\widehat{\mu}_{Z(\lambda,\tau)} - \mu_{Z(\lambda,\tau)}\right) \le x\Big) \right| \xrightarrow{\mathbb{P}} 0,$$

and

$$\sup_{x\in\mathbb{R}} \left| \mathbb{P}^*\Big(\sqrt{n}\,\mathrm{Im}\left(\widehat{\mu}^*_{Z(\lambda,\tau)} - \mathbb{E}^*\widehat{\mu}^*_{Z(\lambda,\tau)}\right) \le x\Big) - \mathbb{P}\Big(\sqrt{n}\,\mathrm{Im}\left(\widehat{\mu}_{Z(\lambda,\tau)} - \mu_{Z(\lambda,\tau)}\right) \le x\Big) \right| \xrightarrow{\mathbb{P}} 0,$$

as $b \to \infty$, $n \to \infty$ *with* $b/n \to 0$*, where* $\mathbb{P}^*$ *and* $\mathbb{E}^*$*, respectively, denote the conditional probability and conditional expectation, given* $(Z_1(\lambda,\tau), Z_2(\lambda,\tau), \ldots, Z_n(\lambda,\tau))$*.*

Proof. See Section 5.1.5. □

Now, let us derive the formula for the optimal block length. For clarity, we focus on the real part of $\mu_{Z(\lambda,\tau)}$, since the results for the imaginary part are analogous. Fix $\lambda = \frac{p}{qT_0}$, where $p, q \in \mathbb{Z}$ are relatively prime, and $\tau \ge 0$. Since $Z_s(\lambda,\tau)$ is a PC time series with a known integer period q, we can apply the result from [3]. Consequently, the optimal block length takes the form $b = lq + 1$, with $l \in \mathbb{Z}$, and is given by

$$b_{\mathrm{opt,Re}} = b_{\mathrm{opt,Re}}(\lambda,\tau) = \sqrt[3]{\frac{2G^2}{D}}\,\sqrt[3]{n}, \tag{5.4}$$

where

$$G = q \sum_{h=-\infty}^{\infty} \left|\left\lfloor \tfrac{h}{q} \right\rfloor\right| \gamma_{\mathrm{Re}(Z)}(h), \qquad D = \tfrac{4}{3}(2\pi q)^2 |f_{\mathrm{Re}(Z)}(0)|^2.$$

Moreover, $\gamma_{\mathrm{Re}(Z)}(h) = \mathrm{Cov}(\mathrm{Re}(Z_s(\lambda,\tau)), \mathrm{Re}(Z_{s+h}(\lambda,\tau)))$ and

$$f_{\mathrm{Re}(Z)}(\omega) = \frac{1}{2\pi} \sum_{h=-\infty}^{\infty} \gamma_{\mathrm{Re}(Z)}(h)\, e^{-i\omega h}.$$

Detailed assumptions for the above results can be found in [3]. The derivation of (5.4) is provided in Section 5.1.5.

Remark 5.1. Note that for the cycle frequency $\lambda = \frac{l}{T_0}$, where $l \in \mathbb{Z}$, of the PC process $X(t)$ yields a mean function for $Z_s(\lambda,\tau)$ with period $q = 1$. Consequently, $Z_s(\lambda,\tau)$ is a stationary time series, and the formula for the optimal block length simplifies to the well-known expression used in the stationary case for the CBB method (see [47, Chapter 7]).

Remark 5.2. The bootstrap approach above can also be applied to the estimation of the cyclic mean function $b(\gamma)$. Specifically, we define the process $Z_s(\gamma)$ as

$$Z_s(\gamma) = \frac{1}{T_0} \int_{(s-1)T_0}^{sT_0} X(t)\, e^{-i2\pi\gamma t}\, \mathrm{d}t, \quad s = 1, 2, \ldots, n,$$

where $n = \lfloor \frac{T}{T_0} \rfloor$. In this case, to obtain results analogous to those in Proposition 5.1, it is not necessary to assume the periodicity of the fourth moments of $X(t)$. The arguments for consistency and the selection of the optimal block length follow in the same manner as those for the cyclic autocovariance function.

The above results are established when the mean function is zero. However, they can be extended to cases where the mean function is periodic, provided that the third moments of $X(t)$ are also periodic with period T_0. This extension follows by applying reasoning analogous to the discussion following Corollary 3.5 in [85].

In contrast to the CEMMB for the sampled process, the focus here is not on constructing simultaneous confidence intervals. Instead, the primary objective is to determine the optimal block length for each frequency.

5.1.3 Application of the bootstrap inference

In this section, we discuss the applications of bootstrap methods in the model (5.1).

As noted previously, the Fourier analysis of the underlying PC process $X(t)$ is crucial for the analysis of the original ECG process $Y(t)$. Specifically, the estimators of $\kappa(\gamma, t, \tau)$ and $\rho(\lambda, t, \tau)$ can be determined by the estimators $\widehat{b}(\gamma)$ and $\widehat{a}(\lambda, \tau)$. In addition, the functions $b(\gamma)$ and $a(\lambda, \tau)$ characterize the cyclical properties of the signal under consideration. Therefore, one may be interested in constructing confidence intervals for them.

The consistency of the bootstrap procedure allows for replacement of the quantiles of the asymptotic distribution with the quantiles of the bootstrap distribution to construct pointwise confidence intervals for the real or imaginary part of cyclic statistical functions $b(\gamma)$ and $a(\lambda, \tau)$. In many practical scenarios, confidence intervals are required for a range of frequencies. To address this, simultaneous confidence intervals can be constructed. The pointwise and simultaneous bootstrap confidence intervals for discrete-time PC processes are discussed in detail, for example, in [28].

Another important application of the bootstrap method is performing hypothesis testing, particularly to identify significant frequencies. Specifically, we can verify at which frequencies the functions $b(\gamma)$ and $a(\lambda, \tau)$ are significantly different from zero. Detecting significant frequencies of $b(\gamma)$ allows us to construct the estimator for the mean function. Identifying significant frequencies of $a(\lambda, \tau)$ provides a deeper analysis of the underlying process. For example, in machine diagnostics, the appearance of a new frequency component can signal mechanical failure [1]. A similar approach can be applied for the ECG signal, where the detection of new frequencies may indicate abnormalities in heart anatomy or function.

Let us formulate the problem of identifying a significant frequency of $a(\lambda, \tau)$. For fixed $\tau \in \mathbb{R}$ and $\lambda \in \mathbb{R}$

$$H_0 : a(\lambda, \tau) = 0,$$
$$H_1 : a(\lambda, \tau) \neq 0.$$

Define two test statistics

$$\operatorname{Re} U_T(\tau) = \nu_T \operatorname{Re} \widehat{a}(\lambda, \tau) \quad \text{and} \quad \operatorname{Im} U_T(\tau) = \nu_T \operatorname{Im} \widehat{a}(\lambda, \tau),$$

where ν_T denotes the appropriate rate of convergence, which depends on the specific bootstrap approach employed. For the CEMBB for the sampled process, we have $\nu_T = \sqrt{T}$, while for the CBB for the average process, we have $\nu_T = \sqrt{\lfloor \frac{T-\tau}{T_0} \rfloor}$.

Both test statistics are asymptotically normal with unknown covariance matrices [18]. Under the null hypothesis, we have

$$\operatorname{Re} \widehat{a}(\lambda, \tau) \xrightarrow{\mathbb{P}} 0 \quad \text{and} \quad \operatorname{Im} \widehat{a}(\lambda, \tau) \xrightarrow{\mathbb{P}} 0 \quad \text{as} \quad T \to \infty,$$

whereas under the alternative hypothesis,

$$\operatorname{Re} \widehat{a}(\lambda, \tau) \xrightarrow{\mathbb{P}} \operatorname{Re} a(\lambda, \tau) \quad \text{and} \quad \operatorname{Im} \widehat{a}(\lambda, \tau) \xrightarrow{\mathbb{P}} \operatorname{Im} a(\lambda, \tau) \quad \text{as} \quad T \to \infty.$$

If the observed test statistic $\operatorname{Re} U_T(\tau)$ or $\operatorname{Im} U_T(\tau)$ deviates far from zero relative to the reference distribution, this suggests that the alternative hypothesis holds. The critical values for the tests are determined using the quantiles of the bootstrap distribution. Under the null hypothesis, we have

$$\mathbb{P}\left(\widehat{u}_{\frac{\alpha}{2}} < \operatorname{Re} U_T(\tau) < \widehat{u}_{1-\frac{\alpha}{2}} \right) \longrightarrow 1 - \alpha \quad \text{as} \quad T \to \infty,$$

whereas under H_1

$$\mathbb{P}\left(\widehat{u}_{\frac{\alpha}{2}} < \operatorname{Re} U_T(\tau) < \widehat{u}_{1-\frac{\alpha}{2}} \right) \longrightarrow 0 \quad \text{as} \quad T \to \infty,$$

with $\widehat{u}_{\frac{\alpha}{2}}$ and $\widehat{u}_{1-\frac{\alpha}{2}}$ denoting the $\frac{\alpha}{2}$ and $1 - \frac{\alpha}{2}$ quantiles, respectively, of the bootstrap distribution corresponding to $\nu_T(\operatorname{Re} \widehat{a}(\lambda, \tau) - \operatorname{Re} a(\lambda, \tau))$. The procedure for the imaginary part $\operatorname{Im} a(\lambda, \tau)$ is analogous.

For PC processes, cyclic functions have non-zero values only at frequencies that are integer multiples of the inverse of the period. However, if the considered process is actually an AM-TW PC, but we assume that it is a PC and estimate the cyclic functions accordingly, the resulting values tend to spread around the cycle frequencies [64]. In such cases, the bootstrap tests described above can be used to verify the significance of frequencies in the neighborhood of cycle frequencies. This approach serves as a useful tool for determining whether the cyclic structure is concentrated at integer multiples of the inverse of the period, which indicates a PC model, or spread across infinitely many frequencies, which would suggest that an AM-TW PC model may be more appropriate.

Additionally, the bootstrap test can be used to evaluate the quality of the underlying PC signal reconstruction. This step is particularly important because the reconstruction is sensitive to the choice of certain parameters. If after reconstruction, the cyclic functions remain spread around the cycle frequency, it may indicate that the parameters need to be adjusted. Alternatively, such dispersion could be due to a time-warping function $\varepsilon(t)$ that varies too rapidly.

5.1.4 Real data example

In this section, the proposed methodology is applied to ECG data. Specifically, we analyze the ECG signal $\widetilde{Y}(t)$ recorded from a 30-year-old Caucasian male who is a non-smoker, leads a sedentary lifestyle, had consumed coffee prior to recording, and was listening to classical music during the session. More details on the data set can be found at `https://physionet.org/physiobank/database/cebsdb/` and [32].

For our analysis, we consider a recording duration of $T = 200$ seconds with a sampling rate of 200 Hz, which corresponds to a discratization step of $h = 0.005\,\mathrm{s}$ and yields a total of $n = 40000$ time points. First, we subtract the overall mean from the ECG signal. From now, we consider the signal $Y(t) = \widetilde{Y}(t) - \frac{1}{T}\int_0^T \widetilde{Y}(s)\,\mathrm{d}s$. The first 15 seconds of the signal $Y(t)$ are shown in Figure 5.1.

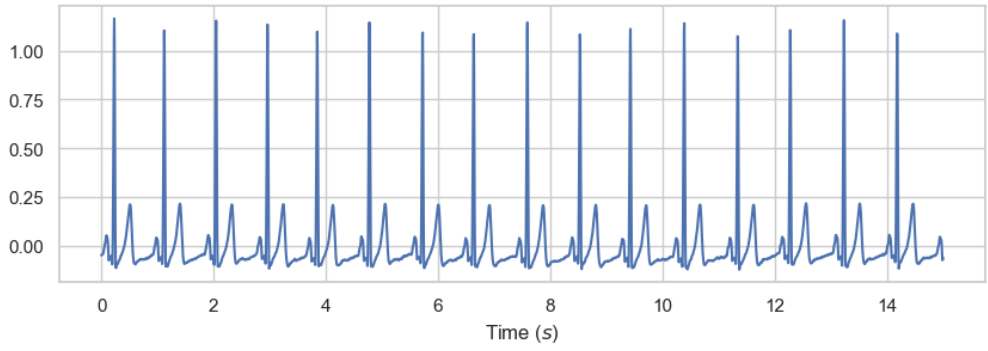

Figure 5.1: A 15-second recording of the signal $Y(t)$.

We assume that $Y(t)$ can be modeled by (5.1). We start with reconstructing the underlying PC signal $X(t)$ from the observed signal $Y(t)$. To achieve this, we apply the amplitude-modulation compensation and de-warping method proposed in [64]. Further implementation details are provided in our paper [31]. A comparison between the observed signal $Y(t)$ and the reconstructed signal $\widehat{X}(t)$ is shown in Figure 5.2. Furthermore, we present the estimated cyclic mean functions of both $\widehat{X}(t)$ and $Y(t)$, assuming that each is a PC process. Note that the cyclic functions of $\widehat{X}(t)$ are more concentrated around the cycle frequency $\alpha_0 = 0.0055244655\,h^{-1}$ compared to those of $Y(t)$.

Next, we estimate the mean function of the underlying PC process using its Fourier series representation. The estimated mean function is given by

$$\widehat{\mu}_X(t) = \sum_{k=-K}^{K} \widehat{b}(k\alpha_0)\, e^{i2\pi k\alpha_0 t},$$

where $K = 90$. This procedure cannot be applied directly to $Y(t)$, as a finite set of significant frequencies cannot be clearly identified for this signal.

We now perform bootstrap inference. First, we test the null hypothesis that $b(\gamma) = 0$ for each $\gamma \in \Lambda_{\alpha_0}$, where

$$\Lambda_{\alpha_0} = \{\alpha_0 + kh\alpha_0 \,:\, k = -14, -13, \ldots, 14\}\,.$$

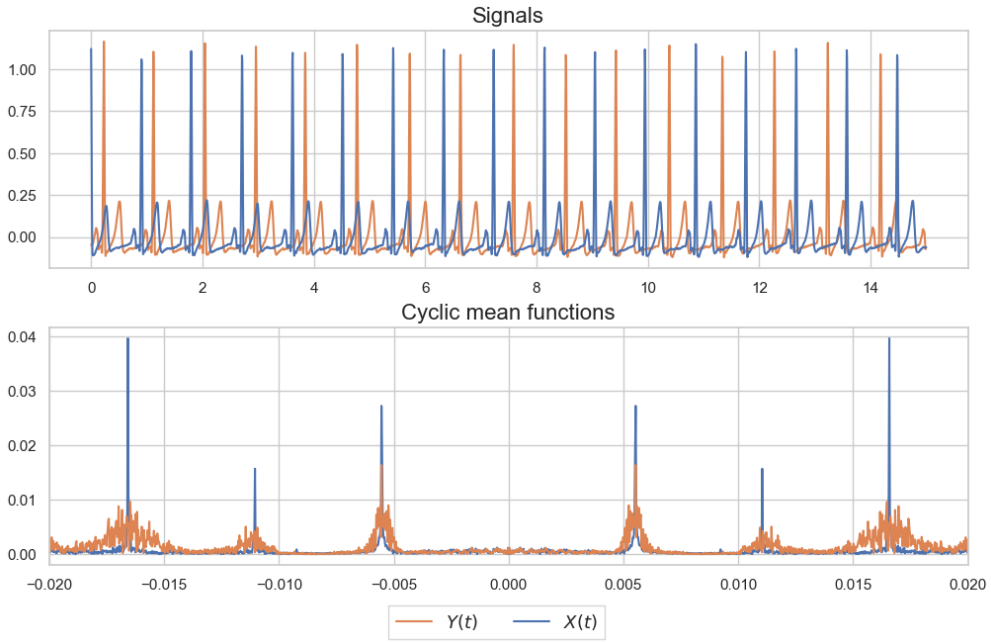

Figure 5.2: Comparison of results for the signal $Y(t)$ and the estimated underlying PC signal $\widehat{X}(t)$. Top panel: signals $Y(t)$ and $\widehat{X}(t)$. Bottom panel: magnitude of the cyclic mean functions $b(\gamma)$ of $Y(t)$ and $\widehat{X}(t)$ for $\gamma \in [-0.02, 0.02]$. Orange line: results for $Y(t)$. Blue line: results for $\widehat{X}(t)$.

The significance level we set to $\alpha = 0.05$. Second, we compute 95% bootstrap confidence intervals for $a(\lambda, 0)$, for each $\lambda \in \Lambda_{\alpha_0}$. For both hypothesis testing and confidence interval construction, we apply the two proposed bootstrap approaches. The results for each method are reported below.

CEMBB for the sampled process. We fix the block size as $b = 10\lfloor \alpha_0^{-1} \rfloor + 1 = 906$. We generate $B = 999$ bootstrap samples and perform hypothesis tests. The results, presented in Figure 5.3, show that the null hypothesis is rejected only at the frequency α_0. Next, we construct 95% bootstrap simultaneous equal-tailed percentile confidence intervals for $a(\lambda, 0)$. These intervals are displayed in Figure 5.4.

CBB for the averaged process. We first compute the optimal block lengths for $b(\gamma)$ separately for each frequency $\gamma \in \Lambda_{\alpha_0}$. Based on these, we generate $B = 999$ bootstrap samples and perform hypothesis tests. The results, presented in Figure 5.5, show that the null hypothesis is rejected only at the frequency α_0. Next, we compute the optimal block lengths for $a(\lambda, 0)$ for each $\lambda \in \Lambda_{\alpha_0}$ individually. We generate $B = 999$ bootstrap samples with new block lengths and construct 95% bootstrap pointwise equal-tailed percentile confidence intervals for $a(\lambda, 0)$, for $\lambda \in \Lambda_{\alpha_0}$. These intervals are displayed in Figure 5.6.

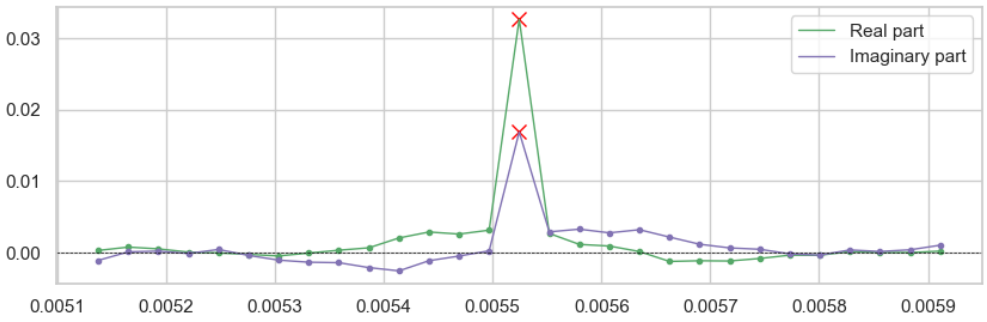

Figure 5.3: Results for the hypothesis tests based on the CEMBB for the sampled process. Green points: real part of the cyclic mean function at frequencies where the null hypothesis is not rejected. Violet points: imaginary part of the cyclic mean function at frequencies where the null hypothesis is not rejected. Red points 'x': real or imaginary part of the cyclic mean function at cycle frequencies where the null hypothesis (that the cyclic statistical function is zero) is rejected.

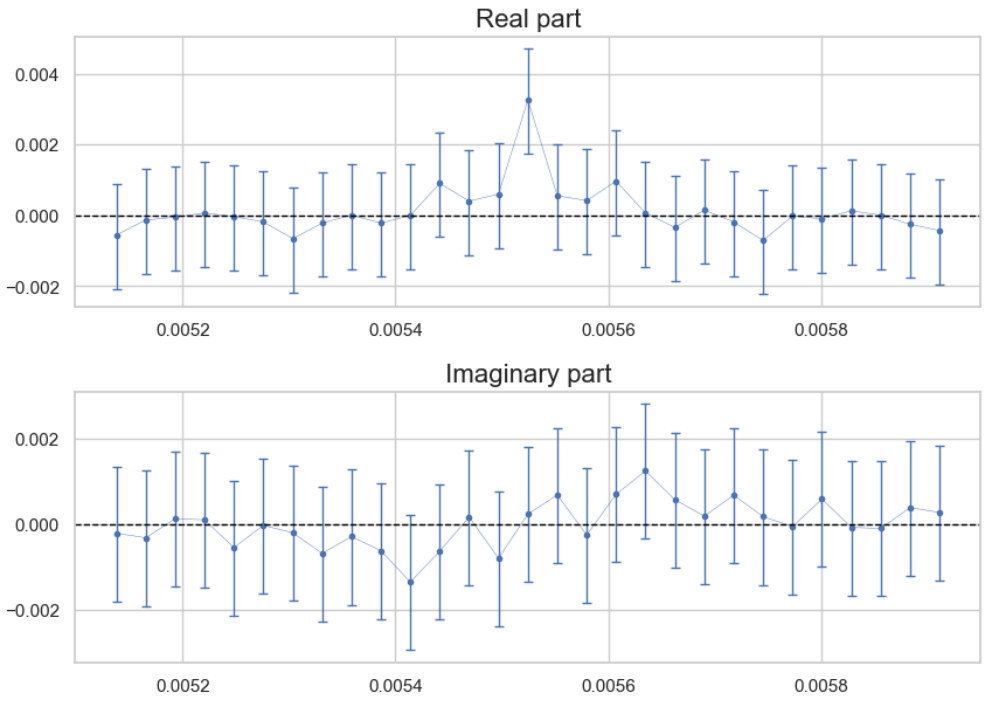

Figure 5.4: Results for the CEMBB for the sampled process. 95% bootstrap simultaneous equal-tailed percentile confidence intervals for the real part (top panel) and the imaginary part (bottom panel) of cyclic function $a(\lambda, 0)$. Blue dots: estimated values of $a(\lambda, 0)$. Vertical blue lines: confidence intervals for $a(\lambda, 0)$.

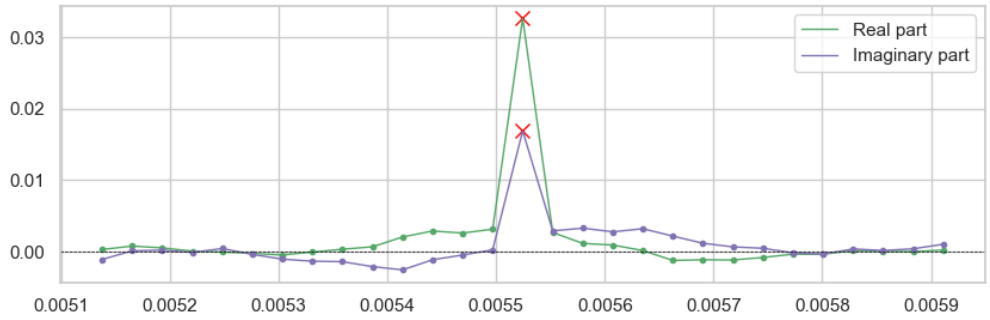

Figure 5.5: Results for the hypothesis tests based on the CBB for the averaged process. Green points: real part of the cyclic mean function at frequencies where the null hypothesis is not rejected. Violet points: imaginary part of the cyclic mean function at frequencies where the null hypothesis is not rejected. Red points 'x': real or imaginary part of the cyclic mean function at cycle frequencies where the null hypothesis (that the cyclic statistical function is zero) is rejected.

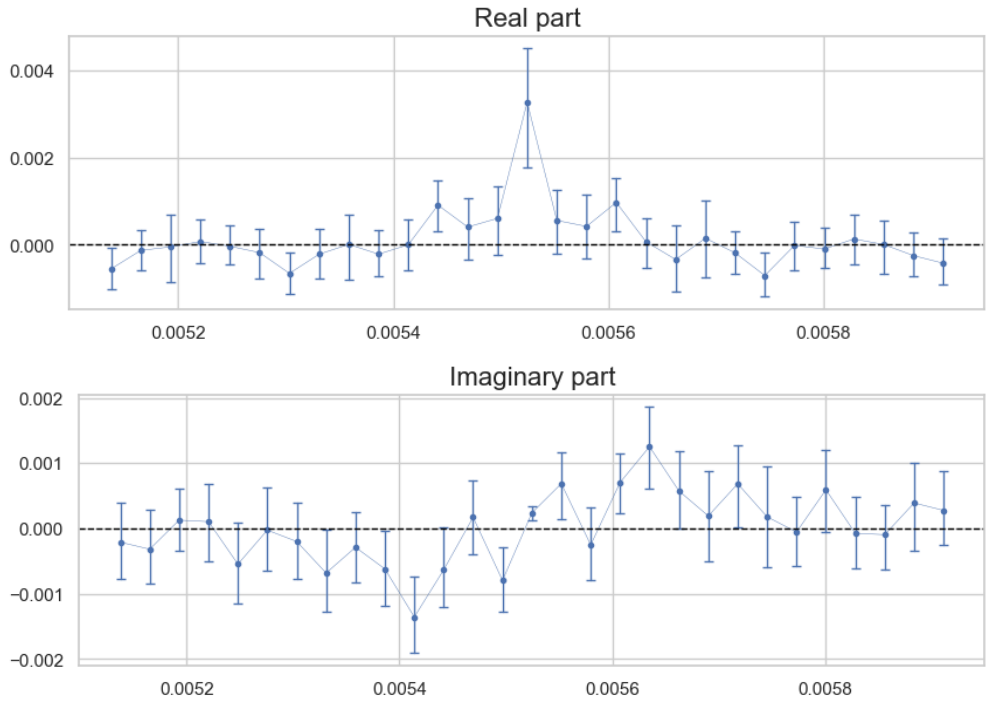

Figure 5.6: Results for the CBB for the averaged process. 95% bootstrap pointwise equal-tailed percentile confidence intervals for the real part (top panel) and the imaginary part (bottom panel) of cyclic function $a(\lambda, 0)$. Blue dots: estimated values of $a(\lambda, 0)$. Vertical blue lines: confidence intervals for $a(\lambda, 0)$.

5.1.5 Proofs of results presented in Section 5.1

This subsection contains proofs of the original results presented in Section 5.1.

Proof of Proposition 5.1. For simplicity, instead of $Z_s(\lambda,\tau)$ we write Z_s. The mean function of Z_s is as follows

$$\begin{aligned}
\mathbb{E}Z_s &= \frac{1}{T_0}\int\limits_{(s-1)T_0}^{sT_0} \mathbb{E}\big[X(t)\,X(t+\tau)\big]\,e^{-i2\pi\lambda t}\,\mathrm{d}t \\
&= \frac{1}{T_0}\int\limits_{0}^{T_0} \mathbb{E}\big[X(t+(s-1)T_0)\,X(t+(s-1)T_0+\tau)\big]\,e^{-i2\pi\lambda(t+(s-1)T_0)}\,\mathrm{d}t \\
&= e^{-i2\pi\lambda(s-1)T_0}\frac{1}{T_0}\int\limits_{0}^{T_0} \mathbb{E}\big[X(t)\,X(t+\tau)\big]\,e^{-i2\pi\lambda t}\,\mathrm{d}t \\
&= \mathbb{E}(Z_1)\,e^{-i2\pi\lambda(s-1)T_0}.
\end{aligned}$$

If $\lambda=\frac{p}{qT_0}$ with $p,q\in\mathbb{Z}$, then the function $e^{-i2\pi\lambda(s-1)T_0}$, viewed as a function of $s\in\mathbb{Z}$, is periodic with period q. As a result, the mean function of the time series Z_s is also periodic with period q.

Applying the same logic to the autocovariance, we show that it is independent of s. Specifically, for each $h\in\mathbb{Z}$, we have

$$\begin{aligned}
\mathrm{Cov}\big(Z_s,Z_{s+h}\big) &= \frac{1}{T_0^2}\int\limits_{(s-1)T_0}^{sT_0}\int\limits_{(s+h-1)T_0}^{(s+h)T_0} \mathrm{Cov}\big(X(t)\,X(t+\tau),X(u)\,X(u+\tau)\big)\,e^{-i2\pi\lambda t}\,e^{i2\pi\lambda u}\,\mathrm{d}t\,\mathrm{d}u \\
&= \frac{1}{T_0^2}\int\limits_{0}^{T_0}\int\limits_{hT_0}^{(h+1)T_0} \mathrm{Cov}\big(X(t+(s-1)T_0)\,X(t+(s-1)T_0+\tau), \\
&\qquad\qquad X(u+(s-1)T_0)\,X(u+(s-1)T_0+\tau)\big) \\
&\qquad\qquad \times e^{-i2\pi\lambda(t+(s-1)T_0)}\,e^{i2\pi\lambda(u+(s-1)T_0)}\,\mathrm{d}t\,\mathrm{d}u \\
&= \frac{1}{T_0^2}\int\limits_{0}^{T_0}\int\limits_{hT_0}^{(h+1)T_0} \mathrm{Cov}\big(X(t)\,X(t+\tau),X(u)\,X(u+\tau)\big)\,e^{-i2\pi\lambda t}\,e^{i2\pi\lambda u}\,\mathrm{d}t\,\mathrm{d}u.
\end{aligned}$$

□

Proof of Theorem 5.1. The proof follows the same reasoning as the proof of Theorem 3 in [23]. □

Proof of Theorem 5.2. It is enough to show that the assumptions of Corollary 3.2 in [84] are satisfied for a PC time series $Z_s=Z_s(\lambda,\tau)$.

Assumption (i) of Corollary 3.2 in [84] is satisfied since the autocovariance function of Z_s does not depend on time.

Assumption (ii) of Corollary 3.2 in [84] follows from Minkowski integral inequality and Hölder inequality

$$\Big(\mathbb{E}|Z_s|^{4+\delta}\Big)^{\frac{1}{4+\delta}} \le \frac{1}{T_0}\int_{(s-1)T_0}^{sT_0}\Big(\mathbb{E}|X(t)X(t+\tau)|^{4+\delta}\Big)^{\frac{1}{4+\delta}}\,\mathrm{d}t \le \left(\sup_{t\in\mathbb{R}}\mathbb{E}|X(t)|^{2(4+\delta)}\right)^{\frac{1}{2(4+\delta)}}.$$

To show that assumption (iii) of Corollary 3.2 in [84] holds, note that

$$\sigma(Z_s) \subset \sigma(\{X(t) \,:\, (s-1)T_0 \le t \le \tau + sT_0\}).$$

Then we get

$$\sigma(\{Z_s \,:\, s \le p\}) \subset \sigma(\{X(t) \,:\, t \le \tau + pT_0\}),$$

and

$$\sigma(\{Z_s \,:\, s \ge p+q\}) \subset \sigma(\{X(t) \,:\, t \ge (p+q-1)T_0\}).$$

Therefore, the mixing coefficient $\alpha_Z(\cdot)$ of Z_s satisfies

$$\alpha_Z(q) \le \alpha_X(qT_0 - T_0 - \tau)$$

for $qT_0 - T_0 - \tau \ge 0$. This shows that (iii) of Corollary 3.2 in [84] is satisfied. □

Proof of the optimal block length eq. (5.4). For simplicity, instead of $Z_s(\lambda, \tau)$ we will write Z_s. The optimal block length for a sample $(\operatorname{Re} Z_1, \ldots, \operatorname{Re} Z_n)$ from the PC time series with period q is given by the following formula

$$b_{\mathrm{opt,Re}} = \sqrt[3]{\frac{2G^2}{D}}\, n,$$

where

$$G = \sum_{s=1}^{q} \sum_{h=-\infty}^{\infty} \left|\left\lfloor \tfrac{h}{q} \right\rfloor\right| \operatorname{Cov}(\operatorname{Re}(Z_s), \operatorname{Re}(Z_{s+h})), \qquad D = \tfrac{4}{3}(2\pi q)^2 \sum_{s=0}^{q-1} |f^s_{\operatorname{Re}(Z)}(0)|^2,$$

and $f^s_{\operatorname{Re}(Z)}(\omega)$, $s = 0, 1, \ldots, q-1$ are spectral densities of PC time series $\operatorname{Re}(Z_t)$, see [3].

In our settings, a time series $\operatorname{Re}(Z_t)$ has a periodic mean function with period $q \in \mathbb{N}$ and the autocovariance function depends only on a lag parameter, i.e. $\gamma_{\operatorname{Re}(Z)}(h) = \operatorname{Cov}(\operatorname{Re}(Z_s), \operatorname{Re}(Z_{s+h}))$, then

$$G = \sum_{t=1}^{q} \sum_{h=-\infty}^{\infty} \left|\left\lfloor \tfrac{h}{q} \right\rfloor\right| \operatorname{Cov}(\operatorname{Re}(Z_t), \operatorname{Re}(Z_{t+h})) = \sum_{t=1}^{q} \sum_{h=-\infty}^{\infty} \left|\left\lfloor \tfrac{h}{q} \right\rfloor\right| \gamma_{\operatorname{Re}(Z)}(h) = q \sum_{h=-\infty}^{\infty} \left|\left\lfloor \tfrac{h}{q} \right\rfloor\right| \gamma_{\operatorname{Re}(Z)}(h).$$

Since the autocovariance $\gamma_{\operatorname{Re}(Z)}(h)$ is constant in time, there is only one non-zero spectral density function, corresponding to the main diagonal, denoted by $f_{\operatorname{Re}(Z)}(\omega)$. Moreover, using the properties of discrete-time PC processes, we have

$$f_{\operatorname{Re}(Z)}(\omega) = \frac{1}{2\pi} \sum_{\tau=-\infty}^{\infty} \gamma_{\operatorname{Re}(Z)}(\tau)\, e^{-i\tau\omega},$$

and hence

$$D = \tfrac{4}{3}(2\pi q)^2 |f_{\operatorname{Re}(Z)}(0)|^2.$$

□

5.2 Statistical properties of oscillatory processes with stochastic modulation in amplitude and time

Continuous-time stochastic processes with irregular cyclicities can be modeled using the approach discussed in Section 5.1. Related methods have also been explored in [16] and in [54]. However, the key limitation of these methods is the lack of asymptotic results for statistical methods. In this section, we introduce the novel semiparametric continuous-time model for signals with irregular cyclicities, which is related to parametric discrete-time models proposed by Lenart in [49, 48]. Unlike Lenart's models, we depart from the assumption of a Gaussian distribution for the phase-shift process. In Section 5.2.1, we introduce our model. In Section 5.2.2, we derive the first- and second-order properties of the model. In Section 5.2.3, we propose estimation methods for a mean and an autocovariance function. In Section 5.2.4, we examine the convergence rate of the autocovariance estimator using Monte Carlo simulations. Finally, Section 5.2.5 includes proofs of the results.

All theorems in this section are original contributions. These results can be found in [26].

5.2.1 Model construction

In [26], we propose a new continuous-time semiparametric model given by

$$X(t) = A(t) \sum_{j=1}^{J} c_j \cos\left(\lambda_j (t + \psi_j + \phi(t) + z(t))\right) + \mu, \quad t \geq 0, \tag{5.5}$$

where $\mu \in \mathbb{R}$ is an overall mean, $0 < \lambda_1 < \lambda_2 < \ldots < \lambda_J < \infty$ are frequencies, $\psi_j \in \mathbb{R}$ are phase-shifts, $c_j \in \mathbb{R}$ with $c_1 = 1$ are amplitudes, and $J \in \mathbb{N}$ is any fixed number of frequencies. Moreover, $A(t)$, $\phi(t)$ and $z(t)$ are stochastic processes.

Assumption 5.1. We impose the following conditions on the processes $A(t)$, $\phi(t)$ and $z(t)$.

(i) $\{A(t),\, t \geq 0\}$ is any second-order stationary stochastic process with $\mathbb{E}A(t) = a \neq 0$ and autocovariance function $\gamma_A(\tau) = \mathrm{Cov}(A(t), A(t+\tau))$, for $t, t+\tau \geq 0$.

(ii) $\{\phi(t),\, t \geq 0\}$ is a fractional Brownian motion (fBm) with Hurst index $h \in (0,1)$ and variance parameter $\sigma_\phi^2 > 0$. That is, $\phi(t)$ is zero-mean Gaussian process that $\phi(0) = 0$ a.s., and it has the following autocovariance function

$$\mathrm{Cov}(\phi(t), \phi(t+\tau)) = \frac{\sigma_\phi^2}{2}\left(|t|^{2h} + |t+\tau|^{2h} - |\tau|^{2h}\right).$$

(iii) $\{z(t),\, t \geq 0\}$ is any zero-mean stochastic process with stationary increments. That is, the distribution of $z(t) - z(s)$ depends only on $t - s$ for all $0 \leq s < t$.

(iv) $A(t)$, $\phi(t)$ and $z(t)$ are mutually independent.

The process $A(t)$ is an amplitude modulation process and $\phi(t) + z(t)$ is the phase shift process of superposition of cosines

$$\sum_{j=1}^{J} c_j \cos(\lambda_j (t + \psi_j)) + \mu. \tag{5.6}$$

Note that (5.6) is an almost periodic function (see Definition 1.4). To model irregular cycles that cannot be captured using almost periodic functions, we introduced a random phase shift $\phi(t) + z(t)$ into our model. The choice of a nonstationary phase shift process $\phi(t)+z(t)$ is motivated by its ability to represent scenarios in which the exact position within the cycle at a given time is unknown. In contrast, if the random phase is stationary, the cycles remain closely synchronized with the reference almost periodic function (5.6), deviating only slightly.

Recall that the Hurst index h of the fBm process measures its long-range dependence. If $h > 0.5$, then increments on non-overlapping time intervals of fBm are positively correlated, while if $h < 0.5$ they are negatively correlated, resulting in more erratic process paths. In the special case $h = 0.5$, fBm reduces to a Brownian motion (also known as the Wiener process) and has independent increments. By changing the value of h, one can control the behavior of the phase shift process in our model. For further details on the fBm process, we refer the reader to [56, 66].

5.2.2 Statistical properties of the model

In this section, we present the first- and second-order properties of the model (5.5). Note that the existence of moments of $X(t)$ is ensured by the existence of moments of $A(t)$.

Below, we present the form of the mean function of a process $X(t)$.

Theorem 5.3. *Let Assumption 5.1 holds. Then for $t \geq 0$, we have*

$$\mathbb{E}X(t) = \mu + a\sum_{j=1}^{J} c_j \mathbb{E}\cos\left(\lambda_j(t + \psi_j + z(t))\right) e^{-\frac{1}{2}\lambda_j^2\sigma_\phi^2|t|^{2h}}.$$

Proof. See Section 5.2.5. □

Observe that the mean function of $X(t)$ is less related to the frequencies $\lambda_1, \lambda_2, \ldots, \lambda_J$ over time. Its almost periodic nature weakens more rapidly as the Hurst index h increases.

Now, we consider the second-order moment of a process $X(t)$.

Theorem 5.4. *Let Assumption 5.1 holds. Then for $t, t+\tau \geq 0$, we have*

$$\mathbb{E}((X(t) - \mu)(X(t + \tau) - \mu)) = \gamma_X(\tau) + W(t, \tau),$$

with

$$\gamma_X(\tau) = \frac{1}{2}(\gamma_A(\tau) + a^2)\sum_{j=1}^{J} c_j^2 e^{-\frac{1}{2}\lambda_j^2\sigma_\phi^2|\tau|^{2h}} \mathbb{E}\cos(\lambda_j(|\tau| + z(|\tau|)))$$

and

$$|W(t, \tau)| \leq C_0 e^{-c_0(|t|^{2h}+|t+\tau|^{2h})}, \tag{5.7}$$

for some positive constants c_0, C_0, which do not depend on t and τ.

Proof. See Section 5.2.5. □

The second-order moment of $X(t)$ can be decomposed into two components. The first component depends on the lag parameter τ and does not depend on time t. In contrast, the second component depends on both τ and t, and vanishes as t increases. For the formula of $W(t,\tau)$, see (5.10).

As a conclusion, we get that as time tends to infinity, the autocovariance gradually loses its nonstationary (cyclic) properties at a rate determined by the Hurst index h.

Corollary 5.1. *Let Assumption 5.1 holds. Then*

(i) $\lim_{t\to\infty} \mathbb{E}X(t) = \mu$;

(ii) $\lim_{t\to\infty} \mathbb{E}((X(t)-\mu)(X(t+\tau)-\mu)) = \gamma_X(\tau)$ *for* $\tau \in \mathbb{R}$;

(iii) $\lim_{t\to\infty} \mathrm{Cov}(X(t), X(t+\tau)) = \gamma_X(\tau)$ *for* $\tau \in \mathbb{R}$.

Proof. See Section 5.2.5. □

In the next subsection, we propose estimators of the mean μ and the autocovariance function $\gamma_X(\tau)$.

5.2.3 Mean-square consistent estimators of mean and autocovariance functions

From the previous subsection, we know that the process $X(t)$ given by (5.1) is nonstationary, however over time its nonstationary properties vanishes in time. Therefore, we propose standard estimators of the mean and autocovariance functions for stationary processes to estimate μ and $\gamma_X(\tau)$, respectively. Fix $T > 0$. Let $\{X(t),\, t \in [0,T]\}$ be an observed sample of the process $X(t)$. Then to estimate μ and $\gamma_X(\tau)$, $\tau \geq 0$, we use the following estimators

$$\widehat{\mu}_T = \frac{1}{T}\int_0^T X(t)\,\mathrm{d}t, \qquad \widehat{\gamma}_{X,T}(\tau) = \frac{1}{T}\int_0^{T-\tau} (X(t)-\widehat{\mu}_T)(X(t+\tau)-\widehat{\mu}_T)\,\mathrm{d}t.$$

Below we establish mean-square consistency of these estimator.

Theorem 5.5. *Under Assumption 5.1, the estimator* $\widehat{\mu}_T$ *is a mean-square consistent estimator of* μ. *Moreover,*

$$\mathbb{E}\,|\widehat{\mu}_T - \mu|^2 = \mathcal{O}\left(T^{-1}\right), \quad \text{as } T \to \infty.$$

Proof. See Section 5.2.5. □

To obtain the mean-square consistency of $\widehat{\gamma}_{X,T}(\tau)$ we impose additional moment and α-mixing conditions. Recall that the concept of α-mixing is introduced in Section 3.1.

Assumption 5.2. Assume that $\{X(t),\, t \geq 0\}$ is α-mixing with an α-mixing coefficient $\alpha_X(\cdot)$. Moreover, there exists some $\delta > 0$ such that $\sup_{t\geq 0} \mathbb{E}|A(t)|^{4+2\delta} < \infty$.

Theorem 5.6. *Under Assumption 5.1 and 5.2, the estimator* $\widehat{\gamma}_{X,T}(\tau)$ *of* $\gamma_X(\tau)$ *is mean-square consistent for any* $\tau \geq 0$. *That is,*

$$\lim_{T\to\infty} \mathbb{E}\,|\widehat{\gamma}_{X,T}(\tau) - \gamma_X(\tau)|^2 = 0.$$

Proof. See Section 5.2.5. □

Compared to the mean estimator $\widehat{\mu}_T$, we did not derive the theoretical convergence rate of the autocovariance estimator $\widehat{\gamma}_{X,T}(\tau)$. Therefore, in the sequel, we examine this rate of convergence using Monte Carlo simulations.

5.2.4 Investigate the rate of convergence of the autocovariance estimator

In this section, based on simulation study, we investigate the convergence rate of $\mathbb{E}|\widehat{\gamma}_{X,T}(\tau)-\gamma_X(\tau)|^2$. Below, we outline the approach used to conduct this investigation.

For each $\tau \geq 0$, we assume for sufficiently large T, we have

$$\mathbb{E}\,|\widehat{\gamma}_{X,T}(\tau) - \gamma_X(\tau)|^2 = C_1(\tau)T^{-\kappa(\tau)}(1 + v_T(\tau)),$$

with some positive constants $\kappa(\tau)$ and $C_1(\tau)$ and with $v_T(\tau) = o(1)$, as $T \to \infty$. In other words, the theoretical convergence rate of $\mathbb{E}|\widehat{\gamma}_{X,T}(\tau) - \gamma_X(\tau)|^2$ is of the order $T^{-\kappa(\tau)}$. Then for sufficient large T, we get

$$\log\left(\mathbb{E}\,|\widehat{\gamma}_{X,T}(\tau) - \gamma_X(\tau)|^2\right) = -\kappa(\tau)\log(T) + \log\left(C_1(\tau)(1 + v_T(\tau))\right).$$

Therefore, based on a linear regression model, we can compute the least squares estimates of $-\kappa(\tau)$. That is, we obtain an estimator of the rate of convergence of $\mathbb{E}\,|\widehat{\gamma}_{X,T}(\tau) - \gamma_X(\tau)|^2$.

For simulation, we consider the process $X(t)$ given by (5.5) that consists of two cosine waves, that is, $J = 2$. We set $\lambda_1 = 0.05$, $\lambda_2 = 0.2$, $c_1 = 1$, $c_2 = 5$, $\mu = 25$, and $a = 10$. For the amplitude process $A(t)$, we consider $A(t) = \mu + \widetilde{A}(t)$, where $\widetilde{A}(t)$ is an Ornstein-Uhlenbeck process defined by the following stochastic differential equation

$$\mathrm{d}\widetilde{A}(t) = -\rho_A\widetilde{A}(t)\,\mathrm{d}t + \sigma_A\,\mathrm{d}W(t), \quad t \geq 0,$$

where $\rho_A, \sigma_A > 0$ and $W(t)$ is the Wiener process. For the process $z(t)$, we consider a fractional Gaussian noise with drift equal to zero, volatility $\sigma_z > 0$, and Hurst index $g \in (0, 1)$. Thus,

$$\mathrm{Cov}(z(t), z(t+\tau)) = \frac{\sigma_z^2}{2}\left(|\tau+1|^{2g} - 2|\tau|^{2g} + |\tau-1|^{2g}\right).$$

We consider four different scenarios **M1**, **M2**, **M3**, and **M4** with different parameter values for $\sigma_A, \rho_A, \rho_z, g, \sigma_\phi, h$. These parameter values are summarized in Table 5.1.

	σ_A	ρ_A	ρ_z	g	σ_ϕ	h
M1	$\frac{1}{20}$	$\frac{1}{2}$	$\frac{1}{5}$	$\frac{3}{5}$	$\frac{4}{5}$	$\frac{3}{10}$
M2	$\frac{1}{100}$	$\frac{1}{20}$	1	$\frac{7}{10}$	$\frac{3}{5}$	$\frac{1}{2}$
M3	$\frac{1}{4}$	$\frac{1}{100}$	5	$\frac{4}{5}$	$\frac{2}{5}$	$\frac{7}{10}$
M4	$\frac{1}{5}$	$\frac{3}{200}$	$\frac{1}{2}$	$\frac{9}{10}$	$\frac{1}{5}$	$\frac{9}{10}$

Table 5.1: Parameters $\sigma_A, \rho_A, \rho_z, g, \sigma_\phi, h$ in scenarios **M1**–**M4**.

We generate realizations from scenarios **M1**–**M4** for $T = 1000, 2000, \ldots, 250000$. For each T we generated $B = 1500$ independent samples and estimate the value $\mathbb{E}|\widehat{\gamma}_{X,T}(\tau) - \gamma_X(\tau)|^2$, for $\tau = 0.5, 1, \ldots, 120$, using a Monte Carlo procedure. The estimates obtained are denoted by $\widehat{MSE}_B(\tau, T)$. We apply the linear regression model for point

$$\left(\log(T), \log\left(\widehat{MSE}_B(\tau, T)\right)\right), \quad T = 1000, 2000, \ldots, 250000,$$

and calculate the least squares estimates $-\widehat{\kappa}_T(\tau)$ of $-\kappa(\tau)$.

In Figure 5.7, we show the estimation results of $\kappa(\tau)$. The left panel presents the estimates as functions of τ. It is evident that the convergence rate depends on the model parameters for a fixed τ. In particular, we observe the following patterns.

- In model **M1**, where $h < 0.5$ ($\phi(t)$ exhibits short-range dependence), the convergence rate appears to be faster than T^{-1}.
- In model **M2**, where $h = 0.5$ ($\phi(t)$ reduces to the Wiener process), the convergence rate is very close to T^{-1}.
- In models **M3** and **M4**, where $h > 0.5$ ($\phi(t)$ exhibits long-range dependence), the convergence rate appears to be slower than T^{-1}.

Furthermore, for each model, the convergence rate clearly depends on τ and exhibits a cyclic pattern. The right panel of Figure 5.7 presents values of the coefficient R^2, which remain close to 1 in all cases. Furthermore, the values of R^2 also show a cyclical pattern with respect to τ. In [26], we presented further simulation studies of the proposed model.

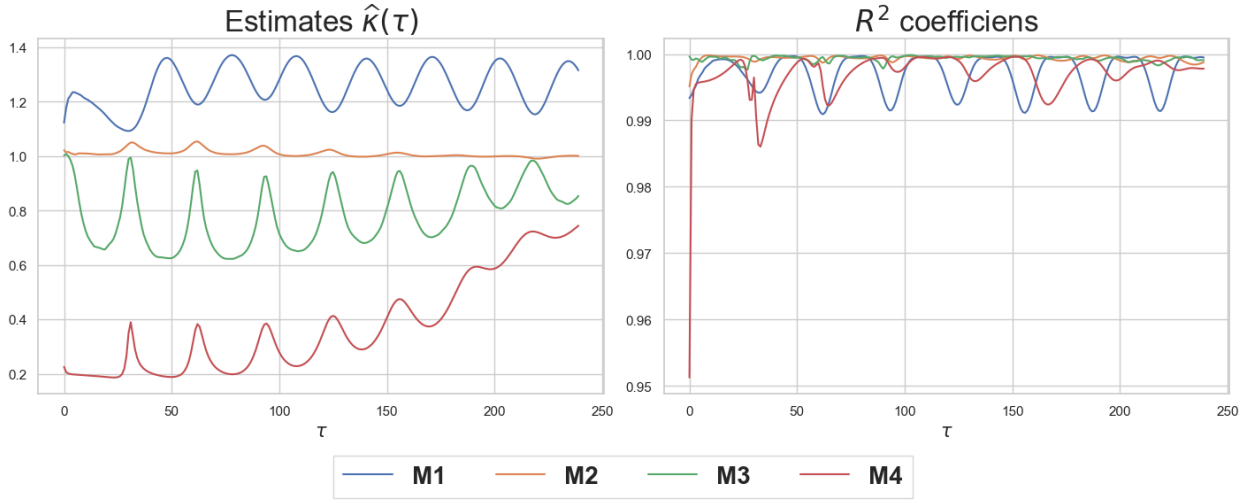

Figure 5.7: Results of convergence rate estimation. Left panel: estimates $\widehat{\kappa}(\tau)$ of $\kappa(\tau)$ for $\tau = 0.5, 1, \ldots, 120$. Right panel: corresponding R^2 for $\tau = 0.5, 1, \ldots, 120$.

5.2.5 Proofs of results presented in Section 5.2

This subsection contains proofs of the original results presented in Section 5.2.

Lemma 5.1. *Let X and Y be independent random variables. Assume that X has a normal distribution with mean $\mu \in \mathbb{R}$ and variance $\sigma^2 > 0$. Then*

$$\mathbb{E}\sin(X+Y) = e^{-\frac{1}{2}\sigma^2}\mathbb{E}\sin(\mu+Y), \quad \mathbb{E}\cos(X+Y) = e^{-\frac{1}{2}\sigma^2}\mathbb{E}\cos(\mu+Y).$$

Proof of Lemma 5.1. The proof follows from the property of the characteristic function of the sum of independent random variables. □

Proof of Theorem 5.3. The proof follows directly from Lemma 5.1. □

Lemma 5.2. *Let $h \in (0,1)$ and $\alpha, \beta > 0$, $\alpha \neq \beta$. Then there exists a positive constant c_0 (which depends only on $\alpha, \beta, h, \sigma_\phi$) such that*

$$\operatorname{Var}(\alpha\phi(t) - \beta\phi(s)) \geq c_0(|t|^{2h} + |s|^{2h}),$$

for $t, s \geq 0$.

Proof. Without loss of generality we take $s = t + \tau$ with some $\tau \geq 0$. We have

$$\begin{aligned}\operatorname{Var}(\alpha\phi(t) - \beta\phi(t+\tau)) &= \alpha^2 \operatorname{Var}(\phi(t)) - 2\alpha\beta \operatorname{Cov}(\phi(t), \phi(t+\tau)) + \beta^2 \operatorname{Var}(\phi(t+\tau)) \\ &= \sigma_\phi^2 \left(\alpha\beta\tau^{2h} + \alpha(\alpha-\beta)t^{2h} + \beta(\beta-\alpha)(t+\tau)^{2h}\right).\end{aligned}$$

It is sufficient to prove that there exist constants $c_1 > 0$ and $c_2 > 0$ such that

$$\alpha\beta\tau^{2h} + \alpha(\alpha-\beta)t^{2h} + \beta(\beta-\alpha)(t+\tau)^{2h} > c_1|t|^{2h}, \tag{5.8}$$

and

$$\alpha\beta\tau^{2h} + \alpha(\alpha-\beta)t^{2h} + \beta(\beta-\alpha)(t+\tau)^{2h} > c_2|t+\tau|^{2h} \tag{5.9}$$

for $t, \tau \geq 0$. Note that for $t = 0$ and any $\tau \geq 0$, as well as for $\tau = 0$ and any $t \geq 0$, the statement holds trivially. Hence, in the sequel, we focus on the case where $t, \tau > 0$. We split the proof into two steps. In the first step, we establish the existence of constant c_1 in the inequality (5.8), and next, we establish the existence of the constant c_2 in the inequality (5.9).

Step 1. In (5.8), we substitute $y = \frac{\tau}{t}$. Then the existence of a constant $c_1 > 0$ satisfying

$$\alpha\beta\tau^{2h} + \alpha(\alpha-\beta)t^{2h} + \beta(\beta-\alpha)(t+\tau)^{2h} > c_1|t|^{2h}$$

is equivalent to the existence of a constant $c_1 > 0$ such that

$$f(y) = \alpha\beta y^{2h} + \alpha(\alpha-\beta) + \beta(\beta-\alpha)(1+y)^{2h} > c_1 > 0,$$

for $y > 0$. The first derivative of $f(y)$ is given by

$$f'(y) = 2\beta h\left(\alpha y^{2h-1} + (\beta-\alpha)(1+y)^{2h-1}\right) = 2\beta(\alpha-\beta)hy^{2h-1}\left(\frac{\alpha}{\alpha-\beta} - \left(\frac{1}{y}+1\right)^{2h-1}\right).$$

If $\beta > \alpha$, then $f'(y) > 0$, which means that $f(y) \geq f(0) = (\alpha-\beta)^2 > 0$ for $y > 0$. If $\alpha > \beta$, then we consider two cases: $h \in (0, \frac{1}{2}]$ and $h \in (\frac{1}{2}, 1)$.

For $h \in (0, \frac{1}{2}]$, we have

$$\left(1+\frac{1}{y}\right)^{1-2h} \geq 1 > 1 - \frac{\beta}{\alpha} = \frac{\alpha-\beta}{\alpha},$$

which implies

$$\frac{\alpha}{\alpha-\beta} > \left(1+\frac{1}{y}\right)^{2h-1}.$$

Consequnelty, $f'(y) > 0$, and hence $f(y) > f(0) = (\alpha-\beta)^2$ for $y > 0$.

For $h \in (\frac{1}{2}, 1)$, the function $f(y)$ has one local minimum at

$$y_0 = \frac{1}{\left(\frac{\alpha}{\alpha-\beta}\right)^{\frac{1}{2h-1}} - 1} > 0,$$

since $f'(y) < 0$ for $y \in (0, y_0)$ and $f'(y) > 0$ for $y \in (y_0, \infty)$. We consider the following substitution

$$\alpha = \frac{\beta x^{2h-1}}{x^{2h-1}-1},$$

with $x > 1$ and $h \in (\frac{1}{2}, 1)$. Then

$$f(y_0) = \frac{\beta^2 \left(\frac{x}{x-1}\right)^{2h} xF(x,h)}{\left(x - x^{2h}\right)^2},$$

with

$$F(x,h) = x^{2h-1} - x^{2h} + (x-1)^{2h} - 1 + x = (x-1)(1 - x^{2h-1} + (x-1)^{2h-1}).$$

Therefore, it is enough to show that $(x-1)^{2h-1} > x^{2h-1} - 1$ for any $x > 1$ and $h \in (\frac{1}{2}, 1)$. We substitute $z = x - 1 > 0$, we obtain $z^{2h-1} + 1 > (z+1)^{2h-1}$ which is true for any $z > 0$ and $h \in (\frac{1}{2}, 1)$. This finishes this step.

Step 2. The proof is similar to that of *Step 1.* In (5.9), we substitute $y = \frac{\tau}{t}$. Then it is enough to show that there exists a constant $c_2 > 0$ such that

$$g(y) = \beta(\beta-\alpha) + \alpha(y+1)^{-2h}\left(\alpha + \beta\left(y^{2h} - 1\right)\right) > c_2 > 0,$$

for $y > 0$. The first derivative of $g(y)$ is

$$g'(y) = 2\alpha\beta h(y+1)^{-2h-1}\left(y^{2h-1} - \frac{(\alpha-\beta)}{\beta}\right).$$

For $\beta > \alpha$ we have $g'(y) > 0$, which means that $g(y) \geq g(0) = (\alpha-\beta)^2 > 0$. For $\alpha > \beta$ the function $g(y)$ has one local minimum at

$$y_0 = \left(\frac{\alpha-\beta}{\beta}\right)^{\frac{1}{2h-1}} > 0,$$

since $g'(y) < 0$ for $y \in (0, y_0)$ and $g'(y) > 0$ for $y \in (y_0, \infty)$. By substitution $\alpha = \beta\left(x^{2h-1} + 1\right)$, with $x > 0$ we get

$$g(y_0) = \beta^2 x^{2h-2}(x+1)^{-2h}\left((x+1)\left(x^{2h} + x\right) - x(x+1)^{2h}\right).$$

Observe that

$$(x+1)\left(x^{2h}+x\right)-x(x+1)^{2h}=x(x+1)\left((x^{2h-1}+1)-(x+1)^{2h-1}\right),$$

and $x^{2h-1}+1>(x+1)^{2h-1}$ for any $x>0$ and $h\in(0,1)$. This finishes the proof. □

Proof of Theorem 5.4. Denote $\xi_j(t)=\lambda_j(t+\psi_j+z(t))$. Using the following trigonometric product-to-sum identity

$$\cos(x)\cos(y)=\frac{1}{2}\left(\cos(x-y)+\cos(x+y)\right),\quad x,y\in\mathbb{R},$$

we have

$$\begin{aligned}
&\mathbb{E}((X(t)-\mu)(X(t+\tau)-\mu))\\
&=\mathbb{E}(A(t)A(t+\tau))\sum_{j_1=1}^{J}\sum_{j_2=1}^{J}c_{j_1}c_{j_2}\mathbb{E}\left(\cos\left(\lambda_{j_1}\phi(t)+\xi_{j_1}(t)\right)\cos\left(\lambda_{j_1}\phi(t+\tau)+\xi_{j_2}(t+\tau)\right)\right)\\
&=\frac{1}{2}\left(\gamma_A(\tau)+a^2\right)\sum_{j_1=1}^{J}\sum_{j_2=1}^{J}c_{j_1}c_{j_2}\Big(\mathbb{E}\left(\cos\left(\lambda_{j_1}\phi(t)-\lambda_{j_2}\phi(t+\tau)+\xi_{j_1}(t)-\xi_{j_2}(t+\tau)\right)\right)\\
&\quad+\mathbb{E}\left(\cos\left(\lambda_{j_1}\phi(t)+\lambda_{j_2}\phi(t+\tau)+\xi_{j_1}(t)+\xi_{j_2}(t+\tau)\right)\right)\Big).
\end{aligned}$$

By Lemma 5.1, we get

$$\mathbb{E}\left(\cos\left(\lambda_{j_1}\phi(t)\pm\lambda_{j_2}\phi(t+\tau)+\xi_{j_1}(t)\pm\xi_{j_2}(t+\tau)\right)\right)=e^{-\eta^{(\pm)}_{j_1,j_2}(t,\tau)}\mathbb{E}\cos\left(\xi_{j_1}(t)\pm\xi_{j_2}(t+\tau)\right),$$

where

$$\begin{aligned}
\eta^{(\pm)}_{j_1,j_2}(t,\tau)&=\frac{1}{2}\mathrm{Var}(\lambda_{j_1}\phi(t)\pm\lambda_{j_2}\phi(t+\tau))\\
&=\frac{1}{2}\left(\lambda_{j_1}^2\mathrm{Var}(\phi(t))\pm2\lambda_{j_1}\lambda_{j_2}\mathrm{Cor}(\phi(t),\phi(t+\tau))+\lambda_{j_2}^2\mathrm{Var}(\phi(t+\tau))\right)\\
&=\frac{1}{2}\sigma_\phi^2\left(\lambda_{j_1}^2|t|^{2h}\pm\lambda_{j_1}\lambda_{j_2}(|t|^{2h}+|t+\tau|^{2h}-|\tau|^{2h})+\lambda_{j_2}^2|t+\tau|^{2h}\right)\\
&=\frac{1}{2}\sigma_\phi^2\left(\lambda_{j_1}|t|^{2h}(\lambda_{j_1}\pm\lambda_{j_2})+\lambda_{j_2}|t+\tau|^{2h}(\lambda_{j_2}\pm\lambda_{j_1})\mp\lambda_{j_1}\lambda_{j_2}|\tau|^{2h}\right)\\
&=\frac{1}{2}\sigma_\phi^2\left((\lambda_{j_1}\pm\lambda_{j_2})(\lambda_{j_1}|t|^{2h}-\lambda_{j_2}|t+\tau|^{2h})\mp\lambda_{j_1}\lambda_{j_2}|\tau|^{2h}\right).
\end{aligned}$$

Note that for $j_1=j_2=j$, by stationary increments of $z(t)$, we obtain

$$e^{-\eta^{(-)}_{j,j}(t,\tau)}\mathbb{E}\cos\left(\xi_j(t)-\xi_j(t+\tau)\right)=e^{-\frac{1}{2}\sigma_\phi^2\lambda_j^2|\tau|^{2h}}\mathbb{E}\cos(\lambda_j(|\tau|+z(|\tau|))).$$

Consequently,

$$\mathbb{E}((X(t)-\mu)(X(t+\tau)-\mu))=\gamma_X(\tau)+W(t,\tau),$$

with

$$\begin{aligned}
W(t,\tau)=\frac{1}{2}\left(\gamma_A(\tau)+a^2\right)\Bigg(&\sum_{j=1}^{J}c_j^2e^{-\eta^{(+)}_{j,j}(t,\tau)}\mathbb{E}\cos\left(\xi_j(t)+\xi_j(t+\tau)\right)\\
&+\sum_{j_1\neq j_2}c_{j_1}c_{j_2}\Big(e^{-\eta^{(-)}_{j_1,j_2}(t,\tau)}\mathbb{E}\cos\left(\xi_{j_1}(t)-\xi_{j_2}(t+\tau)\right)\\
&+e^{-\eta^{(+)}_{j_1,j_2}(t,\tau)}\mathbb{E}\cos\left(\xi_{j_1}(t)+\xi_{j_2}(t+\tau)\right)\Big)\Bigg).
\end{aligned}\tag{5.10}$$

Moreover,

$$|W(t,\tau)| \leq \frac{1}{2}|\gamma_A(\tau)+a^2| \left(\sum_{j_1=1}^{J}\sum_{j_2=1}^{J} |c_{j_1}c_{j_2}| e^{-\eta^{(+)}_{j_1,j_2}(t,\tau)} + \sum_{j_1\neq j_2} |c_{j_1}c_{j_2}| e^{-\eta^{(-)}_{j_1,j_2}(t,\tau)} \right)$$
$$\leq C \left(\sum_{j_1=1}^{J}\sum_{j_2=1}^{J} e^{-\eta^{(+)}_{j_1,j_2}(t,\tau)} + \sum_{j_1\neq j_2} e^{-\eta^{(-)}_{j_1,j_2}(t,\tau)} \right),$$

with

$$C = \frac{1}{2}\left|\sup_{\tau\in\mathbb{R}} \gamma_A(\tau)+a^2\right| \max_{1\leq j\leq J} c_j^2.$$

Finally, by Lemma 5.2 and

$$\begin{aligned}\eta^{(+)}_{j_1,j_2}(t,\tau) &= \frac{1}{2}\left(\lambda_{j_1}^2 \mathrm{Var}(\phi(t)) + 2\lambda_{j_1}\lambda_{j_2}\mathrm{Cor}(\phi(t),\phi(t+\tau)) + \lambda_{j_2}^2\mathrm{Var}(\phi(t+\tau))\right)\\ &\geq \frac{1}{2}\left(\lambda_{j_1}^2 \mathrm{Var}(\phi(t)) + \lambda_{j_2}^2\mathrm{Var}(\phi(t+\tau))\right)\\ &= \frac{1}{2}\sigma_\phi^2\left(\lambda_{j_1}|t|^{2h} + \lambda_{j_2}^2|t+\tau|^{2h}\right),\end{aligned}$$

we end the proof. □

Proof of Corollary 5.1. The proof of *(i)* follows from Theorem 5.3. By Theorem 5.4 we obtain *(ii)* since $\lim_{t\to\infty} W(t,\tau) = 0$ for any $\tau \geq 0$. From *(i)*, *(ii)* and

$$\mathrm{Cov}(X(t), X(t+\tau)) = \mathbb{E}((X(t)-\mu)(X(t+\tau)-\mu)) - \mathbb{E}(X(t)-\mu)\mathbb{E}(X(t+\tau)-\mu),$$

we immediately get *(iii)*. □

Lemma 5.3. *Under Assumption 5.1, we have*

$$\int_0^\infty |W(t,\tau)|\,\mathrm{d}t \leq C_W < \infty,$$

where C_W is some positive constant that does not depend on τ.

Proof. Using (5.7) we get

$$\int_0^\infty |W(t,\tau)|\,\mathrm{d}t \leq C_0 \int_0^\infty e^{-c_0(|t|^{2h}+|t+\tau|^{2h})}\,\mathrm{d}t \leq C_0 \int_0^\infty e^{-c_0|t|^{2h}}\,\mathrm{d}t,$$

with some positive constants $c_0, C_0 > 0$ that does not depend on τ and t. Finally, by the change of variables $u = c_0 t^{2h}$, we obtain

$$\int_0^\infty e^{-c_0 t^{2h}}\,\mathrm{d}t = \frac{1}{2hc_0^{\frac{1}{2h}}}\int_0^\infty u^{\frac{1}{2h}-1}e^{-u}\,\mathrm{d}u = \frac{1}{2hc_0^{\frac{1}{2h}}}\Gamma\left(\frac{1}{2h}\right) < \infty, \tag{5.11}$$

where $\Gamma(x) = \int_0^\infty u^{x-1}e^{-x}\,\mathrm{d}x$, $x > 0$, is the Gamma function. □

Proof of Theorem 5.5. Applying Theorem 5.4, we get

$$\begin{aligned}\mathbb{E}|\widehat{\mu}_T-\mu|^2 &= \frac{1}{T^2}\int_0^T\int_0^T \mathbb{E}((X(t)-\mu)(X(s)-\mu))\,\mathrm{d}s\,\mathrm{d}t\\ &= \frac{1}{T^2}\int_0^T\int_{-t}^{T-t} \mathbb{E}((X(t)-\mu)(X(t+u)-\mu))\,\mathrm{d}u\,\mathrm{d}t \qquad (5.12)\\ &= \frac{1}{T^2}\int_0^T\int_{-t}^{T-t} \gamma_X(u)\,\mathrm{d}u\,\mathrm{d}t + \frac{1}{T^2}\int_0^T\int_{-t}^{T-t} W(t,u)\,\mathrm{d}u\,\mathrm{d}t.\end{aligned}$$

Let us consider the first term on the right-hand side. Using (5.11), we have

$$\frac{1}{T^2}\int_0^T\int_{-t}^{T-t} \gamma_X(u)\,\mathrm{d}u\,\mathrm{d}t \le \frac{\sup_{u\in\mathbb{R}}\mathbb{E}|A(u)|^2}{2T}\sum_{j=1}^{J} c_j^2\int_{\mathbb{R}} e^{-\frac{1}{2}\lambda_j^2\sigma_\phi^2|u|^{2h}}\,\mathrm{d}u = \mathcal{O}\left(T^{-1}\right).$$

Applying Lemma 5.3, for the second term on the right-hand side of (5.12), we obtain

$$\frac{1}{T^2}\int_0^T\int_{-t}^{T-t} |W(t,u)|\,\mathrm{d}u\,\mathrm{d}t \le \frac{1}{T^2}\int_{-T}^{T}\int_0^{\infty} |W(t,u)|\,\mathrm{d}t\,\mathrm{d}u \le \frac{2C_W}{T},$$

where $C_W>0$ is some positive constant. □

Lemma 5.4. *Under Assumption 5.1 and 5.2, for any $\tau\ge 0$ we have*

$$\lim_{T\to\infty}\mathbb{E}\,|\widehat{\gamma}_{X,T}(\tau)-\widetilde{\gamma}_{X,T}(\tau)|^2 = 0,$$

where

$$\widetilde{\gamma}_{X,T}(\tau) = \frac{1}{T}\int_0^{T-\tau}(X(t)-\mu)(X(t+\tau)-\mu)\,\mathrm{d}t.$$

Proof. Note that

$$\begin{aligned}\widehat{\gamma}_{X,T}(\tau)-\widetilde{\gamma}_{X,T}(\tau) &= \frac{1}{T}\int_0^{T-\tau}\left(\widehat{\mu}_T^2-\mu^2+(\mu-\widehat{\mu}_T)(X(t)+X(t+\tau))\right)\mathrm{d}t\\ &= \frac{T-\tau}{T}(\widehat{\mu}_T^2-\mu^2) - (\widehat{\mu}_T-\mu)\cdot\frac{1}{T}\int_0^{T-\tau}(X(t)+X(t+\tau))\,\mathrm{d}t\\ &= \frac{T-\tau}{T}(\widehat{\mu}_T-\mu)(\widehat{\mu}_T+\mu) - (\widehat{\mu}_T-\mu)\,R_T,\end{aligned}$$

where

$$R_T = \frac{1}{T}\int_0^{T-\tau}(X(t)+X(t+\tau))\,\mathrm{d}t.$$

By Minkowski inequality and Hölder inequality, we obtain

$$\left(\mathbb{E}\,|\widehat{\gamma}_{X,T}(\tau)-\widetilde{\gamma}_{X,T}(\tau)|^2\right)^{\frac{1}{2}} \le \frac{T-\tau}{T}\left(\mathbb{E}\,|\widehat{\mu}_T-\mu|^4\cdot\mathbb{E}\,|\widehat{\mu}_T+\mu|^4\right)^{\frac{1}{4}} + \left(\mathbb{E}\,|\widehat{\mu}_T-\mu|^4\cdot\mathbb{E}|R_T|^4\right)^{\frac{1}{4}}.$$

Using Minkowski integral inequality, we get

$$\left(\mathbb{E}\,|\widehat{\mu}_T+\mu|^4\right)^{\frac{1}{4}} \le \left(\mathbb{E}\,|\widehat{\mu}_T|^4\right)^{\frac{1}{4}} + |\mu| = \left(\mathbb{E}\left|\frac{1}{T}\int_0^T X(t)\,\mathrm{d}t\right|^4\right)^{\frac{1}{4}} + |\mu|$$
$$\le \frac{1}{T}\int_0^T \left(\mathbb{E}\,|X(t)|^4\right)^{\frac{1}{4}}\,\mathrm{d}t + |\mu| \le \left(\sup_{t\ge 0}\mathbb{E}\,|A(t)|^4\right)^{\frac{1}{4}} + |\mu| < \infty.$$

Similarly, we have

$$\left(\mathbb{E}|R_T|^4\right)^{\frac{1}{4}} \le \frac{1}{T}\int_0^{T-\tau}\left(\mathbb{E}|X(t)+X(t+\tau)|^4\right)^{\frac{1}{4}}\,\mathrm{d}t \le \frac{1}{T}\int_0^{T-\tau}\left(\mathbb{E}|A(t)|^4\right)^{\frac{1}{4}} + \left(\mathbb{E}|A(t+\tau)|^4\right)^{\frac{1}{4}}\,\mathrm{d}t$$
$$\le 2\frac{T-\tau}{T}\left(\sup_{t\ge 0}\mathbb{E}\,|A(t)|^4\right)^{\frac{1}{4}} = \mathcal{O}(1),$$

as $T\to\infty$. Therefore, it remains to show that $\lim_{T\to\infty}\mathbb{E}\,|\widehat{\mu}_T-\mu|^4 = 0$. We have

$$\mathbb{E}\,|\widehat{\mu}_T-\mu|^4 = \mathbb{E}^2\,|\widehat{\mu}_T-\mu|^2 + \mathrm{Var}\left(|\widehat{\mu}_T-\mu|^2\right).$$

From Theorem 5.5, we have $\lim_{T\to\infty}\mathbb{E}\,|\widehat{\mu}_T-\mu|^2 = 0$. Moreover, by the property of α-mixing measure (see Lemma B.2), we obtain

$$\mathrm{Var}\left(|\widehat{\mu}_T-\mu|^2\right) = \mathrm{Var}\left(\frac{1}{T^2}\int_0^T\int_0^T (X(t)-\mu)(X(s)-\mu)\,\mathrm{d}t\,\mathrm{d}s\right)$$
$$= \frac{1}{T^4}\int_0^T\int_0^T\int_0^T\int_0^T \mathrm{Cov}((X(t)-\mu)(X(s)-\mu),(X(u)-\mu)(X(v)-\mu))\,\mathrm{d}t\,\mathrm{d}s\,\mathrm{d}u\,\mathrm{d}v$$
$$\le \frac{C}{T^4}\int_0^T\int_0^T\int_0^T\int_0^T \alpha_X^{\frac{\delta}{2+\delta}}(\min\{|t-u|,|t-v|,|s-u|,|s-v|\})\,\mathrm{d}t\,\mathrm{d}s\,\mathrm{d}u\,\mathrm{d}v,$$

where

$$C = 8\left(\sup_{t\ge 0}\mathbb{E}|A(t)|^{2(\delta+2)}\right)^{\frac{2}{2+\delta}}.$$

Let us consider the change of variables $x=t-u$, $y=t-v$, $z=s-u$ and $w=s-v$. The Jacobian of this transformation equals $\frac{1}{2}$. Moreover, $(x,y,z,w)\in[-T,T]^4$. Then

$$\mathrm{Var}\left(|\widehat{\mu}_T-\mu|^2\right) \le \frac{C}{2T^4}\int_{-T}^T\int_{-T}^T\int_{-T}^T\int_{-T}^T \alpha_X^{\frac{\delta}{2+\delta}}(\min\{|x|,|y|,|z|,|w|\})\,\mathrm{d}x\,\mathrm{d}y\,\mathrm{d}z\,\mathrm{d}w$$
$$= \frac{4!C}{2T^4}\int_{-T}^T\int_{-T}^w\int_{-T}^z\int_{-T}^y \alpha_X^{\frac{\delta}{2+\delta}}(|x|)\,\mathrm{d}x\,\mathrm{d}y\,\mathrm{d}z\,\mathrm{d}w$$
$$\le \frac{96C}{T}\int_{-T}^T \alpha_X^{\frac{\delta}{2+\delta}}(|x|)\,\mathrm{d}x.$$

Fix $\varepsilon > 0$. Then one can choose $T_0 > 0$ such that $\left|\alpha^{\frac{\delta}{2+\delta}}(\tau)\right| < \varepsilon$ for all $\tau > T_0$. Moreover, $\alpha_X(\tau) \leq \frac{1}{4}$ for $\tau \in \mathbb{R}$, see [21]. Consequently, for $T > \frac{T_0}{4\varepsilon}$, we have

$$\frac{1}{T}\int_0^T \alpha^{\frac{\delta}{2+\delta}}(\tau)\,\mathrm{d}\tau \leq \frac{1}{T}\int_0^{T_0} \alpha^{\frac{\delta}{2+\delta}}(\tau)\,\mathrm{d}tau + \frac{1}{T}\int_{T_0}^T \alpha^{\frac{\delta}{2+\delta}}(\tau)\,\mathrm{d}tau \leq \frac{T_0}{4T} + \frac{T-T_0}{T}\varepsilon < 2\varepsilon, \tag{5.13}$$

which ends the proof. □

Proof of Theorem 5.6. By Minkowski inequity and Lemma 5.4, it is sufficient to show that

$$\lim_{T\to\infty} \mathbb{E}\,|\widetilde{\gamma}_{X,T}(\tau) - \gamma_X(\tau)|^2 = 0.$$

First, we discuss the convergence of $\mathbb{E}\widetilde{\gamma}_{X,T}(\tau)$. Applying Theorem 5.4, we get

$$\begin{aligned}\mathbb{E}\widetilde{\gamma}_{X,T}(\tau) &= \frac{1}{T}\int_0^{T-\tau} \mathbb{E}((X(t)-\mu)(X(t+\tau)-\mu))\,\mathrm{d}t \\ &= \frac{T-\tau}{T}\gamma_X(\tau) + \frac{1}{T}\int_0^{T-\tau} W(t,\tau)\,\mathrm{d}t.\end{aligned}$$

Consequnelty, by Lemma 5.3

$$\frac{1}{T}\int_0^{T-\tau} |W(t,\tau)|\,\mathrm{d}t \leq \frac{1}{T}\int_0^{\infty} |W(t,\tau)|\,\mathrm{d}t \leq \frac{C_W}{T},$$

where $C_W > 0$ is some positive constant. Therefore, $\lim_{T\to\infty} \mathbb{E}\widetilde{\gamma}_{X,T}(\tau) = \gamma_X(\tau)$.

Next, we demonstrate that the variance converges to zero. By inequality for α-mixing processes (Lemma B.2) and the change of variables $u = t - s$

$$\begin{aligned}\mathrm{Var}(\widetilde{\gamma}_{X,T}(\tau)) &= \frac{1}{T^2}\int_0^{T-\tau}\int_0^{T-\tau} \mathrm{Cov}((X(t)-\mu)(X(t+\tau)-\mu),(X(s)-\mu)(X(s+\tau)-\mu))\,\mathrm{d}t\,\mathrm{d}s \\ &\leq \frac{C}{T^2}\int_0^{T-\tau}\int_0^{T-\tau} \alpha_X^{\frac{\delta}{2+\delta}}(\min\{|t-s|,|s+\tau-t|,|t+\tau-s|\})\,\mathrm{d}t\,\mathrm{d}s \\ &= \frac{C}{T^2}\int_0^{T-\tau}\int_{-s}^{T-s-\tau} \alpha_X^{\frac{\delta}{2+\delta}}(\min\{|u|,|\tau-u|,|u+\tau|\})\,\mathrm{d}u\,\mathrm{d}s,\end{aligned}$$

where

$$C = 8\left(\sup_{t\geq 0}\mathbb{E}|A(t)|^{2(2+\delta)}\right)^{\frac{2}{2+\delta}}.$$

Hence,

$$\begin{aligned}
\operatorname{Var}(\widetilde{\gamma}_{X,T}(\tau)) &\leq \frac{C}{T^2} \int_0^{T-\tau} \int_{-T-\tau}^{T-2\tau} \alpha_X^{\frac{\delta}{2+\delta}}(\min\{|u|, |\tau-u|, |u+\tau|\})\,\mathrm{d}u\,\mathrm{d}s \\
&= \frac{C(T-\tau)}{T^2} \int_{-T-\tau}^{T-2\tau} \alpha_X^{\frac{\delta}{2+\delta}}(\min\{|u|, |\tau-u|, |u+\tau|\})\,\mathrm{d}u \\
&= \frac{C(T-\tau)}{T^2} \int_{-T-\tau}^{-\tau/2} \alpha_X^{\frac{\delta}{2+\delta}}(|u+\tau|)\,\mathrm{d}u + \frac{C(T-\tau)}{T^2} \int_{-\tau/2}^{\tau/2} \alpha_X^{\frac{\delta}{2+\delta}}(|u|)\,\mathrm{d}u \\
&\quad + \frac{C(T-\tau)}{T^2} \int_{\tau/2}^{T-2\tau} \alpha_X^{\frac{\delta}{2+\delta}}(|u-\tau|)\,\mathrm{d}u.
\end{aligned}$$

Similarly to (5.13), we obtain that the first and last terms of the above sum tend to zero as $T \to \infty$. Additionally, the second term also converges to zero since $\alpha_X(\tau)$ is bounded by $\frac{1}{4}$. □

CHAPTER 6

CONCLUSIONS AND FURTHER RESEARCH

In this thesis, we presented new results on the statistical inference for nonstationary processes. Mainly, we focused on the spectral analysis of harmonizable whose spectral measure is concentrated on the union of lines. We introduced the periodogram frequency-smoothed along the line as an estimator on the spectral density function. We established its mean-square consistency in the cases where the support line is known and where it must be estimated. Furthermore, we derived its asymptotic distribution. Based on this estimator, we proposed an estimator for the spectral coherence function. Additionally, we introduced a subsampling procedure and proved its consistency for spectral analysis in harmonizable processes with spectral measures concentrated on a union of lines. Finally, we discussed two models for signals that exhibit irregular cyclicity, both consisting of modulation of time and amplitude. The first model is a nonparametric approach proposed by Napolitano [63], where both modulations are deterministic. For this model, we proposed two bootstrap procedures for Fourier analysis. The second model is a newly introduced semiparametric approach in which both modulations are stochastic. We established its statistical properties and discussed the estimation of the mean and autocovariance.

In the following, we outline the problems that will be addressed in the future.

1. **Statistical inference for harmonizable processes whose spectral measure is concentrated on the union of curves.** This thesis examines spectral density estimation for harmonizable processes whose spectral mass is concentrated on lines. However, a more general class of harmonizable processes, known as spectrally correlated (SC) processes, has been studied in the literature [61, Chapter 4]. SC processes are harmonizable processes whose spectral measure is concentrated on a union of curves. Such processes result from frequency wrapping of APC processes [62, Section 13.6.6]. So far, research on SC processes has focused only on point estimation of spectral density functions. We plan to extend the results from Chapters 2 and 3. Specifically, we will investigate a periodogram frequency-smoothed along the estimated support curve and develop statistical inference methods based on subsampling.

2. **Spectral density estimation for discretized harmonizable processes.** In this thesis, we examine continuous-time stochastic processes, which are common in telecommunications, where many physical phenomena are described only in continuous time. In practice, however, we observe discretized data, making spectral estimation challenging due to the aliasing problem (the spectral density function of the sampled process is the superposition of the spectral density functions of the continuous-time process [52]). While significant results exist for stationary processes, research on nonstationary processes, such as APC, remains relatively limited. For stationary processes, the spectral analysis is performed on a line $\mathbb{R}$, while in the case of nonstationary processes, on a two-dimensional plane $\mathbb{R}^2$, making the aliasing effects more complex. Our goal will be to study the estimation of the spectral density of discretized processes whose spectral measure is concentrated on the union of lines.

3. **Further work on models for oscillatory processes with stochastic modulation in amplitude and time.** In Section 5.2, we present the semiparametric continuous-time model for signals exhibiting irregular cyclicity. Our future research will focus on exploring additional theoretical properties of this model, including the asymptotic distributions of estimators for the mean and autocovariance functions, and on aspects of spectral analysis. We also aim to extend the model proposed in [26] since currently we assume that the amplitude and phase-shift processes are independent. In many real-world applications, these processes are interdependent. In ECG signals, amplitude variations occur throughout the cycle, reaching their maxima near the so-called 'R-peak'. Finally, we plan to develop a nonparametric model with stochastic modulation in both amplitude and time. Compared to the semiparametric approach, a nonparametric model would offer greater flexibility.

APPENDIX A

COMPLEX-VALUED RANDOM VARIABLES AND VECTORS

In this chapter, we discuss the characterization of complex-valued random variables and vectors. This is essential to our study, as we consider complex-valued stochastic processes. In addition, spectral density estimators have complex values. The notation in this chapter mostly follows the conventions established in [62, Appendix E].

A.1 Second-order characterization of complex-valued random variables and vectors

A complex random variable Z defined on a probability space $(\Omega, \mathcal{F}, \mathbb{P})$ is a function $Z : \Omega \mapsto \mathbb{C}$ such that $\mathrm{Re}(Z)$ and $\mathrm{Im}(Z)$ are both real-valued random variables on $(\Omega, \mathcal{F}, \mathbb{P})$. If $\mathbb{E}|\,\mathrm{Re}(Z)| < \infty$ and $\mathbb{E}|\,\mathrm{Im}(Z)| < \infty$, then the expectation of Z exists and it is defined as

$$\mathbb{E}Z = \mathbb{E}\,\mathrm{Re}(Z) + i\mathbb{E}\,\mathrm{Im}(Z).$$

Since

$$\max\{|\,\mathrm{Re}(Z)|, |\,\mathrm{Im}(Z)|\} \leq |Z| \leq |X| + |Y|,$$

it follows that $\mathbb{E}|Z| < \infty$ if and only if both $\mathbb{E}|\,\mathrm{Re}(Z)| < \infty$ and $\mathbb{E}|\,\mathrm{Im}(Z)| < \infty$, see [6, Chapter 3].

Now, let us introduce second-order characterization. Let Z and W be two complex-valued random variables such that $\mathbb{E}|Z|^2 < \infty$ and $\mathbb{E}|W|^2 < \infty$.

- The variance of Z exists and is defined as

$$\mathrm{Var}(Z) = \mathbb{E}\big[|Z - \mathbb{E}Z|^2\big];$$

- The covariance of Z and W exists and is defined as

$$\mathrm{Cov}(Z, W) = \mathbb{E}\big[(Z - \mathbb{E}Z)\overline{(W - \mathbb{E}W)}\big] = \mathbb{E}\big[Z\overline{W}\big] - \mathbb{E}Z\,\mathbb{E}\overline{W};$$

- The conjugate covariance (or pseudo-covariance) of Z and W exists and is defined as

$$\operatorname{Cov}(Z, \overline{W}) = \mathbb{E}\big[(Z - \mathbb{E}Z)(W - \mathbb{E}W)\big] = \mathbb{E}\big[ZW\big] - \mathbb{E}Z\,\mathbb{E}W;$$

To fully characterize the second-order properties of complex-valued random variables, one should consider the covariance and conjugate covariance.

A complex random vector $\boldsymbol{Z} = [Z_1, \ldots, Z_M]^{\mathrm{T}}$ defined on a probability space $(\Omega, \mathcal{F}, \mathbb{P})$ is a function $Z : \Omega \mapsto \mathbb{C}^M$ such that

$$[\operatorname{Re}(Z_1), \ldots, \operatorname{Re}(Z_M), \operatorname{Im}(Z_1), \ldots, \operatorname{Im}(Z_M)]^{\mathrm{T}}$$

is $2M$-dimensional real-valued random vector on $(\Omega, \mathcal{F}, \mathbb{P})$. Below we present two approaches to fully describe second-order characteristics of complex-valued random vectors.

- A M-dimensional complex-valued vector $\boldsymbol{Z} = \boldsymbol{X} + i\boldsymbol{Y}$ with two M-dimensional real-valued vectors $\boldsymbol{X}$ and $\boldsymbol{Y}$ can be viewed as $2M$-dimensional real-valued random vector

$$\boldsymbol{V} = [V_1, \ldots, V_{2M}]^{\mathrm{T}} = [\boldsymbol{X}^{\mathrm{T}}, \boldsymbol{Y}^{\mathrm{T}}]^{\mathrm{T}} = [\operatorname{Re}(Z_1), \ldots, \operatorname{Re}(Z_M), \operatorname{Im}(Z_1), \ldots, \operatorname{Im}(Z_M)]^{\mathrm{T}}$$

with a mean vector

$$\boldsymbol{\mu}_{\boldsymbol{V}} = \mathbb{E}\boldsymbol{V} = [\boldsymbol{\mu}_{\boldsymbol{X}}^{\mathrm{T}}, \boldsymbol{\mu}_{\boldsymbol{Y}}^{\mathrm{T}}]^{\mathrm{T}} = [\mathbb{E}\operatorname{Re}(Z_1), \ldots, \mathbb{E}\operatorname{Re}(Z_M), \mathbb{E}\operatorname{Im}(Z_1), \ldots, \mathbb{E}\operatorname{Im}(Z_M)]^{\mathrm{T}},$$

and covariance matrix

$$\Sigma_{\boldsymbol{V}\boldsymbol{V}} = \mathbb{E}\big[(\boldsymbol{V} - \mathbb{E}\boldsymbol{V})(\boldsymbol{V} - \mathbb{E}\boldsymbol{V})^{\mathrm{T}}\big] = \begin{bmatrix} \Sigma_{XX} & \Sigma_{XY} \\ \Sigma_{YX} & \Sigma_{YY} \end{bmatrix},$$

where

$$\begin{aligned} \Sigma_{XX} &= \mathbb{E}\big[(\boldsymbol{X} - \mathbb{E}\boldsymbol{X})(\boldsymbol{X} - \mathbb{E}\boldsymbol{X})^{\mathrm{T}}\big], \\ \Sigma_{YY} &= \mathbb{E}\big[(\boldsymbol{Y} - \mathbb{E}\boldsymbol{Y})(\boldsymbol{Y} - \mathbb{E}\boldsymbol{Y})^{\mathrm{T}}\big], \\ \Sigma_{XY} &= \mathbb{E}\big[(\boldsymbol{X} - \mathbb{E}\boldsymbol{X})(\boldsymbol{Y} - \mathbb{E}\boldsymbol{Y})^{\mathrm{T}}\big] = \Sigma_{YX}^{\mathrm{T}}. \end{aligned}$$

- A M-dimensional complex-valued vector $\boldsymbol{Z}$ can be viewed as $2M$-dimensional complex-valued random vector

$$\boldsymbol{\zeta} = [\boldsymbol{Z}, \overline{\boldsymbol{Z}}]^{\mathrm{T}} = [Z_1, \ldots, Z_M, \overline{Z_1}, \ldots, \overline{Z_M}]^{\mathrm{T}}$$

with a complex-valued mean vector

$$\boldsymbol{\mu}_{\boldsymbol{\zeta}} = [\mathbb{E}\boldsymbol{Z}, \mathbb{E}\overline{\boldsymbol{Z}}]^{\mathrm{T}} = [\mathbb{E}Z_1, \ldots, \mathbb{E}Z_M, \mathbb{E}\overline{Z_1}, \ldots, \mathbb{E}\overline{Z_M}]^{\mathrm{T}}$$

and complex-valued covariance matrix

$$\Sigma_{\boldsymbol{\zeta}\boldsymbol{\zeta}} = \mathbb{E}\big[(\boldsymbol{\zeta} - \boldsymbol{\mu}_{\boldsymbol{\zeta}})(\boldsymbol{\zeta} - \boldsymbol{\mu}_{\boldsymbol{\zeta}})^{\mathrm{H}}\big] = \begin{bmatrix} \Sigma_{\boldsymbol{Z}\overline{\boldsymbol{Z}}} & \Sigma_{\boldsymbol{Z}\boldsymbol{Z}} \\ \overline{\Sigma_{\boldsymbol{Z}\boldsymbol{Z}}} & \overline{\Sigma_{\boldsymbol{Z}\overline{\boldsymbol{Z}}}} \end{bmatrix}$$

where

$$\begin{aligned} \Sigma_{\boldsymbol{Z}\boldsymbol{Z}} &= \operatorname{Cov}\big(\boldsymbol{Z}, \overline{\boldsymbol{Z}}\big) = \mathbb{E}\big[(\boldsymbol{Z} - \mathbb{E}Z)(\overline{\boldsymbol{Z} - \mathbb{E}Z})^{\mathrm{T}}\big], \\ \Sigma_{\boldsymbol{Z}\overline{\boldsymbol{Z}}} &= \operatorname{Cov}\big(\boldsymbol{Z}, \boldsymbol{Z}\big) = \mathbb{E}\big[(\boldsymbol{Z} - \mathbb{E}Z)(\boldsymbol{Z} - \mathbb{E}Z)^{\mathrm{T}}\big]. \end{aligned}$$

Moreover using the Euler formula, i.e., $\mathrm{Re}(z) = \frac{z+\overline{z}}{2}$ and $\mathrm{Im}(z) = \frac{z-\overline{z}}{2i}$ for $z \in \mathbb{C}$, we get

$$\boldsymbol{\mu_V} = \left[\tfrac{\boldsymbol{Z}+\overline{\boldsymbol{Z}}}{2}, \tfrac{\boldsymbol{Z}-\overline{\boldsymbol{Z}}}{2i}\right], \qquad \boldsymbol{\mu_\zeta} = \left[\boldsymbol{\mu}_{\boldsymbol{X}}^{\mathrm{T}} + i\boldsymbol{\mu}_{\boldsymbol{Y}}^{\mathrm{T}}, \boldsymbol{\mu}_{\boldsymbol{X}}^{\mathrm{T}} - i\boldsymbol{\mu}_{\boldsymbol{Y}}^{\mathrm{T}}\right],$$

and

$$\begin{aligned}\Sigma_{\boldsymbol{ZZ}} &= \Sigma_{\boldsymbol{XX}} - i\Sigma_{\boldsymbol{XY}} - i\Sigma_{\boldsymbol{YX}} + \Sigma_{\boldsymbol{YY}},\\ \Sigma_{\boldsymbol{Z\overline{Z}}} &= \Sigma_{\boldsymbol{XX}} + i\Sigma_{\boldsymbol{XY}} + i\Sigma_{\boldsymbol{YX}} - \Sigma_{\boldsymbol{YY}},\end{aligned}$$

and

$$\begin{aligned}\Sigma_{\boldsymbol{XX}} &= \frac{1}{2}\,\mathrm{Re}\left(\Sigma_{\boldsymbol{Z\overline{Z}}} + \Sigma_{\boldsymbol{ZZ}}\right), \qquad \Sigma_{\boldsymbol{XY}} = -\frac{1}{2}\,\mathrm{Im}\left(\Sigma_{\boldsymbol{Z\overline{Z}}} - \Sigma_{\boldsymbol{ZZ}}\right),\\ \Sigma_{\boldsymbol{YX}} &= \frac{1}{2}\,\mathrm{Im}\left(\Sigma_{\boldsymbol{Z\overline{Z}}} + \Sigma_{\boldsymbol{ZZ}}\right), \qquad \Sigma_{\boldsymbol{YY}} = \frac{1}{2}\,\mathrm{Re}\left(\Sigma_{\boldsymbol{Z\overline{Z}}} - \Sigma_{\boldsymbol{ZZ}}\right).\end{aligned}$$

A.2 Cumulant of complex-valued random vectors

Cumulants of random variables are tools to characterize the statistical properties of random variables. In this section, we introduce the cumulants of complex-valued random variables.

Before doing so, we recall the notation of cumulants for real-valued random variables. Let $X_1, \ldots, X_M$ be a real-valued random variables. Assume that, for fixed $M \in \mathbb{N}$, we have $\mathbb{E}|X_j|^M < \infty$ for all $j = 1, 2, \ldots, M$. The joint cumulant of $X_1, \ldots, X_M$ is defined as

$$\mathrm{cum}(X_1, \ldots, X_M) = (-i)^M \frac{\partial^M}{\partial t_1 \ldots \partial t_M} \log\left(\mathbb{E}\left(e^{i\boldsymbol{t}^{\mathrm{T}}\boldsymbol{X}}\right)\right)\Big|_{t_1=\ldots=t_M=0}, \tag{A.1}$$

where $\boldsymbol{t} = [t_1, \ldots, t_M]^{\mathrm{T}}$ and $\boldsymbol{X} = [X_1, \ldots, X_M]^{\mathrm{T}}$. We have the following relationship between moments and cumulants

$$\mathrm{cum}(X_1, \ldots, X_M) = \sum_P (-1)^{p-1}(p-1)! \prod_{i=1}^{p} \mathbb{E}\left[\prod_{l\in\pi_j} X_l\right], \tag{A.2}$$

where P is the set of distinct partitions of $\{1, \ldots, M\}$ each constituted by the subset $\{\mu_j,\, j = 1, \ldots, p\}$. For instance, for a zero-mean random vector, we have

$$\begin{aligned}&\mathrm{cum}(X_1) = \mathbb{E}X_1 = 0,\\ &\mathrm{cum}(X_1, X_2) = \mathbb{E}(X_1, X_2) = \mathrm{Cov}(X_1, X_2),\\ &\mathrm{cum}(X_1, X_2, X_3) = \mathbb{E}(X_1X_2X_3)\\ &\mathrm{cum}(X_1, X_2, X_3, X_4) = \mathbb{E}(X_1, X_2, X_3, X_4) - \mathbb{E}(X_1, X_2)\mathbb{E}(X_3, X_4),\\ &\qquad\qquad - \mathbb{E}(X_1, X_3)\mathbb{E}(X_2, X_4) - \mathbb{E}(X_1, X_4)\mathbb{E}(X_2, X_3).\end{aligned}$$

For more details on cumulants and their properties, we refer to [10, 22, 68]

Using (A.2) we can define the comulants for complex-valued random variables [62, Appendix E]. Let $Z_1, \ldots, Z_M$ be complex-valued random variables. Assume that, for fixed $n \in \mathbb{N}$, we have $\mathbb{E}|Z_j|^M < \infty$ for all $j = 1, 2, \ldots, k$. The joint cumulant of $Z_1, \ldots, Z_M$ is defined as

$$\mathrm{cum}(Z_1, \ldots, Z_M) = \sum_P (-1)^{p-1}(p-1)! \prod_{i=1}^{p} \mathbb{E}\left[\prod_{l\in\pi_j} Z_l\right],$$

where P is the set of distinct partitions of $\{1,\dots,M\}$ each constituted by the subset $\{\mu_j,\, j = 1,\dots,p\}$. Note that (A.1) may not exist if we replace the real-valued vector $\boldsymbol{X}$ by the complex-valued vector $\boldsymbol{Z} = [Z_1,\dots,Z_M]$. For this reason, we use the equation (A.2). Moreover, this definition ensures that all the algebraic properties of the cumulants for real-valued random variables also hold for complex-valued random variables. In contrast to the cumulants of real-valued variables, the second-order cumulant $\operatorname{cum}(Z_1, Z_2)$ is not equal to the covariance $\operatorname{Cov}(Z_1, Z_2)$. Specifically,

$$\operatorname{cum}(Z_1, Z_2) = \mathbb{E}(Z_1 Z_2) - \mathbb{E}Z_1 \mathbb{E}Z_2 = \operatorname{Cov}(Z_1, \overline{Z_2}).$$

In the following, we present a property of cumulants that plays a key role in the proof of Theorem 3.5. To the best of our knowledge, it has not been presented in the literature before.

Let $k \in \mathbb{Z}$ such that $0 \le k \le M$. Note that

$$\begin{aligned}&\operatorname{cum}\left(\operatorname{Re}(Z_1),\dots,\operatorname{Re}(Z_k),\operatorname{Im}(Z_{k+1}),\dots,\operatorname{Im}(Z_M)\right)\\ &\quad= \operatorname{cum}\left(\tfrac{Z_1+\overline{Z_1}}{2},\dots,\tfrac{Z_k+\overline{Z_k}}{2},\tfrac{Z_{k+1}-\overline{Z_{k+1}}}{2i},\dots,\tfrac{Z_M-\overline{Z_M}}{2i}\right)\end{aligned}$$

By $z^{[*]}$ we denote the optional complex conjugation of z, i.e., $z^{[*]} \in \{z, \overline{z}\}$. Applying multilinearity of joint cumulants, the joint cumulants

$$\operatorname{cum}\left(\operatorname{Re}(Z_1),\dots,\operatorname{Re}(Z_k),\operatorname{Im}(Z_{k+1}),\dots,\operatorname{Im}(Z_M)\right)$$

can be rewritten using linear combination of

$$\operatorname{cum}\left(Z_1^{[*]},\dots,Z_M^{[*]}\right).$$

Consequnelty, if

$$\operatorname{cum}\left(Z_1^{[*]},\dots,Z_M^{[*]}\right) = 0$$

for all possible choices of $Z_j^{[*]}$, then

$$\operatorname{cum}\left(\operatorname{Re}(Z_1),\dots,\operatorname{Re}(Z_k),\operatorname{Im}(Z_{k+1}),\dots,\operatorname{Im}(Z_M)\right) = 0.$$

A.3 Complex normal vectors

Let $\boldsymbol{Z} = [Z_1,\dots,Z_M]^{\mathrm{T}}$ be a random vector. We say $\boldsymbol{Z}$ has a M-dimensional complex normal distribution if and only if

$$[\operatorname{Re}(\boldsymbol{Z})^{\mathrm{T}}, \operatorname{Im}(\boldsymbol{Z})^{\mathrm{T}}]^{\mathrm{T}} = [\operatorname{Re}(Z_1),\dots,\operatorname{Re}(Z_M),\operatorname{Im}(Z_1),\dots,\operatorname{Im}(Z_M)]^{\mathrm{T}}$$

has a $2M$-dimensional normal distribution. A complex normal random vector $\boldsymbol{Z}$ can be parameterized in two ways

$$\begin{aligned}\boldsymbol{Z} &\sim \mathcal{N}(\boldsymbol{\mu_V}, \boldsymbol{\Sigma_{VV}}),\\ \boldsymbol{Z} &\sim \mathcal{N}(\boldsymbol{\mu_\zeta}, \boldsymbol{\Sigma_{\zeta\zeta}}).\end{aligned}$$

using the notation from Section A.1. Based on the first parametrization, the characteristic function of $\boldsymbol{Z}$ is given by

$$\phi_{\boldsymbol{V}}(\boldsymbol{t}) = e^{i\boldsymbol{t}\boldsymbol{\mu}_V - \frac{1}{2}\boldsymbol{t}^{\mathrm{T}}\boldsymbol{\Sigma}_{\boldsymbol{V}\boldsymbol{V}}\boldsymbol{t}}, \quad \boldsymbol{t} \in \mathbb{R}^{2M}.$$

As noted in [58], the normal distribution is the only distribution in which the logarithm of the characteristic function is a polynomial. Moreover, it is a quadratic polynomial

$$\log \phi_{\boldsymbol{V}} = i\boldsymbol{t}\boldsymbol{\mu}_V - \tfrac{1}{2}\boldsymbol{t}^{\mathrm{T}}\boldsymbol{\Sigma}_{\boldsymbol{V}\boldsymbol{V}}\boldsymbol{t}.$$

As a result, to prove that a complex-valued random vector $\boldsymbol{Z}$ has a complex normal distribution vector, it is sufficient to show that

$$\operatorname{cum}(V_{t_1}, \ldots, V_{t_k}) = 0,$$

for any $\{t_1, \ldots, t_k\} \subset \{1, \ldots, 2M\}$ and $k \geq 3$. From the observation stated in Section A.2, it is enough to show that

$$\operatorname{cum}\left(Z_1^{[*]}, \ldots, Z_M^{[*]}\right) = 0,$$

for all possible choices of $Z_j^{[*]}$, to obtain that $\boldsymbol{Z}$ has a complex normal distribution vector.

APPENDIX B

LEMMAS

In this chapter, we provide the tools and the auxiliary lemmas used in this thesis.

Let us start with a formula for the joint cumulants of products of random variables. For this purpose, we introduce a notations from Section 2.3 in [10]. Consider a table

$$\begin{matrix} (1,1) & \cdots & (1,R) \\ \vdots & \ddots & \vdots \\ (P,1) & \cdots & (P,R) \end{matrix} \tag{B.1}$$

and a partition $v_1 \cup v_2 \cup \cdots \cup v_M$ of its entries. We say that sets v, u of the partition *hook* if there exist $(i_1, j_1) \in v$ and $(i_2, j_2) \in u$ such that $i_1 = i_2$. We say that sets v and u *communicate* if there exists a sequence of sets $v = v_{m_1}, v_{m_2}, \ldots, v_{m_N} = u$ such that v_{m_n} and $v_{m_{n+1}}$ hook for $n = 1, 2, \ldots, N-1$. A partition is called to be *indecomposable* if all sets communicate.

Lemma B.1 (Theorem 2.3.1 in [10])**.** *Consider random variables $X_{i,j}$, with $i = 1, \ldots, P$ and $j = 1, \ldots, R$. Define*

$$Y_i = \prod_{j=1}^{R} X_{i,j}, \quad i = 1, \ldots, P.$$

Then

$$\operatorname{cum}(Y_1, \ldots, Y_P) = \sum_{\boldsymbol{v}=(v_1,\ldots,v_L)} \operatorname{cum}(X_{i,j},\, (i,j) \in \nu_1) \ldots \operatorname{cum}(X_{i,j},\, (i,j) \in \nu_L),$$

where the summation is over all indecomposable partitions $\boldsymbol{v} = (v_1, \ldots, v_L)$ of a table (B.1)*.*

In Chapter 3 we often use some inequalities for covariance. To present them, we first define the α-mixing measure for two σ-fields $\mathcal{A}$ and $\mathcal{B}$:

$$\alpha(\mathcal{A}, \mathcal{B}) = \sup_{A \in \mathcal{A},\, B \in \mathcal{B}} |\mathbb{P}(A \cap B) - \mathbb{P}(A)\,\mathbb{P}(B)|. \tag{B.2}$$

The measure $\alpha(\mathcal{A}, \mathcal{B})$ is used to measure the dependence between $\mathcal{A}$ and $\mathcal{B}$, see [21]. Below, we present two inequities related to the α-mixing measure.

Lemma B.2 ([21]). *Let X and Y be random variables. Assume that $\mathbb{E}|X|^p < \infty$ and $\mathbb{E}|Y|^q < \infty$, with $p, q > 1$ such that $\frac{1}{p} + \frac{1}{q} < 1$. Then*

$$|\mathrm{Cov}(X, Y)| \leq 8 \left(\mathbb{E}|X|^p\right)^{\frac{1}{p}} \left(\mathbb{E}|X|^q\right)^{\frac{1}{q}} \alpha^{1-\frac{1}{p}-\frac{1}{q}}(\sigma(X), \sigma(Y)).$$

Lemma B.3 ([21]). *Let X and Y be random variables. Assume that there exists $M_X, M_Y > 0$ such that $|X| \leq M_X$ and $|Y| \leq M_Y$ a.s. Then*

$$|\mathrm{Cov}(X, Y)| \leq 4 M_X M_Y \alpha(\sigma(X), \sigma(Y)).$$

In proofs of the asymptotic properties of the periodogram frequency-smoothed along the line, we require auxiliary lemmas concerning the properties of the Fourier transform W of the data-tapering window w (see Chapter 2). These lemmas are provided below.

Lemma B.4. *Assume that w is a continuous function on the interval $\left(-\frac{1}{2}, \frac{1}{2}\right)$ with compact support $\left[-\frac{1}{2}, \frac{1}{2}\right]$. Then*

$$\int_{\mathbb{R}} w\left(\tfrac{t-c_T}{d_T}\right) e^{-i2\pi\nu t} \,\mathrm{d}t = d_T W(d_T\nu) e^{-i2\pi\nu c_T}.$$

Proof. By changing the variables $u = \frac{t-c_T}{d_T}$, we have

$$\int_{\mathbb{R}} w\left(\tfrac{t-c_T}{d_T}\right) e^{-i2\pi\nu t} \,\mathrm{d}t = d_T e^{-i2\pi\nu c_T} \int_{\mathbb{R}} w(u) \, e^{-i2\pi\nu d_T u} \,\mathrm{d}u = d_T W(d_T\nu) e^{-i2\pi\nu c_T}.$$

□

Lemma B.5. *Assume that $W \in L^2(\mathbb{R})$. Then for $a \neq 0$*

$$\lim_{b\to\infty} \int_{\mathbb{R}} |W(x)\, W(ax+b)| \,\mathrm{d}x = 0.$$

Proof. Let $M_b = o(b)$ as $b \to \infty$. For sake of simplicity, we write M instead of M_b. Define $W_M(x) = W(x)\mathbb{1}_{[-M,M]}(x)$. Then we have $\|W - W_M\|_2 \to 0$ as $b \to \infty$. Note that $W_M(x)\, W_M(ax+b) = 0$ for $b > \frac{1}{2}M(a+1)$. Consequently, there exists b_0 such that for $b > b_0$

$$\int_{\mathbb{R}} |W_M(x)\, W_M(ax+b)| \,\mathrm{d}x = 0.$$

Now, we consider

$$\begin{aligned}
&\int_{\mathbb{R}} W(x)\, W(ax+b) \,\mathrm{d}x - \int_{\mathbb{R}} W_M(x)\, W_M(ax+b) \,\mathrm{d}x \\
&\quad = \int_{\mathbb{R}} W(x)\, W(ax+b) \,\mathrm{d}x - \int_{\mathbb{R}} W_M(x)\, W(ax+b) \,\mathrm{d}x \\
&\qquad + \int_{\mathbb{R}} W_M(x)\, W(ax+b) \,\mathrm{d}x - \int_{\mathbb{R}} W_M(x)\, W_M(ax+b) \,\mathrm{d}x.
\end{aligned}$$

Moreover, by Hölder inequality

$$\left|\int_{\mathbb{R}} (W(x)\,W(ax+b) - W_M(x)\,W(ax+b))\,\mathrm{d}x\right|^2 \le \int_{\mathbb{R}} |W(ax+b)|^2\,\mathrm{d}x \int_{\mathbb{R}} |W(x)-W_M(x)|^2\,\mathrm{d}x$$
$$\le |a|^{-1}\|W\|_2^2\,\|W-W_M\|_2^2,$$

and similarly

$$\left|\int_{\mathbb{R}} (W(ax+b)\,W_M(x) - W_M(ax+b)\,W_M(x))\,\mathrm{d}x\right|^2 \le |a|^{-1}\|W\|_2^2\,\|W-W_M\|_2^2,$$

which ends the proof since $\|W-W_M\|_2 \to 0$ as $b\to\infty$. □

Lemma B.6. *Assume that $W \in L^{\frac{4}{3}}(\mathbb{R})$. Then for $a_1, a_2, a_3 \neq 0$*

$$\lim_{b\to\infty} \int_{\mathbb{R}^3} |W(x_1)\,W(x_2)\,W(x_3)W(a_1x_1+a_2x_2+a_3x_3+b)|\,\mathrm{d}x_1\,\mathrm{d}x_2\,\mathrm{d}x_3 = 0.$$

Proof. Let $M_b = o(b)$ as $b\to\infty$. For simplicity, we write M instead of M_b. Define $W_M(x) = W(x)\mathbb{1}_{[-M,M]}(x)$. Then we have $\|W-W_M\|_{\frac{4}{3}} \to 0$ as $b\to\infty$. Also there exists b_0 such that $W_M(x_1)\,W_M(x_2)\,W_M(x_3)W_M(a_1x_1+a_2x_2+a_3x_3+b) = 0$ for $b > b_0$. Consequently, for $b > b_0$

$$\int_{\mathbb{R}^3} |W_M(x_1)\,W_M(x_2)\,W_M(x_3)W_M(a_1x_1+a_2x_2+a_3x_3+b)|\,\mathrm{d}x_1\,\mathrm{d}x_2\,\mathrm{d}x_3 = 0.$$

Let us consider the following change of variables

$$y_1 = a_1x_1,$$
$$y_2 = a_1x_1 + a_2x_2,$$
$$y_3 = a_1x_1 + a_2x_2 + a_3x_3.$$

We have

$$\begin{aligned} R &= \int_{\mathbb{R}^3} W(x_1)\,W(x_2)\,W(x_3)W(a_1x_1+a_2x_2+a_3x_3+b)\,\mathrm{d}x_1\,\mathrm{d}x_2\,\mathrm{d}x_3 \\ &\quad - \int_{\mathbb{R}^3} W_M(x_1)\,W_M(x_2)\,W_M(x_3)W_M(a_1x_1+a_2x_2+a_3x_3+b)\,\mathrm{d}x_1\,\mathrm{d}x_2\,\mathrm{d}x_3 \\ &= (a_1a_2a_3)^{-1} \int_{\mathbb{R}^3} W\left(\tfrac{y_1}{a_1}\right) W\left(\tfrac{y_2-y_1}{a_2}\right) W\left(\tfrac{y_3-y_2}{a_3}\right) W(y_3+b)\,\mathrm{d}y_1\,\mathrm{d}y_2\,\mathrm{d}y_3 \\ &\quad - (a_1a_2a_3)^{-1} \int_{\mathbb{R}^3} W_M\left(\tfrac{y_1}{a_1}\right) W_M\left(\tfrac{y_2-y_1}{a_2}\right) W_M\left(\tfrac{y_3-y_2}{a_3}\right) W_M(y_3+b)\,\mathrm{d}y_1\,\mathrm{d}y_2\,\mathrm{d}y_3. \end{aligned}$$

Therefore, using convolution operator, we can write

$$\begin{aligned} R &= (W_1 * W_2 * W_3 * W_4)(-b) - (W_{1,M} * W_{2,M} * W_{3,M} * W_{4,M})(-b) \\ &= ((W_1 - W_{1,M}) * W_2 * W_3 * W_4)(-b) \\ &\quad + (W_{1,M} * (W_2 - W_{2,M}) * W_3 * W_4)(-b) \\ &\quad + (W_{1,M} * W_{2,M} * (W_3 - W_{3,M}) * W_4)(-b) \\ &\quad + (W_{1,M} * W_{2,M} * W_{3,M} * (W_4 - W_{4,M})(-b), \end{aligned}$$

where $W_j(y) = |W(\frac{y}{a_j})|$ and $W_{j,M}(y) = |W_M(\frac{y}{a_j})|$ for $j = 1, 2, 3$, while $W_4(y) = |W(-y)|$ and $W_{4,M}(y) = |W_M(-y)|$. Applying Young's inequality, we obtain

$$\begin{aligned}((W_1 - W_{1,M}) * W_2 * W_3 * W_4)(-b) &\leq \|(W_1 - W_{1,M}) * W_2 * W_3 * W_4)\|_\infty \\ &\leq \|(W_1 - W_{1,M}) * W_2\|_2 \cdot \|W_3 * W_4\|_2 \\ &\leq \|W_1 - W_{1,M}\|_{\frac{4}{3}} \cdot \|W_2\|_{\frac{4}{3}} \cdot \|W_3\|_{\frac{4}{3}} \cdot \|W_4\|_{\frac{4}{3}},\end{aligned} \tag{B.3}$$

since $\frac{1}{2} + \frac{1}{2} = 1$ and $\frac{3}{4} + \frac{3}{4} = 1 + \frac{1}{2}$. Hence, the left hand-side of the inequality (B.3) converges to zero since $\|W_1 - W_{1,M}\|_{\frac{4}{2}} \to 0$ as $b \to \infty$.

Using the the same reasoning applies to the remaining terms and the fact that $\|W_{j,M}\|^p \leq \|W_j\|^p$ for $j = 1, 2, 3, 4$ and any $p > 1$, we conclude that all terms converge to zero, completing the proof. □

Lemma B.7. *Assume that $W \in L^\infty(\mathbb{R})$ and there exists a positive constant K such that $\sup_{x\in\mathbb{R}} |xW(x)| = K$. Then $W \in L^p(\mathbb{R})$ for all $p > 1$.*

Proof. For any $c > 0$, we have

$$\int_{\mathbb{R}} |W(x)|^p \,\mathrm{d}x = \int_{-c}^{c} |W(x)|^p \,\mathrm{d}x + \int_{\mathbb{R}\setminus(-c,c)} |W(x)|^p \,\mathrm{d}x \leq 2c\|W\|_\infty + 2K \int_c^\infty \frac{1}{x^p} \,\mathrm{d}x < \infty,$$

since $p > 1$. □

Lemma B.8. *Assume that $W \in L^2(\mathbb{R})$. Moreover, $c_T/d_T \to \vartheta \in \mathbb{R}$. Then*

$$\lim_{T\to\infty} \mathcal{E}_{c_T/d_T}(\alpha) = \mathcal{E}_\vartheta(\alpha).$$

Proof. It follows immediately from the dominated convergence theorem since the magnitude of the integrand function is $|W(\eta)W(-\alpha\eta)|$ which is integrable on $\mathbb{R}$. The integrability of $|W(\eta)W(-\alpha\eta)|$ follows from Hölder inequality. Namely,

$$\left| \int_{\mathbb{R}} |W(\eta)W(-\alpha\eta)| \,\mathrm{d}\nu \right|^2 \leq \int_{\mathbb{R}} |W(\eta)|^2 \,\mathrm{d}\nu \int_{\mathbb{R}} |W(-\alpha\eta)|^2 \,\mathrm{d}\nu = |\alpha|^{-1}\|W\|_2^4.$$

□

Lemma B.9. *Assume that $W \in L^\infty(\mathbb{R})$ and there exists a positive constant K such that $\sup_{x\in\mathbb{R}} |xW(x)| = K$. Define $W_M(x) = W(x)\mathbb{1}_{[-M,M]}(x)$ with $M > 0$. Then for constants $a \neq 0$ and $b \in \mathbb{R}$*

$$\int_{\mathbb{R}} |W(x)W(ax + b)| \,\mathrm{d}x = \int_{\mathbb{R}} |W_M(x)W_M(ax + b)| \,\mathrm{d}x + \mathcal{O}\big(M^{-\frac{1}{2}}\big),$$

as $M \to \infty$.

Proof. Note that

$$\int_{\mathbb{R}} |W(x) - W_M(x)|^2 \,\mathrm{d}x = \int_{|x|>M} |W(x)|^2 \,\mathrm{d}x \leq K \int_{|x|>M} |x|^{-2} \,\mathrm{d}x = 2KM^{-1}.$$

Moreover,

$$\begin{aligned}\int_{\mathbb{R}} |W(x)W(ax+b)|\,\mathrm{d}x \le &\int_{\mathbb{R}} |W(x)-W_M(x)|\,|W_M(ax+b)|\,\mathrm{d}x\\ &+\int_{\mathbb{R}} |W(x)-W_M(x)|\,|W(ax+b)-W_M(ax+b)|\,\mathrm{d}x\\ &+\int_{\mathbb{R}} |W_M(x)|\,|W(ax+b)-W_M(ax+b)|\,\mathrm{d}x\\ &+\int_{\mathbb{R}} |W_M(x)W_M(ax+b)|\,\mathrm{d}x.\end{aligned}$$

For the first term on the right-hand side, using Hölder inequality we have

$$\begin{aligned}\int_{\mathbb{R}} |W(x)-W_M(x)|\,|W_M(ax+b)|\,\mathrm{d}x &\le \left(\int_{\mathbb{R}} |W(x)-W_M(x)|^2\,\mathrm{d}x\cdot\frac{1}{a}\int_{\mathbb{R}} |W_M(x)|^2\,\mathrm{d}x\right)^{\frac{1}{2}}\\ &\le \left(\frac{2K}{Ma}\int_{\mathbb{R}} |W(x)|^2\,\mathrm{d}x\right)^{\frac{1}{2}} = \mathcal{O}\big(M^{-\frac{1}{2}}\big).\end{aligned}$$

The function $W\in L^2(\mathbb{R})$ by Lemma B.7. By Hölder inequality, the second term is bounded as follows

$$\int_{\mathbb{R}} |W(x)-W_M(x)|\,|W(ax+b)-W_M(ax+b)|\,\mathrm{d}x \le \frac{1}{\sqrt{a}}\int_{\mathbb{R}} |W(x)-W_M(x)|^2\,\mathrm{d}x = \mathcal{O}\big(M^{-1}\big),$$

For the third term, we have analogously to the first term, i.e.

$$\int_{\mathbb{R}} |W_M(x)|\,|W(ax+b)-W_M(ax+b)|\,\mathrm{d}x = \mathcal{O}\big(M^{-\frac{1}{2}}\big).$$

Note that the boundedness of the above three terms depends on M, K, a, and not on b. □

Lemma B.10. *Assume that $W\in L^\infty(\mathbb{R})$ and there exists a positive constant K such that $\sup_{x\in\mathbb{R}}|xW(x)|=K$. Then for $k\ge 2$ and $a_j\neq 0$, $j=1,2,\ldots,k$ and $b\in\mathbb{R}$*

$$\int_{\mathbb{R}^k} |W(x_1)\ldots W(x_k)W(a_1x_1+\ldots+a_kx_k+b)|\,\mathrm{d}x_1\ldots\mathrm{d}x_k \le C(a_1,\ldots,a_k)<\infty,$$

where $C(a_1,\ldots,a_k)>0$ and does not depend on b.

Proof. Let us consider the following change of variables

$$\begin{aligned} y_1 &= a_1x_1,\\ y_j &= a_1x_1+\ldots+a_jx_j, \qquad j=2,3,\ldots,k.\end{aligned}$$

Thus,

$$\begin{aligned}&\int_{\mathbb{R}^k} |W(x_1)\ldots W(x_k)W(a_1x_1+\ldots+a_kx_k+b)|\,\mathrm{d}x_1\ldots\mathrm{d}x_k\\ &\quad=\prod_{j=1}^{k-1}|a_j|^{-1}\int_{\mathbb{R}^k}\left|W\left(\tfrac{y_1}{a_1}\right)W\left(\tfrac{y_2-y_1}{a_2}\right)\ldots W\left(\tfrac{y_k-y_{k-1}}{a_k}\right)W(y_k+b)\right|\,\mathrm{d}y_1\ldots\mathrm{d}y_k\\ &\quad=\prod_{j=1}^{k-1}|a_j|^{-1}(W_1*W_2*\ldots*W_k)(-b),\end{aligned}$$

where $W_j(y) = |W(\frac{y}{a_j})|$, with $j = 1, 2, \ldots, k-1$, and $W_k(y) = |W(-y)|$. By the Young inequality, we get

$$\begin{aligned}\|W_1 * W_2 * \ldots * W_k\|_\infty &\leq \|W_1\|_{p_1} \|W_2 * \ldots * W_k\|_{p_1} \\ &\leq \|W_1\|_{p_1} \|W_2\|_{p_2} \|W_3 * \ldots * W_k\|_{p_2} \\ &\leq \|W_1\|_{p_1} \|W_2\|_{p_2} \ldots \|W_k\|_{p_k} < \infty,\end{aligned}$$

with $p_1 = 2$ and

$$1 + \frac{1}{p_n} = \frac{1}{p_{n+1}} + \frac{1}{p_{n+1}}, \quad n = 2, 3, \ldots, k.$$

Moreover, it can be shown that

$$p_n = \frac{2^n}{2^n - 1} > 1, \quad n = 1, 2, \ldots, k.$$

By Lemma B.7 functions $W_j \in L^p(\mathbb{R})$, for all $p > 1$. □

BIBLIOGRAPHY

[1] J. Antoni. Cyclostationarity by examples. *Mechanical Systems and Signal Processing*, 23(4):987–1036, 2009.

[2] J. Arteche and P. M. Robinson. Semiparametric inference in seasonal and cyclical long memory processes. *Journal of Time Series Analysis*, 21(1):1–25, 2000.

[3] P. Bertail and A. E. Dudek. Optimal choice of bootstrap block length for periodically correlated time series. *Bernoulli*, 30(3):2521–2545, 2024.

[4] P. Bertail, D. Politis, and N. Rhomari. Subsampling continuous parameter random fields and a bernstein inequality. *Statistics*, 33(4):367–392, 2000.

[5] A. Besicovitch. *Almost Periodic Functions*. Cambridge University Press, 1932.

[6] P. Billingsley. *Probability and Measure*. Wiley series in probability and mathematical statistics. Wiley India, 2017.

[7] P. Bloomfield. *Fourier Analysis of Time Series: An Introduction*. Wiley, New York, 2nd edition, 2000.

[8] H. Bohr. Zur theorie der fastperiodischen funktionen. *Acta Mathematica*, 46:101–214, 1925.

[9] H. Brezis. *Functional Analysis, Sobolev Spaces and Partial Differential Equations*. Universitext. Springer New York, 2010.

[10] D. R. Brillinger. *Time Series: Data Analysis and Theory*. Society for Industrial and Applied Mathematics, 2001.

[11] P. Brockwell and R. Davis. *Time Series: Theory and Methods*. Springer Series in Statistics. Springer, New York, NY, 1991.

[12] S. Chiu. Statistical Estimation of the Parameters of a Moving Source from Array Data. *The Annals of Statistics*, 14(2):559–578, 1986.

[13] P. Ciblat, P. Loubaton, E. Serpedin, and G. Giannakis. Asymptotic analysis of blind cyclic correlation-based symbol-rate estimators. *IEEE Transactions on Information Theory*, 48(7):1922–1934, 2002.

[14] P. Ciblat, P. Loubaton, E. Serpedin, and G. Giannakis. Performance analysis of blind carrier frequency offset estimators for noncircular transmissions through frequency-selective channels. *IEEE Transactions on Signal Processing*, 50(1):130–140, 2002.

[15] R. Dahlhaus, T. Dumont, S. Le Corff, and J. C Neddermeyer. Statistical inference for oscillation processes. *Statistics*, 51(1):61–83, 2017.

[16] S. Das and M. G. Genton. Cyclostationary processes with evolving periods and amplitudes. *IEEE Transactions on Signal Processing*, 69:1579–1590, 2021.

[17] D. Dehay. Spectral analysis of the covariance of the almost periodically correlated processes. *Stochastic Processes and their Applications*, 50(2):315–330, 1994.

[18] D. Dehay and J. Dudek, A. andd Leśkow. Subsampling for continuous-time almost periodically correlated processes. *Journal of Statistical Planning and Inference*, 150:142–158, 2014.

[19] D. Dehay and H. Hurd. Empirical determination of the frequencies of an almost periodic time series. *Journal of Time Series Analysis*, 34(2):262–279, 2013.

[20] P. A. M. Dirac. *The Principles of Quantum Mechanics*. Comparative Pathobiology - Studies in the Postmodern Theory of Education. Clarendon Press, 1981.

[21] P. Doukhan. *Mixing: Properties and Examples*. Lecture Notes in Statistics. Springer New York, 1994.

[22] P. Doukhan and J. León. Cumulants for mixing sequences and applications to empirical spectral density. *Probability and Mathematical Statistics*, 10, 01 1989.

[23] A. E. Dudek. Circular block bootstrap for coefficients of autocovariance function of almost periodically correlated time series. *Metrika*, 78, 08 2015.

[24] A. E. Dudek. Block bootstrap for periodic characteristics of periodically correlated time series. *Journal of Nonparametric Statistics*, 30(1):87–124, 2018.

[25] A. E. Dudek and Ł. Lenart. Spectral density estimation for nonstationary data with nonzero mean function. *Journal of the American Statistical Association*, 0(0):1–11, 2022.

[26] A. E. Dudek, Ł. Lenart, and **B. Majewski**. Statistical Properties of Oscillatory Processes with Stochastic Modulation in Amplitude and Time. *HAL preprint, https://hal.science/hal-04719645*, October 2024.

[27] A. E. Dudek, J. Leśkow, E. Paparoditis, and D. Politis. A Generalized Block Bootstrap For Seasonal Time Series. *Journal of Time Series Analysis*, 35(2):89–114, March 2014.

[28] A. E. Dudek and P. Potorski. Bootstrapping the autocovariance of pc time series - a simulation study. In Fakher Chaari, Jacek Leskow, Radoslaw Zimroz, Agnieszka Wyłomańska, and Anna Dudek, editors, *Cyclostationarity: Theory and Methods – IV*, pages 41–55, Cham, 2020. Springer International Publishing.

[29] A. E. Dudek and **B. Majewski**. Asymptotic distribution and subsampling in spectral analysis for spectrally correlated processes. *HAL preprint, https://hal.science/hal-04675084*, August 2024.

[30] A. E. Dudek, **B. Majewski**, and A. Napolitano. Spectral density estimation for a class of spectrally correlated processes. *Journal of Time Series Analysis*, 45(6):884–909, 2024.

[31] A. E. Dudek, **B. Majewski**, A. Napolitano, and H. Ombao. Inference for signals exhibiting irregular statistical cyclicity with applications to electrocardiograms. *HAL preprint, https://hal.science/hal-04495226*, March 2024.

[32] M. A. García-González, A. Argelagós-Palau, M. Fernández-Chimeno, and J. Ramos-Castro. A comparison of heartbeat detectors for the seismocardiogram. In *Computing in Cardiology 2013*, pages 461–464. IEEE, 2013.

[33] W. Gardner, A. Napolitano, and L. Paura. Cyclostationarity: Half a century of research. *Signal Processing*, 86(4):639–697, 2006.

[34] W. A. Gardner. Statistically inferred time warping: Extending the cyclostationarity paradigm from regular to irregular statistical cyclicity in scientific data. *EURASIP Journal on Advances in Signal Processing*, 2018:1–25, 2018.

[35] F. Ghaderi, S. Sanei, B. Makkiabadi, V. Abolghasemi, and J. G. McWhirter. Heart and lung sound separation using periodic source extraction method. In *2009 16th International Conference on Digital Signal Processing*, pages 1–6, 2009.

[36] E. Gladyshev. Periodically correlated random sequences. *Sov. Math., Dokl.*, 2:385–388, 1961.

[37] E. Gladyshev. Periodically and almost-periodically correlated random processes with a continuous time parameter. *Theory of Probability & Its Applications*, 8(2):173–177, 1963.

[38] N. Gómez Fonseca and M. Noriega Aleman. Cardiac arrhythmia classification based on the rms signal and cyclostationarity. *IEEE Latin America Transactions*, 19(4):584–591, 2021.

[39] E. Hannan. *Multiple Time Series*. Wiley Series in Probability and Statistics. Wiley, 1970.

[40] P. G. Hoel, S. C. Port, and C. J. Stone. *Introduction to Stochastic Processes*. Waveland Press, 1986.

[41] H. Hurd. Correlation theory of almost periodically correlated processes. *Journal of Multivariate Analysis*, 37(1):24–45, 1991.

[42] H. Hurd and A. Miamee. *Periodically Correlated Random Sequences: Spectral Theory and Practice*. Wiley Series in Probability and Statistics. Wiley, 2007.

[43] R. Hyndman, A. B. Koehler, J. K. Ord, and R. D. Snyder. *Forecasting with exponential smoothing: the state space approach*. Springer Science & Business Media, 2008.

[44] Q. Jin, K. M. Wong, and Z. Q. Luo. The estimation of time delay and doppler stretch of wideband signals. *IEEE Transactions on Signal Processing*, 43(4):904–916, April 1995.

[45] S. Kazemi, A. Ghorbani, and H. Amindavar. Cyclostationary modelling of amplitude and frequency modulated signals in heart and respiration monitoring doppler radar systems. *IET Radar, Sonar & Navigation*, 9(2):116–124, 2015.

[46] S. Kazemi, A. Ghorbani, H. Amindavar, and G. Li. Cyclostationary approach to doppler radar heart and respiration rates monitoring with body motion cancelation using radar doppler system. *Biomedical Signal Processing and Control*, 13:79–88, 2014.

[47] S. N. Lahiri. *Resampling Methods for Dependent Data*. Springer New York, NY, 2003.

[48] Ł. Lenart. Properties of stationary cyclical processes. *arXiv preprint arXiv:2405.08907*, 2024.

[49] Ł. Lenart, Ł. Kwiatkowski, and J. Wróblewska. A bayesian nonlinear stationary model with multiple frequencies for business cycle analysis. *arXiv preprint arXiv:2406.02321*, 2024.

[50] Ł. Lenart. Asymptotic properties of periodogram for almost periodically correlated time series. *Probability and Mathematical Statistics*, 28:305–324, 01 2008.

[51] Ł. Lenart. Asymptotic distributions and subsampling in spectral analysis for almost periodically correlated time series. *Bernoulli*, 17(1):290–319, 2011.

[52] K-S. Lii and M. Rosenblatt. Spectral analysis for harmonizable processes. *The Annals of Statistics*, 30(1):258–297, 2002.

[53] M. Loève. *Probability Theory*. D. Van Nostrand Co., Ind., Princeton, NJ, 1963.

[54] S. Lupenko. The rhythm-adaptive fourier series decompositions of cyclic numerical functions and one-dimensional probabilistic characteristics of cyclic random processes. *Digital Signal Processing*, 140:104104, 2023.

[55] F. Maddanu and T. Proietti. Modelling persistent cycles in solar activity. *Solar Physics*, 297(1):13, 2022.

[56] B. B. Mandelbrot and J. W. Van Ness. Fractional brownian motions, fractional noises and applications. *SIAM Review*, 10(4):422–437, 1968.

[57] X. Mao. *Stochastic differential equations and applications*. Elsevier, 2007.

[58] J. Marcinkiewicz. Sur une propriété de la loi de gauß. *Mathematische Zeitschrift*, 44:612–618, 1939.

[59] W. Munk, P. Worcester, and C. Wunsch. *Ocean Acoustic Tomography*. Cambridge Monographs on Mechanics. Cambridge University Press, 1995.

[60] A. Napolitano. Uncertainty in measurements on spectrally correlated stochastic processes. *IEEE Transactions on Information Theory*, 49(9):2172–2191, 2003.

[61] A. Napolitano. *Generalizations of Cyclostationary Signal Processing: Spectral Analysis and Applications*. Wiley-IEEE Press, Hoboken, NJ, USA, 2012.

[62] A. Napolitano. *Cyclostationary Processes and Time Series: Theory, Applications, and Generalizations*. Elsevier Science, London, 2019.

[63] A. Napolitano. An interference-tolerant algorithm for wide-band moving source passive localization. *IEEE Transactions on Signal Processing*, 68:3471–3485, 2020.

[64] A. Napolitano. Modeling the electrocardiogram as oscillatory almost-cyclostationary process. *IEEE Access*, 10:13193–13209, 2022.

[65] A. Napolitano and W. A. Gardner. Algorithms for analysis of signals with time-warped cyclostationarity. In *2016 50th Asilomar Conference on Signals, Systems and Computers*, pages 539–543. IEEE, 2016.

[66] I. Nourdin. *Selected aspects of fractional Brownian motion*, volume 4. Springer, 2012.

[67] H. Ombao and M. Pinto. Spectral dependence. *Econometrics and Statistics*, 32:122–159, 2024.

[68] G. Peccati and M. Taqqu. *Wiener chaos: Moments, Cumulants and diagrams: A survey with computer implementation*, volume 1. Springer Milano, 01 2011.

[69] B. Picinbono. Second-order complex random vectors and normal distributions. *IEEE Transactions on Signal Processing*, 44(10):2637–2640, 1996.

[70] B. Picinbono and P. Bondon. Second-order statistics of complex signals. *IEEE Transactions on Signal Processing*, 45(2):411–420, 1997.

[71] D. Politis. Complex-valued tapers. *IEEE Signal Processing Letters*, 12(7):512–515, 2005.

[72] D. Politis, J. Romano, and M. Wolf. *Subsampling*. Springer Series in Statistics. Springer New York, 1999.

[73] D. N. Politis and J. P. Romano. A general theory for large sample confidence regions based on subsamples under minimal assumptions. Technical Report 399, Department of Statistics. Stanford University, 1992.

[74] D. N. Politis and J. P. Romano. Large sample confidence regions based on subsamples under minimal assumptions. *The Annals of Statistics*, 22(4):2031–2050, 1994.

[75] D.N. Politis and J.P. Romano. *A circular block-resampling procedure for stationary data*. Wiley, New York, 1991.

[76] T. Proietti and F. Maddanu. Modelling cycles in climate series: The fractional sinusoidal waveform process. *Journal of Econometrics*, 239(1):105299, 2024. Climate Econometrics.

[77] W. Rudin. *Real and Complex Analysis*. Mathematics series. McGraw-Hill, 1987.

[78] J. Salas, J. Delleur, and V. Yevjevich. Applied modeling of hydrologic time series. *Water Resources Publications*, 1980.

[79] P. Schreier and L. Scharf. Second-order analysis of improper complex random vectors and processes. *IEEE Transactions on Signal Processing*, 51(3):714–725, 2003.

[80] P. Schreier and L. Scharf. Stochastic time-frequency analysis using the analytic signal: why the complementary distribution matters. *IEEE Transactions on Signal Processing*, 51(12):3071–3079, 2003.

[81] L. Shi, S. Jain, P. Agarwal, M. Mahmoudi, Y. Altayed, and S. Momani. Asymptotic analysis about the periodogram of a general class of time series models with spectral supports on lines not parallel to the main diagonal. *Fractals*, 30(10):2240269, 2022.

[82] A. R. Soltani and M. Azimmohseni. Periodograms asymptotic distributions in periodically correlated processes and multivariate stationary processes: An alternative approach. *Journal of Statistical Planning and Inference*, 137(4):1236–1242, 2007.

[83] A. R. Soltani, A. R. Nematollahi, and M. R. Mahmoudi. On the asymptotic distribution of the periodograms for the discrete time harmonizable simple processes. *Statistical Inference for Stochastic Processes*, 22(2):307–322, 2019.

[84] R. Synowiecki. Consistency and application of moving block bootstrap for non-stationary time series with periodic and almost periodic structure. *Bernoulli*, 13(4):1151–1178, 2007.

[85] R. Synowiecki. *Metody resamplingowe w dziedzinie czasu dla niestacjonarnych szeregów czasowych o strukturze okresowej i prawie okresowej*. PhD thesis, AGH University of Science and Techniology, Krakow, Poland, 2008.